Hashemite Kingdom of Jordan

Jordan Journal of Biological Sciences

An International Peer-Reviewed Scientific Journal

Financed by the Scientific Research Support Fund

http://jjbs.hu.edu.jo/

ISSN 1995-6673

المجلة الأردنية للعلوم الحياتية
Jordan Journal of Biological Sciences (JJBS)
http://jjbs.hu.edu.jo

Jordan Journal of Biological Sciences (JJBS) (ISSN: 1995–6673 (Print); 2307-7166 (Online)): An International Peer- Reviewed Open Access Research Journal financed by the Scientific Research Support Fund, Ministry of Higher Education and Scientific Research, Jordan and published quarterly by the Deanship of Research and Graduate Studies, The Hashemite University, Jordan.

Submission Address

Professor Abu-Elteen, Khaled H
The Hashemite University
P.O. Box 330127, Zarqa, 13115, Jordan
Phone: +962-5-3903333 ext. 5157
E-Mail: jjbs@hu.edu.jo

المجلة الأردنية للعلوم الحياتية
Jordan Journal of Biological Sciences (JJBS)
http://jjbs.hu.edu.jo

International Advisory Board

Associate Editorial Board

Instructions to Authors

Scope

Study areas include cell biology, genomics, microbiology, immunology, molecular biology, biochemistry, embryology, immunogenetics, cell and tissue culture, molecular ecology, genetic engineering and biological engineering, bioremediation and biodegradation, bioinformatics, biotechnology regulations, gene therapy, organismal biology, microbial and environmental biotechnology, marine sciences. The JJBS welcomes the submission of manuscript that meets the general criteria of significance and academic excellence. All articles published in JJBS are peer-reviewed. Papers will be published approximately one to two months after acceptance.

Type of Papers

The journal publishes high-quality original scientific papers, short communications, correspondence and case studies. Review articles are usually by invitation only. However, Review articles of current interest and high standard will be considered.

Submission of Manuscript

Manuscript, or the essence of their content, must be previously unpublished and should not be under simultaneous consideration by another journal. The authors should also declare if any similar work has been submitted to or published by another journal. They should also declare that it has not been submitted/ published elsewhere in the same form, in English or in any other language, without the written consent of the Publisher. The authors should also declare that the paper is the original work of the author(s) and not copied (in whole or in part) from any other work. All papers will be automatically checked for duplicate publication and plagiarism. If detected, appropriate action will be taken in accordance with International Ethical Guideline. By virtue of the submitted manuscript, the corresponding author acknowledges that all the co-authors have seen and approved the final version of the manuscript. The corresponding author should provide all co-authors with information regarding the manuscript, and obtain their approval before submitting any revisions. Electronic submission of manuscripts is strongly recommended, provided that the text, tables and figures are included in a single Microsoft Word file. Submit manuscript as e-mail attachment to the Editorial Office at: JJBS@hu.edu.jo. After submission, a manuscript number will be communicated to the corresponding author within 48 hours.

Peer-review Process

It is requested to submit, with the manuscript, the names, addresses and e-mail addresses of at least 4 potential reviewers. It is the sole right of the editor to decide whether or not the suggested reviewers to be used. The reviewers' comments will be sent to authors within 6-8 weeks after submission. Manuscripts and figures for review will not be returned to authors whether the editorial decision is to accept, revise, or reject. All Case Reports and Short Communication must include at least one table and/ or one figure.

Preparation of Manuscript

The manuscript should be written in English with simple lay out. The text should be prepared in single column format. Bold face, italics, subscripts, superscripts etc. can be used. Pages should be numbered consecutively, beginning with the title page and continuing through the last page of typewritten material.

The text can be divided into numbered sections with brief headings. Starting from introduction with section 1. Subsections should be numbered (for example 2.1 (then 2.1.1, 2.1.2, 2.2, etc.), up to three levels. Manuscripts in general should be organized in the following manner:

Title Page

The title page should contain a brief title, correct first name, middle initial and family name of each author and name and address of the department(s) and institution(s) from where the research was carried out for each author. The title should be without any abbreviations and it should enlighten the contents of the paper. All affiliations should be provided with a lower-case superscript number just after the author's name and in front of the appropriate address.
The name of the corresponding author should be indicated along with telephone and fax numbers (with country and area code) along with full postal address and e-mail address.

Abstract

The abstract should be concise and informative. It should not exceed **350 words** in length for full manuscript and Review article and **150 words** in case of Case Report and/ or Short Communication. It should briefly describe the purpose of the work, techniques and methods used, major findings with important data and conclusions. No references should be cited in this part. Generally non-standard abbreviations should not be used, if necessary they should be clearly defined in the abstract, at first use.

Keywords

Immediately after the abstract, **about 4-8 keywords** should be given. Use of abbreviations should be avoided, only standard abbreviations, well known in the established area may be used, if appropriate. These keywords will be used for indexing.

Abbreviations

Non-standard abbreviations should be listed and full form of each abbreviation should be given in parentheses at first use in the text.

Introduction

Provide a factual background, clearly defined problem, proposed solution, a brief literature survey and the scope and justification of the work done.

Materials and Methods

Give adequate information to allow the experiment to be reproduced. Already published methods should be mentioned with references. Significant modifications of published methods and new methods should be described in detail. Capitalize trade names and include the manufacturer's name and address. Subheading should be used.

Results

Results should be clearly described in a concise manner. Results for different parameters should be described under subheadings or in separate paragraph. Results should be explained, but largely without referring to the literature. Table or figure numbers should be mentioned in parentheses for better understanding.

Discussion

The discussion should not repeat the results, but provide detailed interpretation of data. This should interpret the significance of the findings of the work. Citations should be given in support of the findings. The results and discussion part can also be described as separate, if appropriate. The Results and Discussion sections can include subheadings, and when appropriate, both sections can be combined

Conclusions

This should briefly state the major findings of the study.

Acknowledgment

A brief acknowledgment section may be given after the conclusion section just before the references. The acknowledgment of people who provided assistance in manuscript preparation, funding for research, etc. should be listed in this section.

Tables and Figures

Tables and figures should be presented as per their appearance in the text. It is suggested that the discussion about the tables and figures should appear in the text before the appearance of the respective tables and figures. No tables or figures should be given without discussion or reference inside the text.

Tables should be explanatory enough to be understandable without any text reference. Double spacing should be maintained throughout the table, including table headings and footnotes. Table headings should be placed above the table. Footnotes should be placed below the table with superscript lowercase letters. Each table should be on a separate page, numbered consecutively in Arabic numerals.

Each figure should have a caption. The caption should be concise and typed separately, not on the figure area. Figures should be self-explanatory. Information presented in the figure should not be repeated in the table. All symbols and abbreviations used in the illustrations should be defined clearly. Figure legends should be given below the figures.

References

References should be listed alphabetically at the end of the manuscript. Every reference referred in the text must be also present in the reference list and vice versa. In the text, a reference identified by means of an author's name should be followed by the year of publication in parentheses (e.g.(Brown,2009)). For two authors, both authors' names followed by the year of publication (e.g.(Nelson and Brown, 2007)). When there are more than two authors, only the first author's name followed by "*et al*." and the year of publication (e.g. (Abu-Elteen *et al*., 2010)). When two or more works of an author has been published during the same year, the reference should be identified by the letters "a", "b", "c", etc., placed after the year of publication. This should be followed both in the text and reference list. e.g., Hilly, (2002a, 2002b); Hilly, and Nelson, (2004). Articles in preparation or submitted for publication, unpublished observations, personal communications, etc. should not be included in the reference list but should only be mentioned in the article text (e.g., Shtyawy,A., University of Jordan, personal communication). Journal titles should be abbreviated according to the system adopted in Biological Abstract and Index Medicus, if not included in Biological Abstract or Index Medicus journal title should be given in full. The author is responsible for the sccuracy and completeness of the references and for their correct textual citation. Failure to do so may result in the paper being withdraw from the evaluation process. Example of correct reference form is given as follows:-

Reference to a journal publication:

Ogunseitan OA. 1998. Protein method for investigating mercuric reductase gene expression in aquatic environments. *Appl Environ Microbiol.*, **64 (2)**: 695-702.

Govindaraj S and Ranjithakumari B D. 2013. Composition and larvicidal activity of *Artemisia vulgaris* L. stem essential oil against *Aedes aegypti*. *Jordan J Biol Sci*., **6(1):** 11-16.

Hilly MO, Adams MN and Nelson SC. 2009. Potential fly-ash utilization in agriculture. *Progress in Natural Sci.*, **19**: 1173-1186.

Reference to a book:

Brown WY and White SR.1985. **The Elements of Style**, third ed. MacMillan, New York.

Reference to a chapter in an edited book:

Mettam GR and Adams LB. 2010. How to prepare an electronic version of your article. In: Jones BS and Smith RZ (Eds.), **Introduction to the Electronic Age**. Kluwer Academic Publishers, Netherlands, pp. 281–304.

Conferences and Meetings:

Embabi NS. 1990. Environmental aspects of distribution of mangrove in the United Arab Emirates. Proceedings of the First ASWAS Conference. University of the United Arab Emirates. Al-Ain, United Arab Emirates.

Theses and Dissertations:

El-Labadi SN. 2002. Intestinal digenetic trematodes of some marine fishes from the Gulf of Aqaba. MSc dissertation, The Hashemite University, Zarqa, Jordan.

Nomenclature and Units

Internationally accepted rules and the international system of units (SI) should be used. If other units are mentioned, please give their equivalent in SI.

For biological nomenclature, the conventions of the *International Code of Botanical Nomenclature, the International Code of Nomenclature of Bacteria,* and the *International Code of Zoological Nomenclature* should be followed.

Scientific names of all biological creatures (crops, plants, insects, birds, mammals, etc.) should be mentioned in parentheses at first use of their English term.

Chemical nomenclature, as laid down in the *International Union of Pure and Applied Chemistry* and the official recommendations of the *IUPAC-IUB Combined Commission on Biochemical Nomenclature* should be followed. All biocides and other organic compounds must be identified by their Geneva names when first used in the text. Active ingredients of all formulations should be likewise identified.

Math formulae

All equations referred to in the text should be numbered serially at the right-hand side in parentheses. Meaning of all symbols should be given immediately after the equation at first use. Instead of root signs fractional powers should be used. Subscripts and superscripts should be presented clearly. Variables should be presented in italics. Greek letters and non-Roman symbols should be described in the margin at their first use.

To avoid any misunderstanding zero (0) and the letter O, and one (1) and the letter l should be clearly differentiated. For simple fractions use of the solidus (/) instead of a horizontal line is recommended. Levels of statistical significance such as: $^{*}P < 0.05$, $^{**}P < 0.01$ and $^{***}P < 0.001$ do not require any further explanation.

Copyright

Submission of a manuscript clearly indicates that: the study has not been published before or is not under consideration for publication elsewhere (except as an abstract or as part of a published lecture or academic thesis); its publication is permitted by all authors and after accepted for publication it will not be submitted for publication anywhere else, in English or in any other language, without the written approval of the copyright-holder. The journal may consider manuscripts that are translations of articles originally published in another language. In this case, the consent of the journal in which the article was originally published must be obtained and the fact that the article has already been published must be made clear on submission and stated in the abstract. It is compulsory for the authors to ensure that no material submitted as part of a manuscript infringes existing copyrights, or the rights of a third party.

Ethical Consent

All manuscripts reporting the results of experimental investigation involving human subjects should include a statement confirming that each subject or subject's guardian obtains an informed consent, after the approval of the experimental protocol by a local human ethics committee or IRB. When reporting experiments on animals, authors should indicate whether the institutional and national guide for the care and use of laboratory animals was followed.

Plagiarism

The JJBS hold no responsibility for plagiarism. If a published paper is found later to be extensively plagiarized and is found to be a duplicate or redundant publication, a note of retraction will be published, and copies of the correspondence will be sent to the authors' head of institute.

Galley Proofs

The Editorial Office will send proofs of the manuscript to the corresponding author as an e-mail attachment for final proof reading and it will be the responsibility of the corresponding author to return the galley proof materials appropriately corrected within the stipulated time. Authors will be asked to check any typographical or minor clerical errors in the manuscript at this stage. No other major alteration in the manuscript is allowed. After publication authors can freely access the full text of the article as well as can download and print the PDF file.

Publication Charges

There are no page charges for publication in Jordan Journal of Biological Sciences, except for color illustrations.

Reprints

Twenty (20) reprints are provided to corresponding author free of charge within two weeks after the printed journal date. For orders of more reprints, a reprint order form and prices will be sent with article proofs, which should be returned directly to the Editor for processing.

Disclaimer

Articles, communication, or editorials published by JJBS represent the sole opinions of the authors. The publisher shoulders no responsibility or liability what so ever for the use or misuse of the information published by JJBS.

Indexing

JJBS is indexed and abstracted by:

DOAJ (Directory of Open Access Journals
Google Scholar
Journal Seek
HINARI
Index Copernicus
NDL Japanese Periodicals Index
SCIRUS
OAJSE
ISC (Islamic World Science Citation Center)
Directory of Research Journal Indexing (DRJI)

CABI
EBSCO
CAS (Chemical Abstract Service)
ETH- Citations
Open J-Gat
SCImago
Zoological Records
Scopus
AGORA (United Nation's FAO database)
SHERPA/RoMEO (UK)
International Institute of Organized Research (I2OR) Database

المجلة الأردنية للعلوم الحياتية
Jordan Journal of Biological Sciences (JJBS)
http://jjbs.hu.edu.jo

The Hashemite University

Deanship of Scientific Research and Graduate Studies

TRANSFER OF COPYRIGHT AGREEMENT

Journal publishers and authors share a common interest in the protection of copyright: authors principally because they want their creative works to be protected from plagiarism and other unlawful uses, publishers because they need to protect their work and investment in the production, marketing and distribution of the published version of the article. In order to do so effectively, publishers request a formal written transfer of copyright from the author(s) for each article published. Publishers and authors are also concerned that the integrity of the official record of publication of an article (once refereed and published) be maintained, and in order to protect that reference value and validation process, we ask that authors recognize that distribution (including through the Internet/WWW or other on-line means) of the authoritative version of the article as published is best administered by the Publisher.

To avoid any delay in the publication of your article, please read the terms of this agreement, sign in the space provided and return the complete form to us at the address below as quickly as possible.

Article entitled:----------

Corresponding author: ----------

To be published in the journal: Jordan Journal of Biological Sciences (JJBS)

I hereby assign to the Hashemite University the copyright in the manuscript identified above and any supplemental tables, illustrations or other information submitted therewith (the "article") in all forms and media (whether now known or hereafter developed), throughout the world, in all languages, for the full term of copyright and all extensions and renewals thereof, effective when and if the article is accepted for publication. This transfer includes the right to adapt the presentation of the article for use in conjunction with computer systems and programs, including reproduction or publication in machine-readable form and incorporation in electronic retrieval systems.
Authors retain or are hereby granted (without the need to obtain further permission) rights to use the article for traditional scholarship communications, for teaching, and for distribution within their institution.

☐ **I am the sole author of the manuscript**

☐ **I am signing on behalf of all co-authors of the manuscript**

☐ **The article is a 'work made for hire' and I am signing as an authorized representative of the employing company/institution**

Please mark one or more of the above boxes (as appropriate) and then sign and date the document in black ink.

Signed:_____ Name printed: _____
Title and Company (if employer representative) : _____
Date: _____

Data Protection: By submitting this form you are consenting that the personal information provided herein may be used by the Hashemite University and its affiliated institutions worldwide to contact you concerning the publishing of your article.

Please return the completed and signed original of this form by mail or fax, or a scanned copy of the signed original by e-mail, retaining a copy for your files, to:

Hashemite University
Zarqa 13115 Jordan
Fax: +962 5 3903338
Email: jjbs@hu.edu.jo

EDITORIAL PREFACE

It is my pleasure to present the tenth volume of the *Jordan Journal of Biological Sciences* (JJBS) to the audience. JJBS is a refereed, peer reviewed quarterly international journal issued by the Jordanian Ministry of Higher Education and Scientific Research Support Fund in cooperation with The Hashemite University, Zarqa, Jordan. This journal publishes papers in Biological Sciences encompassing all the branches at molecular, cellular and organismal levels.

A group of distinguished scholars have agreed to serve on the Editorial Board. Without the service and dedication of these eminent scholars, JJBS would have never existed. Now, the Editorial Board is encouraged by the continuous growth of the journal and its formation into a true multidisciplinary publication. I am also honored to have the privilege of working with all members of the international advisory board served by a team of highly reputable researchers from different countries across the globe. I am also delighted with our team of national and international reviewers who are actively involved in research in different biological sciences and who provide authors with high quality reviews and helpful comments to improve their manuscripts.

JJBS has been indexed by SCOPUS, CABI's Full-Text Repository, EBSCO, Zoological Records and National Library of Medicine's MEDLINE\ Pub Med system and others. I would like to reaffirm that the success of the journal depends on the quality of reviewing and, equally, the quality of the research papers published.

In addition to being a hard-copy journal, JJBS is an open access journal which means that all contents are freely available the users and their institutions free of charge. Users are allowed to read, download, copy, distribute, print, search, or link to the full texts of the articles in this journal without asking for prior permission from the publisher or the author. This is in accordance with the BOAI definition of open access.

At the end of this preface, I would like to thank our readers and authors for their continuing interest in JJBS, and each member of our editorial and review boards for their continued hard work, support and dedication, which made it possible to bring another new issue of JJBS to the multidisciplinary international audience. My thanks are also extended to the Hashemite University and Jordanian Scientific Research Support Fund for their continuous support to Jordan Journal of Biological Sciences. I very much appreciate your support as we strive to make JJBS one of the most leading and authoritative journals in the field of Biological Sciences.

December,2017

Prof. Abu-Elteen, Khaled H
Editor-in-Chief
The Hashemite University, Zarqa, Jordan

JJBS

Volume 10, *Number 4, December .2017*
ISSN 1995-6673

Jordan Journal of Biological Sciences

CONTENTS

Original Articles

JJBS

Jordan Journal of Biological Sciences

Volume 10, Number 4,December 2017
ISSN 1995-6673
Pages 221 - 227

Isolation and Characterization of Bacteriocins like Antimicrobial Compound from *Lactobacillus delbrueckii* subsp *lactis*

Narendrakumar Gopakumaran[1,*], Sri Gajani Veerasangili[1] and Preethi Thozhikatu Valliaparambal[2]

[1]*Department of Biotechnology, School of Bio and Chemical Engineering, Sathyabama University, Chennai – 600119*

[2]*Research Scholar, Department of Microbiology, Vels University, Chennai – 600117, India*

Received: April 11, 2017; Revised: August 4, 2017; Accepted: August 13, 2017

Abstract

Bacteriocins are naturally produced antimicrobial peptides that inhibits microorganism in narrow and broad range. *Lactobacillus delbrueckii* subsp *lactis* were isolated from yogurt and screened to produce bacteriocin like compound by Agar diffusion assay, further cultured in shake flask fermentation at 30°C for mass production. Characterization of bacteriocins was done by UV spectrophotometric analysis. At different pH (6-9), incubation time (0-144 hours), temperature (20 – 40) and agitation (50 – 150 rpm) the production of the compound was characterized and checked by agar diffusion assay to perceive the size of zones of inhibition. The study aimed to optimize the growth condition for the enhanced production of bacteriocin by *Lactobacillus delbrueckii* subsp *lactis* using Response Surface Methodology (RSM). Maximum zones of inhibition were observed at pH 8, after 72 hours of incubation at 30°C with an agitation of 100 rpm. The compound was centrifuged and purified using ammonium sulphate precipitation, dialysis and chromatographic techniques. Bacteriocins like polypeptide antimicrobial substance showed activity against Gram positive organisms like *Bacillus cereus* and *Staphylococcus aureus* that proved to be sensitive.

Keywords: Bacteriocins, *Lactobacillus delbrueckii* subsp *lactis*, Response surface methodology (RSM -CCD).

1. Introduction

Lactobacillus delbrueckii subsp *lactis* is a nonpathogenic member and lactic acid emanating bacteria that are largely used in dairy products production, especially in cheese-making and yogurt production. It has the characteristics of diminishing lactose intolerance, changing the intestinal milieu and improving immunity to stimulate physical health (Piard *et al.*, 1992). Recent studies in the field of bacteriocin produced by *L. delbrueckii* have validated that the bacteriocin has a broad spectrum in terms of inhibition on different bacteria and fungi. Lactic acid bacteria's bacteriocin is a kind of antibacterial polypeptide synthesized in the metabolism process (Jagannathan *et al.*, 2015; Larsen *et al.*, 1993; Pingitore *et al.*, 2007; Zhao *et al.*, 2015). There are reports revealing that the bacteriocin was extracted from *Lactobacillus bavaricus* (Larsen *et al.*, 1993); *Lactobacillus brevis* MTCC 7539 (Neha Gautam and Nivedita Sharma, 2009); south Indian special dosa (appam) batter (Pal *et al.*, 20); *Lactobacillus plantarum* (Ray *et al.*, 2009; Ravi Sankar *et al.*, 2012; Zhou *et al.*, 2014). Bacteriocin has an antibacterial effect on Gram-positive pathogens associated with bovine mastitis and helps in eliminating them (Klostermann *et al.*, 2010).

Optimization of cultural parameter is a vital facet in the field of food biotechnology and fermentation to recuperate product yield and trim down the process variability, as well as reducing processing time and costs. Due to the complexity of the culture media, prolonged growth time, and slow agitation for producing bacteriocin from *Lactobacillus delbrueckii* subsp *lactis*, it is practically impossible for a one factor one time to identify an optimum combination of culturing conditions using a predetermined number of experiments. Response Surface Methodology (RSM) is a tactic approach that can be used to analysis the effect of variables and to pursue the conditions for a multivariable system. The aim of this probe was to quest the optimal cultural condition for *Lactobacillus delbrueckii* for mass production by using the statistical tools (Shaileshkumar *et al.*, 2009; Siew *et al.*, 2013; Vidhyalakshmi *et al.*, 2016). Reports relating to the antibacterial properties of these organisms have been constrained.

In the present study, optimal cultural conditions were determined and the effects of these variables on the bacteriocin activity were assessed, using a response

* Corresponding author. e-mail: narendrakumar.biotech@sathyabamauniversity.ac.in.

surface approach that includes statistical and plotting methods for experimental design and analysis.

2. Materials and Method

2.1. Sample Collection

Different bacterial samples were isolated from homemade yogurt.

2.2. Isolation of Bacteria

2.2.1. Isolation of Microorganism

The yogurt samples were brought to the laboratory and 1 gm of yogurt was serial diluted. Appropriate dilutions of 10^{-4}, 10^{-5}, 10^{-6} and 10^{-7} were selected and replicates were maintained throughout the present study. After 24hrs of incubation the bacterial cultures were enumerated, isolated and inoculated in separate Petri plates and vials and stored in the refrigerator for further analysis. The Milk agar plates and slants were labelled properly and were kept undisturbed.

2.2.2. Identification of Microorganisms

2.2.2.1. Physical Identification

Phenotypic identifications were carried out on the basis of their color, colony formation, texture, etc. and they were isolated, stored and classified as 4 isolates.

2.2.2.2. Microscopic Observations

The 4 isolates were Gram stained and observed under the microscope for their morphological appearance. The structure of organisms was identified as bacilli as per Bergey's manual, 1976 and standard methods.

A motility test using semisolid agar tubes was carried out and the motile nature of the organism was observed along the line of inoculation.

2.2.2.3. Biochemical Tests

Identification of these organisms was carried out by conventional biochemical tests, like indole, Methyl red, carbohydrate fermentation, Voges Proskauer, catalase, citrate, urease, triple sugar iron, starch hydrolysis and oxidase test.

2.3. 16s rRNA Analysis

After the isolation and biochemical identification of organism, 16srRNA was performed and the sequence was submitted in EBI (http://www.ebi.ac.uk).

2.4. Bacteriocin Production by Lactobacillus Delbrueckii Subsp Lactis Species

2.4.1. Inoculum Preparation

From the isolated organism, *Lactobacillus delbrueckii* subsp *lactis* was identified, showing an antimicrobial activity. Hence, this organism was used as inoculums to produce bacteriocin like compound. The organism was inoculated in (De Man, Rogosa and Sharpe agar) MRS Broth and incubated 37^{o}C was used for the screening of antimicrobial substance.

2.4.2. Production Media

The cell suspensions were aseptically transferred to experimental flasks for the growth studies. The bacteriocin production was carried out in mineral medium containing: 2.0 mgl^{-1} NH_4NO_3, 0.01 mgl^{-1} $CaCl_2$, 0.5 mgl^{-1} KH_2PO_4, 1.0 mgl^{-1} K_2HPO_4, 0.5 mgl^{-1} $MgSO_4$, 0.1 mgl^{-1} KCl and 0.06 mgl^{-1} yeast extract, respectively. For a large scale production of Bacteriocin like compound, a production medium was optimized and the organism was inoculated. After 72 hours of incubation, the cell free filtrate was analyzed for antimicrobial activity using spectrometry and further by Agar well diffusion method.

2.4.3. Protein Estimation

The protein estimation was carried out according to Lowry's method by using BSA as standard.

2.4.4. Determination of Bacteriocin Activity

A well diffusion assay procedure was used. Aliquots of 50 µl from each bacteriocin dilution were placed in the wells in plates seeded with the bioassay strain. The plates were incubated overnight at 30ºC for lactic acid bacteria indicators and the diameters of the inhibition zone were measured (Rammelsberg and Radler, 1990).

2.4.5. Determination of Bacteriocin titer

The titres of bacteriocin produced were calculated by two-fold serial dilutions of bacteriocin in saline solution and aliquots of 50 µl from each dilution were placed in wells in plates seeded with the bioassay strain. These plates were incubated at 37ºC for 18-24 h and examined for the presence of 2 mm or larger clear zones of inhibition around the wells. The antimicrobial activity of the bacteriocin was defined as the reciprocal of the highest dilution showing inhibition of the indicator lawn and was expressed in activity units per ml (AU ml^{-1}) (Graciela *et al.*, 1995). One AU is defined as the reciprocal of the highest dilution showing a clear zone of growth inhibition.

2.5. Response Surface Methodology RSM- Central Composite Design - CCD

Response surface methodology was used for optimization of bacteriocin production. The selection of parameters was selected from previous literature and the ranges were fixed using one factor at a time (OFAT). The combination of the media influences the production of bacteriocin along with the physical parameter. Table 1 represents the coded value and actual value for all the parameter used (Mandenius and Brundin, 2008)

Table 1. Representing the factors its Coded and Actual value

Factor	Low		High	
	Actual	Coded	Actual	Coded
pH (X_1)	6	-1	10	1
Temperature (X_2) ºC	20	-1	40	1
Incubation time (X_4) h	0	-1	144	1
Agitation (X_4) rpm	50	-1	150	1

Equation $Y = a_0 + a_1X_1 + a_2X_2 + a_3X_3 + a_4X_4 + a_{11}X_1^2 + a_{22}X_2^2 + a_{33}X_3^2 + a_{44}X_4^2 + a_{12}X_1X_2 + a_{13}X_1X_3 + a_{14}X_1X_4 + a_{23}X_2X_3 + a_{24}X_2X_4 + a_{34}X_3X_4$

where Y is the predicted response; X_1, X_2, X_3, X_4, the independent variables, a0 the offset term, a_1, a_2, a_3, a_4, the coefficients of linear effects; a_{11}, a_{22}, a_{33}, a_{44}, coefficients of squared effect, a_{12}, a_{13}, a_{14}, a_{23}, a_{24}, a_{34}, coefficients of interaction terms.

2.6. Spectrophotometric Method (UV – VIS Spectrum)

The crude extra-cellular protein was estimated using spectrophotometer. It was analyzed using Varian Cary 300 UV-VIS spectrophotometer in a spectrum mode and the maximum activity was at a wavelength of 280 nm.

2.7. Gel Permeation Chromatography

Twenty-three 2ml of fraction were separated using Gel permeation method and further subjected to the UV –VIS spectroscopic analysis to 280 nm and the absorption was found maximum in 14 fraction.

2.8. SDS- PAGE (Polyacrylamide Gel Electrophoresis)

2.8.1. Slab gel electrophoresis

This method was performed to establish the molecular weight of the bacteriocin present in the *Lactobacillus delbrueckii* subsp *lactis* sample as it showed maximum protein content in the Lowry's method. The standard protein was kept as Bovine Serum Albumin (BSA). Based on the protein standard the molecular weight of the enzyme was estimated.

2.8.2. FTIR

The absorbance FT-IR spectra of the samples was documented using an FT-IR Perkin–Elmer spectrometer. The spectra were collected within a scanning range of 400-4000 cm^{-1}.

3. Results and Discussion

3.1. Isolation and Identification of Lactobacillus Delbrueckii Subsp Lactis

The organism was isolated from the yogurt and identified as *Lactobacillus delbrueckii subsp lactis* by biochemical and 16s rRNA sequencing. The sequence obtained after sequence is given below:

3.2. Aligned Data

>bi05 Lactobacillus lactis

CCTAAACAGTAGAAATATATTGAAAGCTGTGT
AAACTATGAAATCTCAATCTCTACCTGTAAATATT
CTAGCACTACTTGATAAGGACTGTTTTGTCATGCG
TAGAAACAAAAAACTTGTTCAAGGATCATACCAA
AATGAAGAGCCCTACAATTGTTAGACATAGACAT
CTAACGATTGTGGGGTATTTTTATGACCAAATATT
CATCTGAACAAAAAGTACAAATTGCTTCTGATTAT
CTTTACGGCAGAGACTCATACAATGGATTAAACC
AAAAGTATAATATGGCTGCGTCAATAATTCGTAC
GTGGGTGAAAGCCGCTGAACTTAATGGATTGGAA
CTCATCTTCAATCTATATCTTTTAACAATTGCTGTT
TTCCAAAGTCAATTCACCGCCAAAAGCTTCCAAG
CGATCGACTTCAGCCAGGTAGATTTGGCCAGCAA
TAGTCTGGTACTTGCCAGACGGGTATTGCTCAAA
GCTTAAGGCATCCCCTTCCTTGCTCTTCAAGATGC
CAAATTCTGCTTCTTCCTCATCTTTCATGACAAAG
GACACGACTTGCCCAGCAGCTAATTGCCAGAAGT
CCTGAATCTGCTTGATTTCTGCTGCTTTATCTTGA
ACTTCAAAGGGATCTTCTAATCCTCTTTCCTTAAG
CTGGCCCCGGCAGCGGCTGATATCATGCAAATAC
TCTGATCGATCAATTACTCTGTCAACGGCCTTCTT
CTTAACCTGCAGCAATGAGTCATCCCGGCCAATTT
CGTCAACAGTCAAATACAAGCTGAAGTCGTCATC
AGCACACAATAGCCGACCAACCGCGAATGAAGCT
GGATCTTCTTTCAGATGAACTTCGCACAAACCATC
TACAGTTGTATATTCAGTATCCCGCAACTTAGGAT
TGTCCAGCAACCATTCACCGGAGAAAGCGGCTAG
CCGCCGGAGTTGACAGACAGCAACATTTCCTGCG
AAAGGCTGGTACTTGCCAGAAGGATATGCCGCAA
AATTAACTTGCCCGGCAGAAATATCATCAATATA
TCCCCATTGCTGGTAATCTTCGCCTTCCAGGCAAA
AATATACAACCTGCCCGGGCAATAAGTCCATAAA
GCTTCCGACTGACTTGATTAAGGTAACTTTGTCTT
CCAGCTTGAAAGGATCTGCCAGTCCATTTTGCGTT
AGCAGCTTCCGCCGGCGCTGGATCTCTGCCAAAT
AATGCGATTGATCCAACAGCCGCGTGACCGCTGA
CTTTCTGATCAAGAGCAAGGAATCATCCCGGCCC
AGCTGATCCAAAGTCAAGTAGAGCTGCCAGCCGT
TTTCTTCAAACAAGAGGCGACCGAGTTCAAAACT
GTCCTGAGCAGCGTCTGTGTAGATTTCGTATAATT
TTTCCA

3.3. Identified as Lactobacillus Delbrueckii Subsp Lactis

The sequence was subjected to BLAST and the phylogenetic analysis was reported.

The isolated and confirmed strain was inoculated in the production media for enhanced production of Bacteriocin that can be used as a food preservative (Paul Cotter *et al.*, 2005); it also enhances the immunity of the food against invading pathogens. A database for bacteriocin was classified and created (Hammami *et al.*, 2010).

3.4. Optimization of Bacteriocin Production

Analysis was done to understand the effect of various parameters on the production of Bacteriocin. The ability of the productivity influences the factors that enhance the productivity of the component from the organism. When a single factor analysis was performed the influence of other factors is not understood over the other.

3.4.1. Effect of pH on Bacteriocin Production

The optimum pH for the antimicrobial production by *Lactobacillus delbrueckii subsp lactis* was 8, although a good activity was also achieved at pH 6-9.

3.4.2. Effect of Temperature on Bacteriocin Production

The optimum temperature for the antimicrobial production by *Lactobacillus delbrueckii subsp lactis* was 30ºC.

3.4.3. Effect of Incubation Time on Bacteriocin Production

The maximum antibiotic activity by *Lactobacillus delbrueckii subsp lactis* was achieved at 96 h ours of incubation period.

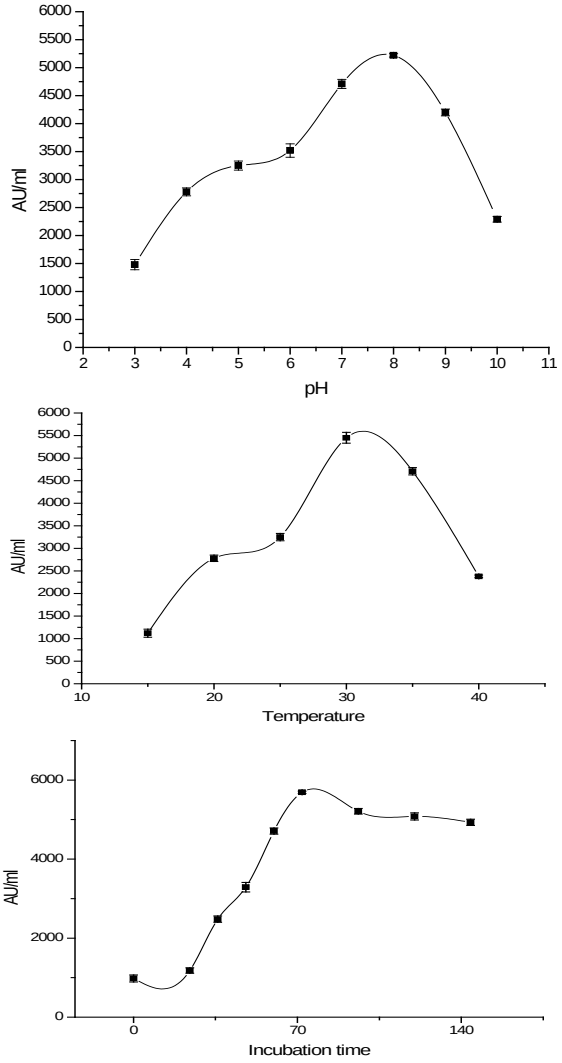

Figure 1. pH, temperature and incubation time with respect to enzyme activity

3.5. Response Surface Methodology

The four-parameter pH (X_1), temperature(X_2), Incubation time (X_3) and Agitation (X_4) were used to Design of Experiment (DOE) using Design expert version 7.0.0 software. After the analysis was performed, the values were loaded into the software again and analysis of variance (ANOVA) was observed. The maximum experimental value 5980AU/ml while the predicted value was estimated at 5646.6 AU/ml, a close correlation with each other. The model was significant and the lack of fit showed non-significance, assign that the design is functional with polynomial equation. The coefficient of determination of terms of R^2 is 0.985702, and the Adj R^2, as 0.972358 with a Pred R^2, was 0.949666. The contour and surface plots represent the interaction between variables.

Table 2. Design table of variable with responses

Run	X_1	X_2	X_3	X_4	Response	
		^oC	H	Rpm	Actual	Predicted
2	6	20	0	50	1500	1734.167
25	10	20	0	50	1770	1617.917
5	6	40	0	50	1750	1954.583
22	10	40	0	50	1470	1575.833
7	6	20	144	50	2920	2892.917
16	10	20	144	50	2270	2489.167
14	6	40	144	50	2560	2490.833
18	10	40	144	50	1790	1824.583
11	6	20	0	150	1880	1969.583
23	10	20	0	150	1750	1900.833
21	6	40	0	150	2570	2432.5
17	10	40	0	150	1950	2101.25
27	6	20	144	150	2610	2585.833
8	10	20	144	150	2310	2229.583
9	6	40	144	150	2150	2426.25
28	10	40	144	150	1960	1807.5
24	4	30	72	100	4020	3849.583
6	12	30	72	100	3150	3114.583
29	8	10	72	100	2980	2877.917
1	8	50	72	100	2780	2676.25
15	8	30	-72	100	1020	799.5833
10	8	30	216	100	1650	1664.583
12	8	30	72	0	1080	907.9167
26	8	30	72	200	1160	1126.25
19	8	30	72	100	5360	5646.667
3	8	30	72	100	5920	5646.667
30	8	30	72	100	5980	5646.667
20	8	30	72	100	5240	5646.667
13	8	30	72	100	5910	5646.667
4	8	30	72	100	5470	5646.667

X_1- pH; X_2- Temperature; X_3- Incubation time; X_4- Agitation

The equation Response = $5646.667 - 183.75\ X_1 - 50.4167\ X_2 + 216.25\ X_3 + 54.58333 X_4 - 65.625\ X_1X_2 - 71.875\ X_1X_3 + 11.875\ X_1X_4 - 155.625\ X_2X_3 + 60.625\ X_2X_4 - 135.625\ X_3X_4 - 541.146\ X_1^2 - 717.396\ X_2^2 - 1103.65\ X_3^2 - 1157.4\ X_4^2$

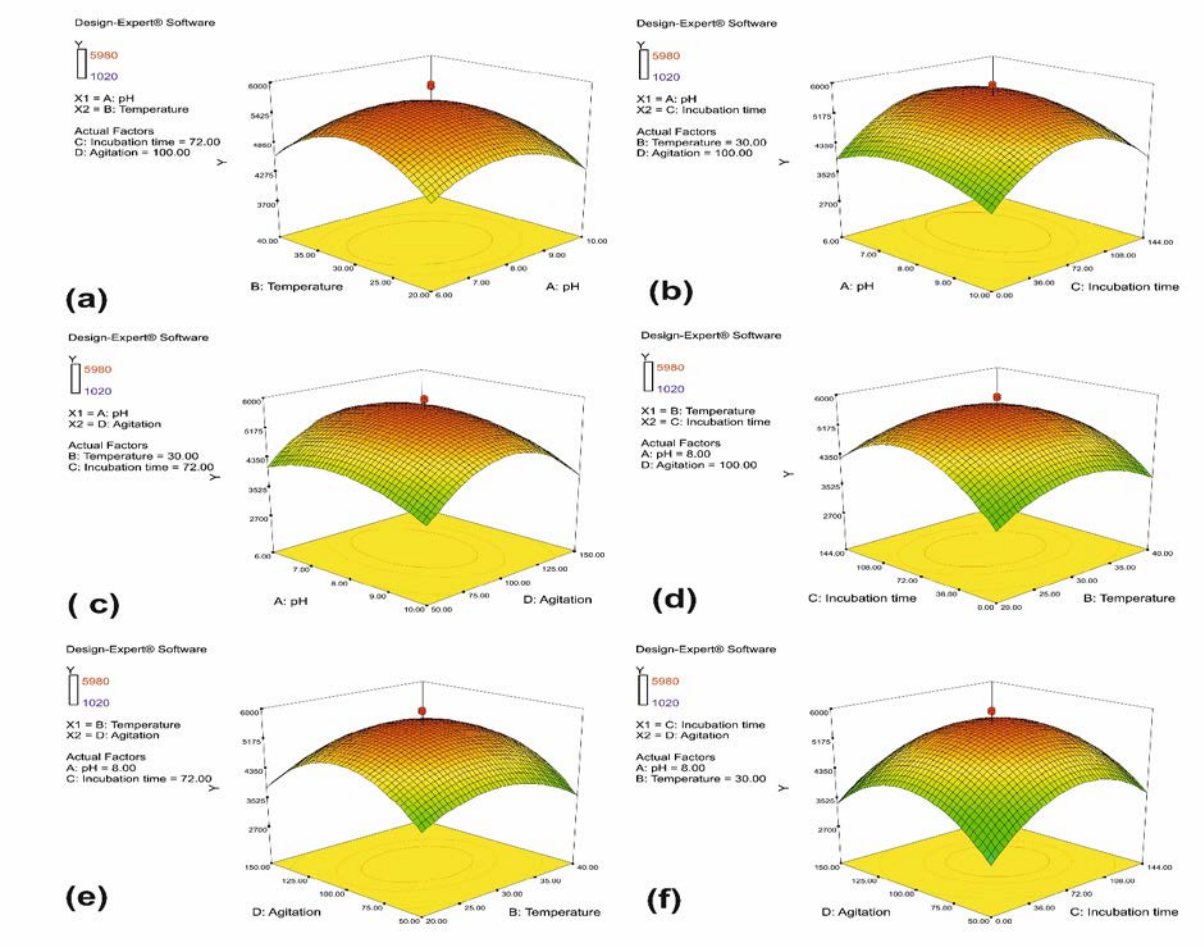

Figure 2. Three dimensional graphs showing the effect of pH (X_1), Temperature (X_2), Agitation (X_3) and Incubation time(X_4) on bacteriocin production

Table 3. ANOVA Table and regression analysis for selected model

Source	Sum of Squares	Df	Mean Square	F Value	p-valueProb > F
Model	71002762	14	5071626	73.8652	< 0.0001
X_1	810337.5	1	810337.5	11.80208	0.0037
X_2	61004.17	1	61004.17	0.888489	0.3608
X_3	1122338	1	1122338	16.34618	0.0011
X_4	71504.17	1	71504.17	1.041415	0.3237
X_1X_2	68906.25	1	68906.25	1.003578	0.3323
X_1X_3	82656.25	1	82656.25	1.203839	0.2899
X_1X_4	2256.25	1	2256.25	0.032861	0.8586
X_2X_3	387506.3	1	387506.3	5.643797	0.0313
X_2X_4	58806.25	1	58806.25	0.856478	0.3694
X_3X_4	294306.3	1	294306.3	4.286395	0.0561
X_1^2	8032150	1	8032150	116.9835	< 0.0001
X_2^2	14116300	1	14116300	205.5955	< 0.0001
X_3^2	33408936	1	33408936	486.5812	< 0.0001
X_4^2	36742357	1	36742357	535.1305	< 0.0001
Residual	1029908	15	68660.56		
Lack of Fit	495975	10	49597.5	0.464454	0.8586
Pure Error	533933.3	5	106786.7		
Cor Total	72032670	29			
Std. Dev.	262.0316		R-Squared		0.985702
Mean	2831		Adj R-Squared		0.972358
C.V. %	9.255796		Pred R-Squared		0.949666
PRESS	3625680		Adeq Precision		26.16025

Significant *$P \leq 0.05$

3.6. Purification and Characterization of Bacteriocin

After optimizing the cultural condition for enhanced production of bacteriocin, the concentration and purification were performed using ammonium sulphate precipitation, dialysis and column chromatography that was confirmed by the method of Lowry *et al.* (1951). The partially purified protein was analyzed for the molecular weight using SDS – PAGE that reveal 42 kDa when compared to that of standard protein marker.

3.7. FT-IR

The FTIR spectrum of bacteriocin from *Lactobacillus delbrueckii* subsp *lactis* is shown below. In bacteriocin treated cells shift in absorbance in low frequency at 3227.4, 2232.1 and 1871.8 cm^{-1} was observed. The shift in absorbance band in the region of 4000-3200 cm^{-1} indicated adsorption of water molecule. In addition, deformation in 2300 -2290 shows -C≡N→O changes take place. There was a shift from 1580 – 1490 to 2250-2670 that indicates the change of NH^{+}. At 1410 – 1260 the peaks were changed, indicating the disappearance of OH group. Similar results were reported by many researchers (Ravi Sankar *et al*., 2012)

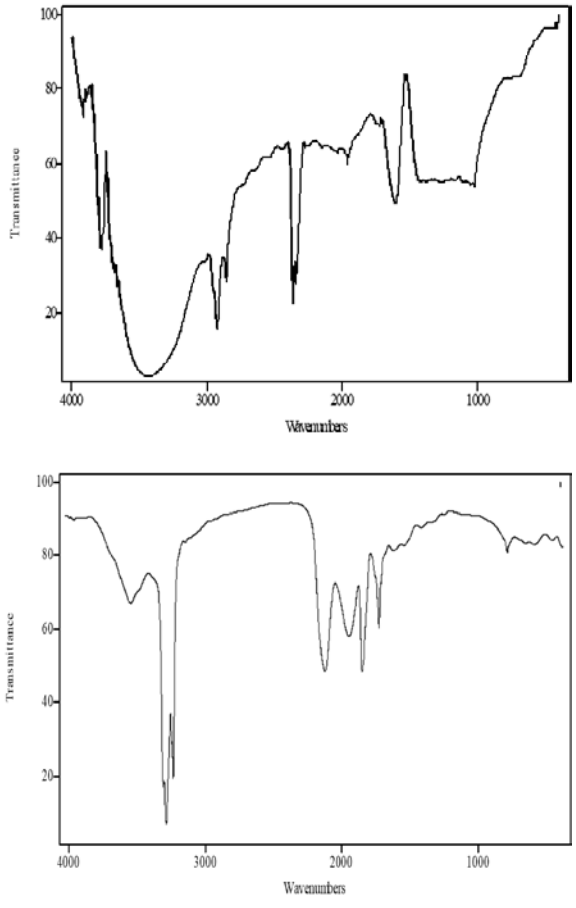

Figure 3. FTIR spectrum

4. Conclusion

Statistical designs (RSM using central composite design) were useful in the identification and optimization of important cultural conditions for bacteriocin production by the isolate from yogurt. Further characterization of the identified bacteriocin and technological evaluation of the isolate for the preparation of antibacterial compound are explored. The prospective application of these antimicrobial substances as bio-preservatives either as protective culture or as additives will be an alternative solution for the carcinogenic preservatives.

References

Graciela M, Vignolo M, de Kairus M, Aida AP, de Rui H and Oliver G. 1995. Influence of growth conditions on the production of lactocin 705, a bacteriocin produced by L. casei CRL 705. *J Appl Bacteriol*, **78**: 5 – 10.

Guinebault P, Colafranceschi C and Bianchetti G. 1990. Determination of mephenesin in plasma by high performance liquid chromatography with fluorometric detection. *J Chromatogr*. **507**:221- 225.

Hammami R, Zouhir A, Lay CL, Hamida JB and Fliss I. 2010. BACTIBASE second release: a database and tool platform for bacteriocin characterization. *BMC Microbiol.,* **10**:22.

Jagannathan A, Muralidharan B and Gayathri V. 2015. A Novel method of optimized bacteriocin production from marine water and testing its efficiency as an anti-microbial agent, *Intern J Innovative Res Sci, Eng Technol.,* **4**: 12.

Klostermann K, Crispie F. Flynn J, Meaney W, Ross R and Paul Hill C. 2010. Efficacy of a teat dip containing the bacteriocin lacticin 3147 to eliminate Gram-positive pathogens associated with bovine mastitis. *J Dairy Res.,* **77**:231-238.

Larsen AG, Vogensen FK and Josephsen J. 1993. Antimicrobial activity of lactic acid bacteria isolate from sour doughs: purification and characterization of bavaricin A, a bacteriocin produced by *Lactobacillus bavaricus* MI401. *J Appl Bacteriol*., **75**:113–122.

Mandenius CF and Brundin A. 2008. Bioprocess Optimization Using Design-of-Experiments Methodology, *Biotechnol. Prog.* **24**:1191-1203.

Neha Gautam and Nivedita Sharma. 2009. Purification and characterization of bacteriocin produced by strain of *Lactobacillus brevis* MTCC 7539. *Indian J Biochem Biophys.,* **49**:337 – 341.

Pal V, Jamuna M, Jeevaratnam K. 2004. Isolation and characterization of Bacteriocin producing lactic acid bacteria from a south Indian special dosa (appam) batter. *JCulture Collections* **4**:53-60.

Paul Cotter D, Colin Hill and Paul Ross R.2005. Bacteriocins: developing innate immunity for food nature reviews, *Microbiology*. **3**:777.

Piard JC, Muriana PM, Desmazaud MJ and Klaenhammer TR. 1992. Purification and partial characterization of lacticin 481, a lanthionine-containing bacteriocin produced by *Lactococcus lactis* subsp. *lactis* CNRZ 481. *Appl Environ Microbiol.,* **58**:279–284.

Pingitore VE, Salvucci E, Sesma F and Nader-Macías ME. 2007. Different strategies for purification of antimicrobial peptides from Lactic Acid Bacteria (LAB). In: Méndez-Vilas A. (Ed.) Communicating Current Research and Educational Topics and Trends in Applied Microbiology, pp:557 – 569.

Rammelsberg M and Radler F. 1990. Antibacterial polypeptides of *Lactobacillus* species. *J Appl Bacteriol.,* **69**: 177-184.

Ravi Sankar N, Deepthi V, Priyanka P, Srinivas Reddy P, Rajanikanth, Kiran Kumar V and Indira M. 2012. Purification and characterization of Bacteriocin Produced by *Lactobacillus plantarum* isolated from cow milk. *Inter J Microbiol Res.*, **3** (2): 133-137.

Ray RC, Sharma P and Panda SH. 2009. Lactic acid production from cassava fibrous residue using *Lactobacillus plantarum* MTCC 1407. *J Environ Biol.,* **30**(5): 847-852.

Shaileshkumar D, Sawale and Lele SS. 2009. Increased dextransucrase production by response surface methodology from *Leuconostoc* species; isolated from fermented *Idli* batter., *Global J Biotechnol Biochem.*, **4** (2): 160-167.

Siew KS, Yee CF and Sulaiman MR. 2013. Optimization of bacteriocin production by *Lactobacillus plantarum* using response surface methodology. Proceedings of the ICNP 2013 *The Open Conference Proceedings J.,* **4**: 81-82.

Ugbe Thomas A. Akpan, Stephen S. Umondak, Uduakobong. J. Udoeka, Ifreke J. Ofem, and Ajah O. 2016. Response surface methodology and its improvement in the yield of pineapple fruit drinks., *Inter J Sci Eng Res.,* **7**:541-553.

Vidhyalakshmi R, Valli NC, Narendrakumar G and Sunkar S. 2016. *Bacillus circulans* exopolysaccharide: Production, characterization and bioactivities, *Int J Biol Macromol.* **87**:405-14.

Zhao R, Duan G, Yang T, Niu S and Wang Y. 2015. Purification, characterization and antibacterial mechanism of Bacteriocin from *Lactobacillus acidophilus* XH1. *Tropical J Pharmaceutical Res.,* **14** (6): 989-995.

Zhou F, Zhao H, Bai F, Dziugan P, Liu Y and Zhang B. 2014. Purification and characterization of the Bacteriocin Produced by *Lactobacillus plantarum,* isolated from Chinese pickle. *Czech J Food Sci.,* **32**(5): 430–436.

JJBS

Volume 10, Number 4,December 2017
ISSN 1995-6673
Pages 229 - 233

Jordan Journal of Biological Sciences

Mentum Deformities in Chironomidae (Diptera, Insecta) as Indicator of Environmental Perturbation in Freshwater Habitats

Isara Thani[1] and Taeng On Prommi[2,*]

[1]Department of Biology, Faculty of Science Mahasarakham University;

[2]Department of Biological Science, Faculty of Liberal Arts and Science, Kasetsart University, Kamphaeng Saen Campus, Nakhon Pathom Province, 73140, Thailand

Received: July 16, 2017; Revised: August 22, 2017; Accepted: August 24, 2017

Abstract

Deformities in the mouthparts of Chironomidae larvae, particularly of the teeth on the mentum, have been proposed as a bioindicator of sediment quality and environmental stress. The Chironomidae larvae were collected in the six-ditch canalization in Kasetsart University, Kamphaeng Saen Campus, Nakhon Pathom Province over a period of six months between October 2016 to March 2017. Three replicates of sampling by aquatic D-frame dip net were used at sampling sites. A total of 1,868 Chironomidae larvae, representing 2 subfamilies, Chironominae and Tanypodinae, were screened for mentum deformities. The observation under the stereomicroscope showed the typical mentum teeth deformity in Chironomidae larvae with various degrees of worn, such as median teeth with moderately worn, substantial worn, median and lateral teeth folked. The percentage of deformities was higher in the ditch canalization received wastewater from dormitory and household than other sites. Data of water quality and chironomids larvae were analyzed with Principal Component Analysis (PCA). Strong correlations were found between Chironomidae larvae and the water quality parameters of orthophosphate (PO_4^{3-}), ammonia-nitrogen (NH_3-N), nitrate-nitrogen (NO_3-N), dissolved oxygen (DO), pH and water temperature.

Key words*:* Chironomidae, Mentum deformities, Ditch canalization**,** Water quality.

1. Introduction

Freshwater bodies in developing countries are subjected to degradation, mainly due to domestic as well as industrial wastes. This will in turn have a serious impact on aquatic organisms. One way of monitoring the health of aquatic ecosystems is through critical observation of benthic macroinvertebrates, especially the chironomids (Cranston, 2007). Because of their ubiquitous distribution, sensitivity to various pollutants and relatively short life cycle, chironomids are an ideal candidate for ecotoxicological studies. The head capsule of chironomid larva is one of the most impacted structures in the body of the organism when the environment, in which it lives, is altered, and it is an indication of stress (Bisthoven and Gerhardt, 2003). Deformities of the head capsule in larval Chironomidae indicate sub-lethal effects of exposure to contaminants and are considered an early warning signal for environmental water quality deterioration (Bisthoven and Gerhardt, 2003). Several studies, especially in the temperate region, have examined the use of head capsules of different species of chironomid larvae in response to a variety of contaminants (Bisthoven and Gerhardt, 2003), including an increase in morphological deformities of antennae and other parts of chironomid larvae as a result of heavy metals elevation in surface water and sediments. Although Chironomidae larval deformities have been successfully used as a biomonitoring tool in other parts of the world, its potential as an indicator of pollution stress in Thai freshwater system is yet to be explored.

Effluent from the domestic and agricultural area consists of a complex mixture of chemicals, varying in composition over time. In the production processes, these plants generate both inorganic and organic wastes (major ions, organic solvents, nutrients etc.) mixed with water, which change the concentration of suspended solids, biological oxygen demand (BOD), conductivity, temperature, color and odor of the receiving water-bodies (Al-Shami *et al*., 2010a). The aim of the present study is to examine the head capsules of Chironomidae larvae for determine the health of freshwater habitats in Kasetsart University, Kamphaeng Campus which are received the effluent-impacted river from domestic and agricultural area.

2. Materials and Methods

2.1. Study Area

Six freshwater ditches (KU_KPS1, KU_KPS2, KU_KPS3, KU_KPS4, KU_KPS5, and KU_KPS6)

* Corresponding author. e-mail: faastop@ku.ac.th.

(Figure 1) were selected to sample water quality parameters and Chironomidae larvae.

2.2. Sampling

Sampling was carried out monthly over a period of 6 months during October 2016 to March 2017. Three replicates of sampling by aquatic D-frame dip net were used at sampling sites (Figure 1). Sample collected in the field were preserved in 95%ethanol. On each sampling occasion, measurements of physicochemical parameters in the field, such as pH, Water Temperature (WT), Dissolved Oxygen (DO), Total Dissolved Oxygen (TDS) and Electrical Conductivity (EC) were made in situ at three randomly selected locations at each sampling site. To analyze selected chemical parameters of water, three separate samples of water from each site were randomly collected using 500-ml plastic bottles. Each appropriately labeled bottle was thoroughly rinsed out with the river water immediately before collecting a s ample. All water samples were transported to the laboratory in an ice chest and kept at 4 °C until analyzed. The ammonium-nitrogen (NH_3-N), nitrate-nitrogen (NO_3-N), orthophosphate (PO_4^{3-}) and turbidity (TUB) were measured at appropriate wavelength using a spectrophotometer HACH 2000. Alkalinity was titration (APHA, 1992).

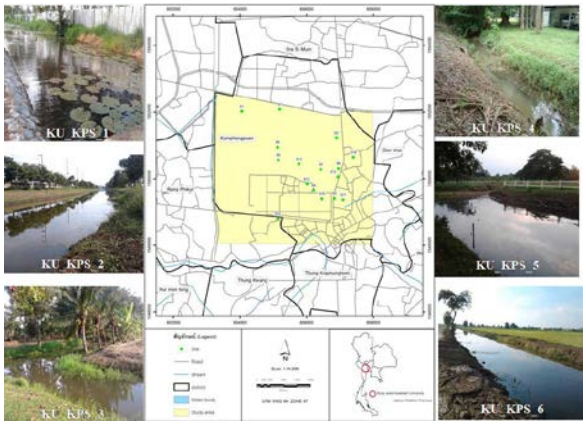

Figure 1. Six sampling sites at Kasetsart University, Kamphaeng Saen Campus, Nakhon Pathom Province

2.3. Chironomid Larval Sampling

Concurrent with physicochemical sampling, Chironomidae larvae were sampled monthly over a period of 6 months from October 2016 to March 2017 at the six sampling sites. A D-frame aquatic dip net was used for collecting the larval samples. Sampling was time-limited. Three minutes total sampling time for each ditch was split equally between different habitat types. Chironomidae larvae were preserved in 95% ethanol and transported to the laboratory for sorting, identification, abundance counts and deformity screening.

2.4. Chironomid Deformities Investigation

The Chironomidae larvae were investigated under light microscope (40X to 400X) for checking normal and deformed head capsule. Head capsules of each deformed Chironomidae larvae were removed from the six sampling sites. All chironomid head capsules were mounted for light microscopical identification following the methods described by Al-Shami *et al*. (2010b) and Gerhardt and Bisthoven (1995). The head capsules were mounted ventral side up a nd squeezed under a cover slip until maximum visibility of mentum was achieved. The mentum structure was systematically screened for morphological deformities (Dickman *et al*., 1992).

2.5. Data Analysis

One-way ANOVA in combination with Tukey's (HSD) *post hoc* test was used to test for physicochemical parameters among various sampling occasions and among the sampling sites using SPSS Version 20.0. The Principal Component Analysis (PCA) was used to evaluate relationships between chironomid deformities and environmental variables with PC-ORD version 5.10. Cluster analysis and non-metric multidimensional scaling (NMDS) were used to classify the sampling sites based on the chironomid deformities using Ward's linkage method with Euclidean distance measure using PC-ORD software.

3. Results and Discussion

3.1. Environmental Variables

The mean and standard errors of the environmental variables at each sampling site are indicated in Table 1. Mean water temperature was significantly lower at site KU_KPS1 compared with sites KU_KPS2 and KU_KPS4 with significantly higher values (p<0.05). Mean concentrations of DO and pH were significantly higher at sites KU_KPS2, KU_KPS4 and KU_KPS6 than at sites KU_KPS1, KU_KPS3 and KU_KPS5 (p<0.05). Mean TDS and EC were higher at sites KU_KPS3 and KU_KPS5 than other sites (p<0.05). Mean water turbidity was lower at the site KU_KPS6 than other sites (p<0.05). Mean alkalinity was higher at the site KU_KPS3 than other sites (p<0.05). Mean nitrate-nitrogen and orthophosphate were higher at the site KU_KPS1 than other sites, whereas mean ammonia-nitrogen was higher at the site KU_KPS6 than other sites (p<0.05). The result suggests that the sites KU_KPS2, KU_KPS4 and KU_KPS6 were relatively free of either dormitory and household wastes compared with the sites KU_KPS1, KU_KPS3 and KU_KPS5.

Table 1. Environmental factors measured at six sampling sites of ditch canalization (October 2016 to March 2017)

Sites/parameter	KU_KPS1	KU_KPS2	KU_KPS3	KU_KPS4	KU_KPS5	KU_KPS6
WT (°C)	26.22±1.24^{a}	31.36±2.40^{c}	27.99±2.13^{ab}	30.74±1.95^{c}	27.56±1.84^{ab}	29.82±1.84^{bc}
DO (mg/L)	1.99±1.49^{a}	7.95±0.67^{b}	2.23±1.36^{a}	7.75±0.34^{b}	3.10±2.22^{a}	8.69±0.49^{b}
pH	7.44±0.24^{a}	8.88±0.16^{b}	7.58±0.07^{a}	8.75±0.19^{b}	7.53±0.23^{a}	8.91±0.43^{b}
TDS (mg/L)	121.70±23.16^{a}	98.04±3.82^{a}	630.67±102.35^{c}	98.58±8.17^{a}	264.25±75.22^{b}	99.52±9.29^{a}
EC (µS/cm)	243.79±45.93^{a}	195.76±7.97^{a}	1263.08±204.90^{c}	199.25±14.24^{a}	527.17±148.53^{b}	198.72±18.82^{a}
TUB (NTU)	36.33±3.23^{c}	27.92±8.43^{bc}	20.08±9.56^{b}	20.75±9.96^{b}	29.67±4.75^{c}	11.25±3.62^{a}
ALK (mg/L)	80.67±8.24^{ab}	79.33±5.61^{a}	271.33±53.82^{c}	78.00±8.78^{a}	108.17±13.76^{b}	78.92±9.28^{a}
NO_3-N (mg/L)	2.05±1.05^{b}	1.10±0.39^{a}	1.05±0.43^{a}	1.25±0.43^{a}	1.18±0.42^{a}	1.43±0.67^{ab}
PO_4^{3-} (mg/L)	0.65±0.20^{b}	0.26±0.12^{a}	0.49±0.32^{ab}	0.37±0.10^{ab}	0.52±0.25^{ab}	0.35±0.39^{a}
NH_3-N (mg/L)	0.57±0.27^{ab}	0.38±0.07^{a}	0.44±0.12^{a}	0.46±0.20^{a}	0.43±0.11^{a}	0.72±0.26^{b}

3.2. Deformity in Chironomidae Larvae

A total of 1868 chironomid larvae belonging to the subfamily Chironominae and Tanypodinae were analyzed for incidence of deformity. The presence of relatively high levels of organic materials at station KU_KPS1 gives credence to the fact that the sediments as well as the water chemistry were severally altered by the effluent. The domestic effluent-impacted site recorded a high percentage (22.85%) of deformed Chironomidae larvae when compared to the other five sites (Table 2). Various types of deformities were encountered in the present study ranging from normal median teeth, normal–moderately worn, worn and folked (Figure 2).

Table 2. The number of normal and deformed mouth parts of Chironominae and Tanypodinae head capsules at each site

Sites	Chironominae					Tanypodinae					Total individual				
	Normal	Abnormal	Total	% Normal	% Abnormal	Normal	Abnormal	Total	% Normal	% Abnormal	Normal	Abnormal	Total	% Normal	% Abnormal
KU_KPS1	204	60	264	77.27	22.73	2	1	3	66.67	33.33	206	61	267	77.15	22.85
KU_KPS2	155	19	174	89.08	10.92	45	14	59	76.27	23.73	200	33	233	85.84	14.16
KU_KPS3	98	26	124	79.03	20.97	9	1	10	90.00	10.00	107	27	134	79.85	20.15
KU_KPS4	183	15	198	92.42	7.58	92	6	98	93.88	6.12	275	21	296	92.91	7.09
KU_KPS5	141	10	151	93.38	6.62	5	1	6	83.33	16.67	146	11	157	92.99	7.01
KU_KPS6	656	65	721	90.98	9.02	56	4	60	93.33	6.67	712	69	781	91.17	8.83
Total	1482	195	163			209	27	236			1646	222	1868		

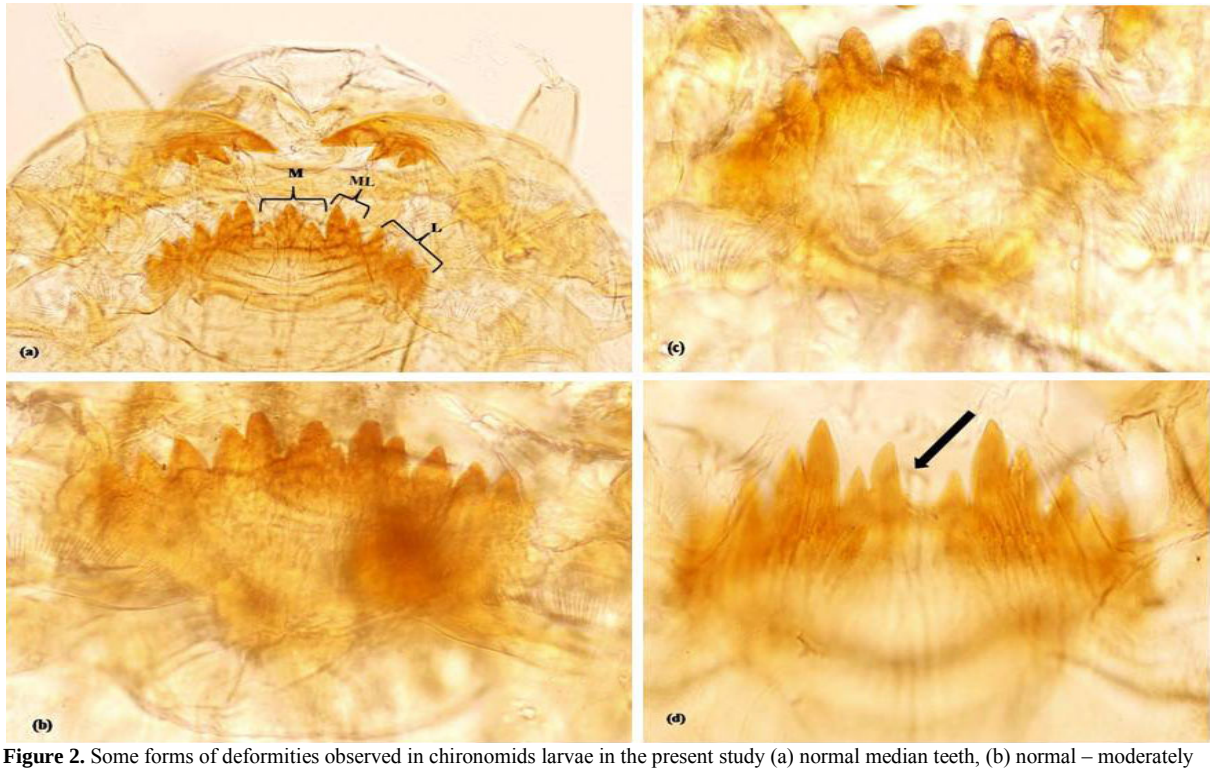

Figure 2. Some forms of deformities observed in chironomids larvae in the present study (a) normal median teeth, (b) normal – moderately worn, (c) worn, and (D) folked. (M=median teeth, ML=median lateral, L=lateral)

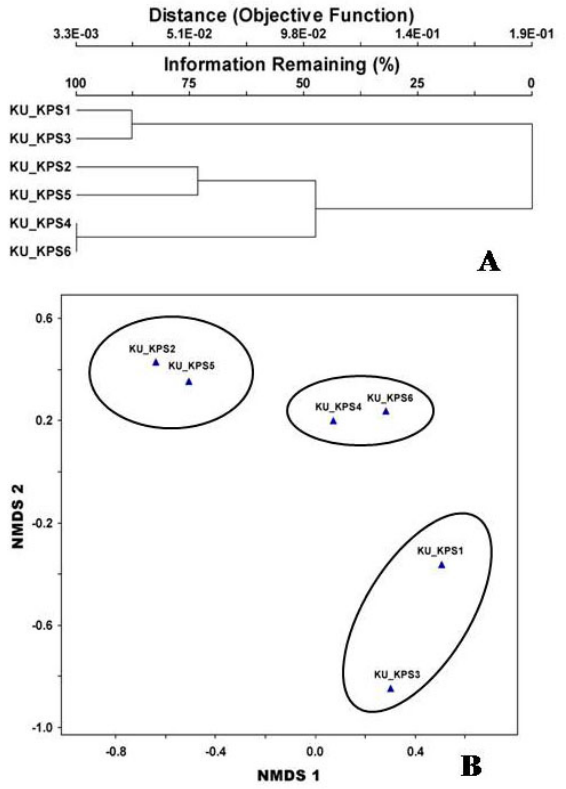

Figure 3. Cluster analysis (A) and Non-metric Multidimensional (NMDS) Scaling (B) of sampling sites based on deformed Chironomidae larvae

Cluster analysis based on Bray-Curtis similarity values showed that sites KU_KPS4 and KU_KPS6 showing high similarity followed by sites KU_KP1 and KU_KPS3, sites KU_KPS2 and KU-KPS6, respectively (Figure 3).

In order to determine the relationship between the physicochemical parameters with the percentage chironomid deformity, a principal component analysis (PCA) was performed. PCA first and second axes were significant and accounted for 75 and 24.9% of the total variance explained, respectively. According to PCA ordination (Figure 4), percentage chironomid deformity was positively correlated with the NO_3-N, PO_4^{3-} and water turbidity. Major nutrient concentration (i.e., PO_4^{3-} and NO_3-N) in an ambient aquatic environment was the primary factor explaining variation in benthic assemblages (Ponader *et al*., 2007). In the present study, PCA showed that proximate determinants, such as water turbidity, PO_4^{3-} and NO_3-N, were vital in explaining the variation in chironomid deformity. Considerable morphological abnormalities were revealed in the mouthparts with various degrees of worn such as, median teeth with moderately worn, substantial worn, median and lateral teeth folked. The deformities reported here are similar to some other chironomid species in polluted waters (Bisthoven and Gerhardt, 2003). These abnormalities represent sub-lethal effects and can be considered as early warning signals of environmental degradation by chemical contaminants (Warwick, 1990). Similarly, Al-Shami *et al.* (2010b) reported high percentage of chironomid deformity in rivers contaminated with industrial discharges from garment and rubber factories. Head capsule deformities can be used as biomarkers for pollution stress.

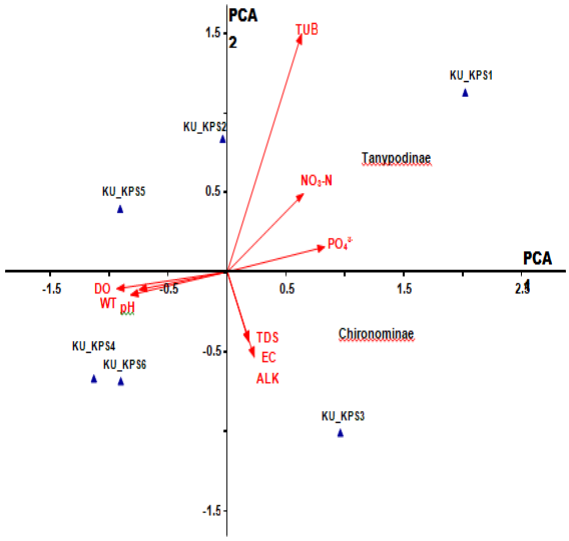

Figure 4. PCA ordination plot based on deformed Chironomidae larvae and environmental variables and sampling sites

4. Conclusions

The present study provides baseline data on s ome physicochemical conditions prevailing in the investigated pond with respect to the site receiving effluent from the domestic and agricultural activities, and could serve as a reference for future investigations. In addition, there was positive influence of domestic effluent discharge in the deformity of Chironomidae larvae inhabiting ponds. Therefore, chironomidae larvae appear to be useful taxa in deformity screening method owing to its ubiquitous distribution and relative abundance in tropical freshwater bodies. Their inclusion in monitoring, especially in Tropical Asian freshwater habitats, will add inferring power to assess ecosystem health and contaminated sediments.

Acknowledgement

The present research work was supported by the Faculty of Liberal Arts and Science, Kamphaeng Saen Campus, Kasetsart University year 2016.

References

Al-Shami SA, Rawi CSM, Ahmad AH and Nor SAM. 2010a. Distribution of Chironomidae (Insecta: Diptera) in polluted rivers of the Juru River Basin, Penang, Malaysia. *J Environ Sci.*, **22**: 1718-1727.

Al-Shami SA, Rawi CSM, Azizah S, Nor SAM, Ahmad AH and Ali A. 2010b. Morphological Deformities in Chironomus spp. (Diptera: Chironomidae) Larvae as a Tool for Impact Assessment of Anthropogenic and Environmental Stresses on Three Rivers in the Juru River System, Penang, Malaysia. *Environ Entomol.*, **39(1)**: 210-222.

American Public Health Association (APHA). 1992. **Standard Methods for the Examination of Water and Wastewater**, *18th edition*. American Public Health Association. Washington, D.C.

Bisthoven L. and Gerhard A. 2003. Chironomidae (Diptera, Nematocera) fauna in three small streams of Skania, Sweden. *Environ Monit Assess.*, **83**: 89-102.

Cranston PS. 2007. The Chironomidae larvae associated with the tsunami-impacted waterbodies of the coastal plain of southwestern Thailand. *Raffles Bull Zool*., **55**: 231-244.

Dickman M, Brindle I. and Benson M. 1992. Evidence of teratogens in sediments of the Niagara river watershed as reflected by chironomid (Diptera: Chironomidae) deformities. *J Great Lakes Res.*, **18**: 467-480.

Gerhardt A. and Bisthoven L. 1995. Behavioural, developmental and morphological responses of *Chironomus gr. thummi* larvae (Diptera) to aquatic pollution. *J Aquat Ecosyst Health*, **4**: 205-214.

Ponader KC, Charles DF and Belton TJ. 2007. Diatom-based TP and TN inference models and indices for monitoring nutrient enrichment of New Jersey streams. *Ecol Indic.*, **7**: 79–93.

Warwick WF. 1990. Morphological deformities in Chironomidae (Diptera) larvae from Lac St. Louis and Laprairie basins of the St. Lawrence River. *J Great Lakes Res.*, **16**: 185-208.

JJBS
Jordan Journal of Biological Sciences

Volume 10, Number 4,December 2017
ISSN 1995-6673
Pages 235 - 237

Morphological Cranial Study and Habitat Preference of *Mus macedonicus* (Petrov & Ruzic, 1983) (Mammalia: Rodentia) in Lebanon

Mounir R. Abi-Said* and Sarah S. Karam

Biodiversity Management/ Mammalogist, Department of Life and Earth Sciences,
Faculty of Science II, Lebanese University .P.O. Box 90656 Jdeideh, Fanar – Lebanon

Received: July 4, 2017; Revised: August 17, 2017; Accepted: August 23, 2017

Abstract

Fifteen Sherman live traps were set at 20 different locations along Ibrahim River in Mount Lebanon. The 1500 trap nights resulted in trapping 15 *Mus macedonicus.* Morphological and cranial measurements were similar to those recorded in other countries except for the length of the head, body and tail that were moderately larger in the Lebanese specimens. Most animals were caught at an altitude above 800m asl. 53% were caught in the agriculture zone very close to cultivated fields, while the rest were recovered in Mediterranean landscape of tall grasses and bushes. Hence, further molecular assessment is recommended for the taxonomic status of Lebanese species.

Keywords: Macedonian mouse, *Mus macedonicus*, Rodentia, Ibrahim River, Lebanon.

1. Introduction

The Macedonian mouse *Mus macedonicus* (Petrov & Ruzic 1983) occurs in the Eastern Mediterranean basin from Yugoslavia to the Near East and from the Balkans to Cyprus (Harrison and Bates 1991; Boursot *et al*. 1993). It was reported from Syria, Jordan and Arabia (Bates and Harrison 1989; Macholan *et al*. 2007). In Israel, Auffray *et al*. (1990a) described *Mus spretoides* that was later referred to as *Mus macedonicus* (Auffray *et al*. 1990b). The *Mus macedonicus* are confined to Mediterranean environments where they live amongst bushes, long grass, cultivated lands or on stream banks, but was never found in human landscape (Auffery *et al*., 1990a; Bates and Harrison, 1989)

In Lebanon, Macholan *et al*. (2007) reported the existence of *Mus macedonicus* only from Byblos and assumed that this species could reach the north-eastern part of Lebanon. In a study on owl pellets (Abi-Said *et al*., 2014), it was speculated that this species may be found in the owl pellets due to the close cranial similarity to *Mus musculus*.

The present study discusses the morphology and the cranial measurement for *Mus macedonicus* based on specimens collected from Lebanon, while comparing them with other populations.

2. Material and Methods

The present study was conducted between May 2016 and May 2017 a long Ibrahim River in Mount Lebanon. Fifteen Sherman live traps baited with peanut butter and grain feed mix were used with a total of 1,500 trap nights. Traps were set at 20 different locations and altitudes along the river, representing various vegetation zones namely Thermo-Mediterranean, EuMediterranean, Supra-Mediterranean and Agricultural Zone. Ten stations were fixed beside the river bank and 10 stations at 500m away. Morphometric measurements of the trapped individuals were recorded (Table 1), photos were taken, and skinned animals were kept at the Lebanese University Natural History Museum Faculty of Sciences II, Fanar-Lebanon.

Six external measurements (HB, T, HL, HW, E, and HF) along with twelve cranial measurements (GTL, CBL, ZB, BB, IC, PC, MXC, MDC, M, RL, BU and ZI) were recorded. Measurements were taken in a straight line using a digital caliper (close to 0.01mm).

3. Results and Discussion

3.1. Habitat Preference

Fifteen *Mus macedonicus* were trapped and examined during the entire study period. A single mouse was trapped

* Corresponding author. e-mail: mabisaid9@gmail.com.

at an altitude of 61m above sea level (asl), while the rest were caught at an altitude above 800m asl. Out of the overall trapped individuals, most (53%) were caught in the agriculture zone very close to cultivated fields, while the rest were recovered in Mediterranean landscape of tall grasses and bushes (20% in Thermo-Mediterranean zone, 20% in Supra-Mediterranean zone and 7% in Meso-Mediterranean zone). No animals were trapped in urban areas. The former two habitats, were in the proximity of a water source either in the form of a river or small streams. Similarly, in Jordan, *M. macedonicus* was collected in both cultivated and semi-wild habitats covered with bushes and long grass (Bates and Harrison, 1989). In the Balkans and Anatolia, it was trapped more often in open areas with tall dense vegetation associated with arable lands and streams and less frequently in cultivated fields (Krystufek and Vohralik, 2006); likewise in Israel, this species inhabited Mediterranean ecosystems (Auffary *et al*., 1990a).

3.2. Morphological and Cranial Measurements

Mus. macedonicus differs from *Mus. musculus* (house mouse) in its pelage color (Figure 1). The dorsal coat fur is characterized by a brownish color, which changes into creamy color on the abdomen rather than the greyish fur that is observed on the body of the house mouse.

There were a difference in the mean measurements between males and females but these measurements remained within the range. This could be referred to the small sample size of females trapped. The tail of *M. macedonicus* is noticed to be shorter than the head and body length. The ratio of head and body length to tail was 1.28 on average (Table 1). This has been found to be consistent with other reported specimens (Auffray *et al*., 1990b; Krystufek and Vohralik, 2009; Aulgnier *et al*., 2009; Harrison and Bates, 1991; Qumsiyeh, 1996). The average ear length (11.40mm) was similar to those reported by Harrison and Bates (1991), Krystufek and Vohralik (2009) and Aulagnier *et al*. (2009). However, the length of the head and body and tail in the Lebanese specimen (Table 1) was found to some extent larger than those reported by Harrison and Bates (1991) from Syria, Jordan and Israel; the reason behind this difference may be explained by the rich habitat and the moderate climate that characterizes the Lebanese landscape.

Figure 1. A male *Mus macedonicus* trapped in the Agricultural Zone along Ibrahim River

The morphometric difference between *M. macedonicus* and *M. musculus* in tail length, tail to body and head length was consistent with Auffray *et al*. (1990a). Additionally, it was observed that the ears of *M. macedonicus* are shorter than those reported by Lewis et al. (1967) and Harrison and Bates (1991) for *M. musculus*.

Table 1. Body measurements of *Mus macedonicus* (N=15) (weight in g, length in mm)

	Male (N=13)			Female (N=2)		
	Mean	SD	Range	Mean	SD	Range
Body Weight	12.18	1.98	10.00 – 17.00	12.50	2.83	10.50 – 14.50
Head and Body (HB)	83.27	3.47	77.36 – 89.16	85.30	7.81	79.78 – 90.82
Tail Length (T)	65.37	3.86	57.66 – 70.35	68.17	3.53	65.68 – 70.67
Head length (HL)	24.08	0.88	22.81 – 25.78	24.85	0.07	22.85 – 24.90
Head width (HW)	11.69	0.46	11.01 – 12.59	11.86	0.52	11.49 – 12.23
Ear (E)	11.40	1.01	9.29 – 13.00	11.73	2.43	10.02 – 13.45
Hind Foot (HF)	17.46	0.82	15.26 – 18.85	18.72	0.04	18.69 – 18.75
Head & Body/Tail	1.28	0.08	1.16 – 1.42	1.27	0.28	1.25 – 1.29

The cranial and teeth (Figure 2) measurements were identical with those reported by Krystufek and Vohralik (2009) and Harrison and Bates (1991). The Zygomatic Index (ZI) (width of malar process/width of the antero-lateral part of the zygomatic arch) which is considered among the determination keys for *Mus macedonicus,* is reported to be not less than 0.52 (Orsini *et al*., 1983; Auffray *et al*., 1990; Harrison and Bates, 1991; Macholan, 1996; Krystufek and Vohralik, 2009; Qumsiyeh, 1996). In these specimens the ZI was within the reported ranges with a mean of 0.81 (range 0.67 – 0.91) for males and 0.84 (0.79 – 0.89) for females (Table 2).

Table 2. Cranial and dental measurements (mm) of *Mus macedonicus* (N=15)

	Male (N=13)			Female (N=2)		
	Mean	SD	Range	Mean	SD	Range
GTL	21.96	0.65	20.66 – 22.59	22.01	0.06	21.97 – 22.06
CBL	20.81	0.82	19.31 – 21.59	20.54	0.42	20.25 – 20.84
ZB	11.01	0.47	10.52 – 11.75	11.13	0.40	10.85 – 11.42
BB	9.78	0.30	9.40 –10.17	10.01	0.35	9.77 – 10.26
IC	3.50	0.06	3.40 – 3.62	3.60	0.64	3.56 – 3.65
PC	6.53	0.31	6.15 – 6.89	6.38	0.37	6.12 – 6.65
MXC	3.46	0.15	3.27 – 3.73	3.38	0.08	3.32 – 3.44
MDC	3.12	0.18	2.80 – 3.40	2.93	0.28	2.74 – 3.13
M	11.30	0.49	10.34 – 11.70	11.08	0.64	10.63 – 11.53
RL	10.64	0.62	9.82 – 11.78	11.19	0.18	11.07 – 11.32
BU	3.56	0.17	3.23 – 3.77	3.66	0.07	3.61 – 3.71
ZI	0.81	0.09	0.67 – 0.91	0.84	0.07	0.79 – 0.89

(GTL= greatest length of the skull, CBL= condylobasal length; ZB= zygomatic breadth; BB= breadth of brain case; IC= interorbital constriction; PC= postorbital constriction; MXC= maxillary cheekteeth; MDC= mandibular cheekteeth; M= mandible length; RL= length of rostrum; BU= bullae; ZI= zygomatic index)

Figure 2. *Mus macedonicus*, dorsal (a), ventral (b) and lateral (c) view of the cranium, and a view of the mandible (d)

4. Conclusion

The habitat preference of this species minimizes its encounter with the house mouse. However, due to the expanding urbanization which is in favour of the house mouse, both species might overlap resulting in house mouse domination and exclusion of the Macedonian from its habitat. In another note, Macholan *et al*. (2007) raised an important question on the genetic characteristic of this species in Lebanon. Hence, molecular assessment of the *Mus macedonicus* population in Lebanon defining its taxonomic status is unambiguously essential. Additionally, the new record of this species along Ibrahim River (0 m asl – 1100 m asl) urges more field studies for assessing its presence in various habitats. It is worth mentioning that intensive human disturbance and habitat destruction have been initiated near Ibrahim River, as a r esult of dam construction, consequently leading to a threat towards many species.

Acknowledgments

The present work was possible through the Lebanese University Research Fund. We would like to thank Eng. Diana Marrouche Abi-Said for reviewing this work and Mr. Mouhammad ElZein and Mouhammad Al-Masri for their technical assistance.

References

Abi-Said MR, Shehab A, and Amr Z. 2014. Diet of the Barn Owl, *Tyto alba*, from Chaddra-Akkar, Northern Lebanon. *Jordan J Biol Sci.,* **7**(2): 109-112.

Auffray JC, Tchernov E, Bonhomme F, Heth G, Simson S and Nevo E. 1990a. Presence and ecological distribution of *Mus "spretoides" Mus musculus domesticus* in Israel: Circum-Mediterranean vicariance in the genus *Mus*. *Zeitschrift. Säugetierkunde*. **55**: 1-10.

Auffray JC, Marshall JT, Thaler L and Bonhomme F. 1990b. Focus on the nomenclature of European species of *Mus*. *Mouse Genome*, **88**: 7-8.

Aulagnier S, Haffner P, Mitchell-Jones AJ, Moutou F and Zima J. 2009. **Mammals of Europe, North Africa and the Middle East**. A&C Black Publisher Ltd. London, UK. Pp 238.

Bates PJJ and Harrison DL, 1989. New records of small mammals from Jordan. *Bonner Zool. Beitr*. **40** (3): 223-226.

Boursot P, Auffray JC, Britton-Davidian J and Bonhomme F. 1993. The evolution of House mouse. *Annual Rev Ecol Systematics*. **24**, 119-152.

Harison DL and Bates PJ. 1991. **The Mammals of Arabia**. 2nd edition. Harrison Zoological Museum, Sevenoaks, Kent, UK. Pp 250-252

Lewis RE, Lewis JH and Atallah SI. 1967. A review of Lebanese mammals. Lagomorpha and Rodentia. *J Zool.,* **153**: 45-70.

Krystufek B. and Vohralik V. 2009. **Mammals of Turkey and Cyprus. Rodentia II: Cricetinae, Muridae, Spalacidae, Calomyscidae, Capromyidae, Hystricidae, Castoridae**. Knjiznica Annales Majora. Slovenia. Pp 146-169

Macholán M. 1996. Key to European house mouse (*Mus*). *Folia Zool*. **45**: 209-217

Macholán M, Vyskocilova M, Bonhomme F, Krystufek B, Orth A and Vohralik V. 2007. Genetic variation and phylogeography of free-living mouse species (genus Mus) in the Balkans and the Middle East. . *Mol Ecol*., **16**: 4774–4788.

Orsini P, Bonhomme F, Britton-Davidian J, Croset H, Gerasimov S and Thaler L. 1983. Le complexe d'espèces du genre *Mus* en Europe centrale et orientale. II. Critères d'identification, repartition et caractéristiques écologiques. *Z. Säugetierkunde*. **48**: 86-95.

Qumsiyeh, MB. 1996. **Mammals of the Holy Land**. Texas Tech University Press, USA. Pp 291-294.

JJBS

Volume 10, Number 4,December 2017
ISSN 1995-6673
Pages 239 - 249

Jordan Journal of Biological Sciences

Lung Cancer Detection Using Multi-Layer Neural Networks with Independent Component Analysis: A Comparative Study of Training Algorithms

Abdelwadood M. Mesleh*

Computer Engineering Department, Faculty of Engineering Technology, Al-Balqa Applied University, Jordan,

Received: May 14, 2017; Revised: June 15, 2017; Accepted: August 10, 2017

Abstract

The present paper presents a Computer-Aided Design (CAD) system that detects lung cancer. Lung cancer detection uses Multi-Layer (ML), Neural Networks (NNs) and Independent Component Analysis (ICA). ICA aims to speed the detection by decreasing the number of features. The ML NNs classifier is trained by Gradient descent algorithm (traingd), Gradient descent with momentum (traingdm), Gradient descent with variable learning rate and momentum (traingdx), Resilient back propagation (trainrp), Fletcher-Reeves Update (traincgf), Polak and Ribiere (traincgp), Powell and Beale Restarts (traincgb), Scaled Conjugate Gradient Algorithm (trainscg), Quasi Newton BFGS (trainbfg), One step secant algorithm (trainoss) and Levenberg–Marquardt (trainlm). The detection algorithm is tuned to determine the existence of cancer in real Computerized Tomography (CT) images and it is validated, trained & tested using 460 CT images, 350 of them belong to lung cancer patients in Jordanian hospitals. The presence of cancer in these images is labeled by experts. The present paper investigates the performance of the ML NN classifier trained by these training algorithms with ICA feature extraction. Results reveal the robustness of the detection algorithm for real CT images. Among the 11 training algorithms, *Levenberg–Marquardt* achieves a classification accuracy of 100% with least number of ICA features.

Keywords: Neural networks, Independent component analysis, Lung cancer detection, Multi-layer neural networks, Training algorithms; Computer aided design, Lung cancer in Jordan.

1. Introduction

Cancer is a disease with an abnormally cell growth, its different types are classified by the type of the initially affected cell, it harms humans when damaged cells divide uncontrollably and it generally forms tumors (Argiris, 2012; Kennedy *et al*., 2000). Tumors grow and interfere with human systems and release hormones that alter body functions. Lung cancer starts in the cells lining the bronchi, bronchioles or alveoli, it starts as areas of precancerous changes that makes the human body cells to grow abnormally, the cell abnormal growth may look a bit abnormal if seen under a microscope, however, it does not form a tumor at this stage and does not cause any symptom. Over time, the abnormal cells progress to true cancer as more genes are changed. Cancer may enable the abnormal cell growth to form a tumor that can be detected on imaging tests. In later stages, cancer cells may spread to other parts of the human body. Most lung cancer cases are not detected until causing symptoms. There are many common symptoms of lung cancer, such as coughing up blood, chest pain, weight loss and loss of appetite, shortness of breath and feeling weak. It is known that tumors (Argiris, 2012; Kennedy *et al*., 2000) are benign or malignant, benign tumors are less than 3 mm, and are curable cancer cases, malignant tumors are greater than 3 mm, and are uncontrollable.

Lung cancer (Miao *et al*., 2016; Howlader *et al*., 2017) is one of the main causes of cancer mortality in many countries, including the United States of America (USA), lung cancer causes more deaths than a combined of breast, prostate, and colorectal cancers, Based on the number of deaths in 2010-2014, lung cancer was the leading cause of death in USA and it was more common for middle and old people, in 2015, 27% of the American deaths were lung cancer patients, lung cancer can be successfully treated at early detected stages, because its symptoms are not noticed until it is at incurable phase, more than half of patients with lung cancer cannot survive more than a year of being diagnosed; moreover, its five-year survival rate is much lower than other cancers. Old attempts, such as chest X-ray that were used to monitor lung cancers cannot provide clinically satisfactory detection of lung cancer. Therefore, a more accurate prescreening method are required (Miao *et al*., 2016). CT imaging (Al Mohammad *et al*., 2017) is among the effective methods to detect lung cancer, as it is able to measure nodule sizes, track the growth of nodules,

* Corresponding author. e-mail: wadood@fet.edu.jo.

support the characterization of morphological lesion and visualize axial sections of chest. The main disadvantage of CT is its radiation that may increase the cause or development of cancer, as a result, it is recommended to use the least radiation dose that assures acceptable quality images. In 2017, the estimated number of new lung cancer cases (Howlader *et al*., 2017) will be 222,500 and the expected number of deaths will be 155,870.

In 2010, the number of cancer cases in Jordan (Tarawneh *et al*., 2010; Al-Sayaideh *et al*., 2012) has increased to 4921, lung cancer cases (males and females) were among the top five cancer cases 380 (7.8%); moreover, its cases were also among the top five cancer cases among Jordanian males 311 (13.3%) and it was a principal cause of death (30.2%) (Tarawneh *et al*., 2010; Al-Sayaideh *et al*., 2012). In 2010, colorectal, lung and Hodgkin lymphoma were the commonest cancer cases for Jordanian males and females, however, colorectal and lung were the most common cancer cases for Jordanian males (age 20-49) and it was the commonest for Jordanian males (age 50+) (Tarawneh *et al*., 2010; Al-Sayaideh *et al*., 2012). In 2010, it is clear that lung cancer was one of the types of cancer cases that most common in males than females, as it affected 311 (13.3%) Jordanian males and 68 (2.7%) Jordanian females (Tarawneh *et al*., 2010; Al-Sayaideh *et al*., 2012).

As mentioned before, it is very important to detect cancer in its early stage to determine the optimal treatment decisions, this treatment may strongly influence the survival opportunity, it is reported that only 15.9% of the lung cancer patients are diagnosed at early stage and their 5-year survival is 55.6% (Howlader *et al*., 2017).

CAD is one of the software technologies to assist radiologists to detect lung nodules efficiently, any CAD cancer detection system (Firmino *et al*., 2015) starts with a preprocessing phase, in which, it converts CT images to grayscale, filters noise if dealing with noisy CT images, converts the grayscale images to binary images using thresholding technique, applies some boundary tracing technique and morphological operation to get rid of unimportant areas of the CT images, and it may apply some smoothing algorithm. In the feature extraction phase, the CAD system minimizes the size of the processed data, and finally, in the classification phase, it classifies / detects lung cancer by implementing data mining or classification methods.

Despite the significant strides to treat cancer cases, lung cancer remains among the unsolved clinical cancer problems. It remains difficult to detect lung cancer in early stage (Argiris, 2012; Kennedy *et al*., 2000). Optimistically, early detection of lung cancer may maximize the treatment opportunity. It is useful to use an invasive biopsy to confirm the detection of lung tumors using imaging techniques, such as CT that are useful in cancer detection. CT is a technique (Herman, 2009; Mayo Clinic Staff, 2017) to better visualize cancer, unfortunately, CT detects lung cancer in late stages, where the chance of survival becomes low. Thus, there is a demand for sophisticated technologies that detect lung cancer in early stages.

The present paper presents a CAD system that detects lung cancer, determines the existence of cancer in CT images for Jordanian patients, provides a computer based second opinion to assist CT interpretation and uses ML NNs classifier with a ICA feature extraction technique (Guyon *et al*., 2006) to speed the detection process by minimizing the number of features. The present paper compares the performance of 11 training algorithm (Bishop, 1995): traingd, traingdm, traingdx, trainrp, traincgf, traincgp, traincgb, trainscg, trainbfg, trainoss and trainlm, and it fills the gap of investigating the performance of lung cancer detection using ML NNs classifier that is trained using 11 different training methods; moreover, it investigates the performance of these training algorithms with ICA feature extraction method in detecting lung cancer in real CT images. Moreover, the present paper is expected to finally promote an ML NN training algorithm that works best with ICA in detecting lung cancer in CT images.

The rest of the present paper is organized as follows: Section 2 presents some of the related previous work, Section 3 presents the related materials and methods, Section 4 presents the results and the discussion and, finally, the Conclusion is presented in Section 5.

2. Previous Work

In Tao *et al*. (2011), an effective screening method for lung cancer using a radial basis NNs is proposed. In Wu *et al*. (2011), many distinct tumor marker groups are combined using NNs to achieve a 92.8% accuracy in lung cancer detection. In Flores-Fernández *et al*. (2012), NNs and Principal Component Analysis (PCA) are used in lung cancer detection and achieved 90% accuracy by evaluating serum biomarkers levels in lung cancer patients. In Taher *et al*. (2012), lung cancer is diagnosed in early stages using Hopfield NNs and a Fuzzy C-Mean clustering algorithm. In (Abdulla and Shaharum, 2012), NNs classifier is used in detecting lung cancer and achieved 90% accuracy. In Sun *et al*. (2013), many machine learning methods used in diagnosing lung cancer in CT images and support vector machine classifier is recommended for this purpose. In Tariq *et al*. (2013), a neuro fuzzy classifier is proposed to detect lung nodules in CT images, and, lung nodules are classified based on properties, such as area, mean, standard deviation, energy, entropy, and eccentricity. In Chen and Suzuki (2013), virtual dual energy chest radiographs images are incorporated to develop an improved detection scheme for lung cancer using NNs; the sensitivity of the proposed detection scheme is substantially improved especially for subtle nodules. In Kuruvilla and Gunavathi (2014), a new proposed training algorithm is used with back propagation NNs, used some common statistical parameters, such as mean, standard deviation, etc. to detect lung cancer in CT images, and, achieved 93.3% accuracy. In Firmino *et al*. (2016), a detection and a diagnosis system for pulmonary nodules on CT images is proposed using watershed and histogram of oriented gradient techniques to recognize nodules, the diagnosis is based on the likelihood of malignancy. Moreover, the proposed systems deployed support vector machine and rule based classifiers. In Syed and Muhammad (2017), some effectiveness cancer detection algorithms for lung cancer, a survey of nodule detection methods, and, a range of feature extraction, classification, and segmentation algorithms are presented. Furthermore, a set of performance measures are also evaluated, so as to provide

as insight into the current advancements in CAD. In Shen *et al.* (2017), the classification of lung nodule malignancy suspiciousness using thoracic CT images is investigated; this investigation used multi-crop convolutional NNs (MC-CNN) in extracting nodule salient information. The proposed classification method achieved accurate classification which was potentially helpful in modeling nodule malignancy. In Tajbakhsh and Suzuki (2017), two dominant classes of end-to-end learning machines are Massive-Training Artificial NNs (MTANNs) and convolutional NNs (CNNs) are compared experimentally and theoretically in the detection of lung nodules and in the distinction between benign and malignant lung nodules in CT images. In addition, it is concluded that MTANNs works better than CNNs especially when dealing with small training datasets. In Manikandan and Bharathi (2017), a hybrid neuro- fuzzy system is proposed to detect lung cancer stages, the algorithm is designed based on the observed symptom values and a classification accuracy of 97.7% is achieved. In Froz *et al.* (2017), a lung nodule classification algorithm, using texture features from CT images, is proposed, the texture features are extracted using artificial crawlers, rose diagram, and, a hybrid model of the artificial crawlers and the rose diagram. In Dimililer *et al.* (2017), an image processing based detection technique for lung cancer is proposed and applied on CT images, these techniques include erosion, filtering, thresholding and feature extraction. Many other NNs classifiers (Ahmad, 2013; Babu *et al*., 2013) are used to detect other cancer cases, such as breast cancer. Moreover, ICA (Nguyen and Dang, 2015) is applied to separate the ribs and other parts in lung images to diagnose lung cancer at early phase resulting in 90% of cases that the ribs are completely and partly suppressed and in 85% of cases increases the nodule visibility.

3. Materials and Methods

3.1. Neural Networks (NNs)

NNs (Bishop, 1995; Haykin, 1999) are efficient processing systems that consist of many neurons. Neurons are highly interconnected processing elements that are connected with each other by links. Links are associated with weights that contain information of input signals. Information signals are used by neuronal networks to solve problems. Neurons have their own activation levels which are the function of the inputs the neurons receive. Gaussian, Linear and Sigmoid are examples of the commonly used activation functions. Learning in NNs is classified into supervised, unsupervised and reinforcement. Consequently, neural network models are specified by interconnections, learning rules to update weights and activation functions. The common neural network architectures are single layer or ML feed forward NNs. Models of NNs differ in architecture, behavior and learning methods; hence they are used to solve different problems, such as character recognition, image compression, pattern recognition and signal processing. Supervised learning is commonly used to train NNs, given input-desired outputs pairs; the NNs process inputs and finally compare the given desired output against the resulted real outputs, errors are propagated back through the network layers are used to adjust weights, this learning process is repeated over and over until achieving high quality results.

In the neural network learning process, it is important to (Haykin, 1999): (i) Pre-process the training examples, and (ii) adjust the architecture of the NNs by tuning the number of layers in the network model, the number of neurons in the input, hidden and output layers, the weights, the transfer function and the training function. In NNs, many training algorithms are used, such as the eleven training methods discussed in the present paper.

3.2. Multi-Layer (ML), Neural Networks (NNs)

ML NNs (Bishop, 1995; Haykin, 1999; Svozil *et al*., 1997), also known as ML NNs (see Figure 1), consist of input layer, output layer and one hidden layer. Noting that each layer has a specific number of neurons. The flow of data inputs starts from input layer, through the hidden layer and finally to output layer. This flow enables the ML to model arbitrary complex functions. Inputs are multiplied by their corresponding weights; then the activation function manipulates the multiplied results and produces the outputs of neurons in the hidden layer. Similarly, the outputs of neurons in the output layer are produced. Sigmoid, hyperbolic tangent, piecewise linear or threshold functions are examples of activation functions in ML networks. An ML operates in training and testing modes: Training aims to minimize the error difference between real outputs of ML and the desired outputs by adjusting weights.

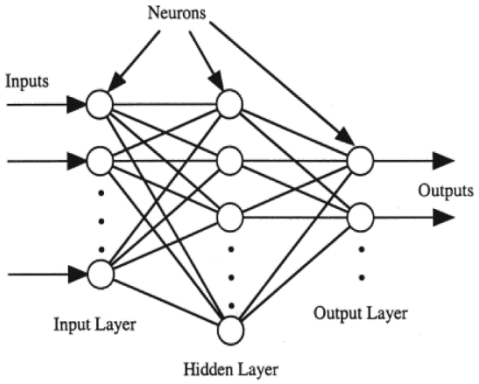

Figure 1. An ML NNs

When the training is completed, the weights of ML NNs are saved in trained states and new (unseen) input data can be presented to the trained ML NNs to determine the appropriate output. It is proved that ML NNs are able to solve larger learning problems; however, more computational efforts are needed to find the correct combination of weights. Back propagation (BP) is a common learning algorithm method that handles many large learning problems, it begins with feeding input data to the neurons in the input layer, passing outputs to neurons in the hidden layer and finally flowing NNs outputs to output layer. BP uses Equation 1 to multiply the neuron's inputs and the corresponding weights for the neurons in hidden and output layers:

$$net_i = \sum_{j \in A} O_j W_{ji}, \forall\, i: i \in B \quad (1)$$

Noting that A represents the neurons in a layer, B represents the neurons in the next layer, O_i represents the

neuron j in the output layer, W_{ij} is the weight between neurons i and j and finally BP uses sigmoid function (see Equation 2) to calculate the output of all neurons (except input neurons).

$$O_i = f(net_i) = 1/1 + e^{-net_i} \quad (2)$$

After calculating the output of neurons, BP estimates error for output neurons using Equation 3:

$$\delta_i = f(net_i).(T_i - O_i), \forall i: i \in C \quad (3)$$

where C represents the output neurons, T_i represents the target value for neuron i, $f(.)$ estimates derivative of the error function (see Equation 2) and δ_i is the error of neuron i. Similarly, The BP algorithm estimates error for neurons in all hidden layers using Equation 4:

$$\delta_i = \acute{f}(net_i).\sum_{j \in E} \delta_j W_{ij}, \forall i, j: i \in A, j \in D \quad (4)$$

where D represents the neurons of the hidden or output layers and E represents the neurons in the next layer.

Then the BP updates the weights of neurons using Equation 5:

$$W_{ij}(t+1) = W_{ij}(t) + \mu.\Delta W_{ij}, \forall i, j: i \in A, j \in B \quad (5)$$

where $\Delta W_{ij} = O_i \delta_i$ and μ is the learning rate that determines the amount of weight adjustments in each iteration.

3.3. Training Algorithms for ML NNs

In the present paper, eleven training algorithms (Bishop, 1995) (traingd, traingdm, traingdx, trainrp, traincgf, traincgp, traincgb, trainscg, trainbfg, trainoss and trainlm) are used to train ML NNs classifier.

Gradient Descent Algorithm (traingd): In *traingd* (Ramesh *et al*., 2008), the NN training starts with random weights, then iteratively updates weights moving shortly toward the direction of the negative gradient, as shown in equation 6:

$$\Delta w(t) = -\mu \nabla E|_{w(t)} \quad (6)$$

where $\nabla E|_{w(t)}$ is the error minima and μ is the learning rate.

Gradient Descent with Momentum (traingdm): *traingdm* adds a new term known as momentum to the *traingd* training algorithm (Ramesh *et al*., 2008) As a result, it smooths the oscillations of gradient of error minima in the weight space. Accordingly, equations 7 shows the *traingdm*:

$$\Delta w(t) = -\mu \nabla E|_{w(t)} + \propto \Delta w(t-1) \quad (7)$$

where $\propto$ is the momentum term.

Gradient Descent with Variable Learning Rate and Momentum (traingdx): While updating the weights in the NNs, *traingdx* (Hagan et al., 1996) adjusts the training variables according to *traingdm*; however, it changes μ to increase the NNs performance. Initially, it calculates the error of the NNs, then, it calculates the modified weights using the current μ, then it re-calculates error again. Finally, it adjusts the training variables according to the *traingdm*. It is clear that *traingdx* discards the updated weights if the new error is bigger than the previous one.

Resilient Back Propagation (trainrp): trainrp (Riedmiller and Braun, 1993) updates weights and biases of NNs by investigating the sign of the partial derivative, it keeps the same change of weight in case of zero partial derivative, it reduces the change of weight in case of weight oscillation and it increases the weight magnitude in the case of continues change in weights.

Conjugate Gradient Algorithms (CGAs): In CGAs (Charalambous, 1992), a search is accomplished in the direction of conjugate gradient so as to minimize the error minima. Moreover, in CGAs, μ determines the length of weight change where the steepest descent direction (SDD) is searched initially. Noting that P_o is the initial search gradient and g_o is the initial gradient, then the following equation 8 is valid:

$$P_o = -g_o \quad (8)$$

Accordingly, given the current weight X_k, the $(k)^{th}$ iteration computes the current search direction P_k from which a new estimate for the next weight vector X_{k+1} (see equation 9):

$$X_{k+1} = X_k + \mu_k P_k \quad (9)$$

where μ_k is the k-th learning rate. It is clear that the direction of the $(k+1)^{th}$ search is conjugate to the direction of the $(k)^{th}$ search as in equation 10:

$$P_k = -g_k + \beta_k P_{k-1} \quad (10)$$

where P_{k-1} is the earlier search direction and β_k is a positive scalar. It should be noted that computation manner of β_k determines the flavor of CGAs.

Fletcher-Reeves Update (traincgf): traincgf obtains β_k by the following equation 11:

$$\beta_k = g_k^t g_k / g_{k-t}^t g_{k-1} \quad (11)$$

Polak and Ribiere (traincgp): *traincgp* obtains β_k by the following equation 12:

$$\beta_k = \Delta g_k^t g_k / g_{k-t}^t g_{k-1} \quad (12)$$

Powell and Beale Restarts (traincgb): In CGAs (Charalambous, 1992), the direction of search is continuously restarted to ensure better performance. *traincgf* and *traincgp* use SDD to restart, *traincgb* is restarted and the direction of search is reset to the negative of the gradient if the following equation 13 is satisfied (Moller, 1993):

$$|g_{k-1}^T g_k| \geq 0.2 \|g_k\|^2 \quad (13)$$

Scaled Conjugate Gradient Algorithm (trainscg): At each iteration, CGAs need line search that requires many calculations related to global error that may raise the complexity of the line search. As a result, *trainscg* combines the model-trust region approach with the conjugate approach to enhance the complexity of the line search.

Quasi Newton BFGS (trainbfg): Quasi Newton BFGS updates weights of NNs according to equation 14:

$$W_{k+1} = W_k - A_k^{-1} g_k \quad (14)$$

where A_k is the Hessian matrix (H) (second derivatives) of the performance index at the current values of the NN weights and biases. Instead of calculating the Hessian matrix, Quasi Newton algorithm updates an approximation of H matrix at each iteration of the algorithm and computes this update as a function of the gradient.

One Step Secant Algorithm (trainoss): *trainoss* (Battiti, 1992) updates the weights of NNs and the related bias values without storing the complete H matrix. *trainoss* assumes that the previous H matrix was the identity matrix

($\mathbf{I}$) and it calculates the new search direction without computing a matrix inverse.

Levenberg–Marquardt (trainlm): trainlm (Hagan and Menhaj, 1994) updates the weights of the NNs according to a standard nonlinear least squares optimization algorithm which is fast enough. However, its optimization algorithm requires more memory than the other training algorithms. Moreover, *trainlm* approximates $\mathbf{H}$ using Jacobian matrix $\mathbf{J}$ which includes the derivative of the NNs error $\mathbf{e}$ as in $\mathbf{H} = \mathbf{J}^{\mathbf{t}}\mathbf{J}$, The gradient can be computed as in $\mathbf{g} = \mathbf{J}^{\mathbf{t}}\mathbf{e}$. it should be noted that calculation complexity of $\mathbf{g}$ is much less than the complexity of computing $\mathbf{H}$. As a result, *trainlm* approximates $\mathbf{H}$ as in equation 15:

$$X_{k+1} = X_k - (J^T J + \mu I)^{-1} J^T e \quad (15)$$

3.4. Independent Component Analysis (ICA)

ICA and PCA (Smith, 1992; Cao and Chong, 2002; Hyvarinen, 1999) techniques are used for feature extraction. Originally, ICA is used in blind source separation (BSS) (Cao and Chong, 2002; Hyvarinen, 1999). It recovers the unknown sources of the original input signals from their linear mixtures. Assume that $\mathbf{x_t}$ is the original linear mixtures and $\mathbf{s_t}$ is the original source input signal, ICA estimates $\mathbf{s_t}$ using the following equation 16:

$$\mathbf{s_t} = \mathbf{U}\mathbf{x_t} \quad (16)$$

where $\mathbf{U}$ is the $\mathbf{m} \times \mathbf{m}$ un-mixing matrix. To identify $\mathbf{s_t} = \mathbf{U}\mathbf{x_t}$, it is required that all the components of $\mathbf{s_t}$ must be independent and non-Gaussian. There are many approaches for implementing ICA. However, Fixed-Point-Fast ICA is among the best algorithms. In Fast ICA, the Negentropy of $\mathbf{s_t}$ is maximized to estimate $\mathbf{s_t}$ using the following Contrast Function (CF) equation 17:

$$J_G(u_i) = [E\{G(u_i^T x_t)\} - E\{G(v)\}]^2 \quad (17)$$

where $\mathbf{u_i}$ is an $\mathbf{m}$ dimensional vector that comprises one of the rows in matrix $\mathbf{U}$. $\mathbf{v}$ is a Gaussian variable. $\mathbf{G}$ is a non-quadratic function. Equations 18, 19 and 20 show the many used functions for $\mathbf{G}$:

$$G_1(s) = \frac{1}{\gamma_1}\log\cosh(\gamma_1 s) \quad (18)$$

$$G_2(s) = -\frac{1}{\gamma_2}\exp(-\gamma_2 s^2/2) \quad (19)$$

$$G_3(s) = \frac{1}{4}s^4 \quad (20)$$

where γ_1 and γ_2 are parameters with $1 \le \gamma_1 \le 2$ and $\gamma_2 \approx 1$. Maximizing $J_G(u_i)$ leads to estimating u_i by equations 21 and 22:

$$u_i^+ = E\{x_t g(u_i^t x_t)\} - E\{\dot{g}(u_i x_i)\}u_i \quad (21)$$

and

$$u_i^* = u_i^+ / \|u_i^+\| \quad (22)$$

where u_i^* is an estimation of u_I, $\mathbf{g}$ is the first derivative of $\mathbf{G}$ and $\dot{\mathbf{g}}$ is the second derivative of $\mathbf{G}$. Based on negentropy, the whole matrix $\mathbf{U}$ is computed by maximizing the sum of one-unit CF taking into account the constraint of decorrelation. In Fast ICA (Hyvarinen, 1999), $\mathbf{x_t}$ is centered by subtracting its mean. PCA (Smith, 1992) is used to achieve whitening and to reduce the dimension of $\mathbf{x_t}$. this minimizes the number of components of $\mathbf{s_t}$. Centering and whitening preprocessing steps are generally used to make the data suitable for the ICA feature extraction process, to speed the ICA convergence, to have better stability properties for the ICA implementation and to find the orthogonal de-mixing matrix which facilitate the implementation of Fast ICA algorithm. Moreover, these preprocessing steps are beneficial to reduce dimensionality (decrease the complexity) of the processed mixtures and to remove the second-order dependencies between the observed input data images or signals.

It should be noted that PCA and ICA feature extraction methods (Hyvarinen *et al*., 2001) are to reduce the number of features. However, when implementing PCA, the first and second moments of the training data sets are utilized to fit Gaussian distribution, on the other hand, higher moments of the training data sets are employed using ICA to serve a wider range of analysis, especially, when dealing with non-Gaussian noisy data. In the present paper, CT images are not indeed Gaussian.

3.5. Dataset

To create successful CAD detection or diagnosis systems, researchers always need a reference standard dataset that is used for training, and testing their systems. Lung Image Database Consortium (LIDC)[1] (Armato *et al*., 2011; Armato *et al*., 2007) is the standard database for lung cancer, LIDC contains CT images for 1010 patients along with their expert cancer annotations, LIDC provides information about the ratings of cancer nodules for only 157 patients, these tumors are rated as 0 for unknnown,1 for benign, 2 for primary malignant, and, 3 for malignant cancer. These ratings are achieved after performing biopsy, surgical resection, progression and reviewing of the radiological CT images, these ratings show the state of nodules at the patient and the nodule levels, this trusted LIDC dataset is acquired for the mentioned patients over a long period using different scanners.

In the present paper, another real (national) dataset is collected from three different Jordanian hospitals: King Hussein Cancer Center, Prince Hamzah Hospital and Al Karak Hospital. At the time of data collection, the average age of the patients was 54 years, the youngest patient was 32 years, the oldest was 77 years, 85% of them are men and the remaining are women. The sizes of their nodules vary from 3 mm to 7 mm. The CT images are labeled as normal or abnormal by experts in the mentioned hospitals.

In the present paper, a dataset of 460 CT images is used to evaluate the performance of the ML NNs detection classifier trained by 11 training algorithms with ICA:

Real dataset: 350 of the 460 CT images belong to the local dataset: King Hussein Cancer Center (100 CT images are normal, 70 CT images are abnormal), Prince Hamzah Hospital (50 CT images are normal, 40 CT images are abnormal) and Al Karak Hospital (50 CT images are normal, 40 CT images are abnormal).

LIDC dataset: 110 of the 460 CT images belong to LIDC lung cancer dataset (60 CT images are normal; 50 CT images are abnormal).

[1] Lung Image Database Consortium Website: http://ncia.nci.nih.gov

It is noted that 260 of the 460 CT images are normal (200 CT images of the real dataset and 60 CT images from the LIDC dataset) while the remaining 200 CT images are infected by cancer (140 CT images of the real dataset and 60 CT images from the LIDC dataset). Figures (2) and (3) show examples of the normal and the abnormal lung images.

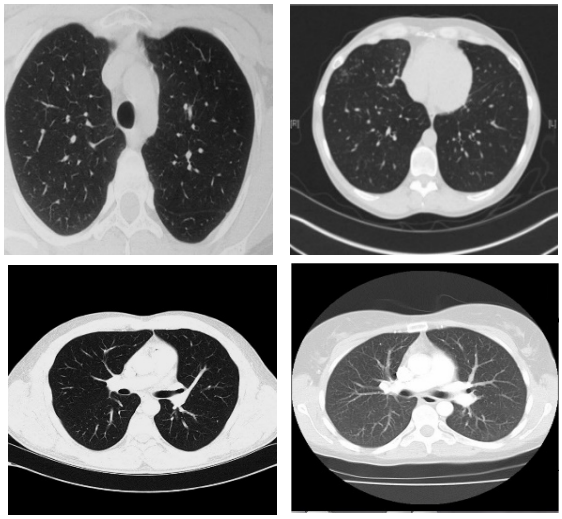

Figure 2. Normal lung CT images

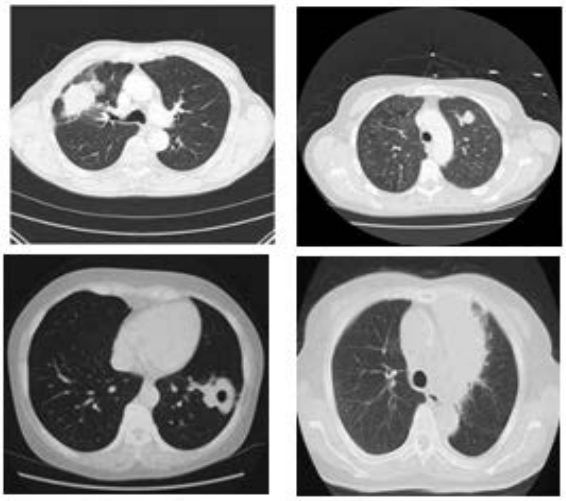

Figure 3. Abnormal lung CT images

3.6. Lung Cancer Detection Algorithm Using ML NNs with ICA

In the medical domain (Suzuki, 2011; Amato *et al*., 2013; Yasmin *et al*., 2013), NNs have been applied in image analysis and interpretation. The proposed lung cancer detection algorithm using ML NNs with ICA is an attempt to solve some of the several challenges that are facing computer aided systems for lung cancer (see El-Baz *et al*., 2013) for challenges discussion).

The proposed algorithm follows the following fundamental steps as shown in Figure (4).

Step 1: Data Collection: in this step, 350 CT lung images were collected for normal and affected lungs from some Jordanian hospitals to train and to test the detection algorithm. Moreover, 110 CT images were selected from the LIDC dataset.

Step 2: Data Preprocessing and Feature Extraction: As a matter of fact, lung images can be directly fed to the input layer of the NNs classifier, but this may negatively affect the complexity of NNs computation. However, to train the classifier more efficiently, data preprocessing procedures are conducted. Data preprocessing is always good since using data with large and small magnitudes may confuse the classification algorithm. In general, when dealing with high dimensional problems, learning algorithms have not been very effective, as a result, the machine learning community has developed many methods (such as ICA) to reduce data dimensions and accordingly to speed the classification process.

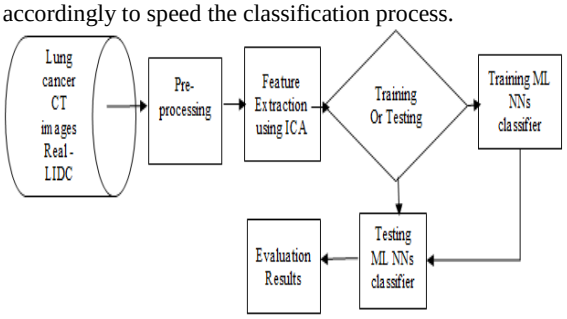

Figure 4. The lung cancer detection algorithm

In the present paper, Otsu method (Otsu, 1979) is used to convert the gray CT images of lungs with a cancerous region to binary images, Otsu method replaced the pixels whose intensities are greater than a threshold level with value '1'and replaced the pixels whose intensities are less than the threshold with value '0'. Otsu method uses the threshold that minimizes the intra-class variance of the black and white pixels. Morphological opening operation uses aperiodic line structuring element to segment lungs in binary images (Gonzalez and Woods, 2008). In morphological operations, structuring is a shape that is used to draw a conclusion on how this shape fits or misses the shapes in the original CT images. In this work, the structuring element contains 2 × 3 members. After the morphological opening operation, the image is inverted and image structures that are lighter than their surroundings and that are connected to the border of the image are suppressed. This high speed and simple segmentation process segmented the CT images correctly. Extracted features for the CT images are represented in a two-dimensional matrix, the number of rows represents the total number of selected features for each CT image and the number of columns represents the total number of CT images. Finally, ICA is used to reduce data dimensions to speed the classification process and to make the detection algorithm applicable in some of the mentioned Jordanian hospitals.

Step 3: NN Classifier Building: in this step, a ML NNs classifier is used to detect the existence of cancer in CT images for real Jordanian patients. Before deploying NNs for lung cancer detection, a parameter selection is involved to select the parameters of the NNs classifiers, these parameters are often selected by some search algorithm or optimized by a tool. Some of these parameters include those which specify the architecture of the NNs itself and some of them include those which determine the behavior, training and testing of the NNs. The number of layers and the number of neurons in the input and the hidden layers

are the most important parameters that affect the overall performance of the presented NN detection algorithm. Researchers in machine learning community (Bishop, 1995; Haykin, 2008) believe that optimizing these parameters may lead to a better performance as more neurons and more layers demand more computations. It is also crucial to determine the parameters that affect the performance of detection algorithms, these parameters include the division of collected CT images into training, validation and testing subsets. As the NNs over-fits data, the validation set error rises. After a predefined number of iterations and when the validation error reaches its minimum value, the training is stopped, and the weights and biases of the epoch, with minimum validation errors are returned as the final NNs structure. In the present paper, a Grid Search (GS) algorithm (Snoek *et al*., 2012) is used for parameter selection. GS is among the well-known parameter selection methods for NNs. GS tries every parameter value over a specified range of values, GS involves an expensive computational cost, fortunately, GS is often parallelized. A user-driven refinement is typically used when searching a large scale of parameter values followed by a fine-tuned or a fine-grained search to achieve better parameter selection. GS parameter selection process used 100 randomly selected CT images in tuning NNs parameters. GS used the Root of Mean Square Error (RMSE) as a performance criterion for the ML NNs detection algorithm. The tuned parameters of the NNs detection algorithm include the number of layers, number of neurons in each layer, the learning rate, momentum term, etc. However, the output layer contains one single neuron.

Step 4: NN Training: in this step, the weights are adjusted so as to minimize the RMSE. Different number of ICA features are evaluated using the above mentioned eleven training algorithms; the number of these features is varied from 1 to 15. At the end of this step, the architecture of the NNs classifier and the other parameters are determined accurately.

Step 5: Testing the Detection Algorithm: in this step, unseen data are exposed to the trained NNs classifier and the performance is evaluated.

4. Results and Discussion

In the present paper, all the experiments are conducted on an Intel Pentium (R) personnel computer with 2.00 GHz Dual-Core CPU and 2 GB RAM, running MS Windows 10 operating system. The lung cancer detection algorithm is programmed using MATLAB version 7.11.0 (R2015a).

The detection algorithm reads the CT images, resizes them to (512 X 512) pixels, converts them to gray images, and, then, converts them to vectors. To prevent overfitting (where the training examples are memorized by the NNs, but the NNs classifier is not able to generalize to new-unseen examples), a validation set of 100 CT images are used to conduct a parameter selection using GS method for the NNs classifier, 50 of them are randomly selected from the real subset and the remaining 50 images are randomly selected from the LIDC subset. This validation set monitors the RMSE of the NNs to terminate the training to avoid overfitting. Finally, best parameter values are selected when achieving best classification accuracy and the least RMSE.

When stopping the training process, the weights of the NNs using the different training algorithms with the corresponding parameter settings are saved at the least error of the validation set. The examples of the training subset are randomly divided into four subsets; each subset contains 115 CT images. An evaluation process is conducted to evaluate the performance of the detection algorithm after tuning its architecture and its related parameters using the mentioned validation set. ICA is implemented as a feature extraction method for each CT image (noting that the extracted features for each CT image are represented in a two-dimensional matrix, the number of rows represents the total number of selected features and the number of columns represents the total number of CT images) and the ICA vector size (k) for each CT image is varied from 1 to 15. It should be noted that the proposed algorithm and the related processing are all implemented using a parallel MATLAB code to speed the detection process and to make the proposed algorithm more applicable for lung cancer detection. Accuracy is the primary performance measure that is used to evaluate the performance of the proposed detection algorithm, it is percentage of true results (both True Positive (TP) and True Negative (TN)) in the population as shown in equation 23:

$$\text{Accuracy} = (TP + TN)/(TP + TN + FP + FN) \quad (23)$$

where TP denotes a CT image that is infected and is classified as cancerous, False Positive (FP) denotes a CT image that is not infected and is classified as cancerous, TN denotes a CT image that is not infected and is classified as non-cancerous and False negative (FN) denotes a CT image that is infected and is classified as non-cancer.

Moreover, sensitivity and specificity are used to evaluate the performance of the NNs classifier trained by the eleven learning algorithms at different numbers of ICA features. Sensitivity is the percentage of positives which are correctly classified. On the other hand, specificity is the percentage of negatives which are correctly classified. Practically, higher sensitivity indicates the ability of detecting those individual CT images with cancer, higher specificity indicates the ability of identifying those individual CT images which actually have no cancer.

The classification accuracy, sensitivity and the specificity values for the ML NNs classifier trained by the eleven training algorithms evaluated over different number of ICA features are shown in Tables 1-3.

For each number of features, the highest classification accuracy values are marked in bold typeface. For each training algorithm, the highest classification accuracy values with the minimum number of features are underlined.

Table 1. Accuracy values for the ML NNs classifier trained by the eleven training algorithms at different numbers of ICA features

No. ICA features	Trainlm	Trainbfg	Trainrp	Trainscg	Traincgb	Traincgf	Traincgp	Trainoss	Traingd	Traingdm	Traingdx
1	89	69	90	89	73	70	75	72	87	84	**94**
2	89	91	81	89	86	79	87	**92**	88	88	86
3	**95**	92	88	**95**	86	86	87	74	84	86	80
4	91	88	92	**96**	86	77	**96**	79	84	80	93
5	**96**	92	89	87	81	83	88	78	95	80	**96**
6	**100**	92	96	85	88	82	85	94	86	92	95
7	**100**	91	88	91	92	96	77	85	95	50	94
8	**100**	83	92	96	92	92	92	83	85	86	94
9	**100**	85	96	92	96	**100**	92	85	85	91	96
10	**100**	73	96	**100**	92	**100**	89	89	96	96	92
11	**100**	**100**	96	**100**	**100**	**100**	**100**	92	92	96	96
12	**100**	**100**	96	**100**	**100**	**100**	**100**	**100**	96	96	96
13	**100**	**100**	**100**	**100**	**100**	**100**	**100**	**100**	**100**	**100**	**100**
14	**100**	**100**	**100**	**100**	**100**	**100**	**100**	**100**	**100**	**100**	**100**
15	**100**	**100**	**100**	**100**	**100**	**100**	**100**	**100**	**100**	**100**	**100**

Table 2. Sensitivity values for the ML NNs classifier trained by the eleven training algorithms at different numbers of ICA features

No. ICA features	Trainlm	Trainbfg	Trainrp	Trainscg	Traincgb	Traincgf	Traincgp	Trainoss	Traingd	Traingdm	Traingdx
1	**100**	84	**100**	**100**	61	58	70	**100**	83	**100**	**100**
2	**100**	90	77	88	83	**100**	81	92	**100**	**100**	**100**
3	**100**	84	84	90	83	**100**	76	50	**100**	**100**	**100**
4	**100**	90	84	91	83	57	**100**	66	57	**100**	**100**
5	**100**	**100**	**100**	76	72	90	76	60	80	**100**	**100**
6	**100**	**100**	**100**	69	83	66	69	87	46	**100**	**100**
7	**100**	**100**	**100**	81	92	**100**	53	69	53	**100**	88
8	**100**	69	**100**	91	92	83	84	69	80	**100**	91
9	**100**	69	0.83	84	**100**	**100**	84	69	61	0.90	**100**
10	**100**	46	**100**	100	84	**100**	76	76	76	**100**	**100**
11	**100**	**100**	**100**	92	**100**	**100**	**100**	84	84	**100**	**100**
12	**100**	**100**	**100**	**100**	**100**	**100**	**100**	92	92	**100**	92
13	**100**	92	**100**	**100**	**100**	**100**	**100**	**100**	83	**100**	**100**
14	**100**	**100**	**100**	**100**	**100**	58	70	**100**	**100**	**100**	**100**
15	**100**	**100**	**100**	**100**	**100**	**100**	81	92	**100**	**100**	**100**

In Table 1, it is clear that increasing the number of ICA features does positively influence the classification accuracy, best accuracy values are achieved by Trainlm training algorithm with 6 features, by *Traincgf* training algorithm with 9 features, by *Trainscg* training algorithm with 10 features, by *Trainbfg*, *Traincgb* and *Traincgp* training algorithms with 11 features, by *Trainoss* training algorithm with 12 features and by *Trainrp*, *Traingd*, *Traingdm* and *Traingdx* training algorithms with 13 features. It is also clear that increasing the features more than 13 does not positively increase the accuracy (see Table 1).

It is known that the sensitivity for cancer detection (Brown, *et al*., 2003) decreases when the size of cancer nodules decreases, for example, cancer detection sensitivity of 91-100% can be achieved when the nodules are bigger than 3 mm in diameter, whereas the sensitivity of detection dropped to 70% when size of nodules are less than 3 mm. A similar detection sensitivity of 91% is achieved for nodules bigger than 3 mm and a sensitivity of 86% for nodules less than 3 mm (Ko *et al*., 2001). Similarly, sensitivity of 94.1% was achieved for solid nodules bigger than 10 mm (Setio *et al*., 2015). Conversely, a good performance is achieved over different sizes of cancer nodules (Marten *et al*., 2005). In 2010, a comparative study of six different CAD systems using the same data set, five of them achieved better detection sensitivity for smaller nodules, the outcome of the present study contradicts the performance achieved in (Ko *et al*., 2001; Brown *et al*., 2003; Marten *et al*., 2005; Setio *et al*., 2015).

In the present work, the best sensitivity values (see Table 2) are achieved by trainlm and traingdm training algorithms. However, *trainoss*, *traincgp* and *traingd* training algorithms have not achieved good sensitivity values. Other training algorithms achieved in between sensitivity values. Moreover, *trainlm*, *trainrp*, *trainsgf*, *trainoss*, *traingdm* and *traingdx* training algorithms achieved best sensitivity values with minimum number of features (with a single feature).

In the present work, the best specificity values (see Table 3) are achieved by *traingdm* and *traingdx* training algorithms; moreover, *traingd*, *trainlm* and *trainrp* work well. However, *traincgb* does not achieve good specificity values. Other training algorithms achieved in between values. Moreover, *traingd*, *traingdm* and *traingdx* training algorithms achieved best specificity values with minimum number of features. After the evaluation process of the detection algorithm and the above reported results, it becomes ready for deployment in real environment, i.e., in one of the mentioned Jordanian hospitals.

It is concluded that Levenberg–Marquardt works best as it achieves the highest detection accuracy of 100% (with only 6 features), 100% specificity and 100% sensitivity. Therefore, results recommend using Levenberg–Marquardt with 6 ICA features as it achieved the best classification accuracy. It should be noted that the elapsed CPU time of training is few seconds and it is noted that the memory requirements is also small for the different training algorithms.

Table 3. Specificity values for the ML NNs classifier trained by the eleven training algorithms at different numbers of ICA features

No. ICA features	Trainlm	Trainbfg	Trainrp	Trainscg	Traincgb	Traincgf	Traincgp	Trainoss	Traingd	Traingdm	Traingdx
1	92	53	88	80	84	81	80	50	**100**	**100**	**100**
2	**100**	90	**100**	88	90	66	0.91	90	**100**	**100**	**100**
3	**100**	**100**	**100**	**100**	90	76	**100**	**100**	90	**100**	**100**
4	**100**	84	**100**	**100**	90	**100**	92	91	**100**	**100**	**100**
5	**100**	84	**100**	**100**	90	76	**100**	**100**	**100**	**100**	**100**
6	**100**	84	**100**	**100**	92	**100**	**100**	**100**	**100**	**100**	**100**
7	**100**	84	**100**	**100**	92	91	**100**	**100**	**100**	**100**	**100**
8	**100**	**100**	**100**	**100**	91	**100**	**100**	**100**	**100**	**100**	**100**
9	**100**	**100**	**100**	**100**	92	**100**	**100**	**100**	**100**	**100**	**100**
10	**100**	**100**	**100**	**100**	**100**	**100**	**100**	**100**	**100**	**100**	**100**
11	**100**	**100**	**100**	**100**	**100**	**100**	**100**	**100**	**100**	**100**	**100**
12	**100**	**100**	**100**	**100**	**100**	**100**	**100**	**100**	**100**	**100**	**100**
13	**100**	**100**	**100**	**100**	**100**	**100**	**100**	**100**	**100**	**100**	**100**
14	**100**	**100**	**100**	**100**	**100**	**100**	**100**	**100**	**100**	**100**	**100**
15	**100**	**100**	**100**	**100**	**100**	**100**	**100**	**100**	**100**	**100**	**100**

5. Conclusion

It is noted that lung cancer is one of the causes of cancer death because of its severity and its late stage when detected. In the present paper, a CAD cancer detection algorithm is implemented to predict the existence of lung cancer in CT images in early stages, the detection system is based on ML NNs classifier with ICA. ICA is to speed the detection algorithm, so as to make it applicable in one of the mentioned Jordanian hospitals, the ML NN classifier is trained by 11 training algorithms. Evaluation used two datasets: one of them is the well-known LIDC dataset, the other dataset is locally collected from three Jordanian hospitals. The paper compares the performance of the 11 training algorithms: *traingd*, *traingdm*, *traingdx*, *trainrp*, *traincgf*, *traincgp*, *traincgb*, *trainscg*, *trainbfg*, *trainoss* and *trainlm*. The present paper investigates the performance of these training algorithms with ICA feature extraction. Among the 11 training algorithms, the *trainlm* training algorithm achieves the highest detection accuracy of 100% with minimum number of features, with specificity of 100% and sensitivity of 100%. i.e., using training algorithm with ICA in ML NN classifier is the best choice to detect lung cancer in CT images collected from the mentioned Jordanian hospitals. The present paper concluded that the ICA is beneficial in cancer classification using NNs especially when dealing with real CT images as it enhances the accuracy and the speed of detection. The proposed detection system is applicable to detect lung cancer at any of the mentioned Jordanian hospitals, this detection is expected to decrease the mortality rate of lung cancer in Jordan.

Acknowledgement

The author likes to thank Al-Balqa Applied University for the financial support to conduct the present work that has been carried out during sabbatical leave granted to the author during the academic year 2015/2016 at Al-Ahliyya Amman University, Jordan. The author likes to thank the Computer Engineering Department at Al-Ahliyya Amman University for providing Plagiarism checker software that was helpful to have a high caliber paper.

References

Abdel-Razeq H, Attiga F and Mansour A. 2015. Cancer care in Jordan. *Hematology/Oncology and Stem Cell Therapy*. **8(2)**: 64-70.

Abdulla A and Shaharum S. 2012. Lung cancer cell classification method using artificial neural network. *Information Eng Let*., **2**: 50-58.

Ahmad F, Isa N, Noor M and Hussain Z. 2013. Intelligent Breast Cancer Diagnosis Using Hybrid GA-ANN. Proceedings of the 2013 Fifth International Conference on Computational Intelligence, Communication Systems and Networks. 9-12.

Al Mohammad B, Brennan P and Mello-Thoms C. 2017. A review of lung cancer screening and the role of computer-aided detection. *Clin Radiol*. **72(6)**: 433-442.

Al Qadire M. 2014. Jordanian cancer patients' information needs and information-seeking behaviour: A descriptive study. *Europ J of Oncology Nursing*. **18(1)**: 46-51.

Al-Sayaideh A, Nimri O, Arqoub K, Al- Zaghal M and Halasa W. 2012. **Annual statistical book**. Directory of Information & Research, Jordanian Ministry of Health.

Amato F, López A, Peña-Méndez E, a hara P, Hampl A and Havel J. 2013. Artificial neural networks in medical diagnosis. *J Appl Biomed*., **11**: 47-58.

Argiris, A. 2012. **Lung Cancer (Emerging Cancer Therapeutics)**. First ed., Demos Medical, New York.

Armato S, McLennan G, Bidaut L, McNitt-Gray M, Meyer C, Reeves A.*et al*., 2011. The Lung Image Database Consortium (LIDC) and Image Database Resource Initiative (IDRI): A Completed Reference Database of Lung Nodules on CT Scans. *Medical Phys*., **38(2)**: 915-931.

Armato S, McNitt-Gray M, Reeves A, Meyer C, McLennan G, Aberle D. *et al*,, 2007. The Lung Image Database Consortium (LIDC): An Evaluation of Radiologist Variability in the Identification of Lung Nodules on CT Scans. *Academic Radiol*., **14(11)**: 1409-1421.

Babu G, Bhukya S and Kumar R. 2013. Feed forward network with back propagation algorithm for detection of breast cancer. Proceedings of the 2013 8th International Conference on Computer Science & Education. 181-185.

Battiti R. 1992. First and second order methods for learning: Between steepest descent and Newton's method. *Neural Computation*. **4(2)**: 141-166.

Bishop C. 1995. **Neural networks for pattern recognition**. Oxford University Press, New York.

Brown M, Goldin J, Suh R, McNitt-Gray M, Sayre J and Aberle D. 2003. Lung micronodules: automated method for detection at thin-section CT-initial experience. *Radiol*., **226(1)**: 256-262.

Cao L and Chong W. 2002. Feature extraction in support vector machine: a comparison of PCA, KPCA and ICA, Proceedings of the 9th International Conference on Neural Information Processing (ICONIP'OZ), 1001-1005.

Charalambous C. 1992. Conjugate gradient algorithm for efficient training of artificial neural networks. *IEEE Proceedings*. **139(3)**: 301-310.

Chen S, Suzuki K. 2013. Computerized Detection of Lung Nodules by Means of "Virtual Dual-Energy" Radiography. *IEEE Transactions on Biomed Eng*., **60(2)**: 369-378.

Dimililer K, Ugur B and Ever Y. 2017. Tumor detection on CT lung images using image enhancement. *The Online J Sci Technol*., **7(1)**: 133-138.

El-Baz A, Beache G, Gimel'farb G, Suzuki K, Okada K, Elnakib A, Soliman A and Abdollahi B. 2013. Computer-Aided Diagnosis Systems for Lung Cancer: Challenges and Methodologies. *Inter J Biomed Imaging*, Hindawi Publishing Corporation, **2013**:1-46.

Firmino M, Angelo G, Morais H, Dantas M and Valentim R. 2016. Computer-aided detection (CADe) and diagnosis (CADx) system for lung cancer with likelihood of malignancy. *Biomed Eng*., **15(1)**: 1-17.

Firmino M, Morais A, Mendoça R, Dantas M, Hekis H and Valentim R. 2014. Computer-aided detection system for lung cancer in computed tomography scans: Review and future prospects. *Biomed Eng OnLine*. **13(41)**: 1-16.

Flores-Fernández J, Herrera-López E, Sánchez-Llamas F, Rojas-Calvillo A, Cabrera-Galeana P, Leal-Pacheco G, González-Palomar M, Femat R and Martínez-Velázquez M. 2012. Development of an optimized multi-biomarker panel for the detection of lung cancer based on principal component analysis and artificial neural network modeling. *Expert Systems with Applications*. **39(12)**: 10851-10856.

Froz B, Filho A, Silva A, Paiva A, Nunes R and Gattass M. 2017. Lung nodule classification using artificial crawlers, directional texture and support vector machine. *Expert Systems with Applications*. **69(1)**: 176-188.

Gonzalez R and Woods R. 2008. **Digital Image Processing**. 3rd Ed. Prentice Hall, New York.

Guyon I, Gunn S, Nikravesh M and Zadeh L. 2006. **Feature Extraction Foundations and Applications**. Springer-Verlag, Berlin Heidelberg.

Hagan M, Demuth H and Beale M. 1996. **Neural Network Design**. 2nd Ed., PWS Publishing, Boston, MA, USA.

Hagan M and Menhaj M. 1994. Training feed-forward networks with the Marquardt algorithm. *IEEE Transactions on Neural Networks*. **5(6)**: 989-993.

Haykin S. 1999. **Neural Networks: A Comprehensive Foundation**. 2nd Ed., Prentice Hall, New York.

Haykin S. 2008. **Neural Networks and Learning Machines**. 3rd Ed. Pearson Education, New York.

Herman G. 2009. **Fundamentals of computerized tomography: Image reconstruction from projection**. 2nd Ed., Springer, London.

Howlader N, Noone A, Krapcho M, Miller D, Bishop K, Kosary C, Yu M, Ruhl J, Tatalovich Z, Mariotto A, Lewis D, Chen H, Feuer E and Cronin K. 2017. SEER Cancer Statistics Review 1975-2014. National Cancer Institute. Bethesda, MD: https://seer.cancer.gov/csr/1975_2014/, based on November 2016 SEER data submission.

Hyvarinen A. 1999. Fast and robust fixed-point algorithms for independent component analysis. *IEEE Transactions on Neural Networks*. **10(3)**: 626-634.

Hyvarinen A, Karhunen J and Oja E. 2001. **Independent Component Analysis**. John Wiley & Sons, INC., New York.

Kennedy T, Miller Y and Prindiville S. 2000. Screening for lung cancer revisited and the role of sputum cytology and fluorescence bronchoscopy in a high-risk group. *Chest J.,* **117(4)**: 72-79.

Ko J and Betke M. 2001. Chest CT: automated nodule detection and assessment of change over timed preliminary experience. *Radiol*., **218(1)**: 267-273.

Kuruvilla J and Gunavathi K. 2014. Lung cancer classification using neural networks for CT images. *Computer Methods and Programs in Biomed.,* **113(1)**: 202-209.

Manikandan T and Bharathi N. 2017. Hybrid neuro-fuzzy system for prediction of stages of lung cancer based on the observed symptom values. *Biomed Res.,* **28(2)**: 588-593.

Marten K, Engelke C, Seyfarth T, Grillhösl A, Obenauer S and Rummeny E. 2005. Computer-aided detection of pulmonary nodules: influence of nodule characteristics on detection performance. *Clin Radiol*., **60(2)**: 196-206.

Mayo Clinic Staff. 2017. CT scan. Mayo Clinic: http://mayoclinic.org, retrieved on May 2017.

Miao Q, Derbas J, Eid A, Subramanian H and Backman V. 2016. Automated Cell Selection Using Support Vector Machine for Application to Spectral Nanocytology. *Biomed Res Inter.,* **2016**: 1-10.

Moller M. 1993. A scaled conjugate gradient algorithm for fast supervised learning. *Neural Networks*. **6**: 525-533.

Nguyen H and Dang T. 2015. Ribs Suppression in Chest X-Ray Images by Using ICA Method. IFMBE Proceedings of the 5th International Conference on Biomedical Engineering in Vietnam. **46**: 194-197.

Otsu N. 1979. A Threshold Selection Method from Gray-Level Histograms. *IEEE Transactions on Systems, Man, and Cybernetics*. **9(1)**: 62-66.

Ramesh J, Vanathi P and Gunavathi K. 2008. Fault classification in phase-locked loops using back -propagation neural networks. *ETRI J.,* **30**: 546-553.

Riedmiller M and Braun H. 1993. A direct adaptive method for faster back propagation learning: the RPROP algorithm. Proceedings of the IEEE International Conference on Neural Networks. San Francisco, CA, USA.

Setio A, Jacobs C, Gelderblom J and Ginneken B. 2015. Automatic detection of large pulmonary solid nodules in thoracic CT images. *Medical Phys.,* **42(10)**: 5642-5653.

Shen W, Zhou M, Yang F, Yu D, Dong D, Yang C, Zang Y and Tian J. 2017. Multi-crop Convolutional Neural Networks for lung nodule malignancy suspiciousness classification. *Pattern Recognition*. **61**: 663-673.

Smith L. 2002. A tutorial on Principal Components Analysis. Downloaded from:

http://www.cs.otago.ac.nz/cosc453/student_tutorials/principal_components.pdf.

Snoek J, Larochelle H and Adams R. 2012. Practical Bayesian optimization of machine learning algorithms. *Advances in Neural Information Processing Systems*. **25**: 2960-2968.

Sun T, Wang J, Li X, Lv P, Liu F, Luo Y, Gao Q, Zhu H and Guo X. 2013. Comparative evaluation of support vector machines for computer aided diagnosis of lung cancer in CT based on a multi-dimensional data set. *Computer Methods and Programs in Biomed.,* **111(2)**: 519-524.

Suzuki, K. 2011. **Artificial Neural Networks Methodological Advances and Biomedical Applications**. Published by InTech Janeza, Croatia

Svozil D, Kvasnicka V and Pospichal J. 1997. Introduction to multi-layer feed-forward neural networks. *Chemometrics and Intelligent Laboratory Syst.,* **39**: 43-62.

Syed M and Muhammad S. 2017. Recent Developments in Computer Aided Diagnosis for Lung Nodule Detection from CT images: A Review. *Current Med Imaging Rev.,* **13(1)**: 3-19.

Taher F, Werghi N, Al-Ahmad H and Sammouda R. 2012. Lung Cancer Detection by Using Artificial Neural Network and Fuzzy Clustering Methods. *Am J Biomed Eng.,* **2(3)**: 136-142.

Tajbakhsh N and Suzuki K. 2017. Comparing two classes of end-to-end machine-learning models in lung nodule detection and classification: MTANNs vs. CNNs. *Pattern Recognition.* **63**: 476-486.

Tao W, Jianping L and Bingxin L. 2011. Research of Lung Cancer Screening Algorithm Based on RBF Neural Network. Proceedings of the 2011 International Conference on Computer and Management (CAMAN), Wuhan, China, 1-4.

Tarawneh M, Nimri O, Arkoob K and AL Zaghal M. 2010. **Cancer Incidence in Jordan 2010**. The fifteenth report, Jordanian Ministry of Health.

Tariq A, Akram M and Javed M. 2013. Lung nodule detection in CT images using neuro fuzzy classifier. Proceedings of the 2013 IEEE Fourth International Workshop on Computational Intelligence in Medical Imaging (CIMI). 49-53.

Wu Y, Wu Y, Wang J, Yan Z, Qu L, Xiang B and Zhang Y. 2011. An optimal tumor marker group-coupled artificial neural network for diagnosis of lung cancer. *Expert Systems with Applications.* **38(9)**: 11329-11334.

Van Ginneken B, Armato S, de Hoop B, de Vorst S, Duindam T, Niemeijer M., Murphy K, Schilham A, Retico A, Fantacci M, Camarlinghi N, Bagagli F, Gori I, Hara T, Fujita H, Gargano G, Bellotti R, Tangaro S, Bolaños L, De Carlo F, Cerello P, Cheran S, Torres E and Prokop M. 2010. Comparing and combining algorithms for computer-aided detection of pulmonary nodules in computed tomography scans: the ANODE09 study. *Med Image Anal.,* **14(6)**: 707-722.

Yasmin M, Sharif M and Mohsin S. 2013. Neural Networks in Medical Imaging Applications: A Survey. *World Appl Sci J.,* **22(1)**: 85-96.

JJBS

Jordan Journal of Biological Sciences

Volume 10, Number 4,December 2017
ISSN 1995-6673
Pages 251 - 255

Biodegradation of Sodium Dodecyl Sulphate (SDS) by two Bacteria Isolated from Wastewater Generated by a Detergent-Manufacturing Plant in Nigeria

Abimbola O. Adekanmbi[*] and Iyanuoluwa M. Usinola

Environmental Microbiology and Biotechnology Laboratory, Department of Microbiology, University of Ibadan, Nigeria.

Received: January 14, 2017; Revised: August 4, 2017; Accepted: August 8, 2017

Abstract

Sodium Dodecyl Sulphate (SDS) is an anionic surfactant widely used all over the world, and it is an important foaming component of shampoos, toothpaste and detergents. Large quantities of SDS are released to the environment and this can cause problems in sewage treatment facilities due to their foaming capabilities and toxicity. The present study aimed at isolating bacteria capable of utilizing SDS from sediment and wastewater samples of a detergent manufacturing plant and laundry section of a student residential hall. Sediment and wastewater samples were collected and cultured on Phosphate Buffered Medium (PBM) supplemented with SDS (PBM-SDS) as the carbon source. Bacterial identification and growth determination were done using conventional methods and the UV visible light spectrophotometer respectively. The SDS-utilizing bacteria were employed in the degradation of SDS in a batch culture for 10 days on a rotary shaker at 150 rpm. The residual SDS concentration was determined using HPLC. A total of eight bacteria belonging to four genera; *Lysinibacillus*, *Staphylococcus*, *Bacillus* and *Paenibacillus* were obtained. All the bacteria tolerated SDS to a concentration of 1000 mM. Two of the eight SDS-degrading bacteria; *Staphylococcus aureus* WAW1 and *Bacillus cereus* WAW2 were selected for the biodegradation set-up based on their growth consistency. *Staphylococcus aureus* WAW1 was able to degrade 36.8% of SDS at the end of the biodegradation study while *Bacillus cereus* WAW2 was able to degrade 51.4%. The bacteria obtained in this study could prove useful in the bioremediation of wastewater laden with SDS, and cleaning up of surfactant from wastewater generated via laundry activities, detergent-manufacturing and other related activities.

Keywords:Detergent-manufacturing, Sodium dodecyl sulphate, Surfactants, Laundry wastewater

1. Introduction

Sodium Dodecyl Sulfate (SDS) otherwise referred to as Sodium Lauryl Sulphate is the most widely used anionic detergent in household products, such as toothpastes, shampoos, shaving foams, bubble baths, cosmetics and detergents (Dhouib *et al*., 2003). In the industries, however, it is used as leather softening agent, wool cleaning agent, penetrant, flocculating agent, de-inking agent in the paper industry; and it is the major components of fire-fighting devices, engine degreasers, floor cleaners, and car wash soaps.

The occurrence of SDS in the environment stems mainly from its presence in domestic and industrial effluents as well as its release directly from some applications (Fendinger *et al*., 1994). Several authors have reported the toxicity of SDS and its effects on the survival of aquatic animals such as fishes, microbes, like yeasts and bacteria (Singer and Tjeerdema, 1992; Sandbacka *et al*., 2000; Martinez and Munoz, 2007). It has also been reported to be toxic to mammals, like mice and humans though to a lesser extent.

The excessive use of detergents domestically and industrially is becoming a serious problem due to the fact that they have detrimental effects on aquatic organisms via the discharge of surfactant-laden wastewater into water bodies and channels (Chukwu and Odunzeh, 2006; Kumar *et al*., 2007). Liwarska-Bizukojc *et al*. (2005) reported that surfactants are ubiquitous and in many untreated effluents, certain classes of surfactants can be present in sufficient concentrations to constitute toxicity problems to aquatic organisms because most of the massive amounts of surfactants used industrially and domestically end up in wastewater flows. Petterson *et al*. (2000) reported that anionic surfactants have toxic effects on various aquatic organisms even at concentrations as low as 0.0025 mg/L thus necessitating the removal of these compounds before they build up to a considerable high concentration in the environment especially water bodies.

Cserhati *et al*. (2002) reported that SDS and other surfactants are considered to be biodegradable by aerobic

[*] Corresponding author. e-mail: bimboleen@yahoo.com.

processes; however, the mass loadings of these compounds into water bodies suggest that, even at these natural removal rates, appreciable amounts of surfactants are released into receiving waters to the extent that a variety of surfactants has been identified in both surface and drinking water (Isobe *et al*., 2004). This has necessitated the need for a system capable of degrading surfactants discharged into water system as a means of augmenting the natural biodegradation of these compounds.

Numerous studies have been carried out in the Nigerian environment on bacteria isolated from wastewater generated by laundry and detergent-manufacturing, and their ability to grow on/degrade different washing detergents; however , none has focused on the ability of bacteria isolated from the same source to subsist on SDS, a surfactant present in detergents. This present study, therefore, investigated the ability of bacteria isolated from laundry and detergent-manufacturing sediments and wastewater to utilize SDS as a sole source of carbon and degrade SDS in a batch culture system spiked with SDS as the carbon source.

2. Materials and Methods

2.1. Chemicals, Culture Media and Reagents

Sodium Dodecyl Sulphate (SDS) was purchased from Merck (Pty) Ltd, Gauteng, 1645, South Africa. Nutrient agar was purchased from Oxoid, UK. Other chemicals, salts and reagents used were of the highest grade available at the time of carrying out the present study. The composition of the Phosphate Buffered Medium (PBM) was (g/L): K_2HPO_4 1.0, KH_2PO_4 1.0, NH_4Cl 1.0, $MgSO_4.7H_2O$ 0.20, NaCl 0.5 and $CaCl_2$ 0.02, (pH 7.5). The medium also contained trace elements (1 mL of stock) having (g/L): $FeCl_3 \cdot 6H_2O$ 0.24, $CoCl_2 \cdot 6H_2O$ 0.04, $CuSO_4 \cdot 5H_2O$ 0.06, $MnCl_2 \cdot 4H_2O$ 0.03, $ZnSO_4 \cdot 7H_2O$ 0.31, $Na_2MoO_4 \cdot 2H_2O$ 0.03. After sterilization, SDS was added to the medium as the sole source of carbon.

2.2. Description of the Study Site

The present study was carried out in Ibadan. Ibadan is located in South-western part of Nigeria. The sampling sites were the wastewater disposal channel of a detergent manufacturing plant located in an industrial estate; and the laundry section of a hall of residence located within the University of Ibadan, Nigeria. The description of the sampling points is shown in Table 1.

Table 1. Description of the Sampling points and GPS readings

Description of sampling point	Source	Type of samples collected	Latitude	Longitude
Point 1	Effluent disposal channel of a detergent manufacturing plant	Soil sediment and wastewater	7.2119N	3.511E
Point 2	Laundry section of a hall of residence	Soil sediment and wastewater	7.2659N	3.5333E

2.3. Sample Collection

Soil sediments were collected in aluminum foil, while wastewater samples were collected in pre-sterilized sample bottles. The samples were transported to the Environmental Microbiology and Biotechnology Laboratory, Department of Microbiology, University of Ibadan, and analyzed within one hour of collection.

2.4. Enrichment and Isolation of SDS-Degrading Bacteria

The SDS-degrading bacteria were isolated from the sediment and wastewater samples using PBM as the enrichment medium. Aliquot (10 mL) of the wastewater sample and ten gram of soil sediment were added separately to 100 mL sterilized PBM supplemented with SDS (100 ppm) in different culture flasks. The set-up was incubated at room temperature for 96 h on a rotary shaker at a speed of 150 rpm. After the incubation period, morphologically distinct colonies of bacteria were picked and repeatedly subcultured on PBM supplemented with SDS (100 ppm) to obtain pure culture (Chaturvedi and Kumar, 2010). The purified cultures of the bacteria were stored in glycerol broth at -80°C. The identity of the SDS-degrading bacteria was determined using conventional morphological and biochemical tests according to Sneath (1996).

2.5. Screening of Bacteria on Increasing Concentration of SDS

The obtained bacteria were screened on PBM containing an increasing concentration of SDS with agar as the solidifying agent. The culture growing on the previous concentration is transferred to the next higher concentration until the final screening concentration of 1000 ppm of SDS. Apart from growth on solid medium, the growth of the SDS-utilizing bacteria was also monitored using a UV-Visible light spectrophotometer, and two bacteria showing consistent increase in OD_{540} within 120 h were selected for the degradation study.

2.6. SDS Degradation Set-up

The degradation study was carried out in 150 mL conical flasks containing 99 mL of PBM supplemented with 10 mM SDS. The inoculum was prepared from overnight cultures of the selected bacterial isolates on nutrient agar plates incubated at 35±2°C. Two-three (2-3) identical colonies of each bacterium were then selected and suspended in saline. The saline suspension was standardized (0.5 McFarland Standard) and 1 mL was used to inoculate PBM-SDS medium to a final volume of 100 mL. The PBM-SDS medium without the bacteria served as the control. The cultures were incubated at room temperature with shaking at 150 rpm for 10 days according to the methods of Rusconi *et al*. (2001) with slight modifications. The rate of degradation was calculated using the formula below:

$$(A-B) \div C$$

where: A= Initial SDS concentration (ppm)

B= Final SDS concentration (ppm)

C= Experimental duration (hour)

2.7. Analysis of the Residual SDS Concentration

The cultures were centrifuged at 10000 rpm for 5 min to remove the bacterial cells and the residual SDS concentration in the growth medium was determined by HPLC using a Water Alliance 1100 series system fitted with a 1260 Infinite Variable Wavelength detector set at 225 nm and an Agilent (3.9 mm × 150 mm, 4 µm) Waters

Novapak C18 column. The isocratic mobile phase gradient of acetonitrile-water, (80-20) was conducted at a flow rate 1.0 mL/min.

3. Results

3.1. Bacterial Isolation, Screening and Characterization

Preliminary screening on PBM-SDS medium gave a total of eight bacteria capable of utilizing SDS as carbon source. All the eight isolates obtained showed consistent and visible growth on PBM-SDS solid medium to a concentration of 1000 mM SDS. The eight bacterial isolates belonged to four genera, which were: *Lysinibacillus* (1), *Staphylococcus* (2), *Paenibacillus* (1) and *Bacillus* (4). The identity of the bacteria and the source of isolation are highlighted in Table 2.

Table 2. Identity of the SDS-utilizing bacteria and their source of isolation

Isolate and code	Sample	Source of isolation
Staphylococcus aureus WAW1	Wastewater	Detergent-manufacturing plant
Bacillus cereus WAW2	Wastewater	Detergent-manufacturing plant
Bacillus firmus WAW3	Soil sediment	Detergent-manufacturing plant
Bacillus siamensis WAW4	Soil sediment	Detergent-manufacturing plant
Paenibacillus amylolyticus BAL1	Soil sediment	Laundry section of a hall of residence
Bacillus lentus BAL2	Soil sediment	Laundry section of a hall of residence
Lysinibacillus sphaericus BAL3	Soil sediment	Laundry section of a hall of residence
Staphylococcus sciuri BAL4	Soil sediment	Laundry section of a hall of residence

3.2. Selection of Bacteria for the Biodegradation Study

Two bacteria, namely *Staphylococcus aureus* WAW1 and *Bacillus cereus* WAW2, were selected for the biodegradation study, based on their consistent increase on PBM-SDS monitored at an optical density of 540 nm. Both bacteria showed no appreciable growth within the first 24 hours of growth. However, there was a noticeable increase in the absorbance from the 48th to the 96th h, before growth started declining again till the end of the experimental duration (120th h) as shown in Figure 1.

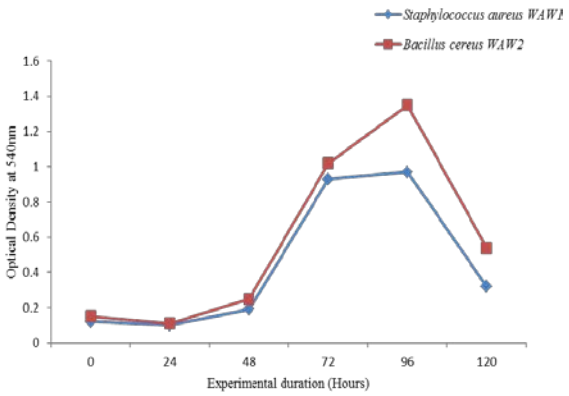

Figure 1. Growth of the two selected SDS-degrading bacteria in PBM-SDS medium

3.3. Residual SDS Concentration

HPLC analysis of the residual concentration of SDS in the samples showed that there was a reduction in the SDS concentration after the 10-day degradation set-up. *Bacillus cereus* WAW2 degraded 5055.70 ppm of the initial SDS in the setup at a degradation rate of 21.07 ppm/h, and eventually degrading 51.4% of the initial SDS concentration, while *Staphylococcus aureus* WAW1 degraded 3615.37 ppm of SDS at a rate of 15.06 ppm/h, leading to a 36.8% reduction in the initial concentration of SDS in the set-up (Table 3).

Figure 2 shows the chromatogram of the control (uninoculated sample) and the samples treated with the two bacteria. The reduction in the height of the peaks in the treated samples in comparison to the uninoculated control gave evidence to the degradation of the surfactant by the two bacterial isolates.

Table 3. Rate of degradation of SDS by the SDS-utilizing bacteria

Bacterial isolate	Amount of SDS degraded (ppm)	Rate of SDS degradation (ppm/h)	Percentage degradation (%)
Staphylococcus aureus WAW1	3615.37	15.06	36.8
Bacillus cereus WAW2	5055.70	21.07	51.4

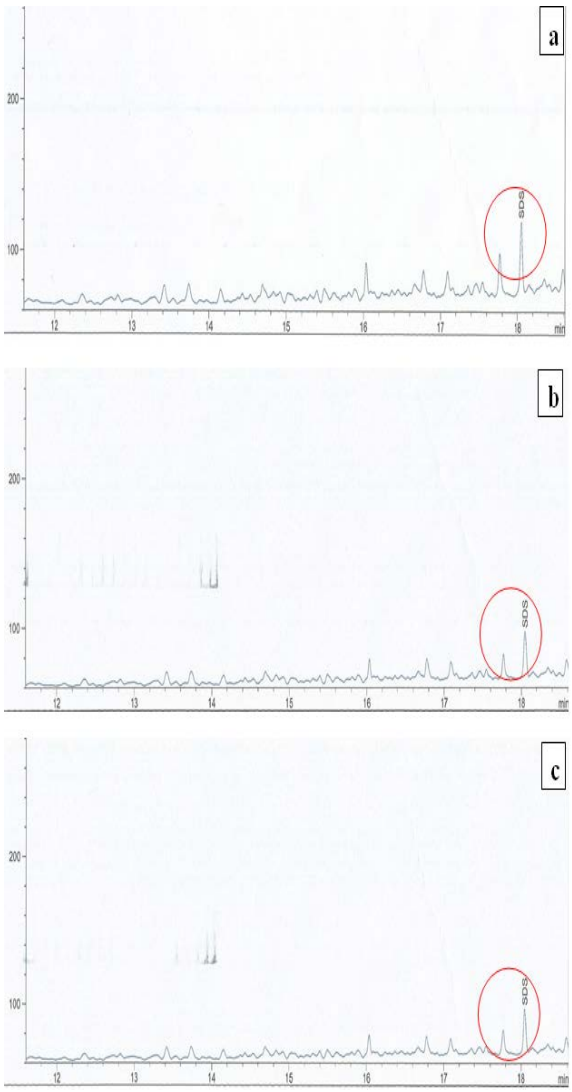

Figure 2. HPLC chromatograms of the (a) uninoculated control (b) *Staphylococcus aureus* WAW1 (c) *Bacillus cereus* WAW2 showing suspected area of degradation (red rings)

4. Discussion

In the present study, a total of eight bacteria capable of utilizing/degrading Sodium Dodecyl Sulphate (SDS) as the sole carbon source were isolated. All the bacteria obtained in the present study were gram-positive organisms; and this is not in agreement with the work of Ojo and Oso (2008) who reported the isolation of a larger percentage of gram-negative organisms capable of growing on detergents. They were of the view that the gram-positive strains showed more tolerance than the gram-negative. This is, however, different from the report of Higgins and Burns (1975) who asserted that gram positive bacteria are noticeably affected by surfactant concentration of 10-20 ppm while gram negative organisms can tolerate several thousand ppm concentration of surfactants without any adverse effect. This is also corroborated by Chaturvedi and Kumar (2010) who reported the isolation of two *Pseudomonas* strains (gram negative bacteria) from a detergent-polluted pond in Varanasi city, India.

Gram positive bacteria similar to the ones obtained in this present study have been reported to utilize surfactants. Anaukwu *et al*. (2016) reported the isolation of *Staphylococcus scuiri* and *Bacillus cereus* capable of degrading or utilizing surfactants as their carbon source. This is not however in accordance with the report of Schleheck *et al*. (2013) who reported the isolation of *Citrobacter* sp., a gram negative bacterium capable of utilizing over 90% surfactant in 35 h of growth in a closed culture. The isolation of gram positive organisms in the present study is not in agreement with the work of Jerabkova *et al*. (1999), who reported the isolation of *Pseudomonas* strains capable of decreasing surfactants concentration by 70% in 20 days; nor is it in agreement with the work of Shukor *et al*. (2009) who reported the isolation and characterization of an SDS-degrading *Klebsiella oxytoca*, also a gram negative bacterium.

The two bacteria, i.e., *Staphylococcus aureus* WAW1 and *Bacillus cereus* WAW2 selected for the biodegradation experiment in the present study have been reported in previous studies. Notable among them was Singh *et al*. (1998) who reported the degradation of SDS by *Bacillus cereus*, which was the first report of biodegradation of SDS by any gram-positive bacterium. Ojo and Oso (2008) also reported the isolation of *Staphylococcus* strain capable of degrading detergent in their study on the isolation and characterization of synthetic degraders from wastewater.

Staphylococcus aureus WAW1 in the present study degraded 36.8% of SDS from an initial concentration of 10 mM in 10 days, and this is lower than the degradation of SDS by *Pseudomonas betelli* (97%) in 10 days as reported by Hosseini *et al*. (2007). In addition, *Bacillus cereus* WAW2 obtained in the present study degraded 51.4% of SDS within the same number of days, which is not in concordance with 96.4% degradation of SDS by *Acinetobacter johnsonii* in 10 days as reported by Hosseini *et al*. (2007). The difference in the degradation could be attributed to several factors including; disparity in the type of bacteria used, concentration of SDS used in the degradation set-up, source of isolation, geographical location and several other environmental factors. Shukor *et al*. (2009) reported that *Klebsiella oxytoca*, a gram negative bacterium isolated from soils and water contaminated with detergent from a car wash outlet in Malaysia was able to degrade 80% of SDS from an initial concentration of 2 g/L within 4 days. This level of degradation is still higher than what was obtained in this present study (36.8% and 51.4%) despite the degradation set-up in the present study being run for longer period (10 days).

In conclusion, the bacteria obtained in the present study are capable of utilizing SDS as their carbon source and could be helpful in the remediation of wastewater contaminated with surfactants. However, more studies need to be carried out on the optimization of culture conditions for the degradation of SDS, degradation of surfactant simultaneously with the removal of other toxicants and the molecular genetics of the SDS-degrading bacteria.

Acknowledgements

The authors would like to appreciate the entire staff of Environmental Microbiology and Biotechnology unit for their assistance during the course of this research.

References

Anaukwu CG, Ekwealor AI, Ezemba CC, Anakwenze VN, Agu KC, Nwankwegu AS, Okeke BC and Awah NS. 2016. Influence of anionic, cationic and non-ionic surfactants on growth of hydrocarbon utilizing bacteria. *Amer J Curr Microbiol*, **4**: 10-16.

Chaturvedi V and Kumar A. 2010. Bacterial utilization of sodium dodecyl sulfate. *Inter J Appl Biol and Pharm Technol*., **3**:1126–1131.

Chukwu LO and Odunzeh CC. 2006. Relative toxicity of spent lubricant oil and detergent against benthic macro-invertebrates of a West African estuarine lagoon. *J Environ Biol.*, **27**: 479-484.

Cserhati T, Forgaes E and Oros G. 2002. Biological activity and environmental impact of anionic surfactants. *Intern J Environ Sci*., **28**: 337–348.

Dhouib A, Hamad N and Hassairi I. 2003. Degradation of anionic surfactants by *Citrobacter braakii*. *Proc Biochem.*, **38**: 1245-1250.

Fendinger NJ, Versteg DJ, Weeg E, Dyer S and Rapaport RA. 1994. Environmental behavior and fate of anionic surfactants in American Chemical Society Washington D.C. *Environ Chem Lakes Reserv.*, **5**: 527-557.

Higgins IJ and Burns RG 1975. **The Chemistry and Microbiology of Pollution**. Academic Press, London. Pp 55-105.

Hosseini F, Malekzadeh F, Amir-mozafari N and Ghaemi N. 2007. Biodegradation of anionic surfactants by isolated bacteria from activated sludge. *Inter J of Environ. Sci Technol*., **4**: 127–132.

Isobe KO, Zakaria MP, Chiem NH, Minh LY, Prudente M, Boonyatumanond R, Saha M, Sarkar S and Takada H. 2004. Distribution of linear alkyl benzenes (LAB) in riverine and coastal environments in South and Southeast Asia. *Water Res*., **38**: 2449-2459.

Jerabkova H, Blanka K and Nahlik J. 1999. Biofilm of *Pseudomonas* C12B on glass support as catalytic agent for continuous SDS biodegradation. *Inter J Environ Sci Technol.*, **44**: 233-241.

Kumar M, Trivedi SP, Misra A and Sharma S. 2007. Histopathological changes in testis of the freshwater fish, *Heteropneustes fossilis* (Bloch) exposed to linear alkyl benzene sulphonate (LAS*). J Environ Biol.*, **28**: 679-684.

Liwarska-Bizukojc E, Miksch K, Jutsz AM and Kalka J. 2005. Acute toxicity and genotoxicity of five selected anionic and non-ionic surfactants. *Chemosphere*, **58**: 1249-1253..

Martinez JF and Munoz MG. 2007. Evaluation of the sensitivity of three cladoceran species widely distributed in Mexico to three reference toxicants. *J Environ Sci and Health*, **42**:1417-1424.

Ojo OA and Oso BA. 2008. Isolation and characterization of synthetic detergent degrader from waste water. *Afric J Biotech.*, **7**: 3753-3760.

Petterson A, Adamson M and Dave G. 2000. Toxicity and detoxification of Swedish detergents and softener products. *Chemosphere*, **41**: 1611-1620.

Rusconi F, Valton E, Nguyen R and Dufourc E. 2001. Quantification of sodium dodecyl sulfate in microliter-volume biochemical samples by visible light spectroscopy. *Annal Biochem.*, **295**: 31-37.

Sandbacka M, Chistianson I and Isoma B.2000. The acute toxicity of surfactants on cells of *Daphnia magna* and fish-a comparative study. *Toxicol Vitro*, **14**: 61–68.

Schleheck D, Lechner M and Svhonenberger R. 2003. Desulfonation of the disulfodiphenylether carboxylates from alkyldiphenyletherdisulfonate surfactants. *Appl Environ Microbiol.*, **69**: 938–944.

Shukor MY, Husin WS, Rahman MF, Shamaan NA and Syed MA. 2009. Isolation and characterization of an SDS-degrading *Klebsiella oxytoca*. *J Environ Biol.*, **30**: 129-134.

Singer MM and Tjeerdema RS. (1992): Fate and effects of the surfactant sodium dodecyl sulfate. *Revised Environ Contamination and Toxicol*., **133**: 95–14916.

Singh KL, Kumar A and Kumar A. 1998. Short communication, *Bacillus cereus* capable of degrading SDS shows growth on variety of detergents. *World J Microbiol Biotechnol*., **14**: 777-779.

Sneath PHA. 1996. **Bergey's Manual of Determinative Bacteriology**. William and Wilkins, Baltimore.

JJBS

Jordan Journal of Biological Sciences

Volume 10, Number 4,December 2017
ISSN 1995-6673
Pages 257 - 264

HPLC-DAD Fingerprinting Analysis, Antioxidant Activity of Phenolic Extracts from *Blighia sapida* Bark and Its Inhibition of Cholinergic Enzymes Linked to Alzheimer's Disease

Oluwafemi A. Ojo[1,*], Basiru O. Ajiboye[1], Adebola B. Ojo[2], Israel I. Olayide[1], Ayodele J. Akinyemi[1], Adewale O. Fadaka[1], Ebenezer A. Adedeji[1], Aline A. Boligon[3] and Marli M. Anraku de Campos[3]

[1] *Department of Biochemistry;* [2] *Department of Medical Biochemistry, Afe Babalola University, Ado-Ekiti, Mail Bag 5454, Nigeria;*

[3] *Graduate Program in Pharmaceutical Sciences, Federal University of Santa Maria, Build 26, room 1115, Santa Maria, CEP 97105-900, Brazil.*

Received: June 21, 2017; Revised: August 13, 2017; Accepted: August 17, 2017

Abstract

In West Africa, the stem of *Blighia sapida* K.D. Koenig are commonly used as remedy against a variety of diseases, including neurodegenerative diseases without scientific basis. The present study characterizes the phenolic constituents, assessed the cholinergic enzymes (acetylcholinesterase and butyrylcholinesterase) and evaluated the antioxidant properties of phenolic extracts from *B. sapida* K.D. Koenig**.** Total phenol and flavonoids content was evaluated as well as antioxidants as illustrated by Fe^{2+} chelation, 2,2-diphenyl-1-picrylhydrazyl (DPPH·) radical scavenging ability and 2,2-azino-bis-(3-ethylbenthiazoline-6- sulphonic acid (ABTS·) radical scavenging ability spectophotometrically. The ability of the extract to inhibit the activities of acetylcholinesterase and butyrylcholinesterase was also evaluated. The extract was found to be rich in phenolic acid (gallic acid, ellagic acid) and flavonoids (Quercetrin and Luteolin). The results show that the phenolic extracts had DPPH radical scavenging abilities (IC_{50} = 90.71 µg/mL), ABTS· radical scavenging ability (IC_{50} = 85.47 µg/mL), iron chelation (IC_{50} = 136.61 µg/mL) and reducing power (Fe^{3+}- Fe^{2+}) (400.08 AAE mg/100g). Extracts of *B. sapida* inhibited acetylcholinesterase (AChE) (IC_{50} = 125.56 µg/mL) and butyrylcholinesterase (BChE) (IC_{50} = 230.63 µg/mL) activities in a concentration dependent manner (20-100 µg/mL). Hence, one probable means through which the stem bark execute their anti-Alzheimer's disease activity might be by inhibiting cholinesterase activities in addition to thwarting oxidative-stress-induced neurodegeneration.

Key words: *Blighia sapida*, HPLC-DAD, Acetylcholinesterase, Butyrylcholinesterase, Alzheimer Disease (AD), Antioxidant.

1. Introduction

Alzheimer's disease (AD) is a neurodegenerative disease associated with progressive loss of memory and cognition, and there are no definitive treatments or prophylactic agents. Cholinergic abnormalities, alongside β-amyloid plaques, neurofibrillary tangles, and extensive neuronal loss, are the major characteristics in AD (Shimohama and Kihara, 2004). AD is clinically characterized by the development of a progressive dementia, with memory loss, disturbances in language, vision spatial relations, and behavior. Among the rudimentary and common characteristics of AD is the severe deterioration of cholinergic neurons projecting from basal forebrain to cortical and hippocampal areas, associated with decrease in acetylcholine content in cholinergic target areas in AD brains (Contestabile, 2011). The biosynthetic enzyme choline acetyltransferase (ChAT) for acetylcholine (ACh), is reduced 60–90% in AD brains, and the degree of its loss is found with the severity of the observed cognitive impairments (Winkler *et al*., 1998). The action of ChAT in the synthesis of cholinergic neurotransmitter acetylcholine is inhibited by acetylcholinesterase (AChE) and butyrylcholinesterase (BuChE) (Nordberg *et al*., 2013). The deterioration of cholinergic nervous system in AD is accompanied by degeneration of many different types of neurons, with a profound loss of forebrain cholinergic neurons, which is accompanied by a progressive decline in acetylcholine. Both the acetylcholine-synthesizing enzyme ChAT, as well in the acetylcholine-hydrolyzing enzyme, AChE are

* Corresponding author. e-mail: oluwafemiadeleke08@gmail.com.

affected. In the development of AD, therapies designed to reverse the cholinergic deficit are in large measure based on the importance of cholinergic function in cognition (García-Ayllón, 2011). The decrease of cholinergic activity can be enhanced by agents that restore or enhance cholinergic transmission in the synaptic cleft. AD and other related disorders are aimed at improving the associated cholinergic deficit by inhibiting AChE, resulting in an enhancement in the cognitive performance and in endogenous level of ACh in the brain (Elufioye *et al*., 2010). Hence, most therapeutic strategies in AD have been directed to the beta-amyloid peptides and cholinergic transmission. The first approach is to act on the Amyloid Precursor Protein (APP) processing while the later to reduce neuronal degradation or increasing cholinergic transmission which will help in the management of cognitive deficits (Mikiciuk-Olasik *et al*., 2007). Butyrylcholineterase (BuChE) has been observed to increases in the brain of AD patients and activity are commonly observed in the cerebral cortex and hippocampus (Elufioye *et al*., 2010). AChE and BuChE play a role in cholinergic signaling; BuChE can hydrolyze ACh and compensate for AChE when levels are depleted (Reid *et al*., 2013). In addition, BuChE genotype may investigate AD risk and rate of disease progression, hence, methods that increase acetylcholine levels, such as cholinesterase inhibitors, demonstrate symptomatic efficacy in AD (Nordberg *et al*., 2013). A study that investigated the effect of a selected brain-target BuChE inhibitor, cymserine analogs, revealed a long-term inhibition of butyrylcholinesterase and elevated extracellular brain acetylcholine in rats. Hence, describing the improvement from cholinergic deficit by inhibiting BuChE (Greig *et al*., 2005). In addition to factors leading to this neurodegenerative disease, oxidative stress also contributes to the development to Alzheimer's disease regarding the fact that tissues in the brain are vulnerable to Oxidative Stress (OS). Increased production of Reactive Oxygen Species (ROS), due to the level of oxygen consumption by the brain, lessen antioxidant systems, and repairing mechanisms to Alzheimer's Disease (AD). Also, mitochondrial dysfunction and ROS have been shown in the cause of AD. Impairments of mitochondrial function and oxidative stress may precede Aβ overproduction and deposition, and neurons in AD exhibit a significantly higher percentage of damaged mitochondria (Barbagallo *et al*., 2015; Pimentel *et al*., 2012). Furthermore, lipid peroxidation, causing damage to membrane phospholipids in AD, produces 4-hydroxynonenal which is found high in AD and causes neuronal death by interfering the ATPases involved in transfer of ions and calcium balance. A study showed that excessive ROS in patients with AZ was abated after the intake of an antioxidant-rich plant extract for 6 months (Christen, 2000).

Blighia sapida K.D. Koenig, commonly known as 'Akee apple', belongs to a plant family called *Sapindaceae*. *B. sapida* is a medicinal plant commonly used by traditional healers in Nigeria, and highly valued in Africa for the treatment of various diseases (John-Dewole and Popoola, 2013). The phytochemical screening of aqueous extract of *B. sapida stem bark* has been shown to contain alkaloids, saponins, cardiac glycosides, reducing sugars and carbohydrates, and it was stated to have several ethnomedicinal purposes; the pulp and leafy juice are used as eye drops in ophthalmic lesions and conjunctivitis (Saidu *et al*., 2013; Hamzah *et al*., 2013). The extracts from stem bark of *B. sapida* have been reported to be used by indigenes of Sagamu, Nigeria, as an antiaging by mixing it with black soap and bathing daily, and were shown to exhibit anti-microbial activity against *S. aureus* and *B. subtilis* (Elufioye, 2012; Udobi *et al*., 2013) and also to ameliorative pancreatic β-cell dysfunction in diabetic rats (Ojo *et al*., 2017). Hence, since limited information is known about the activity of *B. sapida* in management of AD, there is a curiosity to examine the inhibitory activity of phenolic extract from *B. sapida* bark against cholinergic enzymes associated with AD, AChE and BuChE. In addition, AD is associated with increased oxidative stress. Investigating the antioxidant activity of the extracts from *B. sapida* bark against free radicals is essential to reveal its ability to counteract excessive ROS in AD patients.

2. Material and Methods

2.1. Chemicals and Reagents

All chemicals and reagents used in the present study were of analytical grade. Methanol, formic acid, acetic acid, gallic acid and ellagic acid were purchased from Merck (Darmstadt, Germany). Folin-Ciocalteu reagent, 2, 2-diphenyl-1-picrylhydrazyl (DPPH), linoleic acid, and α-tocopherol, quercetin and luteolin were acquired from Sigma Chemical Co. (St. Louis, MO, USA). Acetylcholinesterase (EC.3.1.1.7) and butrylcholinesterase (EC 3.1.1.8) were products of Fluka Co., Germany. Acetylthiocholine iodide (ATChI), butyrylthiocholine chloride (BTChCl), 5:5-dithiobis-2-nitrobenzoic acid (DTNB); eserine and sodium bicarbonate were from Sigma Co. UK. High performance liquid chromatography (HPLC-DAD) was performed with a Shimadzu Prominence Auto Sampler (SIL-20A) HPLC system (Shimadzu, Kyoto, Japan), equipped with Shimadzu LC-20AT reciprocating pumps connected to a DGU 20A5 degasser with a CBM 20A integrator, SPD-M20A diode array detector and LC solution 1.22 SP1 software.

2.2. Plant Material and Preparation

The plant was purchased from Bisi Market, Ado-Ekiti, Ekiti State, Nigeria. The herberia specimen of the plants was prepared and voucher specimens deposited at the Herbarium located at the Biology Department, Afe Babalola University, Ado-Ekiti. The stem barks were washed, air-dried and milled into a fine powder and thereafter weighed.

2.3. Extraction of Phenol Extract

Phenol-rich extract from *B. sapida* K.D. Koenig stem bark was acquired by dissolving the powder in an 80% acetonic solution for 72 h. It was then filtered employing a cheese cloth, concentrated to a small volume to remove the entire acetone using rotary evaporator. Then, it was transferred into a 500 mL beaker and placed in a water bath (40 ˚C) to evaporate to dryness. The extract was kept in a closed container and kept inside the fridge at 4 ˚C for further studies (Marimoutou *et al*., 2015).

2.4. Cholinesterase Activity Assay

Acetycholinesterase and Butyrylcholinesterase activity were, respectively, carried out using the colorimetric method of (Tor *et al*., 1994). The reaction assay mixture consisted 2000 mL 100 mM phosphate butter pH 8.0, 100 mL of test phenol extracted, 100 mL, of enzyme AChE or BuCHE solution at a final concentration of 0.03 U/mL and 0.01 µ/mL, respectively, 100 µL of DTNB (0.3 mM) prepared in 100 M phosphate buffer pH 7.0 containing 120 mM sodium bicarbonate. The mixture was vortexed and then pre-incubated in a water bath at 37^{o}C for 30 min. The reaction was then investigated by the adding 100 µL of ATCI or BTCI at a final concentration of 0.5 mM as a negative control. The absorbance change at wavelength 412 nm was then measured for a period of 5 min. All assays were done in triplicate. Eserine (-) physiotigmine) was used as positive control. The % inhibition was calculated as follows:

% = [(a-b)/a] x 100

where: a = ΔA/min of control; b = ΔA/min of test sample; ΔA = Change in absorbance.

2.5. *Determination of Total Phenolic Content*

All the phenolic contents present in the phenol extract were determined using Folin–Ciocalteu method, slightly modified as described by Boligon *et al*. (2009). Gallic acid was the standard and samples were carried out in triplicate at wavelength 730 nm in a spectrophotometer. The total phenolic content of sample was expressed in mg/100g gallic acid (GAE).

2.6. Determination of Total Flavonoid Contents

Total flavonoid contents were carried according to a slightly modified colorimetric method described by Woisky and Salatino (1998). Briefly, each sample (0.5 mL) was added to $AlCl_3$ (2%, w/v, 0.5 mL). The absorbance was measured at wavelength 420 nm against the blank. Quercetin was used as standard and samples were performed in triplicate. The flavonoid content was expressed in mg/100g quercetin (QE).

2.7. *Radical-Scavenging Activity—DPPH Assay*

The phenol extract was evaluated for its antioxidant activity by monitoring its potency in scavenging the stable free radical DPPH, according to Choi *et al*. (2002). The DPPH quenching ability was expressed as IC50 (the extract concentration required to inhibit 50% of the DPPH in the assay medium). The absorption was measured at 518 nm and ethanol was used to calibrate the spectrophotometer. The test was performed in triplicate and the antioxidant activity was
calculated by the equation:

$$\%\text{inhibition} = 100 - [((Abs_{sample} - Abs_{blank}) * 100)/ Abs_{control}]$$

where Abs_{sample} is absorbance of sample; Abs_{blank} is absorbance of fractions without adding the DPPH; $Abs_{control}$ is absorbance the solution of negative control.

2.8. Determination of Ferric Ion Reducing Antioxidant Power: FRAP Assay

The reducing property of the *B. sapida* stem bark extract was studied by assessing the ability of the extract to scale back $FeCl_3$ solution as delineated by Mukhopadhyay *et al*. (2015). A 2.5 mL aliquot was mixed with 2.5 mL of 200 mM sodium phosphate buffer (pH 6.6) and 2.5 mL of 1% potassium ferricyanide. The solution was incubated for 20 min at 50 °C in a water bath and then 2.5 mL of 10% trichloroacetic acid was added. The sample was then centrifuged at 650 g for 10 min. After that, 5 mL of the supernatant was mixed with an equal water volume and one mL, 0.1% $FeCl_3$. The above-stated process was conjointly applied to a standard ascorbic acid solution, and finally the absorbance was read at 700 nm. The reducing ability was calculated as percentage inhibition.

2.9. Ferrous Ion Chelating Activity Assay

The ferrous ion chelating activity of the phenol extract of *B. sapida* was determined according to Mukhopadhyay *et al*. (2015). In this process, ferrozine, the reaction initiator of the assay, combines with divalent iron to form a stable magenta complex species, the absorbance of which is measured at 562 nm.

The chelating activity of the sample extract was calculated as:

Ferrous ion chelating ability in % = [1-(test sample absorbance/blank sample absorbance)] X 100%

2.10. ABTS Radical Scavenging Assay

ABTS radical scavenging assay was determined by the method of Re *et al*. (1999). Firstly, stock solutions that included 7 mM ABTS solution and 2.4 mM potassium persulfate solution were prepared, mixed together in equal quantities and allowed to react for 12 h at room temperature in the dark. Sample (1 mL) was added to 1 mL of the ABTS solution and the absorbance was taken at 734 nm after 7 min using the spectrophotometer:

%inhibition= [(Abs control –Abs sample)]/ (Abs control)] x 100

Abs control is the absorbance of ABTS radical + methanol; absorbance sample is the absorbance of ABTS radical + sample extract /standard.

2.11. HPLC-DAD Fingerprinting

Bliglia sapida bark extract at 12 mg/mL was taken onto reversed phase Phenomenex C_{18} column (4.6 mm x 250 mm) packed with 5 µm diameter particles. The mobile phases were 0.5% (v/v) aqueous formic acid (solvent A) and 1% (v/v) acetic acid in methanol (solvent B). The binary elution system was as follows: 2% B at initial 5 min used to wash the column, a linear gradient 8% B (25 min), 12% B (45 min), 24% B (60 min). After 80 min, organic phase concentration was taken back to 2% (B) and lasted 10 min for column equilibration. Flow rate of 0.6 mL/min and injection volume 40 µl (Ademosun *et al*., 2016). Thereafter, quantifications were carried out by integrating the peaks using the external standard method, at 257 nm for gallic and ellagic acids; and 366 for quercetin and luteolin. The extract and mobile phase were filtered using 0.45 µm membrane filter (Millipore) and degassed by ultrasonic bath prior to use. Stock solutions of standards references were prepared in the HPLC mobile phase at a concentration range of 0.030 – 0.500 mg/mL. Chromatography peaks were confirmed by comparing its retention time with those of reference standards and by DAD spectra (200 to 700 nm). All chromatography operations were carried out at ambient temperature and in triplicate.

2.12. Data Analysis

The results obtained for DPPH, total flavonoids, total phenols, FRAP, iron chelation, ABTS assays and HPLC were assessed by an analysis of variance model and Tukey's test (HSD multiple range post hoc test). The level of significance for the analyses was set to $p < 0.05$. These analyses were performed by using the free software R version 3.1.1. (R Core Team, 2014) and expressed as mean ± standard error of mean.

3. Results

3.1. Cholinesterase Assay

Acetylcholinesterase inhibitory properties of *B. sapida* phenolic stem bark extract was examined and the result is displayed in Figure 1; the result shows that the phenol extract inhibited AChE activity in a concentration-dependent manner (20–100 μg/mL), having an IC_{50} (extract concentration causing 50% inhibition) value of 125.16 μg/mL as displayed in Table 1. Likewise, the ability of the phenolic extract to inhibit butyrylcholinesterase activity *in vitro* was also assessed, and the result is displayed in Figure 2. The result reveals that the phenol extract inhibited BChE in a concentration-dependent manner (20– 100 μg/mL) having an IC_{50} (extract concentration causing 50% inhibition) value of 230.63 μg/mL as revealed in Table 2.

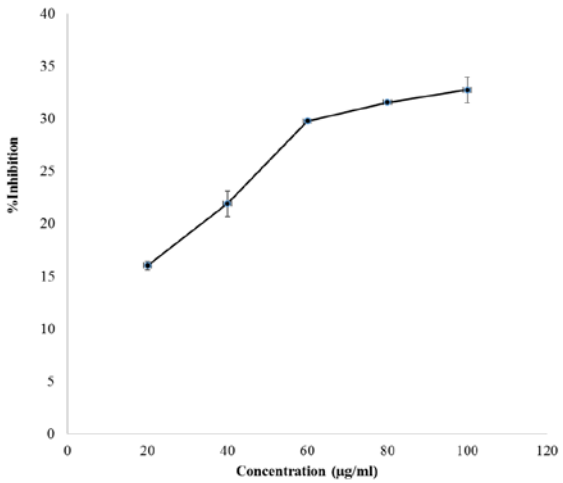

Figure 1. Acetylcholinesterase inhibition by phenolic extract from *Blighia sapida* stem bark
Values are expressed as mean ± SEM for three determinations

Table 1. IC_{50} values for Fe^{2+} chelating ability, DPPH·, ABTS· as well as acetylcholinesterase and butyrylcholinesterase inhibitory activities

Sample	IC_{50} (µg/ml)
Fe Chelation	136.61 ± 7.30
DPPH·	90.71 ± 0.35
ABTS·	85.47 ± 0.30
Acetylcholinesterase	125.16 ± 7.07
Butyrylcholinesterase	230.63 ± 9.07

Values represent means ± standard mean of error

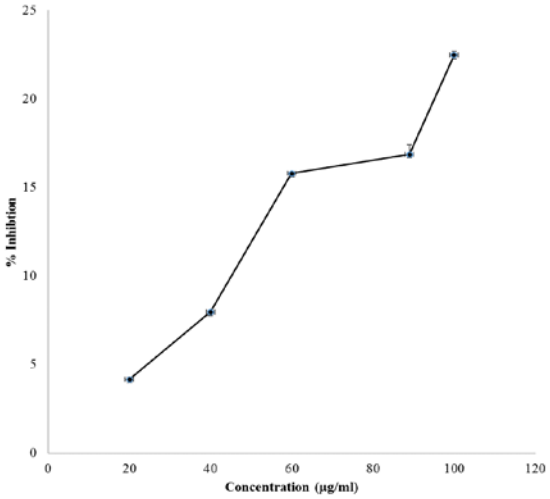

Figure 2. Butyrylcholinesterase inhibition by phenolic extract from *Blighia sapida* stem bark
Values are expressed as mean ± SEM for three determinations

Table 2. Total phenol content, total flavonoid content and reducing properties (FRAP) values of aqueous phenolic extract of *Blighia sapida*

Parameters	Value
Total phenol content (GAE mg/100g)	133.02 ± 32.83
Total flavonoid content (QUE mg/100g)	10.01 ± 1.78
Ferric reducing antioxidant property (AAE mg/100g)	400.08 ± 24.41

* Values represent means ± standard mean of error of triplicate readings. AAE=Ascorbic Acid Equivalent; QUE=Quercetin Equivalent and GAE=Gallic Acid Equivalent

3.2. Phenolic and Flavonoid Content

The results for the total phenol and total flavonoid content of the phenolic extract of stem bark of *B. sapida* are presented in Table 2. The results reveal that *B. sapida* had a total phenol content of 133.02 mg GAE/100g and the total flavonoid content of 10.01 mg QUE/100g.

3.3. DPPH Scavenging Activity

DPPH radical scavenging ability is displayed in Figure 3, with its IC_{50} values (90.71 µg/mL) in Table 2. The result reveals that the phenolic extracts from *B. sapida* scavenged free radicals in a concentration-dependent manner (20-100 µg/mL).

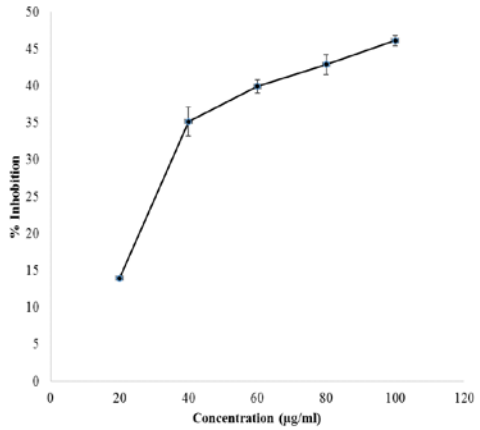

Figure 3. DPPH· scavenging ability of phenolic extract from *Blighia sapida* stem bark.
Values are expressed as mean ± SEM for three determinations

3.4. Reducing Property

The free radical scavenging ability of the *B. sapida* was assessed and the results are presented in Table 2. The results reveal that the *B. sapida* extract (400.08 AAEmg/100g) reduced Fe^{3+} to Fe^{2+} as shown in Table 2.

3.5. Iron (Fe2+) Chelating Ability

Fe^{2+} chelating ability of phenolic extracts from *B. sapida* is presented in Figure 4 and its IC_{50} values of 136.61 µg/mL. The result reveals that the phenolic extract of *B. sapida* exhibited metal chelating activity in a concentration-dependent manner, as shown in Figure 4.

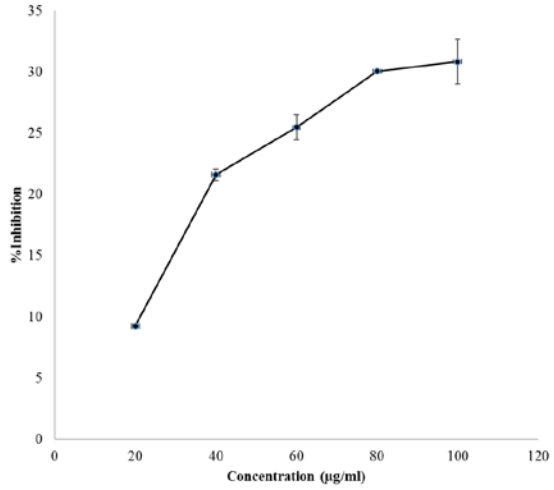

Figure 4. Fe^{2+} chelating ability of phenolic extract from *Blighia sapida* stem bark.
Values are expressed as mean ± SEM for three determinations

3.6. 2,2-Azino-bis3-ethylbenthiazoline-6sulphonic acid (ABTS·) Radical Scavenging Ability

The free radical scavenging ability of the *B. sapida* phenolic stem bark extract was consequently evaluated using the moderately stable ABTS radical (ABTS·) and displayed in Figure 5 with IC_{50} values of 85.47 µg/mL. The results show that the *B. sapida* phenolic extract quenched ABTS radical in a concentration-dependent manner (20-100 µg/mL).

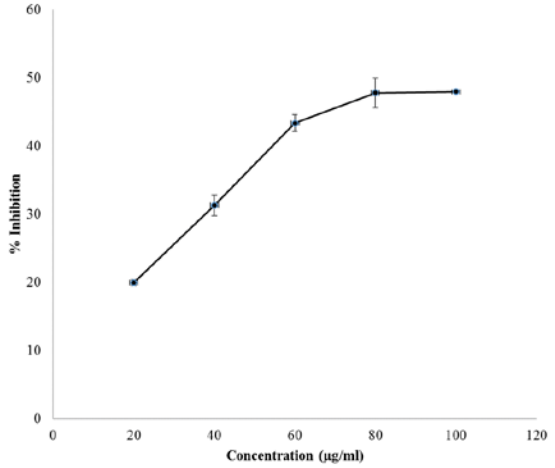

Figure 5. ABTS· scavenging ability of phenolic extract from *Blighia sapida* stem bark
Values are expressed as mean ± SEM for three determinations

3.7. HPLC-DAD Analysis of Phenolic Composition

The phenolics (flavonoids and phenolic acids) composition of *B. sapida* bark as quantified using HPLC-DAD are presented in Table 3. The major phenolic acid was gallic acid, ellagic acid, whereas quercetin and luteolin were the major flavonoids. The result show that the stem bark had high levels of some major flavonoids and phenolic acids of pharmacological importance, including gallic acid, ellagic acid, quercetin and luteolin (Figure 6).

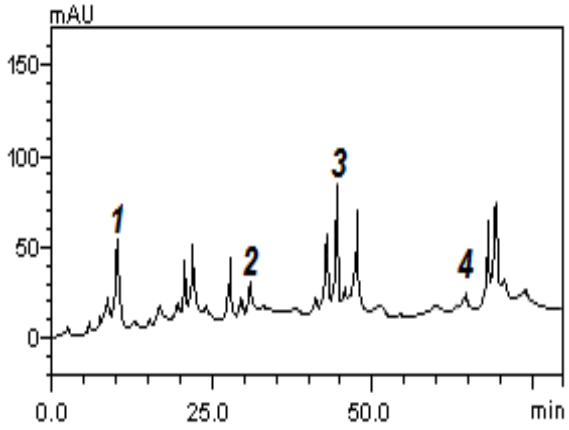

Figure 6. Representative high performance liquid chromatography profile of *Blighia sapida*. Gallic acid (peak 1), ellagic acid (peak 2), quercetin (peak 3) and luteolin (peak 4)

4. Discussion

Mental disorder, also called mental ailment, is a mental or a behavioral pattern of brain functions in life that lead to either suffering or an impaired ability to retain information for a while in the brain. Inhibition of the enzyme linked to Alzheimer's disease with the use of modern drugs has been linked with some side effects that include headache, diarrhoea, drowsiness and vomiting, among others, unlike the use of natural products. The plant parts employed in the present study have been a bailout for those suffering from Alzheimer's disease in traditional medicine although

the mechanism of action remains unknown. Medicinal plants are rich sources of phytochemical, and intakes of these plant chemicals have a protective potential against neurodegenerative diseases (Chu *et al*., 2002; Ojo *et al*., 2013). However, phenolic extracts of *B. sapida* bark inhibited both acetylcholinesterase (AChE) and butyrylcholinesterase (BChE) activity. Inhibition of acetylcholinesterase is well thought out as a probable method for the management of Alzheimer's disease and for doable therapeutic applications in the treatment of Parkinson's disease and ageing (Nochi *et al*., 1995). However, BChE has been considered to be directly connected with the side effects of the AChE inhibitors and the existing drugs of Alzheimer's disease (Tong *et al*., 1996). Medicinal plants that possess a high phenolic content have been reported to inhibit AChE activity *in vitro* (Benamar *et al*., 2010; Adefegha and Oboh, 2012). Cholinesterases inhibition by the *B. sapida* may be of great importance because it could be an appropriate therapeutic approach in the management or treatment of neurodegenerative disorders. Similarly, in certain forms of Alzheimer's disease, BChE variant has been revealed to upsurge brain susceptibility, thus making BChE inhibition of the extract another means in managing neurodegenerative ailments. As soon as AChE is inhibited, acetylcholine degradation in the brain becomes impossible. The subsequent increase in the brain neurotransmitter acetylcholine concentrations enhances the communication between nerve cells that use acetylcholine as a chemical messenger, and this may recover or soothe the symptoms of Alzheimer's disease momentarily (Howes *et al*., 2003). Phenolic extract of *B. sapida* was able to inhibit AChE and BChE activities in a concentration-dependent manner *in vitro*. This AChE and BChE inhibition is partially in agreement with some earlier reports where plant phytochemicals revealed a considerable improvement in the cognitive performance and memory (Maruyama *et al*., 2006). The ability of the extract to inhibit AChE and BChE may be owing to the antioxidant ability of the plant. Phenolic compounds can protect the human body from free radicals, whose formation is associated with the convectional metabolism of aerobic cells. They are strong antioxidants capable of removing free radicals, chelate metal catalysts, activate antioxidant enzymes, reduce α-tocopherol radicals and inhibit oxidases (Marin *et al*., 2004). The antioxidant properties showed a promising result to fight free radicals in the body system. It revealed that phenolic extract of *B. sapida* had a total phenolic (133.02 mg GAE/100g) and total flavonoid (10.01 mg QUE/100g) constituent (Table 2). Flavonoids are regarded as antioxidant molecules and could, hence, reduce cellular oxidative stress (Oboh *et al*., 2007).

DPPH abstracts hydrogen or electrons from stable molecules, turning them into free radicals, as it becomes a stable diamagnetic molecule (Gyamfi *et al*., 1999; Shim *et al*., 2003). Hence, phenolic scavenge DPPH by donating electrons or hydrogen to stabilize the radical. The present investigation reveals that phenolic extracts from *B. sapida* stem bark scavenged DPPH free radicals in a concentration dependent manner (20–100 µg/mL). However, the radical scavenging abilities of the phenol extracts correlate with the total phenolic contents of the stem. Thus, the observed DPPH radical scavenging ability might be attributed to the abundant phenolic constituents in the extracts. This is consistent with the previous studies (Ojo *et al*., 2013; Ojo *et al*., 2014).

The reducing powers of the phenolic extracts of *B. sapida* were evaluated based on their ability to reduce Fe^{3+} to Fe^{2+}. As displayed by the results, *B. sapida* had a reducing property of (400.08 mg AAE/100g). Reducing power is an antioxidant defense system; the two mechanisms that have an effect on this property are electron transfer and hydrogen atom transfer (Tanaka *et al*., 1998; Dastmalchi *et al*., 2007). The reducing capacity of the extracts may be a sign of its potential antioxidant activities due to the presence of reductants.

Metal ions, for example Fe^{2+}, which results in the induction of oxidative stress, have been reported to be coupled with Alzheimer's disease (Tabert *et al*., 2005). The phenolic extract of *B. sapida* significantly chelate Fe^{2+} in a concentration dependent manner (20–100 µg/mL). By chelating Fe^{2+}, the generation of hydroxyl radicals in the Fenton reaction may be attenuated and thus prevent possible damage of hydroxyl radicals to biomolecules. Accumulation of iron has been reported to lead to an increase in the free radicals and development of oxidative stress (Shim *et al*., 2003).

The free radical scavenging ability of the *B. sapida* extracts was studied employing a moderately stable nitrogen-centred radical species (Re *et al*., 1999). The results of the 2,2′-azino-bis (3-ethylbenthiazoline-6-sulphonic acid (ABTS·) radical scavenging ability of the phenolic extracts of *B. sapida* disclose that the extracts are able to scavenge ABTS· radicals in a concentration-dependent manner (20 - 100 µg/mL). The ABTS· scavenging ability of the stem bark might be due to the hydrogen donating ability of the phenolics present in the extract of *B. sapida* to the single pair of ABTS radical.

The antioxidant properties of plant foods have been associated with the presence of an array of important phenolic and nonphenolic phytochemicals, including phenolic acids and flavonoids (Cheplick *et al*., 2007). However, characterization of the extract with HPLC revealed that the major constituents of the phenolic extract from *B. sapida* bark are gallic acid, ellagic acid, quercetin and luteolin of which the level of gallic acid and quercetin were high. The high amounts of gallic acid (2.07 ± 0.01 mg/g) observed in *B. sapida* may be linked to the biological effects of the plant. These phenolic compounds are well acknowledged as potential antioxidants, free radical scavengers, metal chelation agents and inhibitors of lipid peroxidation (Rice-evans *et al*., 1997; Pereira *et al*., 2009).

5. Conclusion

Phenolic extracts of *B. sapida* stem bark are rich in both phenolic and flavonoids compounds that exhibit both anticholinesterase and antioxidant activity. These herbs show a great potential in the management of Alzheimer's disease as it exhibited an inhibitory activity on cholinergic enzymes (acetylcholinesterase and butyrylcholinesterase) in a concentration-dependent manner and exhibit radical scavenging ability due to the phytochemicals present in the extract.

Conflict of Interest

The authors declare that there is no conflict of interests whatsoever throughout the compilation of the manuscript.

Acknowledgments

The authors would like to thank Graduate Program in Pharmaceutical Sciences (Federal University of Santa Maria) for providing the HPLC profile of *B. sapida.*

References

Adefegha SA and Oboh G. 2012. Acetylcholinesterase (AChE) inhibitory activity, antioxidant properties and phenolic composition of two *Aframomum* species. *J Basic Clin Physiol Pharmacol*., **23**:153–161.

Ademosun AO, Oboh G, Passamonti S, Tramer F, Ziberna L, Boligon AA, Athayde ML. 2016. Phenolic composition of orange peels and modulation of redox status and matrix metalloproteinase activities in primary (Caco-2) and metastatic (LoVo and LoVo/ADR) colon cancer cells. *Eur Food Res Technol*., **242**: 1949-1959.

Barbagallo M, Marotta F and Dominguez LJ.2015. Oxidative stress in patients with Alzheimer's Disease: Effect of extracts of fermented papaya powder. *Mediators Inflamm*., **2015**:624801.

Benamar H, Rached W, Derdour A and Marouf A. 2010. Screening of Algeria medicinal plants for acetylcholinesterase inhibitory activity. *J Biol Sci*., **10**: 100–109.

Boligon AA, Pereira RP, Feltrin AC, Machado MM, Janovik V, Rocha JB and Athayde ML. 2009. Antioxidant activities of flavonol derivates from the leaves and stem bark of *Scutia buxifolia* Reiss. *Bioresources Technol*., **100**: 6592–6598.

Cheplick S, Kwon Y, Bhowmik P and Shetty K. 2007. Clonal variation in raspberry fruit phenolics and relevance for diabetes and hypertension management. *J Food Biochem.*, **31**: 656-79.

Choi CW, Kim SC, Hwang SS, Choi BK, Ahn HJ, Lee MY, Park SH, Kim SK. 2002. Antioxidant activity and free radical scavenging capacity between Korean medicinal plants and flavonoids by assay-guided comparison. *Plant Sci*., **163**: 1161–1168.

Christen Y. 2000. Oxidative stress and Alzheimer disease. *Am J Clin Nutr*., **71(2)**: 621– 629.

Chu Y, Sun J, Wu X and Liu RH. 2002. Antioxidant and antiproliferative activity of common vegetables. *J Agri Food Chem.*, **50(23)**: 6910-6916.

Contestabile A. 2011. The history of the cholinergic hypothesis. *Behavioural Brain Res*., **221(2):** 334–340.

Dastmalchi K, Dorman H, Korsa M and Hiltunen R. 2007. Chemical composition of in vitro antioxidant evaluation of a water soluble mediavan balm (*Dracocephalum moldavica* L.) extract. *LWT*. **40**:239–248.

Elufioye TO, Obuotor EM, Sennuga AT, Agbedahunsi JM and Adesanya SA. 2010. Acetylcholinesterase and butyrylcholinesterase inhibitory activity of some selected Nigerian medicinal plants. *Revista Brasileira de Farmacognosia*, **20(4):** 472–477.

Elufioye T. 2012. Ethnomedicinal study and screening of plants used for memory enhancement and Antiaging in Sagamu, Nigeria. *Eur J Med Plants*, **2(3):** 262–275.

García-Ayllón MS. 2011. Revisiting the role of acetylcholinesterase in Alzheimer's disease: Cross-talk with P-tau and β-amyloid. *Front Mol Neurosci* ., **4**: 22.

Greig NH, Utsuki T, Ingram D K, Wang Y, Pepeu G, Scali C, Yu Q-S, Mamczarz J, Holloway HW, Giordano T, Chen D-m, Furukawa K, Sambamurti K, Brossi A and Lahiri DK. 2005. Selective butyrylcholinesterase inhibition elevates brain acetylcholine, augments learning and lowers Alzheimer β-amyloid peptide in rodent. *PNAS*, **102(47)**: 17213–17218.

Gyamfi MA, Yonamine M and Aniya Y. 1999. Free-radical scavenging action of medicinal herbs from Ghana: *Thonningia sanguinea* on experimentally-induced liver injuries. *Gen Pharmacol.*, **32**:661–667.

Hamzah R, Egwim E, Kabiru A and Muazu M. 2013. Phytochemical and *in vitro* antioxidant properties of the methanolic extract of fruits of *Blighia sapida*, *Vitellaria paradoxa* and *Vitex doniana*. *Oxid Antioxid Med Sci*, **2(3):** 215-221.

Howes M, Perry N and Houghton P. 2003. Plants with traditional uses and activities, relevant to the management of Alzheimer's disease and other cognitive disorders. *Phytotherapy Res*., **17**:1–18.

John-Dewole OO and Popoola OO. 2013. Chemical, phytochemical and antimicrobial screening of extracts of *B. sapida* for agricultural and medicinal relevances. *Nat Sci.*, **11(10):**12-17.

Marimoutou M, Le Sage F, Smadja J *et al*. 2015. Antioxidant polyphenol-rich extracts from the medicinal plants *Antirhea borbonica*, *Doratoxylon apetalum* and *Gouania mauritiana* protect 3T3-L1 preadipocytes against H2O2, TNFα and LPS inflammatory mediators by regulating the expression of superoxide dismutase. *J Inflam*., **12(1):** 10.

Marin A, Ferreres F, Tomas-Barberan FA and Gil MI. 2004. Characterization and quantitation of antioxidant constituents of sweet pepper (*Capsicum annuum* L.). *J Agr Food Chem*., **52(12):** 3861-3869.

Maruyama M, Tomita N and Iwasaki K. 2006. Benefits of combining donepezil plus traditional Japanese herbal medicine on cognition and brain perfusion in Alzheimer's disease: a 12-week observer blind, donepezil monotherapy controlled trial. *J Am Geriatric Soc*.,**54**:869–871.

Mikiciuk-Olasik E, Szymaski P and Zurek E. 2007. Diagnostics and therapy of Alzheimer's disease. *Indian J Experimental Biol*.,**45**: 315-325.

Mukhopadhyay D, Rahman HA, Roy D and Dasgupta P. 2015. Evaluation of *In-vitro* antioxidant activity and phytochemical constituents of kulekhara (Hygrophiliaspinosa). *Inter J Pharmaco Phytochem Res*., **7**:1-7.

Nochi S, Asakawa N and Sato T. 1995. Kinetic study on the inhibition of acetylcholinesterase by 1-benzyl-4- [(5,6-dimethoxy-1-indanon)-2-yl] methylpiperidine hydrochloride (E2020). *Biol Pharma Bulletin*, **18(8):**1145–1147.

Nordberg A, Ballard C, Bullock R, Darreh-Shori T and Somogyi M. 2013. A Review of butyrylcholinesterase as a therapeutic target in the treatment of Alzheimer's disease. *Primary Care Companion for CNS Disorders*, **15**:2

Oboh G, Puntel RL and Rocha JBT. 2007. Hot pepper (*Capsicum annuum*, Tepin and Capsicum Chinese, Hernero) prevent Fe^{2+}-induced lipid peroxidation in brain: *in vitro*. *Food Chem* **102**:178–185.

Ojo OA, Oloyede OI, Olarewaju OI and Ojo AB. 2013. *In Vitro* antioxidant activity and estimation of total phenolic content in ethyl acetate extract of *Ocimum gratissimum. Pharmacol Online*, **3**:37-44.

Ojo OA, Oloyede OI, Tugbobo OS, Olarewaju O and Ojo A. 2014. Antioxidant and inhibitory effect of scent leaf (*Ocimum gratissimum*) on Fe^{2+} and sodium nitroprusside induced lipid peroxidation in rat brain *in vitro*. *Advanced Biol Res*., **8(1):**8-17.

Ojo OA, Ajiboye BO, Ojo AB, Oyinloye BE, Imiere OD and Adeyonu O. 2017. Ameliorative potential of *Blighia sapida* K.D. Koenig bark against pancreatic -cell dysfunction in alloxan-induced diabetic rats. *J Complementary and Integrative Med*., DOI: 10.1515/jcim-2016-0145.

Pereira RP, Fachinetto R, De souza prestes A *et al*. 2009. Antioxidant effects of different extracts from *Melissa officinalis* and *Cymbopogon citratus. Neurochem Res*., **34**:973–983.

Pimentel C, Batista-Nascimento L, Rodrigues-Pousada C and Menezes RA. 2012. Oxidative stress in Alzheimer's and Parkinson's diseases: Insights from the yeast *Saccharomyces cerevisiae*. *Oxidative Medicine and Cellular Longevity* Article ID 132146, 9 pages.

R Core Team. 2014. A language and environment for statistical computing," R Foundation for Statistical Computing, Vienna, Austria.

Re R, Pellegrini N, Proteggente A *et al*. 1999. Antioxidant activity applying an improved ABTS radical cation decolorization assay. *Free Rad Biol Med*., **26**: 1231–1237.

Reid GA, Chilukuri N and Darvesh S. 2013. Butyrylcholinesterase and the cholinergic system. *Neurosci*., **234**: 53–68.

Rice-evans CA, Miller NJ and Paganga G. 1997. Antioxidant properties of phenolic compounds. *Trends Plant Sci.*, **2**:152–159.

Saidu AN, Mann A and Ndako M. 2013. Phytochemical studies and effect of the aqueous extract of *Blighia sapida* stem bark on the liver enzymes of albino rats. *Inter Res J Biochem Bioinformatics*, **3(5):** 104-08.

Shimohama S and Kihara T. 2004. Alzheimer's disease and acetylcholine receptors. *Acta Neurobiol Exp*., **64**: 99-105.

Shim YJ, Doo HK and Ahn SY. 2003. Inhibitory effect of aqueous extract from the gall of *Rhus chinensis* on α-glucosidase activity and postprandial blood glucose. *J Ethnopharmacol*., **85**:283–287.

Tabert M, Liu X, Doty R *et al*. 2005. A 10-item smell identification scale related to risk for Alzheimer's disease. *Annals Neurol*., **58**:155–160.

Tanaka M, Kuei CW, Nagashima Y and Taguchi T. 1998. Application of antioxidative maillrad reaction products from histidine and glucose to sardine products. *Nippon Suisan Gakkaishi*, **54**: 1409-1414.

Tong W, Collantes ER, Chen Y and Welsh WJ. 1996. A comparative molecular field analysis study of *N*-benzylpiperidines as acetylcholinesterase inhibitors. *J Med Chem*., **39(2):** 380–387.

Tor ER, Holstege DM and Galey FD. 1994. Determination of cholinesterase activity in brain and blood samples using a plate reader. *J AOAC Int.*, **77**:1308-1313.

Udobi CE, Ubulom PM, Akpabio EI and Eshiet U. 2013. Antimicrobial Activities of Leaf and Stem Bark Extracts of *Blighia sapida. J Plant Studies*, **2(2):** 47-52.

Winkler J, Thal LJ, Gage FH and Fisher LJ. 1998. Cholinergic strategies for Alzheimer's disease. *J Mol Med*., **76(8):** 555–567.

Woisky RG and Salatino A. 1998. Analysis of propolis: some parameters and procedures for chemical quality control. *J Apicultural Res.*, **37**, 99–105.

JJBS

Jordan Journal of Biological Sciences

Volume 10, Number 4,December 2017
ISSN 1995-6673
Pages 265 - 272

Investigation of some Virulence Determents in *Aeromonas hydrophila* Strains Obtained from Different Polluted Aquatic Environments

Mamdouh Y. Elgendy[1*], Waleed S. Soliman[1], Wafaa T. Abbas[1], Taghreed B. Ibrahim[1], Abdelgayed M Younes[1] and Shimaa T. Omara[2]

[1] *Hydrobiology Department, Veterinary Research Division, National Research Centre, 33 El Bohouth Street*

[2] *Microbiology and Immunology Department, Veterinary Research Division, National Research Centre, Dokki, Giza, Egypt*

Received: April 18, 2017; Revised: August 2, 2017; Accepted: August 15, 2017

Abstract

This study aimed to investigate some virulence characteristics of *Aeromonas hydrophila* (*A. hydrophila*) strains obtained from different Egyptian aquatic environments in terms of enzymatic activities, presence of virulence genes and their pathogenicity in *Oreochromis niloticus*. A total of 35 *A. hydrophila* isolates obtained from apparently healthy fish and water samples were examined. Isolates were collected from three different water sources of the River Nile; 15 isolates from El-Sharkawia stream that receives lofty loads of industrial effluents. 11 isolates from El-Rayah El-Towfeky stream at an area known to receive loads of sewage and agricultural discharges and 9 i solates from Bahr Yousuf canal at El-Fayoum governorate. Water and fish samples obtained from the studied areas were also analysed for existence of heavy metals. Isolates obtained from El-Sharkawia stream, exhibited the uppermost enzymatic activities and virulence genes compared to isolates retrieved from other sources. All *A. hydrophila* isolates were pathogenic to *Oreochromis niloticus.* Presence of heavy metal pollutants (Cr, Pb and Mn) in the aquatic environment affected the virulence of *A. hydrophila* isolates with variations in their enzymatic activities and presence of virulence genes.

Key words: *Aeromonas hydrophila,* Virulence, Aquatic Pollution**.**

1. Introduction

Bacteria of the genus *Aeromonas* are distributed widely in the aquatic environments. They have been commonly isolated in greater numbers from; rivers, lakes, streams, canals, sediments, marine as well as chlorinated water especially during hot months (Janda and Abbott, 2010). Certain *Aeromonas* strains have long been considered as serious pathogens in poikilothermic animals, including fish, amphibians and reptiles (Roberts, 2012). These microorganisms also are known to be causative agents of various infections in birds and mammals (Glunder and Siegmann, 1989). Array of human infections relevant to these pathogens also have been described, including gastroenteritis, urinary tract infections, pneumonia, wound infections and septicemia (Chan *et al*., 2003). On the top list of Aeromonads species affecting aquatic animals, *A. hydrophila* has long been considered a pathogen of critical concern in commercial aquaculture causing colossal economic losses (Elgendy *et al*., 2015). Wide spectrum of fresh as well as marine fish species can be common targets for such epizootics (Moustafa *et al*., 2010; Austin and Austin, 2012). As an opportunistic pathogen, fish diseases caused by *A. hydrophila* are linked to unfavorable environmental conditions (Elgendy *et al*., 2015). Pollutants stemming from anthropogenic activities are among the notorious sources of stress conditions overwhelming aquatic species predisposing them to array of microbial infections (Moustafa *et al*., 2015). These pollutants may affect aquatic animals either directly via suppression of immune defense mechanisms or potentially through their effect on the virulence determents of attacking pathogens (Arkoosh *et al*., 1988). Heavy metal pollution affects lysozyme levels and causes alterations of immunoregulatory functions in fish (Sanchez-Dardon *et al*., 1999). Heavy metals also can compromise fish humoral and cell mediated immunity through many pathways, including decreasing levels of antibody and splenic plaque forming cells, reducing proliferation of splenic lymphocytes, and via decreasing disease resistance to bacterial infection (Khangarot *et al*., 1999). The

* Corresponding author. e-mail: mamdouhyousif@yahoo.com; my.abdelaziz@ nrc.sci.eg.

pathogenicity of *A. hydrophila* has been ascribed to numerous virulence determents. A number of virulence factors, including secretion systems, adhesins , toxins, enzymes, quorum systems, iron acquisition and antibiotic resistance, have been identified (Tomas, 2012). In this study, we investigated the presence of six virulence genes (*Act*, *Ast*, *Lip*, *Elast*, *Alt* and *Fla*) in *A. hydrophila* strains obtained from aquatic environments. In addition, the virulence of *A. hydrophila* strains was tested by experimental infection in *O. niloticus*.

2. Material and Methods

2.1. Bacterial Strains and Sampling

A total of 35 *A. hydrophila* isolates obtained from apparently healthy fish and water samples were analyzed in the present study. Isolates were obtained from three water sources; 15 isolates (10 isolates from water and 5 isolates from fish samples) from El-Sharkawia stream (a narrow tributary of the River Nile between Shubra El kheima and El Qanater El Khayreya region, Qaluobyia) which receives lofty loads of industrial effluents coming from numerous factories in that region, like textile, paper, plastic, oil, soap, detergents and small scale services (like petrol stations and garages). 11 isolates (7 isolates from water and 4 isolates from fish) from El-Rayah El-Towfeky stream at Barshoom that receives loads of sewage and agricultural effluents. Additionally, 9 isolates were retrieved from Bahr Yousuf canal at El-Fayoum governorate, a great canal linking the main branch of the River Nile to provide water permanently to the Lake Qarun at El-Fayoum governorate, (5 isolates from water and 4 isolates from fish).

All samples were cultured onto Aeromonas agar base supplemented with Ampicillin, to select for green colonies. All isolates were confirmed with, the commercial Api 20-NE.

2.2. Hemolysin, Protease, Gelatinase and Slime Production

Haemolysis was assayed by spreading each strain onto 5% rabbit erythrocytes agar plates for 24 h at 30°C. Protease activity was demonstrated by spreading *Aeromonas* strains on nutrient agar containing 1.5% skim milk. Plates were incubated for up to 72 h at 30°C, the production of protease was shown by the formation of a clear zone. Gelatinase production was determined using Luria Broth agar containing gelatin (30 g L^{-1}), the plates were incubated overnight at 30°C and then cooled for 5 h at 4°C. The appearance of a turbid halo around the colonies was considered positive for gelatinase production according to Sechi *et al*. (2002).

Slimness was investigated by culturing bacterial isolates onto Brain Heart infusion agar containing 0.8 g l^{-1} Congo Red (Sigma-Aldrich, Milan, Italy). Plates were inoculated at 30°C for 24 h. Slime producing bacteria appeared as black colonies whereas non-slime producers remained non pigmented (Freeman *et al*., 1989).

2.3. PCR for Detection of Virulence Genes

Genomic DNA was extracted from bacterial isolates using DNA extraction kit (Fermentas, Lithuania) according to manufacturer's instructions. The primer pairs used for PCR amplification of six virulence genes (shown in Table 1): cytotoxic heat-labile enterotoxin (Act), cytotonic heat-stable enterotoxin (Ast), Lipase (Lip), elastase (Ela), cytotonic heat-labile enterotoxin (Alt) and flagella A as well as flagella B (Fla), using the same primers sequences and PCR conditions as reported by (Sen and Rodgers, 2004). Briefly, reactions were performed in 25µl volumes, each contained 1 µM of each primer, 12.5 µM of AmpliTaq^{TM} Gold PCR Master mix (2X) containing, $MgCl_2$, AmpliTaq^{TM} Gold DNA polymerase, and dNTPs (Applied Biosystems). 80 ng of DNA template in 5 µl volume was used. Cycling conditions consisted of an initial single cycle at 95°C for 5 min, followed by 25 cycles of 25 s at 95 °C, annealing for 30 s at 55 °C, elongation for 1 min at 72 °C and a final single elongation cycle at 70 °C for 5 min. PCR was performed in Eppendorf Master Cycler gradient thermocycler (Eppendorf AG, Hamburg, Germany).

Table 1. Set of primers used for amplification of virulence genes

Gen	Primer sequence	Size of product bp	Reference
Act	F 5-GAAGGTGACCACCAAG AACA-3 R5-AACTGACATCGGCCTTGAACTC-3	232	Kingombe *et al.,* (1999)
Ast	F5-TCTCCATGCTTCCCTTCCACT-3 R5-TGTAGGGATTGAAGAAGCCG-3	331	Sen and Rodgers (2004)
Fla	F5-TCCAACCGTYTGACCTC-3 R5-GMYTGGTTGCGRATGGT-3	608	Sen and Rodgers (2004)
Alt	F5-TGACCCAGTCCTGGCACGGC-3 R5-GGTGATCGATCACCACCAGC-3	442	Sen and Rodgers (2004)
Lipase	F5-ATCTTCTCCGACTGGTTCGG -3 R5-CCGTGCCAGGACTGGGTCTT-3	382	Sen and Rodgers (2004)
Elastase (Ela)	F5-ACACGGTCAAGGAGATCAAC-3 R5-CGCTGGTGTTGGCCAGCAGG-3	513	Sen and Rodgers (2004)

2.4. Virulence Test

The artificial infection of 12 *A. hydrophila* strains (4 isolates from each site) was carried out by injection in *Oreochromis niloticus* (Table 2). 130 Fish weighing between 40- 50 g were used in the present study. Fish were kept in glass aquaria (60×30×40 cm^3) at a rate of 10 fish / aquarium. The fish were maintained at 27°C and fed with a commercial diet twice a day. Compressed air was pumped continuously into the feed tanks and 50% water was exchanged every day. All bacterial strains were cultured in tryptic soy broth for 24 h at 27°C. All bacterial strains were adjusted to 1 x 10^7 Colony forming Unit (CFU)/ml in Phosphate Buffer Saline. Fish were intraperitoneally injected with 0.2 ml of each bacterial culture while the control group was injected with 0.2 ml Phosphate Buffer Saline and kept under observation for 10 days according to Abu-Elala and Ragaa (2015).

Table 2. Virulence factors of *Aeromonas hydrophila* isolates

source	strain	Haemolysis	Gelatinase	Protease	Slime test	PCR detection of virulence gens					
						ACT	AST	LIP	ELAST	ALT	FLAG
El-Sharkwia stream	1 w *	+	-	+	-	-	-	-	-	-	-
	2 w	-	-	+	-	+	-	-	-	-	-
	3 w	+	-	-	-	-	-	-	-	+	-
	4 w *	+	-	-	-	+	-	+	-	-	-
	5 w	-	-	-	+	-	-	-	+	-	-
	6 w	-	-	+	+	+	-	-	+	-	-
	7 w	-	-	-	-	-	-	-	-	+	-
	8 w	+	-	-	-	-	-	-	+	-	-
	9 w	+	-	-	-	-	-	+	-	-	-
	10 w*	-	-	-	-	-	-	+	-	-	-
	11 f	+	-	+	-	+	-	-	+	-	-
	12 f	+	-	+	+	-	-	-	+	-	-
	13 f	-	+	-	+	+	-	+	-	+	-
	14 f	+	+	-	-	-	-	-	+	-	-
	15 f *	+	-	+	+	+	-	+	-	-	-
El-Rayah El-Towfeky stream	16 w	-	-	-	-	-	-	-	+	-	-
	17 w *	+	-	-	-	-	-	-	-	-	-
	18 w	-	-	-	-	-	-	+	+	-	-
	19 w	-	-	-	+	-	-	-	-	+	-
	20 w *	+	+	+	-	+	-	-	-	-	-
	21 w	-	+	-	-	-	-	-	-	-	-
	22 w*	-	-	-	-	-	-	-	-	-	-
	23 f *	+	+	+	+	-	-	-	-	-	-
	24 f	-	+	-	-	-	-	-	+	-	-
	25 f	-	-	-	-	+	-	+	+	+	-
	26 f	-	-	-	+	-	-	-	-	-	-
Bahr Yousuf at El-Fayoum governorate	27 w *	-	-	-	-	-	-	-	-	-	-
	28 w	-	-	-	-	-	-	-	-	-	-
	29 w	-	-	-	-	-	-	-	-	-	-
	30 w	-	-	+	-	-	-	-	-	-	-
	31 w	-	-	-	-	+	-	-	-	-	-
	32 f *	-	-	-	+	-	-	-	+	-	-
	33 f	-	-	+	-	-	-	-	-	-	-
	34 f *	-	-	-	-	-	-	-	+	-	-
	35 f *	+	-	+	+	-	-	-	-	+	-

*isolates used in pathogenicity testing; W= water; F= fish

2.5. Total Aerobic Count and Total Coliform Count

Bacterial counts were carried out in triplicate. Twenty five gram of fish muscles (5 fish per site) was aseptically cut and transferred into sterile stomacher bag containing 225 ml sterile maximum recovery diluents (Oxoid) according to APHA (1992). Similarly, 25 ml of each water sample (3 samples per site) was mixed with 225 ml of the same recovery diluents. Decimal dilution was prepared up to 10^{-6} and Pour plates were prepared from l0 fold dilutions in plate count agar (Oxoid) for total aerobic enumeration, and violet red bile agar (VRBLA, Oxoid) for total coliforms. All counts were made after incubation of all plates at 35°C for 24 h. Bacterial colonies were counted and expressed in Colony forming Units (CFU) per gram of fish muscles and as (CFU /mL) for water samples (Collins and Lyne, 1984).

2.6. Physiochemical Water Analysis

Temperature, pH and dissolved oxygen (DO_2) were measured on spot at each collection site by digital apparatus, YSI (Yellow Springs, Ohio USA). Chemical Oxygen Demand (COD) was carried out using the potassium permanganate method (Golterman, 1971) and biochemical oxygen demand (BOD) with the five-day incubation method (APHA, 2000). Nitrates (NO_3) and ammonia (NH_3), in water samples were assessed according to methods adopted from (APHA, 2000). Regarding heavy metals, water samples were acidified by concentrated nitric acid (5 mL/L) and then heavy metals (Cd, Co, Cr, Cu, Pb, Ni, Zn and Mn) were measured by atomic absorption spectrophotometer (Perkin-Elmer 3110, USA) (APHA, 2000). Pollution with organochlorines and organophosphates was also analyzed quantitatively using an Agilent gas chromatograph 6890 (Dahshan *et al*., 2016).

2.7. Heavy Metal Analysis in Fish Tissues

Fish were dissected; muscles and liver tissues were isolated, weighed, put in glass vials and digested in concentrated nitric acid (Merck, Darmstadt, Germany); then placed on a hot plate at 100 °C. Samples were cooled in room temperature after complete digestion then, filtered and reached a volume of 10 m1 by distilled water. Heavy metal concentrations (Cd, Co, Cr, Cu, Pb, Ni, Zn and Mn) were determined by atomic absorption spectrophotometry

(Perkin-Elmer 3110, USA) (APHA, 2000). Accumulation Factor (AF) was calculated according to Authman *et al*. (2013).

3. Results

3.1. Hemolysin, Protease, Gelatinase Production and Slime Test

37.14 % of *A. hydrophila* strains were able to lyse rabbit erythrocytes and produced haemolysis on rabbit blood agar plates. 31.42 % of isolates produced protease and hydrolysed Skimmed milk, 17.14 % were gelatinase positive, 28.57 % were positive in slime production test (Table 2).

3.2. PCR for Detection of Virulence Genes

All isolates were found negative for the virulence genes, *Ast* and *Fla* whereas nine strains produced the expected band, 232 bp of *Act*. Seven strains showed a positive band of 382 bp respective for *Lip*. Twelve strains gave the expected band at 513 bp of *Elast*. Six isolates were positive for *Alt* showing expected band at 442 bp (Table 2; Figure 1).

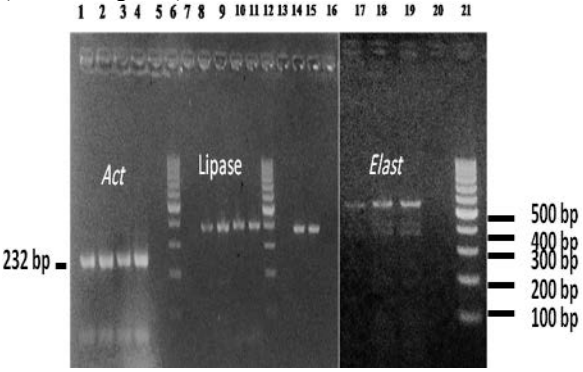

Figure 1: Agarose gel electrophoresis. Lanes 6, 12 and 21: 100 bp DNA marker. Lanes 1,2,3, 4: *Act* positive strains; Lanes 8, 9, 10, 11, 14, 15 are Lipase positive strains; Lanes 17, 18, and 19 are Elastase positive strains; Lanes 5, 7, 13, 20 Negative strains

3.3. Virulence Test

All experimentally infected fish, which were injected with the different *A. hydrophila* isolates (Table 2), died during the period of observation. *A. hydrophila* were re-isolated from the kidney of succumbed fish. Fish showed petechial hemorrhages on different parts of the external body surfaces. Internally, congestion of the liver and spleen were commonly detected. *A. hydrophila* were re-isolated from all succumbed fish. Fish injected with saline showed no mortalities.

3.4. Total Aerobic Count and Total Coliform Count

The mean total aerobic bacterial and total coliform counts in water and fish samples are illustrated in (Table 3). Counts were highest in samples collected from El-Rayah El-Towfeky stream since the total aerobic bacterial counts was $2.5X10^3$ CFU/mL and $1.6X10^4$ CFU/gm in water and fish samples, respectively, while the mean total coliform counts was $6X10^2$ CFU/mL and $4.3X10^3$ CFU/gm, respectively. The lowest bacterial counts were recorded in water and fish samples collected from El-Sharkawia stream; the total aerobic bacterial counts was $1.9X10^3$ CFU/mL and$7.5X10^3$ CFU/gm in water and fish samples while the mean Total coliform count was $2X10^2$ CFU/mL and $1.5X10^3$ CFU/gm, respectively.

Table 3. Total bacterial aerobic count and total coliform count

	Total aerobic count		Total coliform count	
	water	muscles	Water	muscles
El-Sharkawia stream	$1.9X10^3$ CFU/ml	$7.5X10^3$ CFU/gm	$2X10^2$ CFU/ml	$1.5X10^3$ CFU/gm
El-Rayah El-Towfeky	$2.5X10^3$ CFU/ml	$1.6X10^4$ CFU/gm	$6X10^2$ CFU/ml	$4.3X10^3$ CFU/gm
Bahr Yousuf at El-Fayoum governorate	$2.0X10^3$ CFU/ml	$3.5X10^4$ CFU/gm	$3X10^2$ CFU/ml	$2.5X10^3$ CFU/gm

3.5. Physiochemical Water Analysis

The average values recorded for water temperature, pH and dissolved oxygen were within normal values. BOD and COD values were slightly more than the permissible values, especially at El-Sharkawia stream; they were 12.43 and 17 mg/L, respectively. NO_3 and NH_3 were within the permissible limits. Concentrations of heavy metals demonstrated variable levels. Chromium (Cr), Lead (Pb) and Manganese (Mn) showed high values that exceed the permissible limits in El-Sharkawia stream; 1414, 67and 567 µg/L, respectively. Chromium is also the most determined metal in El-Rayah El-Towfeky (1192 µg/L), while Cu was not detected in both locations, and Cd, Ni and Zn were in the permissible limits. On the other hand, Co, Cr, Ni and Mn were not detected in water samples collected from Bahr Yousuf canal. At the same location Cd, Cu, Pb and Zn were within the permissible limits Pesticides; organochlorines and organophosphates were not detected in all investigated water samples (Table 4).

Table 4. Physicochemical water analysis

Permissible Limits		Bahr Yousuf	El-Rayah El-Towfeky stream	El-Sharkawia stream	
USEPA, 2004	Egyptian Environmental Law No.48, 1982				
		25±1.7	26±1.3	26±1.5	Temperature (^{o}C)
	6.5-8.5	8.3±0.6	7.5±0.4	6.9±0.5	pH
	<5	6.4±0.3	6.3±0.6	5.9±0.8	DO_2 (mg/l)
	<6-10	10.8±0.6	11.19±0.5	12.43±0.8	BOD (mg/l)
	<10-15	15±0.8	12±0.9	17±1	COD (mg/l)
	40	0.61±0.02	0.59±0.04	0.59±0.02	No_3 (mg/l)
	< 3	2.1±0.02	1.7±0.03	2.06±0.02	NH_3 (mg/l)
	Heavy metals (µg/l)				
0.25	10	8±0.4	2±0.3	1±0.5	Cd
-	-	nd	21±3	20±1	Co
74	50	nd	1192±70	1414±80	Cr
9	1000	31±1	nd	nd	Cu
2.5	50	28±1	36±0.9	67±1	Pb
52	100	nd	12±6	6±0.2	Ni
120	1000	66±9	11±5	19±3	Zn
-	500	nd	239±10	567±80	Mn
	Pesticides				
		nd	nd	nd	Organochlorines
		nd	nd	nd	Organophosphates

nd (not detected)

3.6. Metals Residues in Fish Tissues

The determined heavy metal concentrations and their bioaccumulation factors in liver tissue were more than that in muscle tissues. Heavy metals exhibited different values of accumulation in fish muscles in both El-Sharkawia and El-Rayah El-Towfeky while in Bahr Yousuf canal all the recorded metals were within the recommended permissible limits (Table 5).

Table 5. Heavy metals residues (mg/Kg wet weight) in muscles and livers of *Oreochromis niloticus* fish from the different studied localities

	El-Sharkawia stream		El-Rayah El-Towfeky stream		Bahr Yousuf at El-Fayoum governorate		Permissible limits	
	M	**L**	**M**	**L**	**M**	**L**	**FAO, 1983**	**IAEA, 407**
Cd	0.18±0.016 (180)	0.16±0.005 (160)	0.16±0.007 (80)	0.14±0.003 (70)	0.004±0.001 (0.5)	0.005±0.0003 (0.63)	0.05	0.189
Co	0.10±0.022 (5)	0.06±0.001 (3)	0.26±0.025 (12.38)	0.52±0.005 (24.76)	nd	nd	---	0.1
Cr	3.40±0.020 (2.40)	6.18±0.012 (4.37)	2.48±0.041 (2.08)	4.92±0.034 (4.13)	nd	nd	1.0	0.73
Cu	1.08±0.092 (--)	3.00±0.071 (--)	4.74±0.111 (--)	36.18±0.311 (--)	0.0003±0.0001 (0.01)	0.001±0.0002 (0.03)	30	3.28
Pb	0.14±0.007 (2.09)	0.24±0.005 (3.58)	0.28±0.033 (7.78)	0.34±0.012 (9.44)	0.009±0.001 (0.32)	0.02±0.002 (0.71)	0.5	0.12
Ni	1.34±0.013 (223.33)	3.06±0.034 (510)	1.66±0.007 (138.33)	3.60±0.014 (300)	0.21±0.003 (--)	0.37±0.012 (--)	---	0.6
Zn	11.44±0.034 (602.11)	24.22±0.36 (1274.74)	18.76±0.097 (1705.45)	21.06±0.29 (1914.55)	0.022±0.002 (0.33)	0.046±0.003 (0.70)	30	67.1
Mn	1.24±0.033 (2.19)	1.16±0.007 (2.05)	1.30±0.005 (5.44)	2.30±0.003 (9.62)	0.26±0.002 (--)	0.41±0.011 (--)	1.0	3.52

M: muscle, L: liver, nd: not detected; Data are represented as mean value of three replicates of pooling tissues ± Standard deviation (Accumulation factor).

4. Discussion

In the present study, virulence determents of *A. hydrophila* isolates are analysed by enzymatic and molecular methods. The present study demonstrates a difference in the enzymatic activities and extracellular products produced by *A. hydrophila* isolates obtained from different environmental sources. Isolates obtained from El-Sharkwia stream that receives high industrial effluents exhibited the uppermost enzymatic activities compared to isolates retrieved from other sources. *A. hydrophila* secretes a wide range of extracellular products, including proteases, lipases, nucleases, and gelatinases that potentiate their virulence as well as adaptation to environmental changes. 37.14 % of *A. hydrophila* strains were able to lyse rabbit erythrocytes; nine isolates from El-Sharkawia stream, three from El-Rayah El-Towfeky stream and only one isolate from Bahr Yousuf canal at El-Fayoum governorate. *Aeromonas* sp. produce two types of hemolysins without enterotoxic properties; α-hemolysins and β- hemolysins which are thermostable and pore forming toxins that lead to osmotic lysis and complete destruction of erythrocytes (Kirov, 1997). Proteases were also detected in some isolates (31.42 %) with high frequencies in strains obtained from El-Sharkawia stream (six isolates). Extracellular proteases allow *Aeromonas* sp. to persist in different habitats and facilitate ecological interactions with other organisms. Proteases enhance the establishment of infections and overcoming the initial host defenses (Leung and Stevenson, 1988). Additionally, proteases promote invasion by direct damage of host tissue or by proteolytic activation of toxins (Kirov, 1997). Gelatinase was completely absent in isolates obtained from the fish farm samples where it was detected in four isolates in El-Rayah stream that receive loads of sewage and agriculture effluents. Gelatinase contribute significantly in the pathogenicity as it enhances the intestinal colonization by bacteria through the disruption of the intestinal barrier.

PCR detection of virulence gens demonstrated absence of *Ast* and *Fla* in all isolates. Sen and Rodgers (2004) detected the genes coding for the polar flagellum protein in 59% of *Aeromonas* strains obtained from drinking water and they alleged that presence of flagella is critical for the adherence process of pathogens since mutations in the polar flagellum *flaA* and *flaB* genes resulted in complete loss of motility and adherence to human epithelial HEp-2 cells. Nine strains produced the expected band for PCR amplification of *Act*, six of these isolates were obtained from samples from El-Sharkawia stream. *Act* is one of the main virulence factors of *A. hydrophila* and have hemolytic, cytotoxic and enterotoxic activities (Tomas, 2012). This cytotoxic enterotoxin perform important roles in Aeromonas infections as it induces early cell signaling in eukaryotic cells, which leads to the production of inflammation mediators in macrophages (Xu *et al*., 1998) and also contributes to apoptosis (Galindo *et al*., 2006). Seven strains showed a positive band of *Lip* none of them from the fish farm. Lipases can affect several immune system functions through the free fatty acids generated by lipolytic activity. *Elast* was detected in twelve isolates while six isolates demonstrated positive results for *Alt*. *Alt* is a cytotonic enterotoxin which does not cause degeneration of crypts and villi of the intestine like the cytotoxic enterotoxin (Chopra and Houston, 1999). A significant link between existence of *alt* and *ast* genes in *Aeromonas* isolates and their ability to cause infections and diarrhea in children harboring such strains (Albert *et al*., 2000). In their study, the authors detected that 54% of the *A. hydrophila* strains obtained from diarrheal children had both genes, while only 15% of the strains recovered from environmental samples were found to have both genes. Harboring of enterotoxins alone may not be sufficient for virulence since these factors have been found in strains isolated from healthy and the ability of the bacterium to adhere and invade the intestinal mucosa are also crucial components of pathogenesis (Schiavano *et al*., 1998). It has been demonstrated that, bacterial strains from environmental sources are s ignificant reservoirs of virulence and fitness genes and acquisition of such genes occurs among autochthonous bacteria as well as hu man pathogens, released via anthropogenic activities, in the aquatic environment (Xie *et al*., 2005; Caburlotto *et al*., 2009). The acquisition of mobile genetic elements, such as plasmids, bacteriophages, transposons and genetic islands allows bacteria to acquire a range of genetic traits that may increase their fitness under different environmental conditions and their virulence potentials (Gennari *et al*., 2012).

Results did not show an obvious correlation between the presence of virulence determents in *A. hydrophila* isolates and pathogenicity to *Oreochromis niloticus*, as some of these strains possess more or less virulence determents. Additionally some of these strains No (22 w* and 27 w *) were pathogenic and resulted in death of all challenged fish, although they do not possess any of the studied virulence determents. This suggests that *A. hydrophila* might have a d ifferent virulence gene system and different pathogenic mechanisms other than the studied and further genotypic studies are still needed to elucidate the hypothesis.

Bacterial counts were higher in water collected from El-Rayah El-Towfeky stream which may be relevant to the surplus sewage and agricultures discharges. Consequently bacterial loads were higher in fish muscles samples collected from the same site since the level of contamination of aquatic animals depends on the extent of pollution in the growing waters (Ekanem and Adegoke, 1995). On the other hand the lowest bacterial counts were detected in Sharkawia stream which may be due to the toxic effects of industrial pollutants on the bacterial communities distributed in the area.

Comparing the physicochemical picture of the water in the three studied locations, El-Sharkawia stream was the most polluted source. It receives high industrial effluents and consequently high BOD and COD values. The water was loaded by high concentrations of some heavy metals (Cr, Pb and Mn) that exceed the Egyptian Environmental law no. 48, (1982) and international guidelines of freshwater of USEPA (2004). The lofty loads of chromium detected in El-Sharkawia and El-Rayah streams may be attributed to the industrial and agricultural discharges (Ahmed *et al*., 2013). The majority of the recorded metals were concentrated and accumulated in fish tissues to levels exceed the international permissible limits FAO, 1983 and IAEA, 2003 especially in liver due to its main detoxification function (Iwegbue, 2008). The variation in

the accumulation of metals in fish organs may be relevant to the availability of metals to specific fish tissues, fish age, species, the existence of ligands in the tissues with a high affinity to the metal and/or to the role of these tissues in the detoxification process (Bashir and Alhemm, 2015). On the other hand, Bahr Yousuf canal was the lowest polluted location, has nearly normal water quality parameters and all the detected metals were within the recommended permissible limits both in water and in tissue samples. The presence of heavy metals pollutants in the aquatic environment can result in deleterious impacts on the ecosystems, with alterations in the biomass, diversity of microbial communities and cycling of elements (Sobolev and Begonia, 2008). The toxic effects of heavy metals on m icroorganisms are influenced by many factors, such as pH, concentration of chelating agents and organic matter (Nwuche and Ugoji, 2008). Long existence of microorganisms in such polluted environments results in selection of certain strains of bacterial populations (Silva *et al*., 2012). Bacterial strains also can exhibit adaptation to heavy metals pollutants in their environment through; changing the metabolic and physiological activities of bacteria (Lima e Silva et *al*., 2012); formation of resistant strains as well as via altering the genetic information (Chudobova *et al*., 2015).

5. Conclusion

Environmental *A. hydrophila* strains have array of virulence attributes and isolates obtained from industrially polluted area demonstrated existence of the highest level of virulence characteristics. The presence of metallic pollutants in the aquatic environment can affect the enzymatic activities as well as the genetic virulence factors of cohabitant bacterial populations. Additionally, *A. hydrophila* retrieved from aquatic environment are highly pathogenic to fish and have diverse pathogenic mechanisms and further genotypic studies are still needed to elucidate the hypothesis.

Acknowledgment

Authors express appreciation to all hydrobiology lab staff. We also thank fishermen for helping us in catching and transporting fish.

References

Abu Elala NM and Ragaa NM. 2015. Eubiotic effect of a dietary acidifier (potassium diformate) on the health status of cultured *Oreochromis niloticus* . *J Advanced Res*., **6**: 621–629.

Ahmed MK, Kundu GK, Al-Mamun MH, Sarkar SK, Akter MS and Khan MS. 2013. Chromium (VI) induced acute toxicity and genotoxicity in freshwater stinging catfish, *Heteropneustes fossilis*. *Ecotoxicol Environ. Safety*, **92**: 64-70.

Albert MJ, Ansaruzzaman M, Talukder KA, Chopra AK, Kuhn I and Rahman M. 2000. Prevalence of enterotoxin genes in *Aeromonas* sp. isolated from children with diarrhea, healthy controls, and the environment. *J Clin Microbiol* , **38**:3785–90.

APHA (American Public Health Association) 2000. **Standard Methods for the Examination of Water and Wastewater**, Washington, D. C.

APHA (American Public Health Association). 1992. **Standard Methods for the Examination of Water and Wastewater.** 18lh ed. Washington. D.C. 2005pp.

Arkoosh MR, Casillas E, Clemons E, Kagley D, Olson R, Paul Reno P, Stein J.E. 1998. Effect of pollution on fish diseases: Potential impacts on salmonid populations. *J Aquat Anim Health*, **10**:182–190.

Austin B and Austin DA. 2012. **Bacterial Fish Pathogens, Disease of Farmed and Wild Fish**, 5th edn. Springer, Media Dordrecht.

Authman MM, Abbas HH and Abbas WT. 2013. Assessment of metal status in drainage canal water and their bioaccumulation in *Oreochromis niloticus* fish in relation to human health. *Environ Monitoring Assessment*, **185**: 891–907.

Bashir FA and Alhemm EM. 2015. Analysis of some heavy metal in marine fish in muscle, liver and gill tissue in two marine fish spices from Kapar Coastal Waters, Malaysia. The Second Symposium on Theories and Applications of Basic and Biosciences 5 September 201.

Caburlotto G, Gennari M, Ghidini V, Tafi MC and L leo MM. 2009. Presence of T3SS2 and other virulence-related genes in tdh-negative *Vibrio parahaemolyticus* environmental

strains isolated from marine samples in the area of the Venetian Lagoon, Italy. *FEMS Microbiol Ecol,* **70**: 506–514.

Chan SS, Ng KC, Lyon DJ, Cheung WL, Cheng AF and Rainer TH. 2003. Acute bacterial gastroenteritis: a study of adult patients with positive stool cultures treated in the emergency department, *Emergency Medicine J*., **20**: 335–338.

Chopra AK and Houston CW. 1999. Enterotoxins in Aeromonas associated gastroenteritis. *Microbes and Infect.,* **1**: 1129–1137.

Chudobova D, Dostalova S, Ruttkay-Nedecky B, Guran R, Rodrigo MA, Tmejova K, Krizkova S, Zitka O, Adam V and Kizek R. 2015. The effect of metal ions on *Staphylococcus aureus* revealed by biochemical and mass spectrometric analyses. *Microbiol Res*., **170**:147-156.

Collins CH and Lyne MP. 1984. **Microbiological Methods**, Fifth ed. Butterworth, London, UK.

Dahshan H, Megahed AM, Abd-Elall AM, Abd-El-Kader MA, Nabawy E and Elbana MH. 2016. Monitoring of pesticides water pollution-The Egyptian River Nile. *Environ Health Sci Eng J*., **14**: 15 - 26.

Egyptian Law 48. 1982. The Implementer Regulations for law 48/1982 regarding the protection of the River Nile and water ways from pollution. Map. Periodical Bull. 3–4 Dec: 12–35.

Ekanem EO and Adegoke GO.1995. Bacteriological study of West African clam (*Egeria radiata* Lamarch) and their overlying waters. *Food Microbiol*, **12** : 381-385.

Elgendy MY, Moustafa M, Gaafar AY and Borhan T. 2015. Impacts of extreme cold water conditions and some bacterial infections on earthen-pond cultured Nile tilapia, *Oreochromis niloticus*. *RJPBCS*, **6**: 136-145.

FAO (Food and Agriculture Organization). 1983. Compilation of legal limits for hazardous substances in fish and fishery products. *FAO Fish Circular*, **464**:5–100.

Freeman DJ, Falkiner FR and Keane CT. 1989. New method for detecting slime production by coagulase negative staphylococci. *Clin Pathol J*, **42**: 872-874.

Galindo CL, Gutierrez JR and Chopra AK. 2006. Potential involvement of galectin-3 and SNAP23 in *Aeromonas hydrophila* cytotoxic enterotoxin-induced host cell apoptosis. *Microbial Pathogenesis*, **40:** 56–68.

Gennari M, Ghidini V, Caburlotto G and Lleo MM. 2012. Virulence genes and pathogenicity islands in environmental Vibrio strains nonpathogenic to humans. *FEMS Microbiol Ecol*, **82**: 563–573.

Glunder G, Siegmann O. 1989. Occurrence of *Aeromonas hydrophila* in wild birds. *Avian Pathol*. **18**: 685-695.

Golterman HL. 1971. **Methods for Chemical Analysis of Freshwaters**. Oxford and Edinburgh: Blackwell Scientific Publications.

Iwegbue CM. 2008. Heavy metal composition of livers and kidneys of cattle from southern Nigeria.*Veterinarski Archiv*, **78**: 401 - 410.

IAEA 407 (International Atomic Energy Agency). 2003. **Analytical Quality Control Services,** Vienna, Austria.

Janda JM and Abbott SL. 2010. The genus *Aeromonas*: taxonomy, pathogenicity, and infection," .*Clin Microbiol Rev*., **23**: 35–73.

Khangarot BS, Rathore RS, Tripathi DM. 1999. Effects of chromium on humoral and cell-mediated immune responses and host resistance to disease in a freshwater catfish, *Saccobranchus fossilis* (Bloch). *Ecotox Environ Safety*, **43**:11-20.

Kingombe, CI, Huys G, Tonolla M, Albert MJ, Swings J, Peduzzi R and Jemmi T. 1999. PCR detection, characterization, and distribution of virulence genes in *Aeromonas* sp. *Appl Environ Microbiol*., **65**: 5293–5302.

Kirov SM. 1997. *Aeromonas* and *Plesiomonas* species in Food Microbiology, In: **Fundamentals and Frontiers**, Doyle, M P., Beuchat L R and Montville T J., Eds., ASM Press, Washington, DC, USA, pp 265-287.

Leung KY and Stevenson RM. 1988. Tn5-induced protease deficient strains of *Aeromonas hydrophila* with reduced virulence for fish, *Infect Immun*., **56**: 2639–2644.

Lima e Silva AA, Carvalho MA, Souza SA, Dias PT, Filho RS, Saramago CM, Bento C M and Hofer E. 2012. Heavy metal tolerance (Cr, Ag and Hg) in bacteria isolated from sewage. *Brazilian J Microbiol*., **112**: 1620-1631.

Moustafa M, Eissa AE, Laila AM, Gaafar AY, Abumourad IM and Elgendy MY. 2015. Investigations into the potential causes of mass kills in mari-cultured Gilthead sea Bream, (*Sparus aurata*) at Northern Egypt. *RJPBCS*, **6**: 466-477.

Moustafa M, Laila AM, Mahmoud MA, Soliman WS and Elgendy MY. 2010. Bacterial infections affecting marine fishes in Egypt. *J Am Sci.,* **6**: 603-612.

Nwuche CO and Ugoji EO. 2008. Effects of heavy metal pollution on the soil microbial activity. *Int J Environ Sci Tech*.,**5**: 409-414.

Roberts RJ. 2012. **Fish Pathology**. 3rd Edn., W.B. Saunders, Philadelphia, PA..

Sanchez-Dardon J, Voccia I, Hontela A, Chilmonczyk S, Dunier M, Boermans H, Blakley B and Fournier M. 1999. Immunomodulation by heavy metals tested individually or in mixtures in rainbow trout (*Oncorhynchus mykiss*) exposed *in vivo* . *Environ Toxicol Chem*., **18**: 1492–1497.

Schiavano GF, Bruscolini F, Albano A and Brandi G. 1998. Virulence factors in *Aeromonas* sp. and their association with gastrointestinal disease. *The New Microbiol.*, **21**: 23–30.

Sechi LA, Deriu A, Falchi MP, Fadda G and Zanetti S. 2002. Distribution of virulence genes in *Aeromonas* sp. isolated from Sardinian waters and from patients with diarrhea. *Appl Microbiol*., **92**: 221-227.

Sen K and Rodgers M. 2004. Distribution of six virulence factors in *Aeromonas* species isolated from US drinking water utilities: a PCR identification. *J Appl Microbiol*., **97**: 1077-1086.

Sobolev D, Begonia MF. 2008. Effects of heavy metal contamination upon soil microbes: lead-induced changes in general and denitrifying microbial communities as evidenced by molecular markers. *Int J Environ Res Public Health*, **5**: 450-456.

Tomas JM. 2012. The main *Aeromonas* pathogenic factors. *ISRN Microbiology*. **2012,** Article ID 256261, 22 pages, 2012. doi:10.5402/2012/256261

USEPA (United States Environmental Protection Agency). 2004. **National Recommended Water Quality Criteria Aquatic Life Criteria.**

Xie ZY, Hu CQ, Chen C, Zhang LP and Ren CH. 2005. Investigation of seven Vibrio virulence genes among *Vibrio alginolyticus* and *Vibrio parahaemolyticus* strains from the coastal mariculture systems in Guangdong, *China Lett Appl Microbiol*., **41**: 202–207.

Xu XJ, Ferguson MR, Popov VL, Houston CW, Peterson JW and Chopra AK. 1998. Role of a cytotoxic enterotoxin in *Aeromonas*-mediated infections: development of transposon and isogenic mutants. *Infect Immun*., **66**: 3501–3509.

JJBS

Volume 10, Number 4,December 2017
ISSN 1995-6673
Pages 273 - 280

Jordan Journal of Biological Sciences

In Silico Screening for Inhibitors Targeting Bacterial Shikimate Kinase

Mohammed Z. Al-Khayyat*

Biology Department, College of Education for Pure Sciences, University of Mosul, Mosul City, Iraq.

Received: February 28, 2017; Revised: July 29, 2017; Accepted: August 10, 2017

Abstract

Shikimic acid pathaway is essential for the biosynthesis of aromatic amino acids in bacteria. Shikimate kinase is one of the enzymes which converts shikimate to shikimate-3-phosphate, may be used as an alternative target in antibiotic design. In the present study, homology modeling and quality assessment of shikimate kinase of four microorganisms; *Campylobacter jejuni*, *Salmonella enterica*, *Pseudomonas* spp. and *Enterococcus faecali* was performed, then two docking software; ArgusLab 4.0.1 and Hex 8.0.0 were used to dock a total of 200 selected compounds, obtained from Drug Bank and ZINC databases against the constructed models. The two approved drugs Dobutamine and oxprenolol, (3,4-dihdroxy-2-nitrophenyl) (phenyl) methanone, and isoxsuprine had their biding affinities higher than the substrate shkimate as control in both tools and in all four models. Therefore, these compounds may be exploited in preliminary screening for new antibacterial agents to combat bacterial infections caused by antibiotic resistant microorganisms.

Key words: Antibacterial design, Homology modeling, Molecular docking, Shikmate kinase.

1. Introduction

The aromatic biosynthetic pathway, also called shikimic acid pathway (Figure 1), is conserved in bacteria, fungi, plants and parasites, like *Plasmodium* spp. and *Toxoplasma gondii*. This pathway is used for the synthesis of chorismate, which is converted into aromatic amino acids and compounds and because it is absent in mammals, this pathway was investigated for inhibitors in drug design due to the widespread antibiotic resistance and the existence of antiparastic agents as well (Daughery *et al*., 2001; Amer *et al*., 2008). The enzyme 3-dehydroquinate dehydratase has been suggested as a molecular target for the developing antibiotics against *mycobacterium tuberculosis* and *Helicobacter pylori* (Amer *et al*., 2008; Gonzalez-Bello, 2016). Flourinated shikimates, 3-deoxy-3,3-difluoro-shikimate, and 3-deoxy-3,3-difluoro-4-epi-shikimate were found to be inhibitors of *P. falciparum in vitro*. Mutagenesis of *aroA*, the gene responsible for production of 5-enolpyruvyl-shikimate-3-phosphate (EPS P) synthase, caused reduction of bacterial virulence in both Gram negative and Gram positive bacteria (Izhar *et al*., 1990). Chorsimate synthase has also been proposed as a molecular target for antimicrobials against *Listeria monocytogenes*, a food-borne pathogen (Hossain *et al*., 2015).

Molecular docking involves the search for possible poses of a compound inside the binding pocket of a molecular target predicts the preferred orientation of a ligand when bound to receptor protein or enzyme. Docking programs use different scoring systems to predict and sort these poses with their binding affinities. Therefore, consensus scoring is necessary to obtain accurate results since each computational tool places different weight on the factors involved in interaction established between the ligand-protein complexes. These tools can also predict the nature of the interactions, e.g., van der Waals, hydrogen bonding and hydrophobic interactions (Lengauer and Rarey, 1996; Monika *et al*., 2010; Simmons *et al*., 2010).

In the present study, homology modeling of shikimate kinases from *Pseudomonas* spp. GM41, *Salmonella enterica* subsp. Enterica serovar Enteridis, *Campylobacter jejuni* subsp. jejuni NCTC11168, and *Enterococcus faecalis* is carried out to build three-dimensional structures of the enzyme. These models represent pathogens that are involved in many human infections; finding novel antibiotics is crucial due to the emergence of resistance to almost all the currently available antibiotics.

* Corresponding author. e-mail: saeed.mohammed62@yahoo.com.

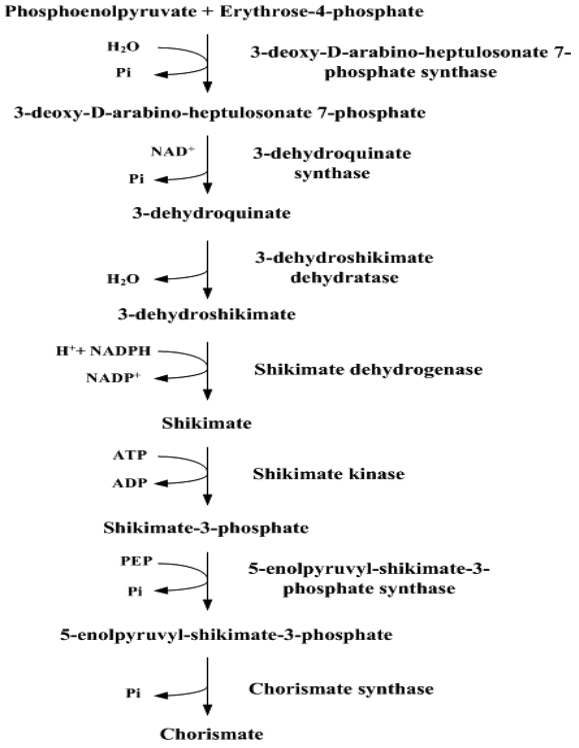

Figure 1. The shikimate acid pathway. PEP: Phosphonolpyruvate, Modified from Gonzalez-Bello, 2016)

2. Materials and Methods

2.1. Homology Modeling and Quality Assessment

Amino acid sequences of shikimate kinase were retrieved from Gene Bank at (http://www.ncbi.nlm. nih.gov/). Models were constructed by an on-line server, RaptorX (Källberg *et al*., 2012), at (http://raptorx. uchicago. edu/) which predicts the binding sites. RaptorX is a statistical method for modeling a protein target using the structural information of experimentally solved template proteins. RaptorX consists of three components: single-template threading, alignment quality prediction and multiple-template threading. The accuracy of the models was assessed by four online tools: (a) ERRAT (Colovos and Yeates, 1993), which can be accessed at (http://services.mbi.ucla.edu/ERRAT/); (b) PROSA (Wiederstein and Sippl, 2007), at (https://prosa.services. came.sbg.ac.at/prosa.php); (c) Qualitative Model Energy ANalysis tool, QMEAN6 (Benkert *et al*., 2009), at: (https://swissmodel.expasy.org/); and (d) Ramachandran plot analysis by RAMPAGE (Lovell *et al.,* 2002), can be accessed at (http://mordred. bioc.cam.ac.uk/~rapper/ rampage.php).

2.2. Ligand Selection

A total of 200 compounds were selected (see supplementary file 1). These include approved and experimental compounds downloaded from Drug Bank V.2 library (http://www.drugbank.ca) (Wishart *et al*., 2008), and natural products obtained from ZINC database (Irwin *et al*., 2012). These two databases also provide the molecular properties of compounds. Compounds for docking were selected according to the study of Sahu and Raval (2016) where molecular weight of 300-500 g/mol, H-bond donors ranged between 2-4, H-bond acceptors ranged between 4-6. The polar surface area was less than 140 Aº (Pajouhesh and Lenz, 2005).

2.3. Molecular Docking

Rigid protein-ligand docking was carried out using Hex 8.0.0. Hex 8.0.0 uses Spherical Polar Fourier (SPF) correlations to accelerate the calculations (Ritchie and Venkatraman, 2010). The settings were: Grid dimension = 0.6, 100 docking solutions, an initial steric scan at N = 18, followed by a final scan at N = 25(N= order of docking correlation), receptor and ligand range 180 degrees. The second docking software, ArgusLab 4.0.1 (Thompson, 2004) which is available at (http://www.arguslab.com/) uses Ascore as an empirical scoring function whose terms have been derived from Xscore. The flexible docking parameters of the latter tool, were: Grid center of 20.0, 20.0 and 20.0 for x, y and z, respectively, grid resolution 0.40 and for 150 evaluations (Wang *et al*., 2002).

3. Results and Discussion

Table 1 shows the templates used to construct the amino acid sequences of shikimate kinases. The first determined structure was that of *Erwinia chrysanthemi* and appeared to be composed of a central sheet of five parallel β-strands flanked by seven α-helices similar in structure to the nucleoside monophosphate kinase family (Krell *et al*., 1998). Similarly, the model of *C. jejuni* in this study has the topology of β1-α1-β2-α2-α3-α4-β3-β4-α5-α6-α7-β5-α8 while the model of *Pseudomonas* spp. has the topology of α1-β1-α2-α3-α4-β2-α5-β3-α6-α7-β4-α8. Both *S. enteridis* and *E. faecalis* have their models of the topology: β1-α1-β2-α2-α3-α4-β3- α5-β4-α6-α7-β5-α8. Two binding sites have been identified in the enzyme, one for ADP and the other for shikimate since the enzyme is responsible for conversion of shikimate to shikimate-3-phosphate by transfer of a phosphate group from ATP. Table 2 lists the amino acid residues involved.

In *H. pylori*, shikimate kinase consists of three domains: (a) the core domain, (b) the shikimate binding domain, and (c) the LID region. Several conserved motifs were also characterized: (1) the Walker A motif GXXGXGKT/S (residues 8 to 15), (2) the DT/SD motif (residues 31 to 33) in which Asp^{33} is essential to interact with O-11 and O-12 of the shikimate, and (3) the GGGXV segment, residues 79 to 83 (Cheng *et al*., 2005). In *M. tuberculosis* Shikimate kinase three domains: (a) a core domain consists of five β-sheets and the Walker A-motif, residues 9-17, forming the binding site for ATP and ADP, lies between β1-α1, (b) the LID domain, residues 112-124, which closes over the active site and has residues also essential for binding ATP, and (c) the substrate binding domain, residues 33-61, which binds shikimate. The last domain comprises Arg^{136}, Arg^{58}, Glu^{61}, Asp^{34}, Arg^{117} and Lys^{15}, and a lipophilic pocket made by Phe^{49}, Phe^{57}, Pro^{118}, Gly^{79}, Gly^{80} and Gly^{81} (Hartmann *et al*., 2006). Figure 2 shows the crystal structure (resolution 1.57A) of *Campylobacter jejuni* (PDB: 1viaA) (Badger *et al*., 2005).

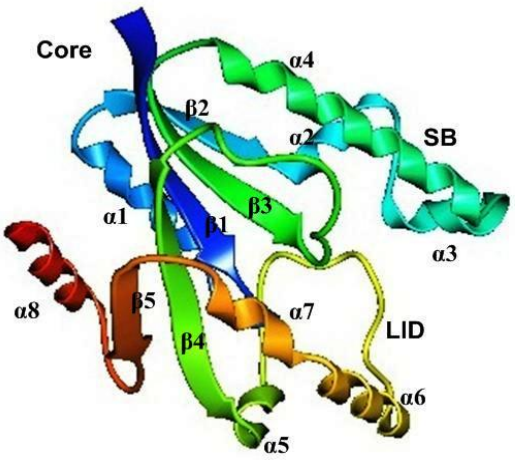

Figure 2. Shikimate kinase of *C. jejuni* (PDB ID: 1viaA). Three domains are present; (a) a core domain, consists of five β-sheets containing the binding site for ATP between β1-α1; (b) the LID domain, comprises residues also essential for binding ATP; and (c) the substrate binding domain, SB, residues which binds shikimate, viewed by ArgusLab 4.0.1 (Thompson, 2004)

Table 1. Models of shikimate kinase built by RaptorX with their quality assessment

Microorganism	Sequence ID	Templates	ProSA	ERRAT (%)	QMEAN6	Ramachandran plot FR[1] (%)	AR[2] (%)	OR[3] (%)
Pseudomonas spp. GM41	EUB76877.1	4y0aA, 1kagA, 3trfA	-6.26	89.032	0.833	159 (98.8)	2 (1.2)	0 (0.0)
S. enterica subsp. enterica serovar Enterdis	KOX84760.1	1e6cA	-6.39	89.595	0.794	176 (98.3)	0 (0.0)	3 (1.7)
C. jejuni subsp. Jejuni NCTC11168	CAL34537.1	1viaA	-6.59	98.726	0.756	158 (96.9)	4 (2.5)	1 (0.6)
E. faecalis	KOA04110.1	4y0aA, 1e6cA, 3nwjA, 3trfA, 3vaaA	-8.86	86.875	0.781	156 (94)	5 (3.0)	5 (3.0)

[1]Residues in favored region, [2]residues in the allowed region, [3]residues in the outlier region

Table 2. Binding sites of shikimate kinases produced by RaptorX

Microorganism	Pocket 1:ADP	Pocket 2:Shikimate-3-phosphate
Pseudomonas spp. GM41	Met[1], Gly[2], Ala[3], Gly[4], Lys[5], Ser[6], Thr[7], Arg[101], Arg[108], Asp[142], Glu[143], Arg[144], Pro[145], Pro[146]	Met[1], Asp[24], Phe[39], Phe[47], Arg[48], Glu[51], Gly[69], Gly[70], Gly[71], Ala[72], Pro[109]
S. enterica subsp. enterica serovar Enteridis	Pro[10], Arg[11], Gly[12], Cys[13], Gly[14], Lys[15], Thr[16], Thr[17], Arg[110], Ala[153], Lys[155], Ala[156], Pro[157]	Arg[11], Lys[15], Thr[33], Asp[34], Val[45], Arg[58], Glu[61], Thr[77], Gly[78], Gly[80], Ile[81], Arg[139]
C. jejuni subsp. jejuni NCTC11168	Met[13], Gly[14], Ser[15], Gly[16], Lys[17], Ser[18], Thr[19], Arg[109], Leu[110], Asp[111], Lys[112], Asp[113], Glu[114], Lys[117], Lys[151], Asn[152], Arg[153], Ile[153]	Ser[35], Asp[36], Val[47], Phe[51], Phe[59], Arg[60], Glu[60], Gly[81],Gly[82], Gly[83], Phe[84], Lys[117], Arg[134]
E. faecalis	Met[10], Gly[11], Ala[12], Gly[13], Lys[14], Thr[15], Thr[16], Arg[109], Thr[151], Asn[152], Arg[153], Ser[154], Pro[155]	Ser[35], Leu[32], Asp[33], Ile[44], Phe[48], Phe[56], Arg[57], Glu[60], Gly[77], Gly[78], Gly[79], Ile[80], Arg[118], Leu[120]

The quality of the predicted models should be determined since it affects their reliability for application in docking experiments. ProSA measures the deviation of the models from native structures that have been solved experimentally in terms of standard deviation of statistical potential energy (Wiederstein and Sippl, 2007). All the models were within the range of X-ray crystallographic and NMR experimental structures (Figure 3). Regarding ERRAT, the model of *C. jejuni* (Figure 4) had the highest overall quality (98.70%) in terms of heavy atomic-pair distributions (CC, CN, CO, NN, NO and OO) while that of *E. faecalis* had the lowest value. It has been suggested that good high-resolution experimental structures usually have quality factors of 95% or even higher but for lower resolution structures a quality of 91% is accepted (Colovos and Yeates, 1993). All the models have QMEAN6 values in the normal range of 0-1. This tool measures the global (overall) and local (for each residue) quality of the model

on the basis of statistical potentials that describes atomic interactions, burial state of residues, and the agreement between the calculated and predicted secondary structure' elements (Benkert *et al*., 2009).

The distribution of backbone dihedral angles, Ramachandran plot, is usually used for quality assessments as stereochemical measure, since that the three backbone dihydral angles ϕ, ψ and ω are the main determinants of the protein folding. Therefore, two-dimensional scatter plots of ϕ and ψ pairs were developed for this purpose (Ramachandran *et al*., 1963; Hooft *et al*., 1997). All the models have more than 90% their amino acids in the favored region. Laskowski *et al*. (1993) suggested that a reliable model generally has a Ramachandran plot in which more than 90% of the residues should be located in the most favored region. (Lovell *et al*., 2003). Arg[55] is in the disallowed region of *C. jejuni* model (Figure 5), while Gln[42], Leu[168] and Pro[169] are in the disallowed region of *S. enterica* model. Ser[68], Gln[94], Glu[115], Glu[123] and Ser[125] are in the disallowed region of *E. faecalis*. MODELLER, another homology modeling software, was used to construct a model of *M. tuberculosis* using tertiary structure of *E. chrysanthem* as a template. Analysis of the Ramachandran plot for this *M. tuberculosis* model by PROCHECK, another stereochemical check tool similar to RAMPAGE, showed that 91.1% of the residues were in the most favorable region and the remaining 8.9% were in the additional allowed regions. In the same research, the analysis for crystallographic *E. chrysanthemi* shikimate kinase structure showed that 93.7% of residues were in the most favorable, 6.1% additional allowed regions, and 0.7% generously allowed regions (de Azevedo *et al*., 2002).

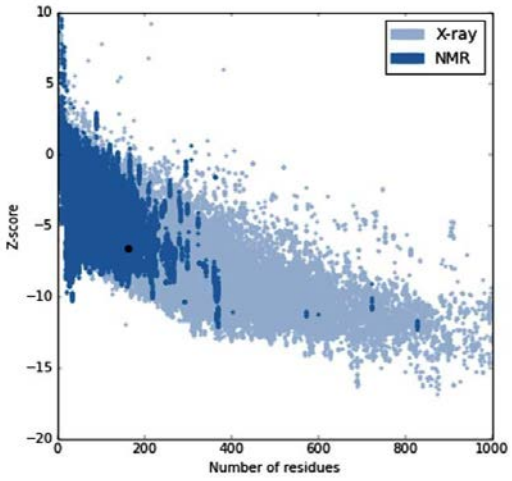

Figure 3. Z-score of *C. jejuni* predicted by ProSA web tool, black dots represent the model compared with the Z-scores of the experimentally determined proteins by NMR spectroscopy and X-ray crystallography

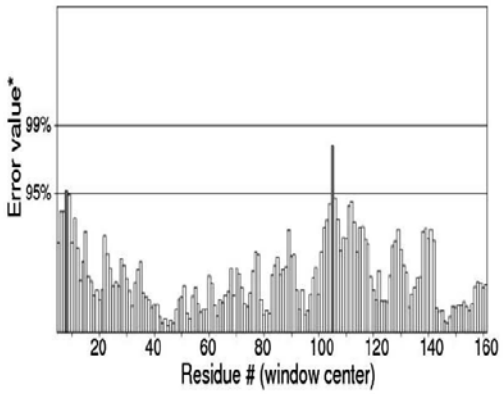

Figure 4. ERRAT result of *C. jejuni*. Black bars represent misfolded regions. On the error axis two lines are drawn to indicate the confidence in which it is possible to reject regions

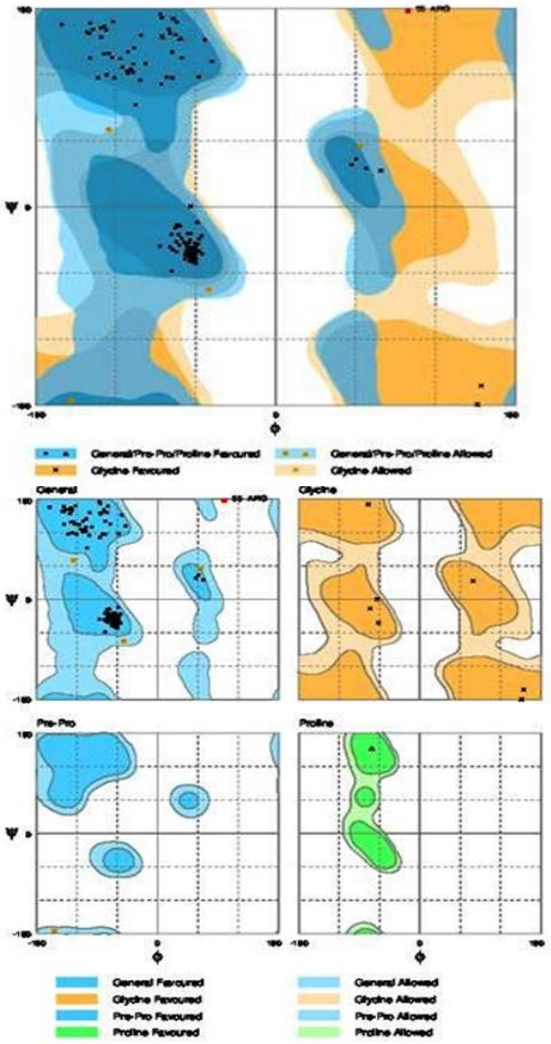

Figure 5. Ramachandran plot of *C. jejuni* model using RAMPAGE. Residues in the disallowed regions are red-colored squares while residues in allowed region are brown-colored squares

Using ArgusLab 4.0.1, a total of 200 compounds were selected and docked against shikimate kinase of *C. jejuni*. The compounds showed that the docking scores were higher than the control, shikimate-3-phosphate (Figure 6), and they were also redocked against the other models and by Hex 8.0.0. R esults are shown in Tables 3 a nd 4. Dobutamine (DB00841), oxprenolol (DB01580), (3,4-dihdroxy-2-nitrophenyl) (phenyl) methanone (DB07462), and isoxsuprine (DB08941), had docking scores higher than the control in all the models and by both docking tools. Their interactions with the residues of shikimate kinase of *C. jejuni* at active site are illustrated in Figures 7 and 8. Their chemical structures are shown in Figure 9 and the molecular properties of compounds are listed in Table 5.

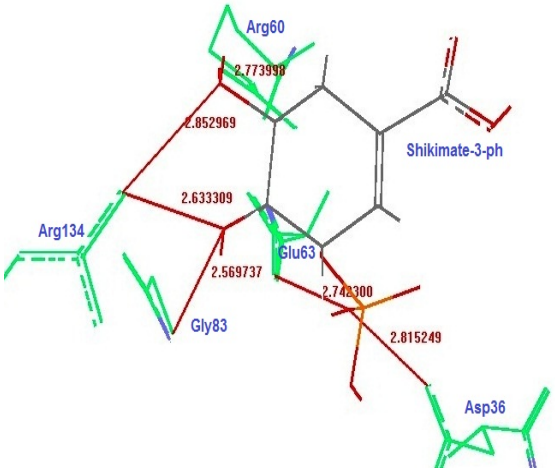

Figure 6. Interaction of shikimate-3-phosphate with its binding site: Shikimate-3-phosphate forms H-bonds with the residues Asp^{36} (2.815 Å), Glu^{63} (2.742 Å), Gly^{83} (2.569 Å), Arg^{60} (2.773 Å) and Arg^{134} (2.633 and 2.852 Å). H-bonds are red colored (numbers refer to distances whereas amino acids are green, viewed by ArgusLab 4.0.1 (Thompson, 2004)

Segura-Cabrera and Rodriguez-Perez (2008) used eHiTS, docking program, to screen for inhibitors of *Mycobacterium tuberculosis* shikimate kinase. Hossain *et al*. (2015) used Autodock in screening libraries of compounds for chorismate synthase inhibitors. Sahu and Raval (2016) screened ZINC database for drug-like molecules against shikimate kinase of *M. tuberculosis*, by using ArgusLab and i-dock tools. Nine ligands were identified whose docking scores above of shikimate. The best two were ZINC34797195 and ZINC72356318. ZINC34797195 forms six hydrogen bonds with the enzyme; Gly^{81} (2.06 Å), Leu^{119} (3.81 Å), Arg^{136} (2.06 Å), Gly^{80} (2.91 Å), Gly^{81} (2.44 Å), Asp^{34} (3.61 Å), and Arg^{117} (2.31 Å). The enzyme also forms six hydrogen bonds with ZINC72356318; Gly^{80} (3.5Å), Gly^{81} (3.66Å), Arg^{136} (2.48Å), Arg^{136} (2.92Å), Leu^{119} (2.65Å), Asp^{34} (3.71Å), and Arg^{117} (2.31 Å). According to Sahu and Raval (2016), the binding site contains the amino acids Asp^{34}, Phe^{57}, Arg^{58}, Gly^{79}, Gly^{80}, Gly^{81}, Leu^{119}, Arg^{117} and Arg^{136}.

Simithy *et al.* (2014) used a library of 400 compounds to identify several compounds that inhibit shikimate kinase of *M. tuberculosis*.

The most active compounds contained either a 2-aminobenzothiazole moiety or an oxadiazole-amide in their structures, with IC_{50} values between 1.9 and 3.8 µM. Using Schrodinger software, shikimate kinase was docked with ligands from Pubchem database and two ligands, SPB01099 and AG538, had docking scores -6.15 and -6.17, respectively, that were higher than shikimate as control (-6.13) (Sinha *et al*., 2013). In addition, Cheng *et al.* (2012) also identified a compound, naphthalene-2-sulfonate, with an IC_{50} value of 4.9 µM as inhibitor of *H. pylori*.

Table 3. Docking results of shikimate kinases using Arguslab 4.0.1

Compound ID	*C. jejuni*	*S. enteridis*	*Pseudomonas* spp.	*E. faecalis*
DB04328*	-8.214	-7.949	-8.988	-9.030
DB00598	-10.321	-11.549	-9.101	-7.929
DB00628	-9.787	-9.609	-7.810	-9.756
DB00841	-11.009	-11.337	-10.066	-9.855
DB01210	-10.758	-9.651	-8.363	-9.322
DB01580	-9.359	-8.533	-9.157	-9.805
DB03601	-8.777	-8.488	-8.085	-9.624
DB07462	-10.748	-10.966	-10.287	-12.179
DB07893	-10.159	-9.486	-8.379	-10.987
DB07894	-9.726	-9.753	-10.477	-9.460
DB08941	-9.486	-10.229	-9.805	-9.071
ZINC00058117	-9.022	-8.558	-8.934	-7.674
ZINC14806959	-9.737	-10.756	-8.355	-9.793

*Shikimate 3-phosphate, control

Combinations of atovaquone (antimalarial drug) with four shikimate analogues 6-R-F-shikimate, 6-R-F-4-epishikimate, 3-deoxy-3,3-difuoro-shikimate, and 3-deoxy-3,3-difuoro-4-epi-shikimate indicated synergy since the combination of Atovaquone with micromolar concentrations of the fuorinated shikimates reduced t he IC_{50} for atovaquone about 250-fold (McConkey, 1999).

Table 4. Docking results of shikimate kinases using Hex 8.0.0

Drug Bank ID	*C. jejuni*	*S. enteridis*	*Pseudomonas* spp.	*E. faecalis*
DB04328	-226.81	-215.55	-223.11	-186.07
DB00598	-251.32	-281.14	-292.19	-250.83
DB00628	-275.24	-271.14	276.30	-259.02
DB00841	-272.10	-250.37	-290.70	-252.92
DB01210	-259.93	-237.83	-273.93	-246.66
DB01580	-243.47	-232.62	-256.22	-230.51
DB03601	-230.27	-272.24	-256.30	-225.92
DB07462	-231.10	-225.94	-255.80	-218.04
DB07893	-268.92	-272.37	-265.04	-253.20
DB07894	-236.01	-215.17	-248.59	-253.20
DB08941	-261.08	-239.82	-296.41	-247.83
ZINC00058117	-247.83	-247.81	-252.87	-226.97
ZINC14806959	-239.66	-243.78	-251.70	-207.61

Table 5. Molecular properties of the best selected compounds

Database ID	Generic name	Mass (g/mol)	LogP	HBD	HBA	PSA (Aº)
DB04328	Shikimate 3-phosphate	254.02	-2.07	5	7	144.52
DB00598	Labetalol	328.18	1.73	4	4	95.58
DB00628	Clorazepate	314.05	2.68	2	4	78.76
DB00841	Dobutamine	301.17	2.97	4	4	72.72
DB01210	Levobunolol	291.18	2.06	2	4	58.56
DB01580	Oxprenolol	265.17	2.44	2	4	50.72
DB03601	5-deoxyflavanone	256.07	2.79	2	4	66.76
DB07462	(3,4-dihdroxy-2-nitrophenyl)(phenyl) methanone	259.05	2.36	2	5	103.35
DB07893	Phenyl[1-(N-succinylamino) pentyl] phosphonate	343.12	1.46	3	5	112.93
DB07894	4-(2-hydroxy-4-fluorophenylthio)-butylphosphonic acid	278.02	1.32	3	4	77.76
DB08941	Isoxsuprine	301.17	2.06	3	4	61.72
ZINC00058117	Eridoicytol	288.26	1.63	4	6	107.00
ZINC14806959	Baicalein	254.24	2.13	3	5	87.00

Staurosporine is a kinase competitive inhibitor but a toxic one; compounds 670–672 are pyrazolone analogs that have been shown to be shikimate kinase inhibitors. However, there are no *in vivo* studies on these compounds; however, *in vitro* studies were conducted using ultrafiltration-liquid chromatography/mass spectrometry to measure binding affinities and an LC/MS-based MtSK to measure the amount of shikimate-3-phosphate in the presence of an inhibitor (Mulabagal and Calderón, 2010; Bandodkar and Schmitt, 2007).

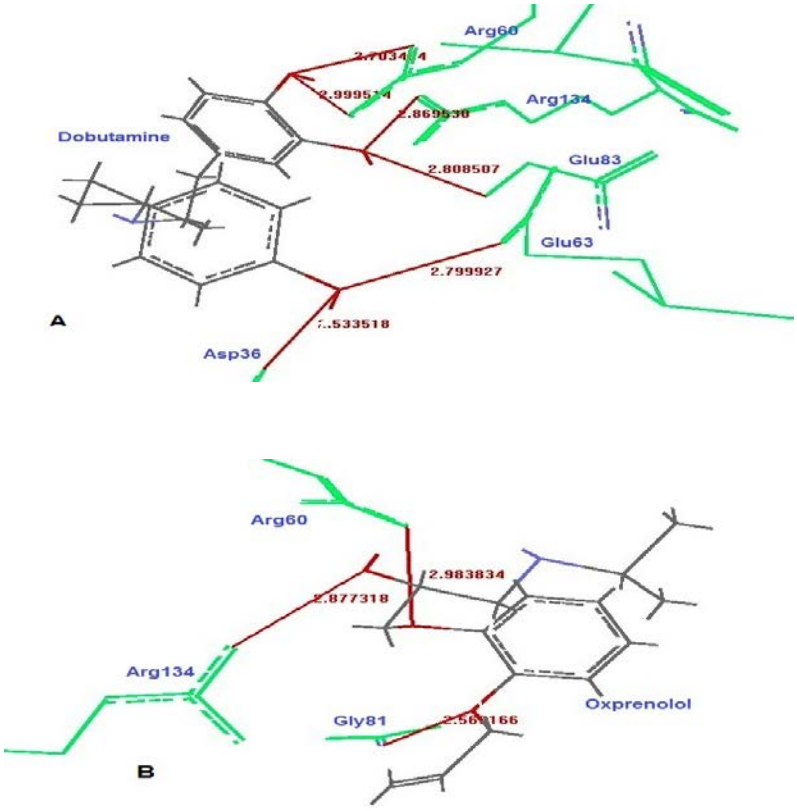

Figure 7. (A) Dobutamine (DB00841) forms H-bonds with the residues Asp[36] (2.533Å), Arg[60] (2.703 and 2.999Å), Glu[63] (2.799Å), Gly[83] (2.808Å) and Arg[134] (2.869Å). (B) Oxprenolol (DB01580) forms H-bonds with the Arg[60] (2.983Å), Gly[81] (2.565Å), and Arg[134] (2.877Å). H-bonds are red colored (numbers refer to distances) whereas amino acids are green, viewed by ArgusLab 4.0.1 (Thompson, 2004)

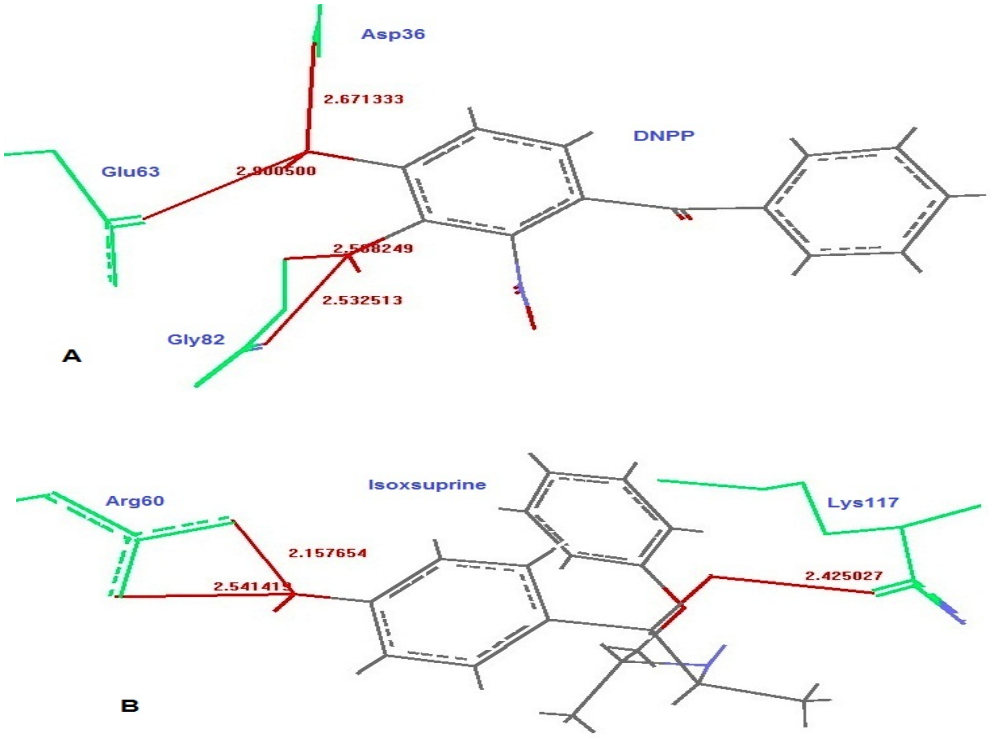

Figure 8. (A) (3,4-dihdroxy-2-nitrophenyl) (phenyl) methanone (DB07462), designated DNPP, forms H-bonds with Asp[36] (2.671Å), Glu[63] (2.900Å) and Gly[82] (2.533 and 2.588Å). (B) Isoxsuprine (DB08941) forms H-bonds with Arg[60] (2.157 and 2.541 Å), and Lys[117] (2.425Å). H-bonds are red colored (numbers refer to distances) whereas amino acids are green, viewed by ArgusLab 4.0.1 (Thompson, 2004).

4. Conclusion

Shikimate kinase may serve as an alternative target in developing antibacterial, antiparasitic agents and herbicides. Oxprenolol (used to treat hypertension), dobutamine (treating cardiac arrhythmias) and isoxsuprine (vasodilator) had binding affinities higher than shikimate, the substrate as control, in docking experiments suggesting that may be used in screening for new compounds in antibacterial drug design. However, *in silico* screening methods should be followed by *in vitro* and *in vivo* experiments, pharmacokinetics and toxicity studies in order to explore their efficacy and usefulness to human.

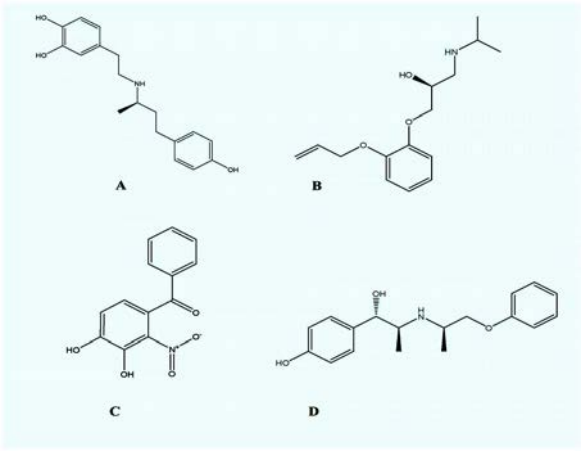

Figure 9. Chemical structures of (A) dobutamine (B) oxprenolol (C) (3,4-dihdroxy-2-nitrophenyl)(phenyl) methanone, and (D) isoxsuprine

Acknowledgement

The author thanks Concepcion Gonzalez-Bello for permission to reproduce the scheme of shikimate pathway. The author wishes to acknowledge the institutions for free online access to bioinformatics' tools especially Chicago Technical Inst., Scripps Research Inst., MBI Lab at UCLA, SIB and Biozentrum at Basel University, Biochemistry department of Cambridge University; CAME laboratory at Salzburg University.

References

Amer FA, El-Behedy EM and Mohtady HA.2008. New targets for antibacterial agents. *Biotechnol Mol Biol Rev*., **3**:46-57.

Badger J, Sauder JM, Adams JM, Antonysamy S, Bain K, Bergseid MG et al. 2005. Structural analysis of a set of proteins resulting from a bacterial genomics project. *Proteins*,**60**:787-796.

Bandodkar BS and Schmitt S .2007.Pyrazolone derivatives for the treatment of tuberculosis. *Patent*, WO/2007/020426 A1.

Benkert P, Kunzli M and Schwede T.2009. QMEAN server for protein model quality estimation. *Nucleic Acids Res.*, W510-514.

Cheng W-C, Chen Y-F and Wang H-J.2005. Structural basis for shikimate-binding specificity of *Helicobacter pylori* shikimate kinase. *J Bacteriol.*, **187**: 8156-8163.

Cheng W-C, Chen Y-F, Wang H-J, Hsu K-C, Lin S-C, Chen T-J, Yang J-M and Wang W-C.2012. Structures of *Helicobacter pylori* shikimate kinase reveal a selective inhibitor-induced-fit mechanism. *PLoS ONE*, **7**: e33481

Colovos C and Yeates TO.1993. Verification of protein structures: Patterns of non-bonded atomic interactions. *Protein Sci.*, **2**:1511-1519.

Daughery M, Vonstein V, Overbeek R and Oserman A .2001. Archaeal shikimate kinase, a new member of the GHMP-kinase family. *J Bacteriol.*, **183**: 292-300.

de Azevedo Jr WF, Canduri F, de Oliveira JS, Basso LA, Palma MS, Pereira JH and Santos DS.2002. Molecular model of shikimate kinase from *Mycobacterium tuberculosis*. *Biochem Biophys Res Commun.*, **295**:142-148.

Gonzalez-Bello C.2016. Inhibition of shikimate kinase and type II dehydroquinase for antibiotic discovery: Structure-based design and simulation studies. *Curr Topics Med Chem.*, **16**:960-977.

Hartmann MD, Bourenkov GP, Oberschall A, Strizhov N and Bartunik HD.2006. Mechanism of phosphoryl transfer catalyzed by shikimate kinase from *Mycobacterium tuberculosis*. *J Mol Biol.*, **364**:411-423.

Hooft RWW, Sander C and Vriend G.1997. Objectively judging the quality of a protein structure from a Ramachandran plot. *CABIOS*, **13**:425-430.

Hossain MM, Roy PK, Jannatul Mosnaz ATM, Shakil SK, Hasan MM and Prodhan SH.2015. Structural analysis and molecular docking of potential ligands with chorismate synthase of *Listeria monocytogenes*: A novel antibacterial drug target. *Indian J Bioch Bioph.*, **52**:45-59.

Irwin JJ, Sterling T, Michael MM, Bolstad ES and Coleman RG.2012. ZINC: A free tool to discover chemistry for biology. *J Chem Inf Model.*, **52**:1757-1768.

Izhar M, DeSilva L, Joysey HS and Hormaeche CH.1990. Moderate immunodeficiency does not increase susceptibility to *Salmonella typhimurium aroA* live vaccines in mice. *Infect Immun.*, **58**:2258-2261.

Källberg M, Wang H, Wang S, Peng J, Wang Z, Lu H and Xu J.2012. Template-based protein structure modeling using the RaptorX web server. *Nat Protocols*, **7**:1511-1522.

Krell T, Coggins JR and Lapthorn AJ .1998. The three-dimensional structure of shikimate kinase. *J Mol Biol.*, **278**:983-997.

Laskowski RA, MacArthur MW, Moss D and Thornton JM .1993. PROCHECK: A program to check the stereochemical quality of protein structures. *J Appl Crystal*, **26**:283-291.

Lengauer T and Rarey M .1996. Computational methods for biomolecular docking. *Curr Opin Struct Biol.*, **6**:402-406.

Lovell SC, Davis IW, Arendall 3rd WB, de Bakker PI, Word JM, Prisant MG, Richardson JS and Richardson DC.2003. Structure validation by Cα geometry: Phi, psi and Cβ deviation. *Proteins: Struct Funct Genet*, **50(3)**:437-450.

McConkey GA .1999. Targeting the shikimate pathway in the malaria parasite *Plasmodium falciparum*. *Antimicrob Agents Chemother.*, **43**:175-177.

Monika G, Punam G, Sarbjot S and Gupta GD.2010. An overview on molecular docking. *Int J Drug Dev Res.*, **2**:219-231.

Mulabagal V and Calderón A.2010.Development of an ultrafiltration-liquid chromatography/mass spectrometry (UF-LC/MS) based ligand-binding assay and an LC/MS based functional assay for *Mycobacterium tuberculosis* shikimate kinase. *Anal Chem.*, **82**:3616–3621.

Pajouhesh H and Lenz GR.2005. Medicinal chemical properties of successful central nervous system drugs. *Neuro Rx.*, **2**:541-553.

Ramachandran GN, Ramakrishnan C and Sasisekharan V.1963. Stereochemistry of polypeptide chain conformations. *J Mol Biol.*, **7**:95-99.

Ritchie DW and Venkatraman V.2010. Ultra-fast FFT protein docking on graphics processors. *Struct Bioinformatics*, **26**:2398-2405.

Sahu PK and Raval MK.2016.Virtual screening for inhibitors of shikimate kinase of *Mycobacterium tuberculosis*. *Pharma Biol Eval.*, **3**:320-326.

Segura-Cabrera A and Rodriguez-Perez MA.2008. Structure-based prediction of *Mycobacterium tuberculosis* shikimate kinase inhibitors by high throughput virtual screening. *Bioorg Med Chem Lett.*, **18**:3152-3157.

Simithy J, Reeve N, Hobrath JV and Reynolds RC.2014. Identification of shikimate kinase inhibitors among anti-*Mycobacterium tuberculosis* compounds by LC-MS. *Tuberculosis*, **94**:152-158.

Simmons KJ, Chopra I and Fishwick CWG.2010. Structure-based discovery of antibacterial drugs. *Nature Rev Microbiol.*, **8**:501-510.

Sinha S, Rajasulochana P, Ramesh Babu PB and Krishnamoorthy P.2013. Comparative modeling of shikimate kinase (M Tb) and molecular docking studies of its known inhibitors. *Res J Pharma Biol Chem Sci.*, **4**:715-720.

Thompson M.2004. ArgusLab 4.0.1. Planaria Software LLC. Available at (http://www.arguslab. com). Seattle, Washington, USA.

Tohge T, Watanabe M, Hoefgen and Fernie AR.2013. Shikimate and phenylalanine biosynthesis in the green lineage. *Front Plant Sci.*, **4**:1-13.

Wang R and Lai L and Wang S.2002. Further development and validation of empirical scoring functions for structure-based binding affinity prediction. *J Comp Aided Mol Design*, **16**:11-26.

Wiederstein M and Sippl MJ .2007. ProSA-web: Interactive web service for the recognition of errors in three-dimensional structures of proteins. *Nucleic Acids Res.*, **35**:W407-410.

Wishart DS, Knox C, Guo AC, Cheng D, Shrivastava S., Tzur D, Gautam B and Hassanali M .2008. Drug Bank: A knowledgebase for drugs, drug actions and drug targets. *Nucleic Acids Res.*, **36**: 901-906.

JJBS

Volume 10, Number 4,December 2017
ISSN 1995-6673
Pages 281 - 287

Jordan Journal of Biological Sciences

Quantitative Analysis of Macrobenthic Molluscan Populations Inhabiting Bandri Area of Jiwani, South West Pakistan Coast

Abdul Ghani[1], Nuzhat Afsar[1,*] and Solaha Rahman[2]

[1]Institute of Marine Science (IMS);
[2]Department of Zoology, University of Karachi, Karachi-75270 – Pakistan

Received: May 7, 2017; Revised: August 14, 2017; Accepted: August 17, 2017

Abstract

The present study is done by using quadrate sampling techniques to estimate macrobenthic molluscan population structure on three tidal levels at two selected stations along the Bandri beach of Jiwani coast, Balochistan for the first time during October 2014 to March 2015. Generally calculated values show a higher species composition, abundance and density at station two (ST-II) which has a predominately rocky bottom profile, while species frequency and diversity are found to be higher at station one (ST-I) which has a sandy muddy bottom composition. Calculating the species composition values reveals that only 4 species give more than 1 % mean cover (overall an average composition %) at ST-I which are *Umbonium vesterium* (94.34 %), *Mitrella blanda* (2. 37 %), *Branchiodontes variabilis* (1.79%) and *Nassarius (Plicalcularia) persicus* (1.17 %), whereas at ST-II only one sp. provides more than 1 % mean cover which is *Branchidontes variabilis* (98.46 %). Overall *Umbonium vesterium* and *Branchiodontes variabilis* dominated the populations at ST-I and II, respectively, at all three tidal levels. Besides calculating species similarities between two stations and over total area, it remained maximum in November 2014 (0.44) and minimum in March 2015 (0.11).

Key words: Molluscan diversity, Bandri beach, Jiwani, Arabian Sea.

1. Introduction

Molluscs are dominating animal group in term of the diversity in the intertidal areas, and due to their ecological adaptation they are found in nearly every habitats; from deepest ocean trenches to the intertidal zone, land and freshwater where they cover a wide range of habitats. Due to easy accessibility, intertidal zones always remain highly sampled than any other ambiance. (Vaghela and Kundu, 2011; Khade and Mane, 2012). For its biodiversity, the intertidal zone has been extensively studied (Little and kitching, 1996). In the intertidal zone measures of species richness, density and abundance are dependent in the difference between spatial patterns of mobile and sessile taxa (Davidson *et al*., 2004). Within the area of few meters of the intertidal zone numerous kind of fauna and flora are observed and is considered as the most productive and diverse (Underwood, 2000). Rocky intertidal zones are found with different zones and bands, containing different biodiversity in which vertical zonation is the most effective phenomena or process to observed rocky intertidal fauna and flora from lower to upper intertidal area (Bandel and Wedler, 1987; Ellis, 2003).

Certainly, many factors or anthropogenic activities that affect the natural habitats of coastal molluscan populations are mainly overexploitation, urbanization of coastal areas, pollution, and conversion of natural area, industrialization and development of public facilities (Ahmed, 1997; Lardicci *et al.*, 1997). However, estuaries and coastal zone are used for a variety of purposes because of their socioeconomic and ecological significance and these activities are subjected to increasing pressure and anthropogenic impact on coastal habitats, which in turn results in environmental stress public health issues. From the research point of view, factors controlling the biodiversity of an area and their functions are mainly in focus (Tilman, 2000). Comparable and meaningful measures of biodiversity are needed to grow awareness related to biodiversity issues to take these into a sharp focus (Gray, 1997; McCann, 2000).

Several published reports from Pakistan are available on molluscan fauna found along the Sindh and Balochistan coast's containing details of species diversity, abundance, population structure, seasonal variations, zonation patterns, etc. (Barkati and Rahman, 2005). However, in the present study, attempts have been made to record macrobenthic molluscan diversity, species composition and population structure at Bandri beach area of Jiwani coast, Balochistan

* Corresponding author. e-mail: nuzhatafsar259@hotmail.com.

for the first time. This site has never been explored previously; therefore, there is no available published record of molluscan diversity from the subjected area, except for a brief systemic account of two flag pen shells from the area (Ghani and Afsar, 2017). Moreover, Bandri is a cl eaner site and anthropogenic pressures are uncommon there so far.

2. Material and Methods

2.1. Study Area

Bandri beach along the Jiwani coast, Balochistan is located at 25.0667° N, 61.8000° E (Figure 1). Study surveys were made during October 2014 to March 2015. In the present study, the site was selected in Jiwani is Bandri beach, which is located along Gawatar Bay, touching the boundary line between Iran and Pakistan, and facing entrance of Gulf of Oman. Two stations were selected side by side along the Bandri beach that is open to direct surf action. Generally, substrate of the beach is hard with plain surface of extremely low slope occupied by boulders. Some parts of substrate appeared to form low profiled rocky overhangs and cave, like shelters. Primarily, the physical substrate profile is a bit different at both stations, such as at 1st station there is no or very small cave-like shelters are present with sandy and muddy substrate, whereas 2nd station is flourish through boulders and rocks with prominent cave-like shelters.

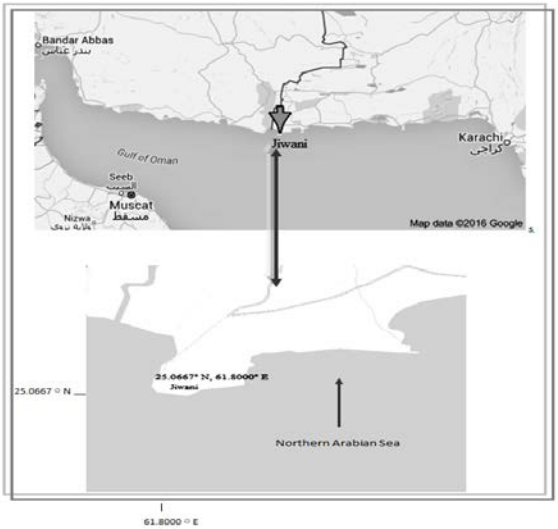

Figure 1. Map is showing collection site Bandri beach, Jiwani.

2.2. Sample Collection and Data Analysis

Quadrate sampling technique is used to carry out the field surveys by placing random quadrates (0.19 m²) on upper mid and lower tidal zones to measure benthic molluscan assemblages by means of quantitative analysis. Data collected by this method are summed up for data analysis; species abundance, density, frequency, diversity, richness, evenness and dominance were calculated by statistical software (PRIMER 5). Formulas of all calculated indices are given below:

Abundance: Total number of individual's recorded/Total number of quadrate where the individuals occurred.

Density: Total number of individuals recorded from the quadrate/ Total number of quadrate studied.

*Frequency (%)***:** Number of quadrate where the species occurred X 100/ Total number of quadrate where the individual occurred.

*Margalef's Diversity Index***:** Dmg = (S-1) /ln N. Where, N= the total number of individuals in the sample; S= the number of species recorded; Ln= natural logarithm.

*Shannon's Diversity Index***:** H= ∑ pi*ln pi. Where, Pi= S/N; S= number of individuals of one species; N= Total number of all individual in the sample or number of individuals (of all species); Ln= natural logarithm.

*Pielou's Evenness Index***:** E = H/lnS. Where, H= Shannon's-Wiener Diversity Index; S= Total number of species in the sample.

*Berger-Parker Dominance Index***:** D = N max/S. Where, N max = the number of individual of most abundant species; S = Total number of observed species.

3. Results

During the present study, by using randomly placed quadrate sampling technique, collectively a total of (13) molluscan species were recorded along station one. Calculation revealed that only 4 species given more than 1% mean cover (overall an average composition %), while rest contributed less than 1% of the total mean cover (Table 1). Whereas a total of (31) molluscan species were found at station two. Among 31 species, gastropod amounted 24 species 6 bivalves and 1 polyplchopora, and not more than 21 species were found constantly in any single collection. There is only one species provided more than 1% mean cover that is *Branchidontes variabilis* (98.46%). Whereas other 30 m olluscan species showed less than 1% mean cover during the study period as detailed in Table 2.

Table 1. Molluscan species composition, abundance, density and frequency (no/0.19m²) along Bandri Beach (ST-I). Whereas ST-I= station one; A.C= Average Composition; A.A= Average Abundance; A.D= Average Density and A.F= Average Frequency.

S. No	Species Names	A.C	A.A	A.D	A.F
	Gastropods				
1	*Anachis fauriti*	0.29	1.96	0.44	22.22
2	*Anachis terpischore*	0.23	1.50	0.33	22.22
3	*Cellana radiata*	0.16	2.00	0.22	11.11
4	*Cerithium caeruleum*	0.33	4.33	0.48	11.11
5	*Clypeomorus bifaciata*	0.59	5.00	1.11	22.22
6	*Mitrella blanda*	2.42	5.79	3.65	51.11
7	*Nassarius(Plicarcularia) fissilabiris*	0.46	6.00	0.67	11.11
8	*Nassarius(Plicarcularia) persicus*	1.26	3.75	1.91	46.30
9	*Nerita albicilla*	0.63	2.88	0.89	27.78
10	*Siphonaria savignyii*	0.18	2.50	0.44	11.11
11	*Lunella cronata*	0.61	3.05	0.19	31.11
12	*Umbonium vesterium*	94.11	132.82	126.32	95.45
	Bivalves				
13	*Branchidontes variabilis*	1.79	30.00	3.33	11.11

Table 2. Molluscan species composition, abundance, density and frequency (no/0.19m²) along Bandri Beach (ST-II). Whereas A.C= Average Composition; A.A= Average Abundance; A.D= Average Density and A.F= Average Frequency.

S. No	Species Names	A.C	A.A	A.D	A.F
	Gastropods				
1	*Anachis terpischore*	0.01	2.67	0.29	11.11
2	*Bullia tranquabarica*	0.01	1	0.11	11.11
3	*Cellana radiata*	0.01	2.50	0.28	11.11
4	*Cerithium caeruleum*	0.03	3.40	0.64	17.78
5	*Clypeomorus bifaciata*	0.10	14.20	1.73	13.33
6	*Diodora funiculata*	0.02	2.25	0.33	13.89
7	*Euchelus asper*	0.01	2.25	0.25	11.11
8	*Hexaplex kuesterianus*	0.01	1.50	0.17	11.11
9	*lunella cronata*	0.08	4.06	1.54	37.03
10	*Mitrella blanda*	0.03	5.00	0.56	11.11
11	*Morula granulata*	0.02	2.67	0.45	18.52
12	*Morula nodulosa*	0.01	1.33	0.25	11.11
13	*Nassarius(Plicarcularia) fissilabris*	0.01	2.00	0.22	11.11
14	*Nassarius deshyesiana*	0.03	6.00	0.67	11.11
15	*Nassarius marmmorius*	0.01	2.00	0.22	11.11
16	*Nerita albicilla*	0.12	4.28	2.20	51.85
17	*Nerita longii*	0.01	2.33	0.26	11.11
18	*Planaxis sulcatus*	0.07	5.25	0.17	18.52
19	*Purpura persicus*	0.01	2.00	0.22	11.11
20	*Siphonaria asghar*	0.10	12.83	1.74	14.81
21	*siphonaria savignyii*	0.02	2.50	0.37	14.81
22	*Thais lacera*	0.07	5.50	0.81	14.81
23	*Thais tissoti*	0.13	4.50	2.35	50.00
24	*Trochus eurytheus*	0.05	3.29	0.91	25.92
	Bivalves				
25	*Barbatia obliquata*	0.01	1.00	0.11	11.11
26	*Branchidontes variabilis*	98.54	2138.12	1847.90	87.03
27	*Crassostrea madrasenses*	0.75	44.04	14.11	33.33
28	*Perna viridis*	0.01	1.00	0.11	11.11
29	*Saccostrea cuccullata*	0.01	1.33	0.18	14.81
30	*Saccostrea echinata*	0.02	2.67	0.35	14.81
	Polyplacophora				
31	*Chiton perguiensis*	0.01	1.00	0.11	11.11

A varying abundance of different species was found over the study period at ST-I. The highest value of average abundance was calculated (132.82 no/0.19 m²) for *Umbonium vesterium*, while the highest abundance value was found in the month of January 2015 and lowest in March 2015; however mid tidal zone with highest value of abundance followed by low and high tidal range, and lowest average abundance (1.50 no/0.19 m²) was calculated for *Anachis terpischore* that falls in February 2015 (Table 3). Moreover, average highest molluscan species abundance at ST-II was shown by *Branchidontes variabilis* (2023 no/0.19 m²). The maximum average abundance found in January 2015 and the minimum in December 2014, while along tidal levels it was higher in mid tide followed by low and high tide zones (Table 3).

Table 3. Temporal and spatial variation in the number of molluscan species in three different tidal levels and total area along Bandari Beach Jiwani, ST-I and ST-II. T.A=Total Area.

	ST-I				ST-II			
Months	High	Mid	Low	T.A	High	Mid	Low	T.A
Oct 2014	6	4	3	7	7	10	6	16
Nov 2014	4	8	3	8	8	11	7	19
Dec 2014	3	7	3	7	9	10	7	21
Jan 2015	8	5	3	10	8	7	6	16
Feb 2015	6	5	3	9	8	7	6	16
Mar 2015	2	2	2	4	8	6	4	14

Average molluscan species density at ST-I was observed, and the calculated values showed that among all the species *Umbonium vesterium* the population density remained higher on average (126.32 no/0.19 m²). The same pattern of variation was observed for the density values as for abundance in the months and the tidal range. Other species, found with a very less density values, are shown in Table 1. By calculating the species density, ST-II revealed the highest population density of *Branchidontes variabilis*, which remained dominant all along the study period. The average density of *Branchidontes variabilis* remained 1774.39 no/0.19 m². The highest species density was observed in the month of February 2015 and lowest in December 2014; the rest of the species along station two with their average density are given in Table 3.

The average species frequency remained higher for *Umbonium vesterium* (95.45 no/0.19 m²) at ST-I (Table 1). The highest frequency values were observed in the months of November and December 2014 and lowest in the month of March 2015. Average high frequency at ST-II was shown by *Branchidontes variabilis* (88.89 no/0.19 m). The average frequency was calculated maximum in the month of October 2014 and minimum in December 2014, as detailed in Table 3.

The number of molluscan species during the present study was found highest at ST-I in the month of January 2015 with total number (10), and the lowest was observed during March, 2015 with (4) numbers of species (Table 3). The Number of the individuals of the molluscan species during January 2015 was found maximum (565±359.87)

and minimum in the month of March 2015 with a total number of (98±62.55) (Table 4); whereas at ST-II the overall calculated values per total area showed the highest number of molluscan species in December'14 with an average value (21/0.19 m²) and lowest in March 2015 (14/0.19 m²), as illustrated in Table 3. Along tidal levels, it was maximum in mid tide followed by high and low; while the average number of molluscan individuals remained higher in November 2014 (6495±7073.07) and lower in January 2015 (5146±5161.60) (Table 4).

Table 4. Temporal and spatial variation in the number of individuals of molluscan species in three different tidal levels and total area (± standard deviation); ST-I= Station one; ST-II= Station two and T.A= Total Area along Bandri Beach.

	ST-I				ST-II			
Months	High	Mid	Low	T.A	High	Mid	Low	T.A
Oct 2014	69	733	415	406 ± 332.10	3685	10043	2339	5356 ± 4114.76
Nov 2014	123	598	584	435 ± 270.29	3035	14632	1818	6495 ± 7073.07
Dec 2014	118	855	524	499 ± 369.14	1841	12039	4038	5973 ± 5367.22
Jan 2015	171	876	649	565 ± 359.87	1637	11073	2729	5146 ± 5161.60
Feb 2015	51	871	364	429 ± 413.81	1238	12023	3522	5594 ± 5683.31
Mar 2015	26	129	139	98 ± 62.55	1985	10059	3518	5187 ± 4288.05

3.1. Diversity Indices (ST-I) (Figures 2-6)

Along the study, area samples were collected by using quadrate method from three different tidal levels, which were summed up and analyzed. The Shannon Diversity index showed that the overall average species diversity was found to be higher in November 2014 (0.39), whereas the least diversity (0.09) was found in March 2015. Whereas on tidal levels on average remained higher along the high tide zone (0.84), followed by mid (0.23) and low (0.17). The highest variation was observed along the high tide followed by mid and low tide.

Generally, calculated indices (Margalef's Richness Index) showed that with an increase in the number of species in the sample plot, the value of richness also increases. Average molluscan species richness of the total area was found higher in January 2015 (1.42) and remained lower in March 2015 (0.65). On tidal levels, with an average, values were high tide zone (1.08), mid (0.75) and low (0.36), while the variation pattern was the same as observed for the diversity.

The value of evenness (Pielou's Evenness Index) became minimum if a s ingle species became more and more dominant in a sample, while species evenness became maximum when all species were distributed evenly in a sample; and maximum species evenness of the total area was observed in November 2014 (0.19) and minimum in March 2015 (0.06). At tidal levels, average species evenness was observed to be high in high tide (0.54) followed by low (0.16) and mid (0.14). Generally, there was no significant changes in evenness between mid and low tidal range because both tidal levels were dominated with a s ingle species *Umbonium vesterium*, as compared to the high tide that had small rock boulders harbored with various species.

On the other hand, dominance (Berger-Parker Dominance Index) per total area remained highest during December 2014 (200.57) and lowest during March 2015 (72.50). Species dominance, on average, along tidal levels, showed a maximum activity in low tidal range (145.17), followed by mid (126.31) and high (16. 24), while the greatest variation was observed in low and mid tide.

3.2. Diversity Indices (ST-II) (Figures 2-6)

Along station two, the maximum diversity (Shannon's Diversity Index) was observed during March 2015 (0.12) and the minimum during February 2015 (0.08). Species diversity along tidal levels was highest in high tide (0.37), followed by mid (0.08) and low (0.07).

By calculating species richness (Margalef's Richness Index) for each month during the study period, the highest value was observed during December 2014 (2.30) and the lowest during March 2015 (1.52). On tidal levels, the maximum was in high tide (1.10), followed by mid (0.91) and low (0.75).

Species evenness (Pielou's Evenness Index) showed the greatest value (0.04) during October 2014 and January, March 2015, while the lowest value (0.03) was in the months of November & December 2014 a nd February 2015. For the tidal range, it was highest in high tide (0.18) and lowest in mid and low tidal range with (0.04).

Species dominance (Berger-Parker Dominance Index) was observed per total area and it was higher in March 2015 (1092.86) and lower in January 2015 (950). On tidal levels, it was observed as maximum in mid tide followed by low and high tidal zone.

3.3. Species Similarity between Two Stations

Molluscan species similarity (Soreson's similarity index) remained maximum during November 2014 (0.44) and minimum during March (0.11). Among tidal ranges, it was calculated as high at high tide with a similarity value (0.30), followed by mid tide (0.14) and low tide (0.00) with a minimum similarity.

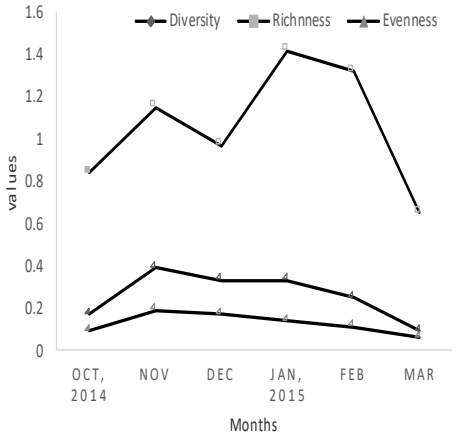

Figure 2. Mean monthly diversity (Shannon's Diversity Index), richness (Margalef's Diversity Index) and evenness (Pielou's Evenness Index) for ST-I

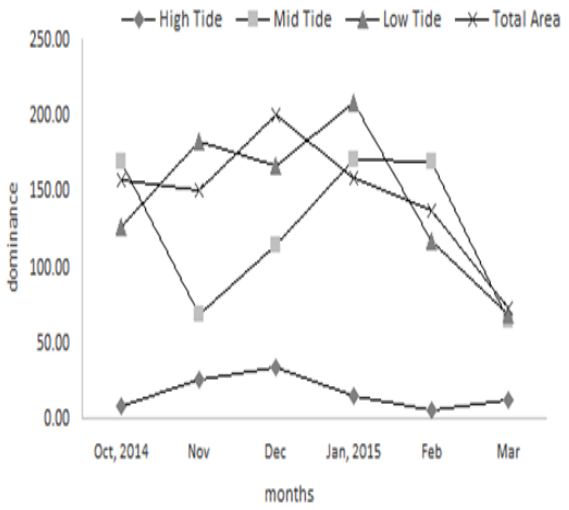

Figure 3. Temporal and spatial variation (no/0.19m²) in species dominance (Berger-ParkerDominanceIndex) for ST-I

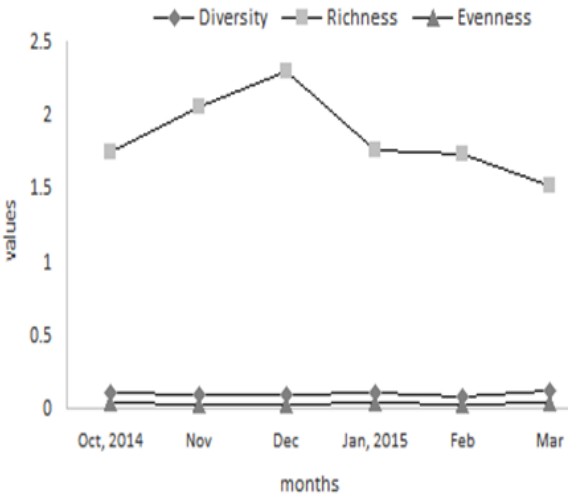

Figure 4. Mean monthly diversity (Shannon's Diversity Index), richness (Margalef's Diversity Index) and evenness (Pielou's Evenness Index) for ST-II.

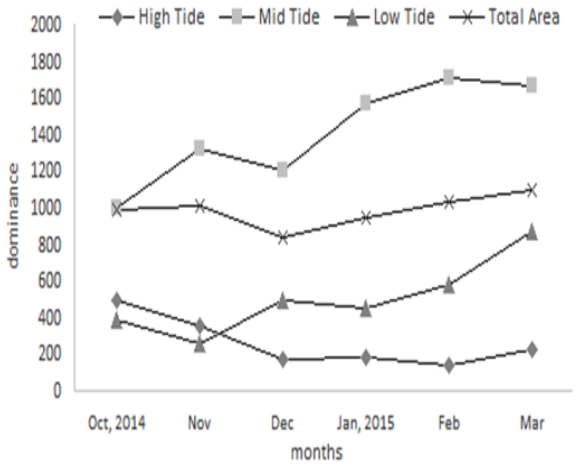

Figure 5. Temporal and spatial variation (no/0.19m²) in species dominance (Berger-Parker Dominance Index) for ST-II.

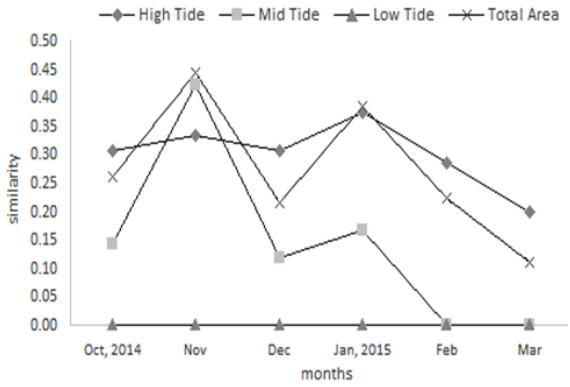

Figure 6. Temporal and spatial variation in species similarity (Sorenson's Similarity Index) between two stations and three tidal levels.

4. Discussion

During the present study, efforts have been made to analyze macro benthic molluscan assemblages found along the Bandri beach, Jiwani for the first time on species level, in addition to species composition, abundance, density, frequency, dominance, etc. that were calculated to establish a baseline study, by using quadrate analysis techniques, which can assist in future detailed studies and resource management of the area. During the present study, by using a randomly placed quadrate sampling technique collectively, a total of (34) molluscan species were found and identified for the first time from the Bandri beach along the Jiwani coast. Specimens were procured from selected stations (ST-I and ST-II). While 10 species were found common in both stations.

Formerly, Ahmed *et al*. (1982) studied the distribution and abundance of the intertidal organisms on s ome beaches of Makeran coast, Baluchistan and a total of 51 species were recorded from the Gawadar West Bay; whereas on the Gawader east Bay 39 species were reported. On the other hand, 42 species were found at Jiwani along the Rest House Beach (Now WWF-Pak Office), among which 24 w ere molluscs. Comparing the composition, abundance and density of common molluscan species at two stations, the calculated values showed that, in general, the overall composition, abundance, density values remained higher at station two, which has a predominately rocky intertidal profile as compared to station one, which offers a sandy muddy habitat to dwell in. Whereas, the maximum distribution was found at mid tidal zones of both of the stations specifically. At Daya Bay, according to China Rongguan *et al.* (1993), the highest vertical distribution of species remained higher at mid tidal zone. From Pakistan, Barkati and Burney (1991) also estimated the highest number of individuals from mid tidal region at Buleji abide throughout the year. Species composition for station two one species only had provided more than 1 % mean cover, which is *Branchidontes variabilis* (98.54 %). *Branchidontes* dominated the species composition (%) at the second station and overall at all three tidal levels. *Branchidontes variabilis* was investigated on species level for the first time from Pakistan. Moreover, the collective list of species found in quadrate sampling showed that

among the 13 species no more than 10 species were found persistently in any single collection during October 2014 to March 2015 at station one; and no more than 21 species were found constantly in any single collection at station two. Similar findings were presented by Bight and Littler (1980) from all the 10 study sites along the Southern California, where they found only 15 species out of 227 macro invertebrates to be common to all the 10 study sites over the study period. Along the station, one average molluscan species density showed that, among all species population densities, *Umbonium vesterium* remained higher on average (132.82/0.19 m²), whereas at station two the calculated species density revealed the highest population density of *Branchidontes variabilis* which remained dominant all along the study period. On average, the density of *Branchidontes variabilis* remained (1847.90/0.19 m²) among all species. It seems that this difference in indices is due to the topographic conditions of substratum, as the benthic profile, at station one, is more sandy muddy, unlike station two, where the bottom profile is predominantly rocky. Several other such studies dealing with molluscan ecology, explaining the faunal composition and distribution of macro benthic molluscan communities, also showed similar findings and rocky intertidal systems were found largely rich in fauna and flora when compared to sandy muddy habitats (Atapattu, 1972; Fuxue *et al.*, 1994). Benthic species composition and distribution were strongly related to environmental factors, such as tidal flow, sediment forms, water currents and temperature. Species horizontal distribution shows the effect of sediment forms on benthos while the vertical distribution of species is concerned by the tidal action (McQuaid *et al.*, 1985; Ruxing *et al.*, 1991; Warwick *et al.*, 1991; Barkati and Burney, 1991). Spight (1978) suggested that the distributional patterns may reflect a habitat selection but it may also be due to random colonization and subsequent biotic interaction.

In contrast, comparatively, species frequencies and diversity were found to be higher at station one; and, on average, the molluscan species frequency and species diversity along station one remained higher throughout the study period. Calculated species frequency for *Umbonium vesterium* dominated the profile (95.45/0.19m²) at station one. Whereas, on average, high frequencies at station two were shown by *Branchidontes variabilis* (87.03/0.19m²). It is believed that there are so many factors which can affect the distribution of communities in the intertidal areas. Therefore, it is suggested that a quantitative horizontal distribution of communities in the intertidal area may be related to wave exposure and tidal currents which are more prevalent at sandy shores due to the absence of barriers that break the force (Kaandorp, 1986; Rauxing *et al.*, 1991; Ghamrawy, 1991).

The comparison of species richness between two stations revealed an average richness between two stations, which was found higher at station two. While comparing the variation between tidal level and total area in station one showed the greatest variation in species richness at high and mid tidal zone with a gradual decreasing trend from mid to high zone. In contrast, molluscan inhabiting Parangua Bay (Brazil) showed a subsequent decrease in the species richness and abundance from low tidal zone to high tidal zone, as observed by Boehs *et al.* (2004). According to Rahman and Barkati (2012), the individuals and the number of species of molluscs generally decrease from low to high tide mark, while remain highest in mid tide zone.

The comparison of species evenness at two stations of Bandri exhibited an average evenness that remained high at station one among the three tidal levels and total area. Generally, along station one and station two, species evenness decreased from high tide to low tide. However, comparing the variation of species evenness in station one showed a higher variation among the three tidal levels and the total area, compared to station two. Whilst comparing species dominance studies revealed that both stations were dominated by different species; station one was dominated by *Umbonium vesterium* and station two by *Branchidontes variabilis.* Observations showed that species dominance remained much higher along station two as compared to station one at three tidal levels and total area, but the overall dominance was found much pronounced at mid tidal zone. Barkati and Rahman (2005) observed seasonal changes in species diversity among the three mangroves associated sites of Karachi coast; at the sands spit coast species richness was found minimum during summer, while it remained maximum during autumn (1.25-3.1); whereas in spring it ranged between 3.83 to 5.7 in autumn. Calculated evenness values were found to be lower during spring and higher during summer. Similarly, from Clifton, the minimum richness was recorded during spring and the maximum in summer, whereas lower evenness was recorded in winter and higher in summer.

Diversity Indices are normally used to characterize the biodiversity of a habitat with respect to the abundance of each species, their richness, and evenness, etc. For instance, species diversity refers to the measure of diversity in an ecological community; whereas species richness is the number of different species representing an ecological community. Species evenness refers to how each species is closely distributed in number in an environment; these measures may affect the species diversity. Moreover, species richness increases in response to the decreasing sand particle size as both grain size and beach slope contribute positively in the species richness at a global scale (Barboza and Dafeo, 2014). A community dominated by one or two species is considered to be less diverse than one in which several different species have similar abundance. Therefore, species richness and evenness increase tends to increase in diversity as it is found higher at ST-I. Seapy and Littler (1978) studied the macro invertebrates along the California coast, and concluded that, at sheltered beaches, species richness remained higher, while by calculating Shannon's index and evenness values it pointed a higher diversity on exposed Sea stack. Richness was of a greater value (9.18) on boulder beach as compared to (7.40) at Sea stack. McQuaid and Branch (1984) studied species richness and evenness based on their observation and they found high evenness whereas richness was low; they concluded that this difference was due to unstable substratum.

Rahman and Barkati (2012) found, while studying molluscan fauna along 4 rocky beaches of Karachi coast Pakistan (Buleji, Nathiagali, Manora and Cape Monze), that between sites, there were no significant changes in species diversity, richness and evenness. Datta *et al.*

(2010) found that species richness (Margalef Richness Index) ranged from 2.93-5.71, and evenness (Pielou's Evenness Index) ranged from 0.81-0.83 while studying three different sites of Mumbai, India. David (2013) studied the biodiversity and distribution of marine gastropod (Mollusca) during pre and post-monsoon season along the Goa coastline India, and calculated Shannon's-Weiner biodiversity index which ranged from 2.1749 during pre-monsoon to 5.7641 in post-monsoon month. Species richness ranged from 0.5412 in pre-monsoon to 4.4866 in the post-monsoon, while evenness values ranged from 0.9128 during pre-monsoon months to 1.9534 during the post-monsoon.

In light of the discussion above, it is concluded that these findings have presented a better insight into the molluscan assemblages and their natural habitats along the Bandri beach of Jiwani coast, Baluchistan for the first time. Obtained data and baseline studies could be useful in the bio resource management of the area. Research based quadrate analysis and taxonomic identifications (Ghani and Afsar 2017) are useful to initiate detailed studies on commercially important species of the area, to investigate their reproductive patterns, biochemical properties, natural product research, physicochemical properties, etc.

References

Ahmed M. 1997. Natural and human threats to biodiversity in the marine ecosystem of coastal Pakistan**.** In**:** Haq BU, Haq SM, Kullenberg G and Stel J H. (Eds**): Coastal Zone Management Imperative for Maritime Developing Nations.** Kluwer Academic Publishers, Netherland, pp, 319-332.

Ahmed M, Rizvi SHN and Moazzam M. 1982. The distribution and abundance of intertidal organisms of some beaches of Makran coast in Pakistan (Northern Arabian Sea). *Pak J Zool*, **14**: 175-184.

Atapattu JH. 1972. The Distribution of Mollusks on littoral rocks in Ceylon, with notes on their ecology. *Mar Biol,* 16: 150-164.

Bandel K and Wedler E. 1987. Hydroid, amphineuran and gastropod zonation in the littoral of the Caribean Sea, Colombia. *Senckenbergiana Maritima,* **19**: 1-129.

Barboza FR and Defeo O. 2014. Global diversity patterns in sandy beach macrofauna: a biogeographic analysis. *Sci Reports*,**5**:14515.

Barkati S and Rahman S. 2005. Species composition and faunal diversity at three sites of Sindh Mangroves. *Pak J Zool,* **37**: 17-31.

Barkati S and Burney SMA. 1 991. **Biomass and species composition of a littoral rocky shore of the Karachi coast. Annual report, department of Zoology UoK: NSRD. Islamabad** pp. 90.

Boehs G, Absher TM and Cruz-Khade AD. 2004. Composition and distribution of benthic mollusks on intertidal flats of Paranagua Bay (Parana, Brazil). *Sci Mar.,* **68**: 537-543.

Datta SN, Chakraborty SK, Jaiswar AK and Ziauddin G. 2010. A comparative study on intertidal faunal biodiversity of selected beaches of Mumbai coast. *J Environ Biol.,* **31**: 981-986.

David A. 2013. Biodiversity and distribution of marine gastropods (Mollusca) during pre and post monsoon season along the Goa Coastline, India, *The Mar Biol Assoc India,* **55**:17-24.

Davidson IC, Crook AC and Barnes DKA. 2004. Quantifying spatial patterns of intertidal biodiversity: Is movement Important?. *Mar Ecol.,* **25**: 15-34.

Fuxue L, Lizhe C and Ping D. 1994. Studies on ecology of molluscan on rocky intertidal zone in Xiaman Harbour. *J Oceanogr Taiwan Strait,* **13**: 43-51.

Ghamrawy MS. 1991. Zonation of organisms on rocky shores of northern Jeddah. *J. King Abdulaziz University: Mar Sci,* **2**: 137-147.

Ghani A and Afsar N. 2017. New record of two flag pen shells (Mollusca: Bivalvia) from Bandri beach, Jiwani coast, Pakistan. *Int J Biol Biotech.,* **14**: 75-78.

Gray JS. 1997. Marine biodiversity: patterns, threats and conservation needs. *Biodiv Conserve,* **6**: 153– 175.

Kaandorp JA. 1986. Rocky substrate community of the infralittoral fringe of the Boulonnais Coast, N.W. France a quantitative survey. *Mar Biol.,* **92**: 255-265.

Khade SN and Mane UH. 2012. Diversity of bivalves and gastropods mollusks from selected localities of raigad district, Maharashtara, west coast of India. *World J Sci Technol.*, **2**: 35-41.

Lardcci, C, Rossi F and Castelli A. 1997. Analysis of macro zoobenthic community structure after sever dystrophic crises in a Mediterranean coastal lagoon. *Mar Poll Bull,* **34:** 536- 547.

Little C and Kitching JA. 1996. **The Biology of Rocky Shores.** Oxford. Uni. Press. NY. USA, 240 pp.

McCann KS. 2000. The diversity-stability debate. *Nature* **405**: 228–233.

McQuaid CD, Branch GM and Crowe AA. 1985. Biotic and abiotic influence on rocky intertidal biomass and richness in the Southern Benguela region. *South African J. Zool.,* **20**: 115-122.

Rahman S and Barkati S. 2012. Spatial and temporal variation in the species composition and abundance of benthic molluscs along 4 rocky shores of Karachi. *Turkish J Zool.,* **36**: 291-306.

Rongguan L, Jinxiang J, Lin L, Fengwu Z, Qiquan W and Chuanyar L. 1993. Species composition and distribution of benthose in intertidal zone of Daya Bay. *Oceonol Limnol Sin. / Haiyang Yu Huzhao,* **24**: 527-535.

Ruxing C, Feng Z, Yihao W, Yaoping D, Zhuoming Y, Yingshang Z, Lianghao J and Weihui S. 1991. Studies on ecology of Zhoushan intertidal zone II. Quantities and distribution. *Donghai Mar Sci,* **9**: 58-72.

Seapy RR and Littler MM. 1978. The distribution, abundance, community structure and primary productivity of macro organisms from two central California rocky intertidal habitats. *Pacific Sci.,* **32**: 293-314.

Spight TM. 1978. Temporal changes in a tropical rocky shore snail community. *Veliger,* **21**: 137-143.

Tilman D. 2000. Causes, consequences and ethics of biodiversity. *Nature,* **405**: 208–211.

Underwood AJ. 2000. Experimental ecology of rocky intertidal habitats: what are we learning? *J Exp Mar Biol Ecol.,* **250**: 51–76.

Vaghela A and Kundu R. 2011. Spatiotemporal variations of hermit crabs (crustacea: decapod) inhabiting rocky shore along saurashtra coast, western part of India. *Indian J Mar Sci.,* **41:** 146-151.

Warwick RM, Goss-Custard JD, Kirby R, George CL, Pope ND and Rowden AA. 1991. Static and dynamic environmental factors determining the community structure of estuarine macrobenthose in Britain: Why is the severn Estuary different? *J. Appl. Ecol.,* **28**: 329-345.

JJBS

Volume 10, Number 4,December 2017
ISSN 1995-6673
Pages 289 - 295

Jordan Journal of Biological Sciences

Immobilization of Moderately Halophilic *Bacillus* sp. 2BSG-PDA-16 cells: A Promising Tool for Effective Degradation of Phenol

Eman Z. Gomaa*

Department of Biological and Geological Sciences, Faculty of Education, Ain Shams University, Cairo, Egypt.

Received: March 26, 2017; Revised: August 22, 2017; Accepted: September 8, 2017

Abstract

Phenolic compounds are hazardous pollutants known to be toxic at low concentration. Removal of phenols from industrial wastewater streams before their discharge into receiving water bodies is thus obligatory. Numerous phenol-degrading non-halophilic bacterial isolates have been described, but detailed information regarding phenol degradation by halophiles is rather sparse. The present study aims at evaluating the capacity of phenol degradation by new species of *Bacillus*. Halophilic bacteria were isolated from mangrove region on the western coast of the Red Sea of Egypt. Bacterial isolate showed the highest potentiality of phenol degradation was identified using 16S rRNA sequencing method as *Bacillus* sp. 2BSG-PDA-16. The optimum conditions for achieving high phenol degradation were 300 mg/l phenol concentration, 1% glucose, peptone, 5% NaCl, pH7, 30°C and 6% (v/v) inoculum size. Upon applied all these conditions, the phenol degradation reached 85.6 % removal. Calcium alginate was employed to immobilize the cells. Compared to free cells, the immobilized cells were not only able to tolerate high concentration of phenol but also are able to degrade it completely in a shorter time. Free cells degrade 600 mg/l in 10 days, whereas the immobilized cells could completely degrade 800 mg/l in 8 days. It could be concluded that this moderately halophilic *Bacillus* sp. 2BSG-PDA-16 might be useful for the degradation of phenol, particularly in saline environments.

Keywords. Biodegradation, Phenol, Halophilic bacteria, Immobilizations.

1. Introduction

Several industries including olive oil mills, pickled vegetables, fish processing, meat canning, dairy products, tanning process and oil refining process generate wastewaters containing high salt content and organic contaminants (Loh *et al*., 2000). Phenol and other phenolic compounds are common organic contaminants found in saline wastewaters formed by some of these industries (Gerrard *et al*., 2006). Presence of these recalcitrant compounds in the environment possess significant health risks to humans. The substituted phenolic compounds are carcinogenic and toxic environmental pollutants which are massively discharged into the environment from anthropogenic activities (Murthy and Gayathri, 2017). Phenol causes irritation of eye, swelling and finally blindness. Moreover, exposure to high concentration of phenol causes hepatic damage, paralysis, cancer and nervous disorders (Juang and Tsai, 2006; Indu Nair *et al*., 2008). In respect to phenol effect on prokaryotes, it is toxic to microorganisms even at low concentration (Yang and Lee, 2007).

Numerous methods have been developed to treat phenols in wastewater including membrane separation (Kujawski et *al*., 2004), adsorption (Roostaei and Tezel, 2004), oxidation (Idris and Saed, 2002) and extraction by liquid membrane (Lin *et al*., 2007). However, these physicochemical methods have their own limitations viz. reaction inefficiency, high energy consumption, production of sludge containing iron, and insufficient capacity (Chen *et al*., 2007). Biodegradation, as a technology for decontaminating of phenols, is gaining great attention due to its eco-friendly characteristics and cost-effectiveness (Adav *et al*., 2007; Catia *et al*., 2010; Ravikumar *et al*., 2011). Among the various practiced approaches for its removal, bacterial utilization gets attraction due to its eco-friendly and cost effective nature (Ahmad *et al*., 2016). However, biodegradation processes are difficult to perform under saline conditions (Kafilzadeh *et al*., 2010). One alternative is the use of efficient halophilic organisms which are adapted to live in such saline conditions.

The aim of the present study is to evaluate phenol degradation efficiency of a bility of *Bacillus* sp. 82BSG-PDA-16 isolated from saline environment.

* Corresponding author. e-mail: emann7778@yahoo.com.

Degradation of phenol was optimized with respect to various nutritional environmental parameters. Batch experiments were carried out in order to obtain the maximum phenol biodegradation rates by analyzing the influence of the immobilization in sodium- alginate gel beads on biodegradation performance.

2. Materials and Methods

2.1. Isolation of Phenol Degrading Halophilic Bacteria

Halophilic bacterial strains were isolated from soil and water samples collected from mangrove region on the western coast of the Red Sea, Egypt. Water (5 mL) and soil (3 g) samples were mixed in 10 mL sterile nutrient broth containing peptone (3 g/L) and beef extract (5 g/L) and incubated at 30°C on a shaking incubator at 150 rpm for 24 h. Bacterial cultures were isolated by repeated culturing in mineral salt medium (MSM) containing (g/L) KH_2PO_4, 0.5; K_2HPO_4, 1.5; NaCl, 10; Mg SO_4. $7H_2O$, 0.5; NH_4Cl, 1; $FeSO_4$. $7H_2O$, 0.01 and $CaCl_2$. $2H_2O$, 0.01 in a 250 mL conical flask (Bai *et al*., 2007). Phenol was filter sterilized separately using 0.2 µm nitrocellulose membrane filter and added to the sterilized medium after cooling to room temperature at a concentration of 100 mg/L. The isolates were incubated at 30°C with shaking at 150 rpm. After five cycles of culturing, serial dilutions of the cultures were prepared and streaked onto plates of mineral salt agar medium supplemented with phenol and incubated at 30°C for 72 h. Isolates exhibiting distinct colonies were further purified by repeated sub-culturing into solidified basal salt medium.

2.2. Identification of Phenol-Degrading Bacterium

Bacterial isolate showing the highest phenol degradation was tested for species identity using the 16S rRNA sequencing method (Rochelle *et al*., 1995). The gene sequencing was done at Macrogen (South Korea). DNA sequences were aligned using Gene Mapper v4.1 & Data Collection v 3.1 Communication Patch1. To extract the genomic DNA, bacterial colonies are picked with a sterilized toothpick, and suspended in 0.5 ml of sterilized saline, then centrifuged at 10,000 rpm for 10 min. After removal of supernatant, the pellet was suspended in 0.5 mL of Insta Gene Matrix (Bio-Rad, USA), incubated at 56 ^oC for 30 min and then heated to 100 ^oC for 10 min. After heating, the supernatant can be used for the PCR reaction. Bacterial 16S rRNAs were amplified by using the following universal bacterial 16S rRNA primers: forward primer 27F (50-AGAGTTTGATCMTGGCTCAG-30) and reverse primer 1792 R (50-TACGGYTACCTTGTTACGACTT- 30). Polymerase chain reaction was performed using kits with Ampli Taq DNA polymerase (FS enzyme; Applied Biosystems). One microlitre of template DNA was added to 20 µL of PCR reaction solution. Amplification was performed using 35 cycles at 94 ^oC for 45 s, 55 ^oC for 60 s, and 72 ^oC for 60 s. The PCR amplicon was purified using a Montage PCR clean up kit (Millipore). The purified PCR products of approximately 1,400 bp were sequenced by using 2 primers 518 F (50-CCA GCA GCC GCG GTA ATA Cg-30) and 800R (50-TAC CAG GGT ATC TAA TCC-30). Sequencing was performed using a Big Dye terminator cycle sequencing kit (Applied BioSystems, USA). Sequencing products were resolved on an Applied Biosystems model 3730XL automated DNA sequencing system (Applied BioSystems, USA). Sequence analysis was performed with sequences in the National Center for Biotechnology Information (NCBI), USA database using Basic Local Alignment Search Tool for Nucleotides (BLASTN) (Altschul *et al*., 1997).

2.3. Biodegradation of Phenol

A loopful of pure bacterial strain was inoculated into Luria–Bertani (LB) medium and incubated at 30^oC for 24 h. Phenol degradation experiments were carried out in 250 mL Erlenmeyer flasks containing 50 mL MSM amended with various concentrations of phenol and inoculated with 6 % (v/v) inoculums of the prepared seed cultures. The flasks were incubated at 30 ^oC on a rotary shaker (150 rpm) for 72 h. The culture suspension was centrifuged at 10,000xg for 20 min for removal of the biomass. The biodegradation of phenol was assessed spectrophotometrically by the method of Yang and Humphrey (1975). Briefly, 50 mL of diluted sample were added to 0.3 ml of 2% aqueous 4-amino- antipyrine solution and 1 mL of 2N NH_4OH. After mixing the content thoroughly, 1mL of 2 % K_3FeCN_6 is added. Absorbance of red color produced is measured at 510 nm and the percentage degradation of phenol was calculated by the following equation:

Phenol degradation (%) = OD (control) – OD (sample)/ OD (control) x 100. Where uninoculated flasks were prepared in a parallel method and used as controls.

2.4. Cell Growth

Cell growth was monitored by measuring the optical density at 600 nm using spectrophotometer (UV-VIS Double Beam PC, Labomed INC). To measure biomass concentration, ten milliliter culture medium was centrifuged at 10,000 xg, 4°C for 20 min and the cell pellets were washed with 10 mL distilled water. The cell pellet was harvested by centrifugation and dried at 105°C for 48 h, or till constant weight was obtained. Cell mass concentration was determined by the standard calibration curve between OD 600 and cell dry weight.

2.5. Optimization of Phenol Degradation

In order to optimize the nutritional and environmental factors affecting phenol degradation by *Bacillus* sp. 2BSG-PDA-16, the following variables were assayed: phenol (100-800 mg/L), additional carbon sources (glucose, sucrose, maltose, cellulose, fructose, lactose, starch), different nitrogen sources (peptone, yeast extract, urea, ammonium chloride, ammonium sulphate, sodium nitrate, leucine, asparagine, proline), NaCl (1-15 %), pH (5-9) and temperature (20- 40°C) and inoculum size (2-12 % (v/v). All assays were performed in triplicate. Uninoculated controls were prepared parallel in all experiments. Following incubation, samples were collected and analyzed for growth and phenol degradation. After determination the optimum for each parameter, an experiment was performed by applying all the optimized nutritional and environmental factors.

2.6. Immobilization Protocol

The microbe of choice was encapsulated in calcium-alginate beads. Liquid cultures were centrifuged in a 50 ml

centrifuge tube (10,000 xg) at 4°C for 20 min and the supernatant was discarded. The pellet was resuspended with a previously autoclaved solution of sodium alginate to a final concentration of 4% (w/v) and 10% (v/v) bacterial biomass. The alginate-bacterial mixture was added drop wise with sterile syringe (20 mL) fitted with a wide bore needle (1 mm diameter) from a height of about 20 cm into an autoclaved solution of calcium chloride (3% (w/v), adjusted to pH 7.0), where beads formed immediately. The beads were left in this hardening solution overnight at 4°C before being harvested by filtration (Abd-elhaleem *et al*., 2003).

2.7. Batch Degradation Studies

Batch experiments on phenol degradation using free cells were performed in 250mL Erlenmeyer flasks containing 100 mL of growth medium. Phenol concentration was varied in the range of 100 to 800 mg/L. Freshly grown seed culture was inoculated to media. Inocula concentration was 6 % (v/v).

For biodegradation experiment with Ca-alginate immobilized cells, 5 g (wet weight) of beads were placed in 250 mL flasks containing 100 mL mineral salts medium and phenol was added at concentrations ranging from 100 to 800 mg/L. The flasks were placed in a rotary shaker at 150 rpm at 30°C. Every 24 h, samples were collected, centrifuged and analyzed for biomass and remaining phenol concentrations.

2.8. Long-Term Degradation Studies

To determine the long-term stability of phenol degradation by immobilized cells, the system was used for repeated batch degradation. After each cycle of incubation period (72 h), the spent medium was decanted and beads were washed with sterile water and transferred into a fresh sterile mineral salts medium (100 mL) containing 500 mg/L phenol . The degradation process was carried out under identical conditions and the spent medium was analyzed for the residual substrate.

2.9. Statistical Analysis

All experiments were done in triplicate, and the results were presented as mean± standard deviation. The experimental data were analyzed by using SPSS. Statistical significance was accepted at a level of $p< 0.05$.

3. Results and Discussion

In the present study, twenty-three morphologically different halophilic bacterial species capable of phenol degradation were isolated using enrichment culture technique. The most potent strain was identified using16S rRNA gene sequence analysis. The sequence alignment using BLASTN software for the comparison up to 1,500 bp of the analysis gave a high homology of 98.8 % to *Bacillus* sp. 2BSG-PDA-16. The strain was selected for further studies because of its high phenol-degrading rate (up to 800 mg / L within 72 h). This might be due to the production of different enzymes including oxygenases, hydroxylases, etc by this strain. Moreover, the enzymes responsible for the oxidizing of the phenolic compounds were very effectively (Indu Nair *et al*., 2008).

Parameters, such as pollutant concentrations, viable biomass, concentrations, existence of inhibitor, temperature, pH, microbial completion and microbial adaptation, are the most important parameters that affect phenol biodegradation rate. Microorganisms can be detrimentally affected if the initial concentration of the pollutant is very high (Nair *et al*., 2008). Hence, in order to know the tolerance levels of *Bacillus* sp. 2BSG-PDA-16, different concentrations of phenol were tried. The highest phenol degradation activity (37.3 %) was recorded at a concentration of 300 mg/l (Figure 1). As phenol concentration was increased from 400 to 800 mg/L, there was a decrease in cell density and this had an impact on phenol degradation. The results, thus, indicated that the higher concentrations of phenol were having a negative effect on the cells. Annadurai *et al*. (2002) confirmed that *Pseudomonas putida* suffered from substrate inhibition, whereby growth and consequently phenol degradation was inhibited at high phenol concentrations.

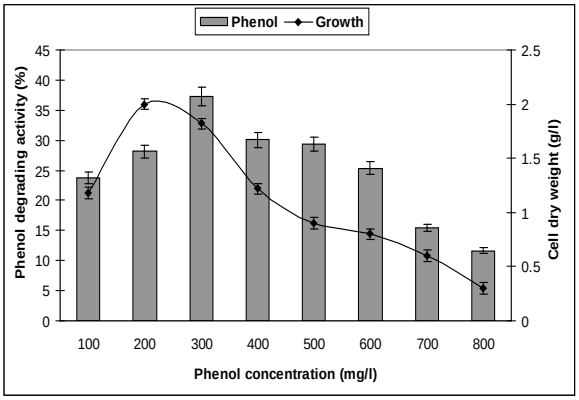

Figure 1. Effect of phenol concentrations on growth and phenol degrading activity of *Bacillus* sp. 2BSG-PDA-16. Results are means of three independent determinations and error bars represent the standard deviation

Various methods have been proposed to overcome substrate inhibition in order to treat high strength phenolic wastewater. These include selection and adaption of the cells to higher phenol concentration (Masque *et al*., 1987), immobilization of the cells (Loh *et al*., 2000) and using genetically engineered microorganisms (Soda *et al*., 1998). Another possible method increasing the tolerance of the cells to substrate inhibition is to supplement the growth medium with conventional carbon sources, such as glucose. In the present study, the phenol removal efficiency was investigated by the addition of various carbon sources and results cited in Figure 2 shows maximum degradation of phenol with the addition of 1 % glucose (62.07 %). This might be due to the fact that glucose acts as a growth substrate in presence of phenol due to its simple structure as compared to phenol. The influences of supplementary conventional carbon source on enhancing the biotransformation rates of phenol as the primary substrate has been studied by medium augmentation with conventional carbon sources (Loh and Wang, 1998).

Effect of different nitrogen sources on the removal capacity of phenol by the selected strain was tested and the results suggested that peptone supported the best degradation of phenol (80.18 %).

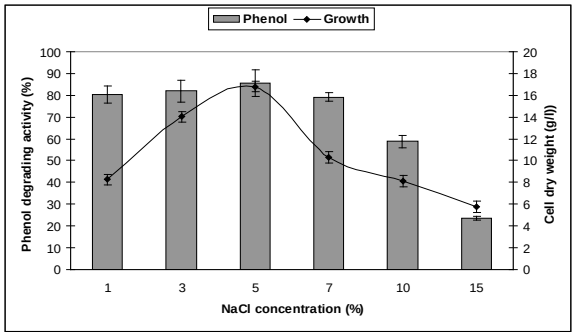

Figure 2. Effect of additional carbon sources on growth and phenol degrading activity of *Bacillus* sp. 2BSG-PDA-16. Control : MSM containing 300 mg/L phenol without any sugar addition. Results are means of three independent determinations and error bars represent the standard deviation

A considerable increase in the bacterial biomass (9.67 g/L) was recorded in the presence of peptone (Figure 3). Effect of different concentrations of NaCl on the biodegradation of phenol was also carried out. The results revealed that using 3% NaCl, the degradation efficiency of phenol by *Bacillus* sp. 2BSG-PDA-16 reached 82 % and the efficiency reached maximum up to 85.6 % at 5% NaCl. Using NaCl concentration of 7 %, 10 % and 15 %, the degradation efficiency decreased to 79.1 %, 58.74 % and 23.6 %, respectively (Figure 4). T hus, the selected bacterial strain was moderately halophilic in nature.

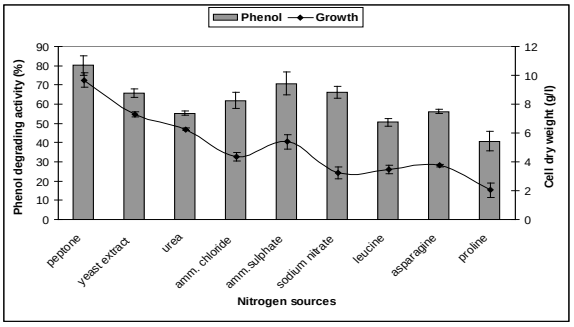

Figure 3. Effect of nitrogen sources on growth and phenol degrading activity of *Bacillus* sp. 2BSG-PDA-16. Results are means of three independent determinations and error bars represent the standard deviation

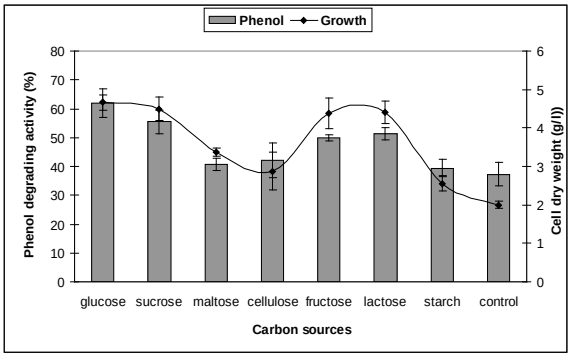

Figure 4. Effect of NaCl concentrations on growth and phenol degrading activity of *Bacillus* sp. 2BSG-PDA-16. Results are means of three independent determinations and error bars represent the standard deviation

Providing good environmental condition is one of the important parameter for bacterial bioremediation (Shweta and Handayuthapani, 2013). pH significantly affects the biochemical reactions required for phenol degradation.

Bacillus sp. 2BSG-PDA-16 showed the maximum degradation of phenol at pH 7 (data not shown). Similarly, the optimum pH for phenol degradation is 7.0 for *Pseudomonas putida* NICM 2174 (Annadurai *et al*., 2000). Below and above this optimal initial pH values, the growth rate and phenol degradation decreased gradually because the acids and bases which can easily entered in to the cell which affect the metabolic pathway and denature the proteins finally leads to lethality (Annadurai *et al*., 2000a). Furthermore, temperature plays an important role than nutrient availability in the degradation of organic pollutants. To assess the influence of the temperature changes, phenol degradation efficiency was compared under a temperature range from 20 t o 40 °C with maximum activity attained at 30ºC. Similar results were recorded by Ramzan and Rehman (2016) who reported that *Stenotrophomonas maltophilia* and *Bacillus subtilis* showed maximum survival and phenol degradation in the presence of phenol up to 300 µg/mL at 30°C and pH 7. Further increase in temperature resulted in marginal reduction in phenol degradation activity (data not shown). Higher temperatures seemed to have a negative effect on the activity of the bacteria and hence hindered its biodegradation capabilities. It may have a d etrimental effect on the bacterial enzymes, which is the main step in the biological degradation process. Annadurai *et al*. (1999) described that when the temperature increased from 30°C to 34°C no phenol degradation was observed due to cell decay, which shows that the phenol degradation is a temperature dependent process.

On studying the effect of initial inoculum concentration on phenol degradation, results reveled that an inoculum concentration of 6 % showed the maximum phenol degradation reached 85.6 % and decreased afterwards. An experiment was performed by applying all the optimized nutritional and environmental factors and confirmed that the strain could efficiently degrade phenol.

The efficiency of the phenol degradation could be further enhanced by the process of cell immobilization (Annadurai *et al*., 2000a). Immobilized microbial cells create opportunities in a wide range of sectors including environmental pollution control. Compared w ith conventional s uspension s ystem, t he i mmobilized microorganism technology offer a multitude of advantages, such as high biomass, h igh metabolic activity and strong resistance to toxic chemicals (Liu *et al*., 2012; Martins *et al*., 2013). Moreover, immobilized microorganisms could be cost effective since they can be used several times without significant loss of activity (Devi and Sridhar, 2000). Therefore, i mmobilized microorganism t echnology ha s be en e xplored a s promising for wastewater treatment (Ahmad *et al*., 2012). C alcium-alginate has been widely employed for immobilization of enzymes or whole cells since it is less toxic than synthetic polymers, easily gelled under mild conditions and inexpensive (Wang *et al*., 2007).

The cell immobilization emerged as an alternative for enzyme immobilization. Immobilization of cells containing specific enzymes has further advantages, such as the elimination of long and expensive procedures for enzymes separation and purification and its vitality in expanding their application by enabling easy separation and purification of products from reaction mixtures and

efficient recovery of catalyst (Junter and Jouene, 2004). In comparison with immobilized enzymes, immobilized cells provide new possibilities since they can be used as natural, water-insoluble carriers of required enzyme activities (Stolarzewicz *et al*., 2011).

Results illustrated in Figure 5 reveal that within the time period examined, the immobilized cells showed higher phenol degradation rate with all phenol concentrations tested. In encapsulated cell culture, the carrier material act as a protective cover against toxicity of phenol by forming networks of the beads, a diffusion barrier for phenol is build up which is not present in free cell culture (Chen *et al*., 2002). Moreover, the immobilization of whole cells tends to improve the stability of enzymes by retaining them in their natural surroundings during immobilization and subsequent continuous operation.

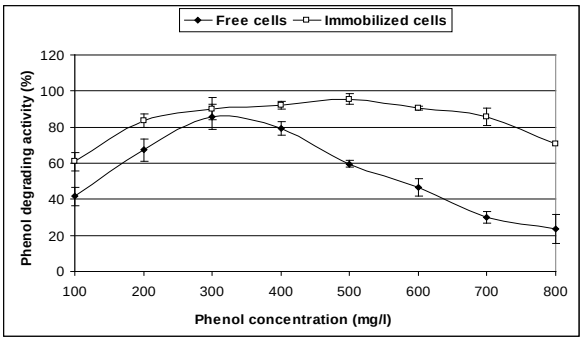

Figure 5. Effect of initial phenol concentrations on biodegradation rate by free and immobilized cells of *Bacillus* sp. 2BSG-PDA-16. Results are means of three independent determinations and error bars represent the standard deviation

Phenol biodegradation rate depends on the period in which the culture was adapted to phenol. The profiles of phenol degradation illustrated in Figure 6 show that as initial phenol concentration increased, appropriate removal efficiencies were obtained in a prolonged durations; time interval for degradation of low phenol concentrations e.g. 100 and 200 mg/Lwas at 5 days. As phenol concentration increased to 300, 400 and 500 mg/L, the degradation period was slightly prolonged. Complete removal of 300,400 and 500 mg/L phenol was achieved in 7 and 9 days, respectively. Initial phenol concentration of 600 mg/L was entirely degraded in 10 days. Further increase in phenol concentration resulted in a lower removal efficiency; for instance 62.53 % for 800 mg/L phenol in 11 days (Figure 6).

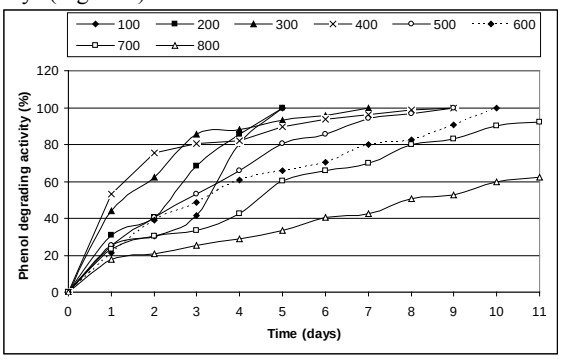

Figure 6. Time profiles of phenol biodegradation by free cells of *Bacillus* sp. 2BSG-PDA-16. Error bars represent the standard deviation

The cells immobilized in the Ca-alginate beads were not only able to tolerate high concentration of phenol but were also able to degrade it completely in a very short span of time. Figure 7 depicts the phenol degradation profiles of immobilized cells for initial phenol concentrations of 100-800 mg/L. It was observed that phenol concentrations of 200, 300 and 400 mg/L were completely degraded in 6 days. Furthermore, complete degradation of 500, 600 and 700 mg/L in 7 days and of 800 mg/L in 8 days. It seems that the tolerance of immobilized organisms against substrate inhibition has increased. In consequence, their capacity for phenol uptake was satisfactorily improved.

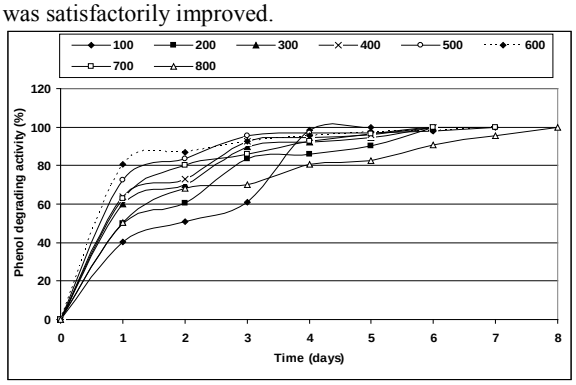

Figure 7. Time profiles of phenol biodegradation by immobilized cells of *Bacillus* sp. 2BSG-PDA-16. Error bars represent the standard deviation

It has been shown by several workers that immobilized microorganisms are better protected against phenolic compounds than are free cells. The advantages of immobilized cells in comparison with suspended ones include the retention in the reactor of higher concentrations of microorganism, protection of cells against toxic substances and prevention of suspended bacterial biomass in the effluent. Immobilization appeared as a promising procedure in overcoming substrate inhibition of phenol concentrations greater than 1000 mg/L (Loh *et al*., 2000).

Immobilized cells of *Pseudomonas putida* have been used successfully to degrade phenol at concentrations ranging from 100 to 1200 ppm in membrane and airlift bioreactors operated in batch and continuous mode (Muftah *et al*., 2009). In addition, cells of *Pseudomonas aeruginosa* adsorbed on diatomaceous earth pellets (celite R-635) and packed in column bioreactors were used to degrade phenol up to 1200 ppm in inorganic defined medium (Durham *et al*., 1994). *Alcaligenes latus* cells immobilized in polyurethane foam showed 100% degradation up to 350 ppm (1.05 mM) and 57% degradation at 500 ppm (1.5 mM). Degradation rate of Ca-alginate immobilized cells was less as compared to that of polyurethane foam immobilized cells (Usha *et al*., 2010).

In addition to this, stability during long-term operation is important for practical application of the immobilized cell system. In order to determine if there was deactivation of cells after repeated use, the immobilized cells were tested in twelve consecutive phenol degradation processes. The results showed that phenol degrading ability only decreased slightly after the immobilized cells were reused in seven cycles (Figure 8), demonstrating that the calcium alginate retained high mechanical strength. The reuse of immobilized cells might be advantageous because it can decrease waste of cells, save time, and cut down

cultivation cost. This facilitates the development of semicontinuous and continuous fermentation processes and leads to simplification of the separation of products from the fermentation broth .

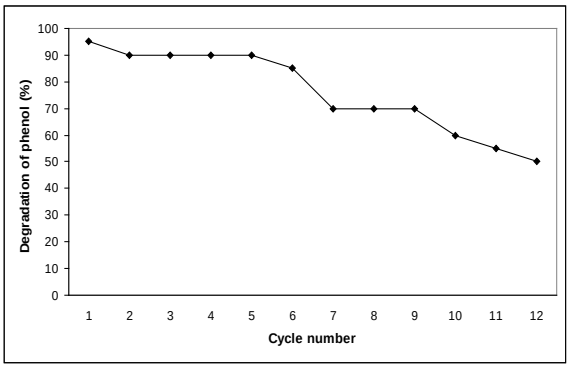

Figure 8. Repeated batch degradation of phenol by immobilized cells of *Bacillus* sp. 2BSG-PDA-16

The present findings show that immobilized cells in calcium alginate are promising for application in bio-degradation schemes in order to degrade phenol and possibly other related aromatic compounds at high concentrations in industry generated wastewater which leads to a reduction in time for complete phenol removal in relation to free cells.

4. Conclusion

The present study demonstrates that the isolated moderately halophilic *Bacillus* sp. 2BSG-PDA-16 is a potential candidate for the treatment of industrial saline wastewater contaminated with phenolic wastes. Immobilized cells in calcium alginate are promising for application in bio-degradation schemes in order to degrade phenol and possibly other related aromatic compounds at high concentrations in industry generated wastewater which leads to a reduction in time for complete phenol removal in relation to free cells.

References

Abd-elhaleem A, Beshay U, Abdelhamid A, Moawad H and Zaki S. 2003. Effects of mixed nitrogen sources on biodegradation of phenol by immobilized *Acinetobacter* sp. Strain W-17. *Afr J Biotechnol,* **2:** 8–12.

Adav S S, Chen MY, Lee D J and Ren N Q. 2007. Degradation of phenol by *Acinetobactor* strain isolated from aerobic granules. *Chemosphere,* **67:** 1566-1572.

Ahmad N, Ahmad I, Iqbal M, Khalid N, Abbas S, Mehboob F and Ahad K. 2016. Biodegradation of phenol by *Stenotrophomonas* sp.and *Staphylococcus* sp. isolated from contaminated sites. *Appl Ecol Environ Res*, **14**: 107-120.

Ahmad SA, Shamaan NA, Noorliza MA, Koon GB, Shuko MYA and Syed MA. 2012. Enhanced phenol degradation by immobilized *Acinetobacter* sp. strain AQ5NOL 1. *World J Microb Biot*, **28 :** 347-352.

Altschul SF, Thomas LM, Alejandro AS, Zhang J, Zhang Z, Miller W and Lipman D J. 1997. Gapped BLAST and PSI-BLAST, a new generation of protein database search programs. *Nucleic Acids Res,* **2517:** 3389–3402.

Annadurai G, Balan MS and Murugesan T. 2000a. Design of experiments in the biodegradation of phenol using immobilized *Pseudomonas pictorium* NICM – 2077 on activated carbon. *Bioprocess Engin,* **22:** 101-107.

Annadurai G, Juang RS and Lee DJ. 2002. Microbiological degradation of phenol using mixed liquors of *Pseudomonas putida* and activated sludge. *Waste Manag*, **22**: 703-710.

Annadurai G, Rajesh Babu S, Mahesh KPO and Murugesant T. 2000b. Adsorption and biodegradation of phenol by chitosan-immobilized *Pseudomonas putida* (NICM 2174). *Bio process Eng*, **22**: 493-501.

Annadurai G, Mathalai Balan S and Murugesan T. 1999. Box-Behnken design in the development of optimized complex medium for phenol degradation using *Pseudomonas putida* (NICM 2174). *Bio process Eng*, **21**: 415-421.

Bai J, Wen JP, Li HM and Jiang Y. 2007. Kinetic modeling of growth the biodegradation of phenol and m-cresol using *Alcaligenes faecalis*. *Process Biochem,* **42:** 510-517.

Cátia TD, Mariano M, Janaína FK and Carlos A. 2010. Biodegradation of phenol by free and encapsulated cells of a new *Aspergillus* sp. isolated from a contaminated site in southern Brazil. *Afri J Biotechnol,* **940:** 6716-6720.

Chen IP, Lin SS, Wang CH and Chang SH. 2007. CWAO of phenol using CeO2/γ-Al2O3 with promoter, effectiveness of promoter addition and catalyst regeneration. *Chemosphere,* **66:** 172-178.

Chen KC, Lin YH, Chen WH and Lin YC. 2002. Degradation of phenol by PAA-immobilized *Candida tropicalis*. *Enzyme Microb Technol,* **31:** 490-797.

Devi S and Sridhar P. 2000. Production of cephamycin C in repeated batch operations from immobilized *Streptomyces clavuligerus*. *Proc Biochem,* **36:** 225-231.

Durham DR, Marshall LC, Miller JG and Chmurny AB. 1994. Characterization of inorganic bio carriers that moderate system upsets during fixed-film biotreatment processes. *Appl Environ Microbiol,* **60:** 3329-3335.

Gerrard AM, Junior JP, Kosteckova A, Paca J, Stiborova M and Soccol CR. 2006. Simple models for the continuous aerobic biodegradation of phenol in a packed bed reactor. *Braz Arch Biol Technol,* **494:** 669-676.

Idris A and Saed K 2002. Degradation of phenol in wastewater using anolyte produced from electrochemical generation of brine solution. *Int J,* **3:** 139-144.

Indu Nair C, Jayachandran K and Shashidhar S. 2008. Biodegradation of phenol. *Afr J Biotechnol,* **725:** 4951-4958.

Juang RS and Tsai SY. 2006. Enhanced biodegradation of mixed phenol and sodium salisylate by *Pseudomonas Putida* in membrane contactors. *Water Res,* **40:** 3517-3526.

Junter GA and Jouenne T. 2004. Immobilized viable microbial cells: from the process to the proteome in leader or the cart before the horse. *Biotechnol Adv*, **22**: 633-658.

Kafilzadeh F, Farhangdoost MS and Tahery Y. 2010. Isolation and identification of phenol degrading bacteria from lake parishan and their growth kinetic assay. *Afr J Biotechnol,* **940:** 6721-6726.

Kujawski W, Warszawki A, Ratajczak PT, Capala W and Ostrowski I. 2004. Removal of phenol from wastewater by different separation techniques. *Desalination* , **163:** 287-296.

Lin CW, Chen LH and Chiang WF. 2007. Microbial community structure during oxygen-stimulated bioremediation in phenol-contaminated groundwater. *J Hazard Mat,* **140:** 221-229.

Liu H, Guo L, Liao S and Wang G. 2012. Reutilization of immobilized fungus *Rhizopus* sp. LG04 to reduce toxic chromate. *J Appl Microbiol,* **112:** 651-659.

Loh KC, Chung TS and Ang W.F. 2000. Immobilized cell membrane bioreactor for high strength phenol wastewater. *J Environ Eng*, **126:** 75–79.

Loh KC and Wang SJ. 1998. Enhancement of biodegradation of phenol and a non growth substrate 4- chlorophenol by medium augmentation with conventional carbon sources. *Biodegradation*, **8**: 329-338.

Masque C, Nolla M and Bordons A. 1987. Selection and adaptation of a phenol degrading strain of Pseudomonas. *Biotechnol Lett*, **9:** 655-660.

Martins SC, Martins CM, Fiúza L M and Santaella ST. 2013. Immobilization of microbial cells, A promising tool for treatment of toxic pollutants in industrial wastewater. *Afr J Biotech,* **1228:** 412-4418.

Muftah H, Shaheen A, Al-Muhtaseb A and Souzan M. (2009). Biodegradation of phenol by *Pseudomonas putida* immobilized in polyvinyl alcohol (PVA) gel. *J Hazard Mater*, **164:** 720-725.

Murthy A, Gayathri KV. 2017. Halotolerant bacterial consortium able to degrade substituted phenolic compounds isolated from saline environment. *Environ risk assess remed,* **1** : 22-29.

Nair CI, Jayachandran K and Shankar S. 2008. Biodegradation of phenol. *Afr J Biotechnol*, **25:** 4951-4958.

Ramzan M and Rehman A. 2016. Characterization of phenol degrading bacteria isolated from industrial effluents. *Pak J Zoo.,* **48:**1865-1870.

Ravikumar S, Parimala PS and Gokulakrishnan R. 2011. Biodegradation of phenolic compounds by using halotolerant microbes. *IJPAES,* **12:** 38-45.

Rochelle PA, Will JA, Fry JC, Jenkins GJ, Parkes RJ, Turley, CM and Weightman A J. 1995. In: Trevors JT, van Elsas JD (Eds), **Nucleic Acids in the Environment**. Springer, Berlin, pp. 219–239.

Roostaei N and Tezel F H. 2004. Removal of phenol from aquaeos solution by absorption. *J Environ Manag,* **70:** 157-164.

Shweta S and Handayuthapani R. 2013. Optimization of phenol biodegradation by *Pseudomonas putida* isolated from industrial effluent. *Int J Pharm Bio Sci,* **43:** 405 – 413.

Soda S, Ike M and Fujita M. 1998. Effects of inoculation of genetically engineered bacterium on performance and indigenous bacteria of sequencing batch activated sludge process treating phenol. *J Ferment Bioeng*, **86**: 90-96.

Stolarzewicz I, Bialecka-Florjañczyk E, Majewska E and Krzyczkowska J. 2011. Immobilization of yeast on polymeric supports. *Chem Biochem Eng*, **25:** 135-144.

Usha MS, Sanjay MK, Gaddad SM and Shivannavar CT. 2010.Degradation of H-acid by free and immobilized cells of *Alcaligenes latus*. *Braz J Microbiol*, **41:** 931-945

Wang Y, Tian Y, Han B, Zhao HB, Bi JN and Cai BL. 2007. Biodegradation of phenol by free and immobilized *Acinetobacte*r sp. strain PD12. *J Environ Sci,* **19:** 222-225.

Yang CF and Lee CM. 2007. Enrichment, isolation, characterization of phenol-degrading *Pseudomonas resinovorans* strain P-1 and *Brevibacillus sp.* Strain P-6. *Int Biodet Biodeg,* **59:** 206-210.

Yang RD and Humphrey AE. 1975. Dynamic and steady state studies of phenol biodegradation in pure and mixed cultures. *Biotechnol Bioengin,* **17:** 1211-1235.

JJBS

Jordan Journal of Biological Sciences

Volume 10, Number 4,December 2017
ISSN 1995-6673
Pages 297 - 302

Evaluation of the Anti-Cancer Potential of Amphidinol 2, a Polyketide Metabolite from the Marine Dinoflagellate *Amphidinium klebsii*

Rafael A. Espiritu[1,2,*], Maria Carmen S. Tan[1] and Glenn G. Oyong[3,4,*]

[1]Department of Chemistry, De La Salle University, [2]Department of Chemistry, Graduate School of Science, Osaka University, Toyonaka, Osaka 560-0043, Japan; [3]Department of Biology, [4]Center for Natural Science and Ecological Research, De La Salle University, 2401 Taft Avenue, Manila 0922, Philippines.

Received: June 27, 2017; Revised: August 30, 2017; Accepted: September 11, 2017

Abstract

The increasing incidence of new cancer cases and the appearance of cancer cells resistant towards standard chemotherapeutic drugs have prompted active research on finding novel compounds with promising anti-cancer properties. In this regard, marine organisms could provide interesting and unique compounds that may be of use in the treatment of this disease. Amphidinols (AMs) belong to a class of polyketide metabolites isolated from the marine dinoflagellate *Amphidinium klebsii*. These compounds are known to perforate the membrane via sterol interaction ultimately leading to pore formation and cell death. Herein, the activity of amphidinol 2 (AM2) against HCT-116, HT-29, and MCF-7 cancer cells was evaluated and compared with normal HDFn cells. Cell viability assays revealed that AM2 was cytotoxic to all cells tested, but it was significantly lower in normal cells; its IC_{50} against HDFn cells was 135.5 µg/mL compared with 1.2–8.5 µg/mL for the three cancer cell lines. Gene expression experiments showed that the presence of AM2 resulted in the upregulation of the pre-apoptosis markers *cfos* and *cjun* in all cancer cell lines tested, which may explain its observed cytotoxic action. These results demonstrate the potential of AM2, and possibly this class of compounds, as an effective anti-cancer therapeutic.

Key words: *Amphidinium klebsii*, Amphidinol 2, Apoptosis, Cytotoxicity.

1. Introduction

The incidence of cancer has increased significantly over the past decades transforming it into a major public health concern worldwide, both in terms of human and financial costs. In the United States, for example, it was projected that over 1.7 million new cases will be diagnosed in 2016 that will result in approximately 600,000 deaths (Siegel *et al*., 2017). This group of related diseases is characterized by 8 hallmarks including resisting apoptosis, sustained proliferative signaling, insensitivity to growth suppressors, replicative immortality, angiogenesis, invasion and metastasis, altered energy metabolism, and evasion of the body's immune responses (Hanahan and Weinberg, 2011). Understanding these traits will provide a better insight into this disease and consequently, the development of new ways to treat it, such as increasing the vulnerability of cancer cells to apoptosis. One of the promising research related to this is on the tumor necrosis factor-related apoptosis-inducing ligand (TRAIL), which is known to promote cancer cell death but not of normal cells. It was previously demonstrated that *cfos* and *cjun* protein products repress the transcription of the anti-apoptotic molecule c-FLIP(L), thus sensitizing prostate cancer cells to TRAIL-induced apoptosis (Li *et al.*, 2007). Furthermore, resistance to TRAIL-induced apoptosis was also observed upon binding to and repression of *cfos* by the anti-apoptotic molecule FBXL10 (Ge *et al.*, 2011). In addition to these, a number of studies also provided support for the notion that protein products of *cfos* and *cjun* are involved in inducing cancer cell death (Chan *et al.*, 2010; Shyu *et al.*, 2014).

* Corresponding author. e-mail: rafael.espiritu@dlsu.edu.ph; glenn.oyong@dlsu.edu.ph.

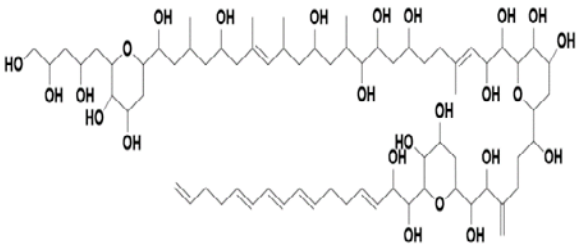

Figure 1. Chemical structure of AM2

Together with the increasing number of new cancer cases is the problem associated with resistance of cancer cells to chemotherapy and molecularly targeted therapies, prompting active research into finding new molecules with anti-cancer potential. Marine dinoflagellates are promising sources in the continuing search for new and unique bioactive secondary metabolites to combat cancer and other diseases. One of the very interesting bioactive natural products obtained from these organisms are the amphidinols (AMs), polyketide metabolites first reported from the dinoflagellate *Amphidinium klebsii* (Satake *et al*., 1991). This class of compounds is defined by unique structural features, namely a linear polyhydroxy moiety, two tetrahydropyran rings, and a polyene chain of varying length. In addition to *A. klebsii*, AMs have also been isolated from *A. carterae*, and currently 19 homologues are known (Satake *et al*., 1991; Paul *et al*., 1995; Paul *et al*., 1997; Murata *et al*., 1999; Echigoya *et al*., 2005; Morsy *et al*., 2005; Morsy *et al*., 2006; Meng *et al*., 2010; Nuzzo *et al*., 2014), as well as a number of structurally-related compounds from other dinoflagellate species (Doi *et al*., 1997; Huang *et al*., 2004; Washida *et al*., 2006; Suguhara *et al*., 2011; Inuzuka *et al*., 2014; Waters *et al*., 2015). Amphidinols have been shown to exhibit antifungal and hemolytic activities which are believed to arise from its ability to permeabilize the membrane via preferential interaction with 3β-hydroxysterols, ultimately leading to cell death (Morsy *et al*., 2008; Espiritu *et al*., 2014). Previous investigations on membrane permeabilization by AMs suggest that the molecule could form both toroidal and barrel-stave pores (Houdai *et al*., 2005; Espiritu *et al*., 2014). Amphidinol 2 (AM2, Figure 1) is unique among the known AM homologs since this molecule has shown permeabilization of the cell membrane even in the absence of sterols (Morsy *et al*., 2008). Furthermore, in addition to being hemolytic, AM2 was also previously reported to be cytotoxic against primary rat hepatocytes (Qi *et al*., 2007), prompting us to investigate whether this molecule can be used as an effective anti-cancer agent.

Thus, the aim of this study is to explore on the chemotherapeutic potential of AM2 against HCT-116 human colorectal carcinoma, HT-29 human colorectal adenocarcinoma and MCF-7 human breast adenocarcinoma, and determine its effects on *cfos* and *cjun* gene expression, the protein products of which are critical in cancer progression. To the best of our knowledge, this is the first report on the anti-cancer activity of this class of molecules as well as on their effect on the aforementioned cancer-related genes.

2. Materials and Methods

2.1. Materials

Amphidinol 2 (AM2) was isolated as reported previously (Paul *et al*., 1995). Human primary fibroblasts, neonatal HDFn (Invitrogen, USA) and cancer cell lines HT-29, HCT-116 and MCF-7 (American Type Culture Collection, USA) was provided by the Molecular Science Unit Laboratory of the Center for Natural Science and Ecological Research, De La Salle University. All cell lines were cultured in Dulbecco's Modified Eagle's Medium (DMEM) supplemented with 10% fetal bovine serum (FBS, Invitrogen, USA) and 1x antibiotic-antimycotic (Invitrogen, USA) and incubated at 37C with 5% CO_2 and 98% humidity.

2.2. Cell Viability Assay against Amphidinol 2

HDFn, HT-29, HCT-116 and MCF-7cells, previously cultured to 90% confluence in a T-flask, were seeded into wells (2.4 x 10^5 cells/well) of a 9 6-well culture plate (Falcon, USA) and incubated for 24 hours to complete cell attachment. Afterwards, 100 µL of the compound, previously filter-sterilized, were subjected to two-fold serial dilution in the corresponding wells. Similar serial dilutions (two-fold) of colchicine (Sigma Aldrich, USA) were used as positive control. The plates were then incubated for 4 days, followed by addition of 10 µL of PrestoBlue® (Molecular Probes, Invitrogen) into each well, and an additional incubation of 30 minutes to 1 hour. Absorbance measurements were performed on a microplate reader (Biotek ELx800, BioTek Instruments, USA) at 570 nm and normalized to 600 nm values (reference wavelength). Background color was corrected by including wells containing only DMEM. Untreated wells with no added AM2 served as untreated controls.

Optical density readings obtained were used to calculate the cell viability index of the drugs using the equation, cell viability (%) = 100 – [100 – ($A_{treated}$ / $A_{untreated}$ x 100)], where $A_{treated}$ and $A_{untreated}$ is the absorbance of the treated and untreated cells, respectively. This was plotted against the corresponding treatment concentrations to derive IC_{50} (defined as the concentration of the drug necessary to inhibit cell growth by 50%) values whenever applicable.

2.3. cfos and cjun Transcript qRT-PCR Assay

Expression of the early apoptosis genes *cfos* and *cjun* was determined for HCT-116, HT-29, and MCF-7 cells, where AM2 exhibited significant cytotoxic activity, following the protocol reported previously (Shyu *et al*., 2014). Briefly, 100 µL of the corresponding cells (2.4 x 10^5 cells/mL) were seeded separately into 96-well microplates and were incubated for 24 hours to attach the cells as monolayers. The cells were then exposed to AM2 for 30 minutes by adding the appropriate sample volume corresponding to the IC_{50} value for each cell. The positive control used was bleomycin, while the negative control included only the cancer cells. Afterwards, the total RNA was extracted from the cells with the TriZol Reagent (Invitrogen, USA) following the manufacturer's protocol.

All qRT-PCR reactions were performed using the Rotor-Gene 3000 thermocycler utilizing a final volume of 10 µL which contains the following: RNA template (1 µL),

2x KAPA FAST SYBR (5 µL; KAPA Biosystems, USA), 10 µM of the forward and reverse primers for *cfos* and *cjun* (0.3 µL each), and diethylpyrocarbonate-treated water (3.4 µL; Invitrogen, USA). The primer sequences used were: F: 5'-AAGGAGAATCCGAAGGGAAAGGAATAAGA-TGGCT-3',R: 5'-AGACGAAGGAAGACGTGTAAGCA GTGCAGCT-3' for *cfos*, and F: 5'-GCATGAGGAACC GCATTGCCGCCTCCAAGT-3',R: 5'-GCGACCAAGTCCTTCCCACT-CGTGCACACT-3' for *cjun.*

Synthesis of cDNA was carried out at 50 °C for 3 minutes, and subsequent amplification consisting of 40 cycles of the cDNA was performed for 20 seconds at 95 °C, for 30 seconds at 55 °C, and for 35 seconds at 72 °C, while melting analysis was carried out between 72 and 95 °C. The amplified transcript levels were quantified using an internal standard, human glyceraldehyde-3-phosphate dehydrogenase (GAPDH), which was also amplified at the same time, at different known magnitudes, specifically, 10^9, 10^8, 10^7, 10^6, and 10^5 copies. Quantification was done using the Rotor-Gene 3000 software ver. 6.1.93, where the critical threshold values were determined from the obtained standard curve.

2.4. Statistical Analysis

The average value of the treatment responses for the different assays were compared and analyzed with one-way analysis of variance ($p < 0.05$) and Tukey multiple comparisons test ($p < 0.05$). For nonlinear regression analysis (least squares method), the concentrations used were transformed to logarithmic scale to determine the IC_{50} values. GraphPad Prism ver. 7.02 was used for these analyses.

3. Results

In this study, the anti-cancer potential of AM2 was investigated, as well as on how it affects the gene expression of *cfos* and *cjun*, whose proteins products have been implicated as being crucial in cancer progression.

3.1. Cytotoxicity of AM2 against Various Cell Lines

The cytotoxicities of the aqueous solutions of AM2 on the four cell lines, based on cell viability assay, are shown in Figures 2 and 3. For the assays conducted, colchicine, an anti-cancer alkaloid that destabilizes microtubules (Lin *et al.*, 2013), served as the positive control. Results showed that addition of either AM2 or colchicine resulted in a concentration-dependent decrease in cell viability for all cell lines tested (Figure 2). However, analysis of the data revealed a n otable difference between the two compounds' activities: significantly higher cell viability was recorded in normal cells compared with all three cancer cell lines upon treatment with AM2, starting at a concentration of 3.125 µg/mL (Figure 2A). In contrast, colchicine exhibited a comparable activity across all four-cell lines, except at a concentration of 100 µg/mL against HT-29 colon cancer cells (Figure 2B) where it was significantly higher.

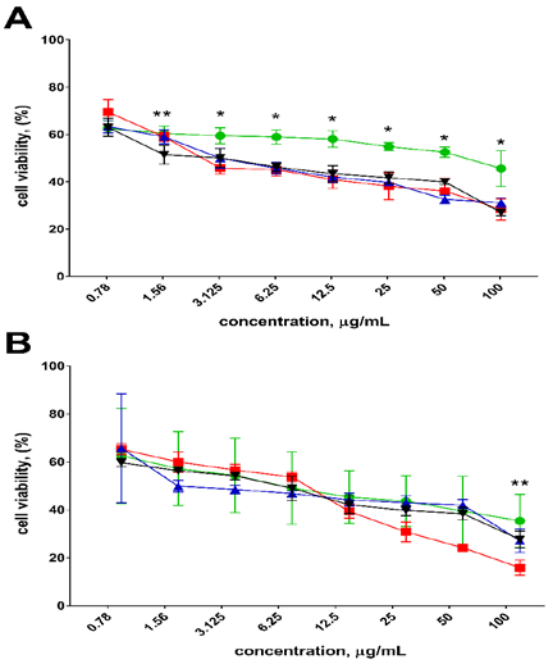

Figure 2. Average cytotoxicity values of AM2 (A) and colchicine (B) against normal (HDFn) and cancer (HCT-116, HT-29, MCF-7) cells. Green, black, red, and blue lines correspond to HDFn, HCT-116, HT-29, and MCF-7 cell viability, respectively. Error bars indicate the standard deviation of three independent trials. * indicates significant difference between normal and all cancer cell lines, while ** indicates significant difference between normal cell and only one cancer cell line (for A is HCT-116, and for B is HT-29).

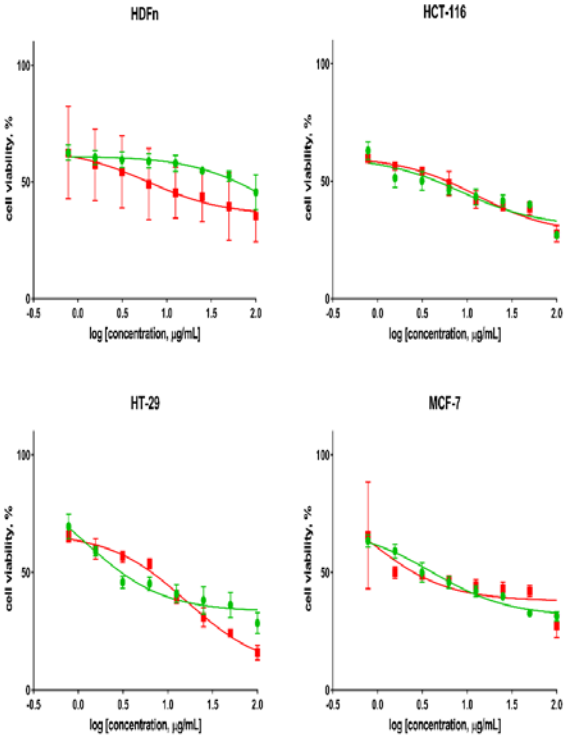

Figure 3. Nonlinear regression analysis of the average cytotoxicity values of AM2 and colchicine against the different cell lines used for IC_{50} determination. Green and red lines correspond to AM2 and colchicine curve-fitting, respectively. Error bars indicate standard deviation of three independent trials.

Nonlinear regression analysis of the dose-response curves (Figure 3) to determine IC_{50} values, or the half-maximal inhibitory concentration, provided more evidence of a better selectivity of AM2 towards cancer cells. The compound exhibited an IC_{50} value of 135.5 µg/mL against the normal HDFn cell, which was around 15- to 112-fold higher against the three cancer cells. In contrast, colchicine was roughly 22-fold more cytotoxic towards normal cells than AM2. Moreover, AM2 showed an approximately 13-fold and 1.5-fold greater activity against HT-29 and HCT-116 cancer cells, respectively, than colchicine, although it was less active against MCF-7 as shown in Table 1.

Table 1. Summary of IC_{50} values for AM2 and colchicine against normal and cancer cell lines obtained from curve-fitting

	AM2	Colchicine
HDFn	135.5 µg/mL	6.1 µg/mL
HCT-116	8.5 µg/mL	12.8 µg/mL
HT-29	1.2 µg/mL	16.3 µg/mL
MCF-7	4.1 µg/mL	0.7 µg/mL

3.2. Effect of AM2 on the Gene Expression of cfos and cjun

Gene regulation of the early apoptotic markers *cfos*/*cjun* significantly increased in all carcinoma cells incubated with AM2 (Figure 4). HCT-116 treated with colchicine and AM2 were statistically similar for both *cfos* and *cjun* whereas untreated HCT-116 cells gave significantly lower values. The *cfos*/*cjun* expression levels in both HT-29 and MCF-7 trials also followed a similar trend. These data are consistent with the comparable cytotoxicity of AM2 against these cancer cell lines. The expression of *cfos*/*cjun* in the aberrant cells incubated with AM2 and colchicine were approximately 100,000-fold higher than in untreated ones.

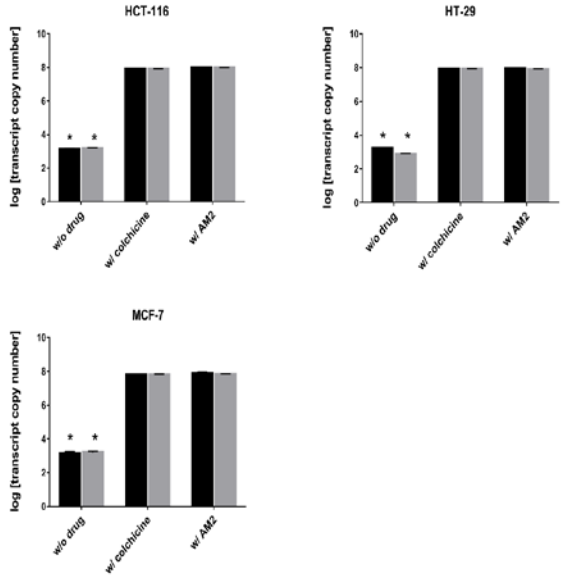

Figure 4. Average transcript copy numbers of the early apoptosis markers cfos (black) and cjun (gray) in untreated and treated HCT-116, HT-29, and MCF-7 cancer cell lines obtained using qRT-PCR. Error bars indicate standard deviation of three independent trials. * indicate significant difference ($p < 0.05$) between the untreated and treated cells.

4. Discussion

The results of the cytotoxicity assays revealed that cancer cells are more sensitive to AM2 than normal ones, pointing to a better selectivity of the compound towards aberrant cells. Furthermore, the results also suggest that normal cells are able to tolerate, and thrive at, AM2 concentrations that would otherwise kill malignant cells, as evidenced by the significantly higher IC_{50} value for normal, HDFn cells. Solid tumors and many malignancies are known to have elevated levels of cholesterol compared with normal cells, primarily brought about by an increased uptake of low-density lipoproteins and the enhancement of cholesterol biosynthesis (Cruz *et al.*, 2013; Silvente-Poirot and Poirot, 2014; Li *et al.*, 2016). This may account for the higher sensitivity of the cancer cells tested towards AM2 since amphidinols have been shown to preferentially interact with membrane sterols leading to more extensive membrane binding, leading to membrane disruption and ultimately, cell death (Morsy *et al.*, 2008; Espiritu *et al.*, 2014). Higher cholesterol content in the membrane will result in a greater accumulation of AM2 on the membrane surface resulting in critical biological effects, such as possibly pore formation. Although it is not possible with these data to ascertain pore formation as the mode of cytotoxic action of AM2, involvement of this mechanism in killing cancer cells have been reported earlier (Lopez *et al.*, 2013). Another distinct possibility to account for the observed selectivity of AM2 towards cancer cells is that its interaction with membrane cholesterol could prevent the sterol from exerting its proper physiological function, such as its role in lipid rafts. Lipid rafts are membrane microdomains rich in cholesterol and sphingolipids that are known to be platforms for various signalling processes, including cell survival, and have been reported to have a higher occurrence in cancer cells than in normal ones (Zhuang *et al.*, 2005; Li *et al.*, 2006; Mollinedo and Gajate, 2015). AM3, a homologue of AM2, has been previously demonstrated to interact with raft-forming liposomes suggesting that it also recognizes cholesterol in this liquid-ordered domain (Espiritu, 2017). Therefore, it is reasonable to suggest that AM2 might behave similarly, given their similarities in structure and bioactivity, resulting in impaired sterol function in lipid rafts that eventually results to cell death. In fact, lipid rafts have been proposed earlier to be viable targets for cancer management (Zhuang *et al.*, 2005; Li *et al.*, 2006). Moreover, the cytotoxicity of AM2 against the three cancer cell lines tested was comparable ($p < 0.05$), indicating that the observed effects of the compound does not depend on the cell type and most probably a general mechanism of cell killing may be involved.

Breast and colon adenocarcinomas are refractory and resistant to a number of broadly used anticancer agents which renders them ineffective. Deregulation of cell death pathways have been linked to the multifactorial mechanisms which have been associated to this inherently resistant phenotype (Holohan *et al.*, 2013). In HT-29, MCF-7, HCT-116 cell lines, it has been established that the integrity of the p53/p21 regulatory system or function thereof has been damaged causing a failure in the body's natural ability to rid itself of irreversibly damaged cells

(Mitkin *et al.*, 2015; Wang *et al.*, 2015). The stalemate between p53 and p21-driven genes and drug sensitivity remains controversial since cytotoxicity of these medical agents can injure both the targeted carcinoma cells and the normal ones. For example, upon interaction with DNA damaging agents, normal cells with intact p53/p21 function suggest the existence of a checkpoint that delays replication, and that may extend the time available for DNA repair. This lack of repair mechanism could suggest that the chemotherapeutic activity of AM2 could follow this process since a highly elevated concentration is needed to reach the IC_{50} for HDFn as compared to the p53-defective aberrant cells. Furthermore, previous research have demonstrated that impairment of the apoptotic pathway, for instance by activation and upregulation of the Akt pathway involved in cellular repair mechanisms, leads to increased survival of cancer cells (Mundi *et al.*, 2016).

The results of this experiment strongly suggest that the increased cytotoxicity for HCT-116, HT-29, and MCF-7 cells incubated with AM2 may be associated with a molecular pathway involving an upregulation of the early apoptotic gene markers *cfos* and *cjun*. Cellular survival pathways in the mutant cell lines seem to have been circumvented since the presence of elevated markers *cfos*/*cjun* have indicated that programmed cell death has ensued. This apoptosis-related cell death may also be caused by impairment of the cell's natural repair mechanisms, although further research needs to be done to confirm this. Finally, given the potent hemolytic activity of AM2 that limits its therapeutic potential (Paul *et al.*, 1995), among others, structure-activity relationship studies must also be conducted to obtain the most effective structure for anti-cancer use, while at the same time minimizing its unwanted side effects.

5. Conclusions

The results of the study showed that AM2 was cytotoxic against the mutant cell lines HCT-116, HT-29, MCF-7, as evidenced by their respective low IC_{50} values, but it was significantly less active against normal HDFn cells. The cytotoxic activity recorded here may be due to the observed upregulation of the early apoptotic gene markers *cfos* and *cjun*, which was significantly higher in the treated cells than in untreated ones, and similar to the positive control colchicine. These suggest that AM2 could result in the eventual activation of the apoptotic pathway as a means to kill cancer cells. These results provide support for the role of AM2 as a potential chemotherapeutic agent, especially for colorectal and breast adenocarcinoma.

Acknowledgement

The authors wish to express their gratitude to Prof. Michio Murata of Osaka University for his assistance with AM2 isolation. A research grant from the De La Salle University Science Foundation through the University Research Coordination Office is gratefully acknowledged.

References

Chan QKY, Lam HM, Ng CF, Lee AYY, Chan ESY, Ng HK, Ho SM and Lau KM. 2010. Activation of GPR30 inhibits the growth of prostate cancer cells through sustained activation of Erk1/2, c-jun/c-fos-dependent upregulation of p21, and induction of G2 cell-cycle arrest. *Cell Death Differ*, **17**:1511-1523.

Cruz PMR, Mo H, McConathy WJ, Sabnis N and Lacko AG. 2013. The role of cholesterol metabolism and cholesterol transport in carcinogenesis: a review of scientific findings, relevant to future cancer therapeutics. *Front Pharmacol*, **4**:1-7.

Doi Y, Ishibashi M, Nakamichi H, Kosaka T, Ishikawa T and Kobayashi J. 1997. Luteophanol A, a new polyhydroxyl compound from symbiotic marine dinoflagellate *Amphidinium* sp.. *J Org Chem*, **62**:3820-3823.

Echigoya R, Rhodes L, Oshima Y and Satake M. 2005. The structures of five new antifungal and haemolytic amphidinol analogs from *Amphidinium carterae* collected in New Zealand. *Harmful Algae*, **4**:383-389.

Espiritu RA. 2017. Membrane permeabilizing action of amphidinol 3 and theonellamide A in raft-forming lipid mixtures. *Z Naturforsch C*, **72**:43-48.

Espiritu RA, Matsumori N, Tsuda M and Murata M. 2014. Direct and stereospecific interaction of amphidinol 3 with sterol in lipid bilayers. *Biochem*., **53**:3287-3293.

Ge R, Wang Z, Zeng Q, Xu X and Olumi AF. 2011. F-box protein 10, and NF-κB dependent anti-apoptotic protein, regulates TRAIL-induced apoptosis through modulating c-fos/c-FLIP pathway. *Cell Death Differ*, **18**:1184-1195.

Hanahan D and Weinberg RA. 2011. Hallmarks of cancer: the next generation. *Cell*, **144**:646-674.

Holohan C, van Schaeybroeck S, Longley DB and Johnston PG. 2013. Cancer drug resistance: and evolving paradigm. *Nat Rev Cancer*, **13**:714-726.

Houdai T, Matsumori N and Murata M. 2008. Structure of membrane-bound amphidinol 3 in isotropic small bicelles. *Org Lett*, **10**:4191-4194.

Huang X, Zhao D, Guo Y, Wu H, Trivellone E and Cimino G. 2004. Lingshuiols A and B, two new polyhydroxy compounds from the Chinese marine dinoflagellate *Amphidinium* sp.. *Tetrahedron Lett*, **45**:5501-5504.

Inuzuka T, Yamada K and Uemura D. 2014. Amdigenols E and G, long carbon-chain polyol compounds, isolated from the marine dinoflagellate *Amphidnium* sp.. *Tetrahedron Lett*, **55**:6319-6323.

Li J, Gu D, Lee SSY, Song B, Bandyopadhyay S, Chen S, Konieczny SF, Ratliff TL, Liu X, Xie J and Cheng JX. 2016. Abrogating cholesterol esterification suppresses growth and metastasis of pancreatic cancer. *Oncogene*, **35**:6378-6388.

Lin Z, Wu C, Chuang Y and Chuang W. 2013. Anti-cancer mechanisms of clinically acceptable colchicine concentrations on hepatocellular carcinoma. *Life Sci*, **93**:323-328.

Li W, Zhang X and Olumi AF. 2007. MG-132 sensitizes TRAIL-resistant prostate cancer cells by activating c-fos/c-jun heterodimers and repressing c-FLIP(L). *Cancer Res*, **67**:2247-2255.

Li YC, Park MJ, Ye SK, Kim CW and Kim YN. 2006. Elevated levels of cholesterol-rich lipid rafts in cancer cells are correlated with apoptosis sensitivity induced by cholesterol-depleting agents. *Am J Pathol*, **168**:1107-1118.

Lopez JA, Jenkins MR, Rudd-SchimdtJA, Brennan AJ, Danne JC, Mannering SI, Trapani JA and Voskoboinik I. 2013. Rapid and unidirectional perforin pore delivery at the cytotoxic immune synapse. *J Immunol*, **191**:2328-2334.

Meng Y, van Wagoner RM, Misner I, Tomas C and Wright JLC. 2010. Structure and biosynthesis of amphidinol 17, a haemolytic compound from *Amphidinium carterae*. *J Nat Prod*, **73**:409-415.

Mitkin NA, Hook CD, Schwartz AM, Biswas S, Kochetkov DV, Muratova AM, Afanasyeva MA, Kravchenko JE, Bhattacharyya A and Kuprash DV. 2015. p53-dependent expression of CXCR5 chemokine receptor in MCF-7 breast cancer cells. *Sci Rep*, **5**:9330.

Mollinedo F and Gajate C. 2015. Lipid rafts ad major platforms for signalling regulation in cancer. *Adv Biol Regul*, **57**:130-146.

Morsy N, Houdai T, Konoki K, Matsumori N, Osihi T and Murata M. 2008. Effects of lipid constituents on membrane-permeabilizing activities of amphidinols. *Bioorg Med Chem*, **16**:3084-3090.

Morsy N, Houdai T, Matsuoka S, Matsumori N, Adachi S, Oishi T, Murata M, Iwashita T and Fujita T. 2006. Structures of new amphidinols with truncated polyhydroxyl chain and their membrane-permeabilizing activities. *Bioorg Med Chem*, **14**:6548-6554.

Morsy N, Matsuoka S, Houdai T, Matsumori N, Adachi S, Murata M, Iwashita T and Fujita T. 2005. Isolation and structure elucidation of a new amphidinol with a truncated polyhydroxyl chain from *Amphidinium klebsii*. *Tetrahedron*, **61**:8606-8610.

Mundi PS, Sachdev J, McCourt C and Kalinsky K. 2016. AKT in cancer: new molecular insights and advanced in drug development. *Br J Clin Pharmacol*, **82**:943-956.

Murata M, Matsuoka S, Matsumori N, Paul GK and Tachibana K. 1999. Absolute configuration of amphidinol 3, the first complete structure determination from amphidinol homologues: Application of a new configuration analysis based on carbon-hydrogen spin-coupling constants. *J Am Chem Soc*, **121**:870-871.

Nuzzo G, Cutignano A, Sardo A and Fontana A. 2014. Antifungal amphidinol 18 and its 7-sulfate derivative from the marine dinoflagellate *Amphidinium carterae*. *J Nat Prod*, **77**:524-1527.

Paul GK, Matsumori N, Konoki K, Murata M and Tachibana K. 1997. Chemical structure of amphidinols 5 and 6 isolated from marine dinoflagellate *Amphidinium klebsii* and their cholesterol-dependent membrane disruption. *J Mar Biotechnol*, **5**:124-128.

Paul GK, Matsumori N, Murata M and Tachibana K. 1995. Isolation and chemical structure of amphidinol 2, a potent haemolytic compound from marine dinoflagellate *Amphidinium klebsii*. *Tetrahedron Lett*, **36**:6279-6282.

Qi XM, Yu B, Huang XC, Guo YW, Zhai Q and Jin R. 2007. The cytotoxicity of lignshuiol: A comparative study with amphidinol 2 on membrane permeabilizing activities. *Toxicon*, **50**:278-282.

Satake M, Murata M, Yasumoto T, Fujita T and Naoki H. 1991. Amphidinol, a polyhydroxy-polyene antifungal agent with an unprecedented structure, from a marine dinoflagellate, *Amphidinium klebsii*. *J Am Chem Soc*, **113**:9859-9861.

Shyu PT, Oyong GG and Cabrera EC. 2014. Cytotoxicity of probiotics from Philippine commercial dairy products on cancer cells and the effect on expression of cfos and cjun early apoptotic-promoting genes and interleukin-1β and tumor necrosis factor-α proinflammatory cytokine genes. *Bio Med Res Int*, 491740/1-491740/10.

Siegel RL, Miller KD and Jemal A. 2017. Cancer Statistics, 2017. *Ca-Cancer J Clin*, **67**:7-30.

Silvente-Poirot S and Poirot M.2014. Cancer. Cholesterol and cancer, in the balance. *Science*, **343**:1445-1446.

Sugahara K, Kitamura Y, Murata M, Satake M and Tachibana K. 2011. Prorocentrol, a polyoxy linear chain compound isolated from the toxic dinoflagellate *Prorocentrum hoffmanianum*. *J Org Chem*, **76**:3131-3138.

Wand G, Cao X, Lai S, Luo X, Feng Y, Wu J, Ning Q, Xia X, Wang J, Gong J and Hu J.2015. Altered p53 regulation of miR-148b and p55PIK contributes to tumor progression in colorectal cancer. *Oncogene*, **34**:912-921.

Washida K, Koyama T, Yamada K, Kita M, Uemura D. 2006. Karatungiols A and B, two novel antimicrobial polyol compounds, from the symbiotic marine dinoflagellate *Amphidinium* sp.. *Tetrahedron Lett*, **47**:2521-2525.

Waters AL, Oh J, Place AR, Hamann MT. 2015. Stereochemical studies of the karlotoxin class using NMR spectroscopy and DP4 chemical-shift analysis: Insights into their mechanism of action. *Angew Chem*, **54**:15705-15710.

Zhuang L, Kim J, Adam RM, Solomon KR and Freeman MR. Cholesterol targeting alters lipid rafts composition and cell survival in prostate cancer cells and xenografts. *J Clin Invest*, **115**:959-968.

JJBS

Jordan Journal of Biological Sciences

Volume 10, Number 4,December 2017
ISSN 1995-6673
Pages 303 - 308

Mycological Quality of Fresh and Frozen Chicken Meat Retailed within Warri Metropolis, Delta State, Nigeria

Gideon I. Ogu[1,*], Inamul H. Madar[2,3], Jude C. Igborgbor[4] and Judith C. Okolo[5]

[1] *Department of Biological Sciences, Novena University, Ogume, Delta State, Nigeria;*

[2] *Department of Biotechnology and Genetic Engineering, Bharathidasan University, Tiruchirappalli, Tamil Nadu, India;*

[3] *Department of Biochemistry, Islamiah College, Vaniyambadi, Vellore District, Tamil Nadu, India;*

[4] *Department of Biology, College of Education Agbor, Delta State, Nigeria;*

[5] *Department of Environmental Biotechnology and Bioconservation, National Biotechnology Development Agency, Abuja, Nigeria.*

Received: March 26, 2017; Revised: September 22, 2017; Accepted: October 10, 2017

Abstract

Chicken meat continues to gain global acceptance. The unhygienic processing and retailing conditions, in most Nigerian States, expose the meat to microbial contaminations. Though, economically useful, most fungi are mycotoxigenic. The present study investigated the mycological quality of fresh and frozen chicken meat retailed in three major markets (Effurun, Ekpan, and Uborikoko) within Warri metropolis, Delta State, Nigeria. The spread plate technique was used to culture the samples on sterile potato dextrose agar (supplemented with antibiotics) at 28 ± 2 ^{o}C. Out of the 60 samples analyzed, 38 (63.3 %) yielded fungal growth, with 25 (65.7 %) and 13 (34.2 %) for fresh and frozen samples, respectively. The fungal loads ranged from 1.1 - 2.2 x 10^4 CFU/g and 1.3 - 4.0 x 10^2 CFU/g for the fresh and frozen samples, respectively. The fungal loads were not significantly different, except in frozen samples from Epkan market. *Penicillium* (20.8 -26.7 %), *Aspergillus* (20.0 - 22.9 %), *Cladosporium* (10.4- 23.3 %), *Mucor* (10.4-13.3 %), *Fusarium* (8.3 - 16.7 %), *Rhizopus* (0 - 12.5 %), *Alternaria* (0 - 8.3 %), and *Candida* spp. (0 - 6.3 %) were the major fungal isolates. The fresh chicken samples were more contaminated than the frozen samples, though not significantly different (P>0.05). Poor processing environment and use of unhygienic retail equipments could be the possible contamination routes. The relatively high proportions of *Penicillium, Aspergillus, Cladosporium* and *Fusarium* spp. is of public health concern, and highlights the need for public education on good hygienic practices, proper environmental sanitations, and adequate thermal treatment of chicken meat before consumption.

Keywords: Warri metropolis, Chicken meat, Potato dextrose agar, Fungi.

1. Introduction

Globally, poultry sector has been recognized as a very significant and vital source of animal protein in the daily diet of an average household (Salawu *et al*., 2014). Chicken has been generally reared for their meat and eggs. The meat is most widely accepted over beef or pork in Nigeria because of its excellent source of proteins, high digestibility, taste, low fat/cholesterol (Javadi and Safarmashaei, 2011) and without religious or health taboo. Nigeria's chicken population is about 150.682 million of which 25 % are commercially farmed, 15 % semi-commercially, and 60 % in backyards (Salawu *et al*., 2014). Generally, the steps involved in processing chicken meat include slaughtering or bleeding, scalding, defeathering and evisceration, which could be manually or mechanically done.

Microorganisms are ubiquitous and resident in wide varieties of foods of plants and animal origin. All foods possess a finite risk of microbiological contamination, but according to Roberts (1990), the highest risk factors include raw and animal foods. Chicken meat is one of such kind of products. Like every other animal, live chickens are hosts to diverse microorganisms residing on their skin, feathers and alimentary tract. These microorganisms can possibly contaminate the meat during processing chain, such as slaughtering, feather plucking, evisceration, and storage (Kozačinski *et al*., 2006; Bhaisare *et al*., 2014). Moreover, when processed in unhygienic environments, others microorganisms present in the processing

* Corresponding author. e-mail: gideoniogu@gmail.com.

environment, equipment, and processors hands/apron can contaminate the final meat product.

Over the years, there have been outbreaks of infections associated with consumption of contaminated chicken products, and the predominant microorganisms isolated included *Salmonella* spp., *Campylobacter* spp., *Staphylococcus* spp., *Shigella* spp., *Escherichia* spp., *Listeria* spp., *Yersinia* spp., *Aeromonas* spp. and *Clostridium* spp. (De Boer *et al*., 1991; Bhaisare *et al*., 2014). Reports abound on the bacteriological quality of commercial poultry and other livestock's products (Akbar and Anal, 2013; Adeyanju and Ishola, 2014; Bhaisare *et al*., 2014; Omorodion and Odu, 2014; Firildak *et al*., 2015; Chuku *et al*., 2016, Zakki *et al*., 2017). Information on mycological quality of raw chicken meat is scanty. Fungi and their spores are ubiquitous in the environments. Some genera, such as *Aspergillus* spp., have been found to elaborate hazardous mycotoxins that are mutagenic, teratogenic, hepatotoxic, immunotoxic and nephrotoxic (Atanda *et al*., 2013; Greco *et al*., 2014; Żukiewicz-Sobczak, 2015; Adeyeye, 2016). The severity of fungal diseases ranges from superficial to deep-seated organ damages if not well managed. The presence of such fungi in edible food is of great public health importance. Considering the fact that the levels of acceptability and demand for chicken meat over other meats remain on the high side, it is pertinent to periodically assess them for fungal contamination and public health safety.

The present study, therefore, investigates the fungal quality of fresh and frozen chicken meat sold in Warri metropolis with a view to ascertaining their mycological portability and public health safety.

2. Materials and Methods

2.1. Study Location

The study area was within Warri, a major city in Delta State, South-South Nigeria (Figure 1). Geographically, it is located at coordinates 5°31°N 5°45 °E and 5.517 °N 5.750°E. It is one of the major hubs of Petroleum activities and businesses in Southern Nigeria, with an estimated population of about 7,056,289 (Anon, 2017). It shares boundaries with Ughelli/Agbarho, Sapele, Okpe, Udu and Uvwie, although most of these places, notably Udu, Okpe and Uvwie, have been integrated to the larger cosmopolitan Warri. Effurun serves as the gateway to and the economic nerve of the city.

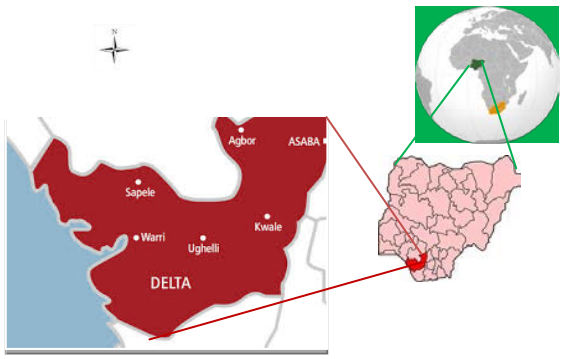

Figure 1. Map showing Warri in Delta State, Nigeria, West Africa.

2.2. Collection of Sample

Three major markets located within Warri metropolis, namely Effurun, Ekpan, and Uborikoko, served as sample collection centres. A total of 60 fresh and frozen chicken thigh samples, processed and retailed with the selected main markets were randomly sourced, purchased and labelled appropriately. The collected samples were placed in sterile ice-packed containers and conveyed to the Laboratory for analysis within 2 h. The sampling regime was between April – June, 2016.

2.3. Preparation of Sample

Twenty-five grams (25 g) of each chicken thigh sample were mixed with 225 mL of sterile (0.1%) peptone water in sterile beaker and thoroughly homogenized under aseptic conditions. Thereafter, the homogenized samples were serially diluted to 10^6 as described by APHA (2001).

2.4. Determination of Fungal Load in Collected Samples

The fungal load for each sample was determined using the streak plate technique (APHA, 2001) on sterile Potato Dextrose Agar (PDA) (Hi-media), previously prepared according to the manufacturer's specifications. The antibiotic, streptomycin (100 mg/L) was added to the culture media to make it more selective for fungal growth. From the dilutions, particularly (10^2, 10^4 and 10^6),made above, 0.1 mL aliquot was taken and aseptically inoculated onto the pre-set antibiotic-supplemented PDA, before spreading evenly with a s terile glass spreader. The inoculated agar plates were incubated on previously disinfected work bench at 28 ± 2 ° C for 3-5 days. The observed colonies were enumerated mechanically. The fungal loads were determined using the formula below, and results were expressed as CFU/g of sample:

$$\text{Total fungal count (CFU/g)} = \frac{\text{Average plate count}}{\text{Volume Cultured x dilution factor}}$$

2.5. Isolation and Characterization of Isolates

The prominent fungal colonies on the culture media plates were sub-cultured by inoculating them onto fresh sterile PDA media for further characterization. The growth pattern, pigmentation, and size of colonies were observed and recorded during the incubation period to aid identification of the organisms. The colonial morphology was examined using lactophenol (LP) cotton blue stain. A drop of lactophenol was placed on a cl ean microscopic slide. A small portion of each fungal isolate was taken using a sterile needle and placed in the drop of lactophenol. A clean cover glass was gently placed over the suspension and observed microscopically. The observed cultural and microscopic morphological characteristics for each stained isolates were compared with standard reference keys and atlas for their probable identities (Alexopoulos and Mims, 1979; Fawole and Oso, 1988; Jay, 1992; De Hoog *et al*., 2000).

2.6. Statistical Analysis

Data were analyzed using the descriptive statistic SPSS (version 20). Differences in mean of analyzed data were considered significant at $P<0.05$.

3. Results and Discussion

Food-borne pathogens have continued to be a major threat to food safety, especially in developing countries where proper hygiene and sanitation facilities are often

poor. The global incidence of food borne infections has greatly increased in recent years due to gross neglect of set food safety standards (EFSA, 2016). Millions of people throughout the world have been reported to die annually as a result of illness traced to food-borne pathogens (CDC, 2013). One of such foods with global epidemiological reports as important sources of human food-borne ailments is poultry products (EFSA, 2007; Arora *et al*., 2015).

In the present study, fresh and frozen chicken samples retailed within three major markets in Warri, Delta State, were analyzed for their fungal concentration and quality. Out of the 60 chicken thighs sampled, 38 (63.3 %) yielded significant fungal growth, with 25 (65.7 %) and 13 (34.2 %) for the fresh and frozen samples, repectively (Figure 2).This is an indication that the fresh chicken samples were probably more contaminated by fungi within the processing, retailing and or storage equipment. The mean fungal counts for fresh chicken samples ranged from 1.1 - 2.2 x 10^4 CFU/g (Figure 3). The highest fungal load was recorded from Effurun market samples, while the lowest was found in Ekpan samples. For the frozen chicken samples, the highest mean fungal load (4.1 x 10^2 CFU/g) was found in Epkan samples, while the least load was from Iborikoko market (1.3 x 10^2 CFU/g) (Figure 4). Statistical analysis of the results revealed that the contamination of the fresh samples were not significantly ($P>0.05$) higher than the frozen samples. These findings were comparable to the previous reports. An earlier study reported a fungal contamination of 0 - 8.0 x 10^4 CFU/g in chicken meat retailed in three different markets (Creek road market, Mile 3 market and Rumokoro market) in Port Harcourt, Rivers State (Omorodion and Odu, 2014). The fungal load reported for fried ready-to-eat chicken meat sold in two selected motor park points within Abakaliki, Ebonyi State, Nigeria, ranged from 0.25x10^5 to 0.25x10^4 CFU/mL. Vural *et al.* (2013) reported a fungal contamination level of 0 - 2.2 x 10^4 CFU/mL in frozen turkey meat sold in Diyarbakır, Turkey. Stagnitta *et al*. (2006) reported a mould and yeast counts of 10^3-10^5 CFU/g for processed meat food samples from retail stores located in San Luis city, Argentina. The fungal loads obtained in the present study were significantly lower than those (5.787 x 10^5 - 1.840 x 10^6 CFU/g) reported for fresh fish retailed in Benin City, Edo State, Nigeria (Udochukwu *et al*., 2016). However, relatively higher fungal contaminations were reported for non-chicken meat (Ajiboye *et al.*, 2011; Haleem *et al*., 2013; Ehigiator *et al.*, 2014).

The presence of fungi in more than half of the total chicken samples possibly suggests environmental contamination, since fungi are ubiquitous in soil, water, air, feeds and processing materials (Greco *et al*., 2014). Additionally, earlier studies reported fungal spores to be abundant in air and dust particles around waste dumpsites (Igborgbor and Ogu, 2015), and, thus, are easily carried by wind from the wastes dumpsites to exposed meat products in their vicinities. All the markets from which the samples were collected had huge waste dumpsites at various locations within and around the markets. This could be the reason for the lack of statistical differences between the levels of fungal load in the three markets. However, the observed variations could be attributed to differences in the levels of storage/retail facilities and handling practices in various markets/shops. The frozen samples were expected to be yield insignificant levels of fungal counts, but this study suggested otherwise. Freezing/refrigeration is a common preservation method for meat and vegetables. The detection of relatively high proportion of psychrotrophic fungi in the frozen chicken samples, despite the relatively low temperature of the storage facilities, is of public health significance. This finding is in concordance with previous study (Altunatmaz *et al*., 2013; Vural *et al.*, 2013; Oranusi *et al*., 2014). It further underscores the need to constantly maintain the recommended storage temperature of $\leq 4\ ^oC$ and adequate thermal treatment of frozen meats before consumption to prevent mycotoxicoses.

A total of seventy-eight fungi belonging to eight genera were isolated from the fresh and frozen samples, and included *Aspergillus, Mucor, Fusarium, Penicillium, Cladosporium, Alternaria*, *Rhizopus* and *Candida* species (Table 1). The frequencies of fungal isolates in the fresh chicken samples were *Aspergillus* 11 (22.9 %), *Penicillium* 10 (20.8 %), *Rhizopus* 6 (12.5 %), *Cladosporium* 5 (10.0 %), *Mucor* 5 (10.0 %), *Fusarium* 4 (8.3 %), *Alternaria* 5 (8.3 %), and *Candida* 3 (6.3 %) (Figure 5). For the frozen sample, the frequencies of isolation were *Penicillium* 8 (26.7 %), *Aspergillus* 6 (20.0 %), *Cladosporium* 7 (23.3 %), *Fusarium* 5 (16.7 %), and *Mucor* sp. 4 (13.3 %) (Figure 6). Previous studies have reported the presence of some of the fungi in various commercial poultry meat. *Candida* and *Cryptococcus* spp. were reported in poultry meat (drumstick and breast) retailed in Local Iraqi Markets (Haleem *et al*., 2013). Only *Aspergillus* spp. was reported by Oranusi *et al.* (2014) for chicken meat retailed in Ogun State, Nigeria. The genera, *Penicillium* spp. 3 (21.4 %), *Aspergillus* spp. 5 (35.7 %), *Neocosmospora* spp. 2 (14.2 %) and *Mucor* spp. 4 (28.5 %) were reportedly isolated from processed chicken meat retailed in two selected motor park points in Abakaliki, Ebonyi State, Nigeria (Jerry *et al.*, 2015). Ajiboye *et al*. (2011) isolated *Aspergillus niger, Aspergillus flavus, Penicillium* sp. and *Rhizopus* sp. from dried meat samples retailed in Oja-Oba market in Ilorin, Nigeria. Recently, *Aspergillus niger, A. fumigates, A. flavus, Penicillium chrysogenum, Rhizopus stolonifer, Fusarium equiseti* and *F. avenaceum* were reported in chicken meat retailed in Lahore City, Pakistan (Zakki *et al*., 2017). Our findings were in agreement with the previous reports, except for the presence of *Cladosporium, Mucor and Alternaria* spp. Differences in fungal distribution from one environment to another could be attributed to the observed variations. The spores of the moulds isolated in the present study are abundantly distributed in soil, water and air and can easily contaminate exposed and poorly processed food (Lange, 2014; Żukiewicz-Sobczak *et al.*, 2015).

Some fungi, under certain environmental conditions, release secondary metabolites, generally known as mycotoxins. Mycotoxins were reported to cause serious disorders in plants, humans and animals (Sule *et al.*, 2015). Different types of mycotoxins have been reported, but the agro-medically important types include aflatoxins, ochratoxins, trichothecenes, zearalenone, fumonisins, tremorgenic toxins, and ergot alkaloids (Zain, 2011). Some of the major mycotoxigenic fungi are distributed among the genera *Asperigullus, Fusarium* and *Penicillium* (Zain, 2011; Ismaiel and Papenbrock, 2015). Prolong exposure to

food contaminated by mycotoxin-producing moulds in food have been reported to cause severe health hazards, particularly among which are allergic reactions, cancer, and organ damages (Tasic and Tasic,2007; Atanda *et al.*, 2013; Greco *et al*., 2014; Żukiewicz-Sobczak*et al*., 2015; Wigmann *et al*., 2015). Although, there is paucity of information on t he acceptable limit for fungal contaminants in water and food, the presence of mycotoxigenic fungi could be of concern to the public health. It is, however, important to point out that the presence of mould is not a direct indication of myco-toxin contamination, because mycotoxin production depends on the type of fungal species and extent of growth, substrate components, aeration, relative humidity, temperature and storage environment (Ashiq, 2015). Moreover, previous studies have shown that relatively high temperature and humid conditions majorly favours fungal proliferation and secretion of mycotoxins (Atanda *et al*., 2013, Ashiq, 2015). The detection of relatively high number of potential mycotoxigenic fungi in the present study calls for improved sanitary, processing and storage facilities by the chicken processors or retailers and consumers alike to prevent impending dangers of ingesting toxins of fungi.

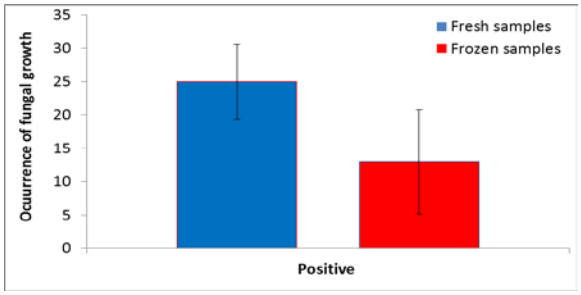

Figure 2. Occurrence of fungal growth in chicken meat samples from markets within Warri metropolis, Delta State

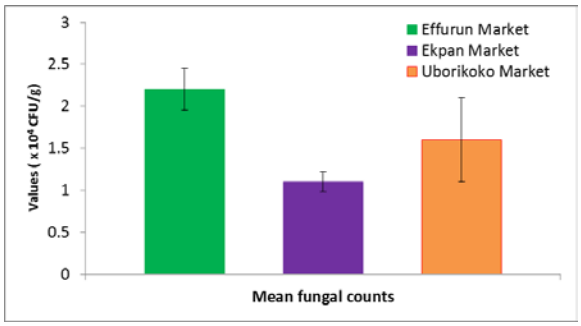

Figure 3. Mean fungal count for fresh chicken meat samples

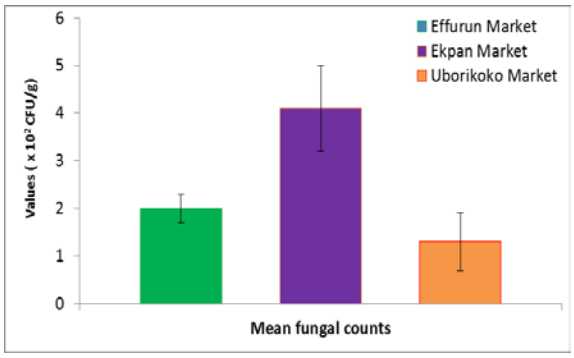

Figure 4. Mean fungal count for frozen chicken meat samples

Table 1. Characteristics and identity of fungal isolates from chicken sample

Isolate code	Description of fungal isolates	Fungal identity
1	The colony has black filaments at its centre which was surrounded by whitish and hairy edge. The reverse of the plate was yellowish.	*Aspergillus* sp.
2	The colony has blue-green centre surrounded by white hyphae. The reverse was greenish yellow	*Penicillium* sp.
3	The colony was whitish, loose, fluffy, cotton like and filamentous mould with reverse being whitish or light cream	*Mucor* sp.
4	The colony was a white, loose filamentous mould with black spores. Hyphae spread to cover the whole plate. The reverse was whitish. The fungus resembles cotton wool in its appearance.	*Rhizopus* sp.
5	White thick mycelium and white colour at bottom of plate	*Fusarium* sp.
6	Flat white cottony growth on plate, erect conidiophores, septate hyphae with cylindrical conidia	*Alternaria* sp.
7	Medium-size hyphae, white with loose filaments, reverse side on plate is white when young.	*Cladosporium* sp.
8	White cream smooth colonies, spherical, budding	*Candida* sp.

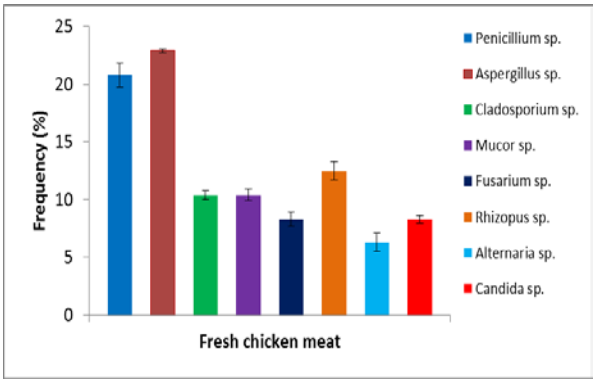

Figure 5. Frequency of fungal isolates from fresh chicken meat samples

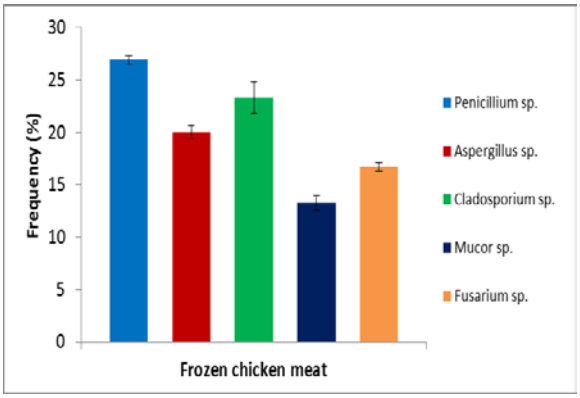

Figure 6. Frequency of fungal isolates from frozen chicken meat samples

4. Conclusion

Commercial fresh and frozen chicken meat samples in major markets within Warri metropolis were found to be contaminated by diverse levels of opportunistic, pathogenic, and saprophytic moulds and yeasts. The fresh chicken meat samples were more contaminated than the frozen samples, though not significantly different (*P>0.05)*. Considering the occurrence of relatively high proportions of *Penicillium, Aspergillus*, *Cladosporium*, *Fusarium* species in both frozen and fresh chicken samples, and their potential health hazards, regular environmental sanitation, good handling practices, proper storage temperatures and adequate thermal treatment of fresh and frozen chicken meat before consumption are recommended.

Acknowledgements

Special appreciation to the Director and Staff of Light Path Medical Laboratory, Warri, Delta State for provision of equipment/reagents and technical support during the study.

References

Ajiboye, EA, Sani A, Adedayo RM, Kolawole MO and Oladosu OT. 2011. Physicochemical properties and microorganisms isolated from dried meat obtained in Oja-Oba market in Ilorin, Nigeria. *Adv Appl Sci Res*., **2** (4): 391-400.

Alexopoulos CJ and Mims CW. 1979. **Introductory Mycology**. 3rd Edition. John Wiley and sons, Newyork. pp 269.

Altunatmaz SS and Issa G and Aydin A. 2012. Detection of airborne psychrotrophic bacteria and fungi in food storage refrigerators. *Braz J Microbiol.,* **43** (4): 1436-1443.

Anonymous. 2017. Warri population. Accessed at https://www.population.city/nigeria/warri/ 17th June, 2017.

APHA. 2001. **Compendium of Methods for the Microbiological Examination of Foods**, 4th Edition. American Public Health Association, Washington DC.

Arora D, Kumar S, Jindal N, Narang G, Kapoor PK and Mahajan NK. 2015. Prevalence and epidemiology of *Salmonella enterica* serovar *Gallinarum* from poultry in some parts of Haryana, India. *Vet World,* **8** (11):1300-1304.

Ashiq S. 2015. Natural occurrence of mycotoxin in food and feed: Pakistan perspective. *Compreh. Rev Food Sci Food Safety*. **14**(2): 159-175

Atanda O, Makun HA, Ogara IM, Edema M, Idahor KO Eshiett ME and Oluwabamiwo BF. 2013. Fungal and mycotoxin contamination of Nigerian foods and feeds. In: Mukun HA, editor. **Mycotoxin and Food Safety in Developing Countries**. Croatia. *In Tech.*, pp 3-38.

Bhaisare DB, Thyagarajan D, Churchil RR and Punniamurthy N. 2014. Bacterial pathogens in chicken meat: review. *Int J Life Sci Res*., **2**(3):1-7.

CDC. 2013. Incidence and trends of infection with pathogens transmitted commonly through food foodborne diseases active surveillance network, 10 U.S. sites, 1996–2012. *Weekly Rep*., **62** (15): 283–287.

Chuku A, Etim LB, Obande GA, Asikong BE and Sani BE. 2016. Bacteriological quality of fresh raw beef and chevon retailed in Lafia Metropolis, Nigeria. *J Microbiol Res.,* **6**:29-34.

De Boer E, Jansen JT, and Van der Zee H. 1991. Potentially pathogenic microorganisms in chicken products from retail stores. AW de Vries and RWAW. Mulder (Eds.). Proceedings of the Symposia on the quality of Poultry Products, III. Safety and Marketing Aspects, Doorwerth, Netherlands. pp 135-144.

De Hoog GS, Guarre J and Gene JF. 2000. **Atlas of Clinical Fungal**, 2nd Edition, The Netherland Publishers, pp 450-453.

EFSA. 2007. European Food Safety Authority. EU-wide survey on *Salmonella* levels in broilers. Available at http://www.efsa.europa.eu/en/pressroom/pressrelease/przoon Salmonellabroilers.html. Accessed on 15-12-2015.

EFSA/ECDPC. 2016. The European Union summary report on trends and sources of zoonoses, zoonotic agents and food-borne outbreaks in 2015. *EFSA J.,* **14** (12): 4634; doi: 10.2903/j.efsa.2016.4634.

Ehigiator FAR, Akise OG and Eyong MM. 2014. Bacteria and fungi load of raw processed shrimp from different meat shops in Benin metropolis. *Nig J Agric Food Environ.,* **10** (3):1-7.

Fawole MO and Oso BA. 1988. **Laboratory Manual of Microbiology.** Spectrum books limited. pp 127.

Greco MV, Franchi ML, Golba, SLR, Pardo AG and Pose GN. 2014. Mycotoxins and mycotoxigenic fungi in poultry feed for food-producing animals. *The Sci World J.,* **2014**:1-9.

Haleem AM, Al-bakri SA and Al-Hiyaly SAK. 2013. Determination of microbial content in poultry meat in local Iraqi markets. *J Microbiol Res.,* **3**(6): 205-207.

Igborgbor JC and Ogu GI. 2015. Microbial assessment of air in the vicinity of some dumpsites in Delta State. *J Eng.*, **5**(1): 2278-8719.

Ismaiel AA and Papenbrock J. 2015. Mycotoxins: Producing Fungi and Mechanisms of Phytotoxicity. *Agric.,* **5**:492-537.

Javadi A and Safarmashaei S. 2011. Microbial profile of marketed broiler meat. *Middle-East J Sci Res.,* **9**(5): 652-656.

Jay JM. 1998. **Food Spoilage in Modern Food Microbiology**, 4th Edition, Chapman and Hall Inc. New York, pp 195.

Jerry O, Emmanuel U, Chika E, Eucharia O, Agabus N, Ikechukwu M, Emmanuel N, Nnabuife A and Lilian O. 2015. Microbial contamination of ready-to-eat fried chicken meat sold in two selected motor park points in Abakaliki, Ebonyi State, Nigeria. *Int J Pure Appl Biosci.,* **3** (4): 271-275.

Lange L. 2014. The importance of fungi and mycology for addressing major global challenges. *IMA Fungus*, **5**(2): 463–471.

Omorodion NJPN and Odu NN. 2014. Microbiological quality of meats sold in Port Harcourt metropolis, Nigeria. *Nat Sci.,***12** (2): 58-62.

Oranusi S, Obioha TU and Adekeye BT. 2014. Investigation on the microbial profile of frozen foods: fish and meat. *Int J Adv Res Biol Sci.,* **1**(2): 71-78.

Roberts D. 1990. Foodborne illnesses. Source of infection: Food. *The Lancet*, **336**: 859-861.

Tasic S and Tasic NM. 2007. *Cladosporium* spp. -cause of opportunistic mycoses. *ACTA FAC MED NAISS*, **24 (1):** 15-19.

Salawu MB, Ibrahim AG, Lamidi LO and Sodeeq AE. 2014. Consumption and consumer preference for poultry meat typesin Ibadan metropolis. *J Econ Sust. Dev.,* **5** (28): 20-25.

Stagnitta PV, Micalizzi B and Stefanini de Guzmán AM. 2006. Prevalence of some bacteria yeasts and molds in meat foods in San Luis, Argentina. *Cent Eur J Publ Health*, **14** (3): 141–144.

Sule EI, Orukotan A, AdoA and Adewumi AAJ. 2015. Total aflatoxin level and fungi contamination of maize and maize products. *Afr J Food Sci Technol.,* **6**(8): 229-233.

Udochukwu U, Inetianbor J, Akaba SO, Omorotionmwan FO. 2016. Comparative assessment of the microbiological quality of smoked and fresh fish sold in Benin City and its public health impact on consumers. *Am J Microbiol. Res.,* **4** (1): 37-40.

Vural A, Erkan ME, Guran HS, Durmusoglu H. 2013. A study about microbiological quality and species identification of frozen turkey meat. *Int J Nutr. Food Sci.,* **2** (6): 337-341.

Wigmann EF, Saccomori F, Bernardi AO, Frisvad JC and Copetti MV. 2015. Toxigenic penicillia spoiling frozen chicken nuggets. *Food Res Int*., **67**: 219–222.

Zain ME. 2011. Impact of mycotoxins on humans and animals. *J Saudi Chem Soc.,* **15**:129–144.

Zakki SA, Qureshi R, Hussain A, Ghias W, Sharif M and Ansari F. 2017. Microbial quality evaluation and prevalence of bacteria and fungus in different varieties of chicken meat in Lahore. *J Pharm Pharm Sci*., **5**(1):30-37.

Żukiewicz-Sobczak W, Cholewa G, Sobczak P, Zagórski J and Wojtyła-Buciora P. 2015. Health risks associated with exposure to fungi. *Agric Sci Procedia*., **7**: 313-317.

JJBS

Jordan Journal of Biological Sciences

Volume 10, Number 4,December 2017
ISSN 1995-6673
Pages 309 - 316

Homology Modeling and *In silico* Docking Studies of DszB Enzyme Protein, Hydroxyphenyl Benzene Sulfinate Desulfinase of *Streptomyces* sp. VUR PPR 101

Praveen Reddy P and Uma Maheswara Rao Vanga*

Department of Botany and Microbiology, Acharya Nagarjuna University, Nagarjuna Nagar-522 510, Guntur District, Andhra Pradesh, India

Received: June 16, 2017; Revised: September 3, 2017; Accepted: September 5, 2017

Abstract

Biodesulfurization of organosulfur compounds in fossil fuels by employing microbes is advantageous over traditional hydrodesulfurization. Dibenzothiophene (DBT) is the most common model organosulfur compound used in biodesulfurization studies by means of microbes. The microbial desulfurization of DBT via the 4S pathway involves four enzymatic steps. The present study investigated the activity of wild type DszB (Hydroxyphenyl benzene sulfinate desulfinase), the last enzyme in the 4S pathway, and several mutant forms. The 3-D protein model of DszB was developed and mutant proteins of DszB viz., Q65H, Y63F and Y63A were constructed. Docking studies were done between wild DszB and the substrate, hydroxy phenyl benzene sulfinate (HPBS) as well as between mutant DszB proteins and HPBS. Based on the libdock scores obtained from docked complexes, mutant protein Y63A was found to have highest affinity towards the substrate, HPBS likely suggesting highest activity.

Keywords: Biodesulfurization, Dibenzothiophene (DBT), Hydroxyphenyl benzene sulfinate (HPBS), 4S pathway, DszB, Docking.

1. Introduction

Fossil fuels, containing organosulfur compounds, get oxidized during their utilization for various purposes and release various hazardous gases including sulfur dioxide leading to air pollution (Rhee *et al.*, 1998). Sulfur dioxide, during its persistence period of one to seven days, transforms into sulfates under the influence of sunlight and photochemical oxidants and hence, serves as reservoir of toxic sulfates and sulfuric acid in the air (Rall, 1974). Chronic exposure of humans to sulfur dioxide results in respiratory infections, pulmonary impairment, asthma, Emphysema, etc. (Badenhorst, 2007; Mehta, 2010). Sulfur dioxide also causes deleterious effects in plants by decreasing photosynthetic efficiency as well as promoting enhanced opening of stomata, which results in excessive loss of water in plants, and ultimately leads to the reduction of quality and quantity of plant yield (Varshney *et al.*, 1979). Acid rain with sulfurous acid, formed from sulfur dioxide in the air, as one of the major components is hazardous to aquatic life, vegetation and human health. Human beings may suffer from brain damage, kidney problems and Alzheimer's disease, when they consume plant or animal products that absorbed soil toxins that leached due to acid rain (Wondyfraw, 2014).

The hydrodesulfurization process normally employed by oil refineries to eliminate the organosulfur compounds from oil is not so effective particularly in the removal of polycyclic aromatic organosulfur compounds (Rhee *et al.*, 1998). Biodesulfurization by means of microorganisms that selectively attack organosulfur compounds and remove sulfur atoms appears to be a most viable and genuine method over the traditional hydrodesulfurization (Calzada *et al.*, 2009). Organosulfur compounds mainly dibenzothiophene (DBT) and its derivatives are unaffected by traditional hydrodesulfurization of crude oils. Therefore, DBT is treated as a model compound for desulfurization studies (Abo-State *et al.*, 2014). In nature, some microorganisms degrade organosulfur compounds by breaking the ring skeleton of organosulfur compounds leading to a reduction of the calorific value of the fuel. Hence, such microbes are not considered commercially viable. In the contrary, some microorganisms metabolize organosulfur compounds by selectively removing the sulfur atom without breaking the ring structure of the compounds. Such microorganisms are equipped with a specialized enzymatic pathway called the 4S pathway, which specifically removes the sulfur atom from DBT, the

* Corresponding author. e-mail: umrvanga@yahoo.co.in.

model organosulfur compound (Campos-Martin *et al*., 2010). Hence, microbes exhibiting DBT desulfurization via the 4S pathway which includes four enzymatic reactions, are obviously commercially important. The prominent DBT desulfurizing bacteria exhibiting the 4S pathway include *Rhodococcus rhodochrous* IGTS8, *Rhodococcus erythropolis* D-1, *Corynebacterium* sp. strain SY1, etc. (Rhee *et al*., 1998). The first enzyme, DBT monooxygenase, catalyzes a two-step oxidation reaction which results in the formation of $DBTO_2$ (Dibenzothiophene oxide) from DBT. The second enzyme, $DBTO_2$ monooxygenase, catalyzes the conversion of $DBTO_2$ to HPBS (Hydroxyphenyl benzene sulfinate). The third enzyme, HPBS desulfinase, catalyzes the hydrolysis of HPBS to form the end products of the pathway, 2-HBP (2-Hydroxy biphenyl) and sulfite (Folsom *et al*., 1999). The 4S pathway enzymes are synthesized by *dsz* operon genes, *dszA*, *dszB* and *dszC*. The *dszA* and *dszC* genes encode flavin dependent $DBTO_2$ monooxygenase (DszA) and DBT monooxygenase (DszC), respectively. The *dszB* gene synthesizes HPBS desulfinase (DszB) (Duarte *et al*., 2001). Using PCR, *dsz* operon genes can be amplified and sequenced (Shavandi *et al*., 2010).

The DBT desulfurization activity is directly proportional to the overall activity of the 4S pathway enzymes. To enhance the DBT desulfurization activity, the activity of the 4S pathway enzymes must be increased. The activity of the 4S pathway enzymatic proteins can be enhanced using computational programs in protein engineering. Protein engineering emphasizes on developing modified proteins by replacing amino acids at specific sites and substrate interaction at the catalytic site (Prokop *et al*., 2000). The current study presents the results of docking studies between wild type DszB protein, translated from the nucleotide sequence of *dszB* gene of *Streptomyces* sp. VUR PPR 101, and the substrate, HPBS, as well as between mutant DszB proteins, constructed via protein engineering by replacing single amino acids at selected sites and HPBS. These results demonstrate the reactivity of wild type and mutant DszB enzyme proteins towards HPBS.

2. Material and Methods

2.1. Translation of dszB Gene Sequence into Protein Sequence

The sequence of *dszB* gene of *Streptomyces* sp. VUR PPR 101 was submitted to NCBI-ORF Finder in FASTA format to generate different reading frames and the frame with highest length was selected for the study (Hung and Lin, 2013).

2.2. Homology Modeling of DszB Protein

The sequence of DszB protein in FASTA format was submitted to SWISS-MODELWORKSPACE automated mode to develop a protein model by homology modeling (Bordoli *et al*., 2008). DszB protein and its sequence were designated as target protein and query sequence, respectively.

2.3. DszB Protein Validation

The modeled DszB protein quality was validated by Ramachandran plot using Rampage (Read *et al*., 2011) and in SPDBV (Deep View – Swiss – Pdb Viewer) version 4.10 based on the RMSD value obtained by superimposing the DszB protein model on its template (Savarino, 2007).

2.4. Energy Minimization and Refinement of Modeled Protein DszB

The modeled DszB protein valency and chemistry were corrected in Discovery Studio (DS) (Accerlys 2.1). To obtain a protein with least energy, energy minimization and refinement were performed by employing CHARMm force field (Nousheen *et al*., 2014; Jin *et al*., 2015).

2.5. Construction and Energy Minimization of DszB Mutant Proteins

Mutant DszB proteins of *Streptomyces* sp. VUR PPR 101 were constructed using "Build Mutant" protocol (Nousheen *et al*., 2014; Raghunathan *et al*., 2012). The substitution of single residues at 63 and 65 positions were made in the modeled DszB protein to generate mutant DszB proteins following the model of Ohshiro *et al.* (2007). Table 1 shows the positions at which amino acid residues in the DszB protein were replaced with different amino acids. Energy of mutant proteins was minimized by applying CHARMm force fields in DS (Hanyog *et al*., 2015).

Table 1. Positions on DszB protein at which amino acids were replaced to generate mutant DszB proteins

ID.	Position of amino acid in DszB protein	Original amino acid	New amino acid
1.	63	Tyrosine	Phenylalanine
2.	63	Tyrosine	Alanine
3.	65	Glutamine	Histidine

2.6. Generation of Substrate Structures

Chemical structures were drawn in the front end of the chemsketch software (ACDLABS 12.0 version software). The substrate structure, i.e., HPBS, which was used for binding at active sites of wild type and mutant DszB proteins, was drawn in Chemsketch and saved in mol2 format to obtain a three-dimensional structure in DS (Archana *et al*., 2014; Park *et al*., 2009).

2.7. Prediction of Active Site

ERASER algorithm of DS 2.1 (Shanthipriya and Victor, 2013; Naika *et al*., 2015) was used to identify the active site pocket of modeled DszB wild type and mutant proteins. In the pocket site, substrate interacting amino acids were determined.

2.8. Docking Studies

The optimized substrate compound HPBS was docked at the catalytic sites of wild type and DszB mutant enzyme proteins using the Libdock algorithm in DS 2.1 utilizing default Libdock parameters. The ligand (substrate) was allowed to be flexible to determine the correct conformation and configuration having minimum energy structures (de Maglhaes *et al*., 2004; Bai *et al*., 2014; Abdel-Hamid and McCluskey, 2014). The parameters used for docking studies are,100 hotspots and docking tolerance of 0.25. User specified docking preferences were employed and the FAST algorithm was used as the endorsement method.

3. Results and Discussion

3.1. Translation of dszB Gene Sequence to Amino Acid Sequence

Submission of *dszB* gene sequence of *Streptomyces* sp. VUR PPR 101 to NCBI-ORF Finder in FASTA format (Figure 1A) resulted in generation of six different reading frames (Figure 1B). The frame showing highest length was selected leading to a protein with a sequence of 259 amino acids. This protein with a linear sequence of amino acids was the DszB protein (primary structure).

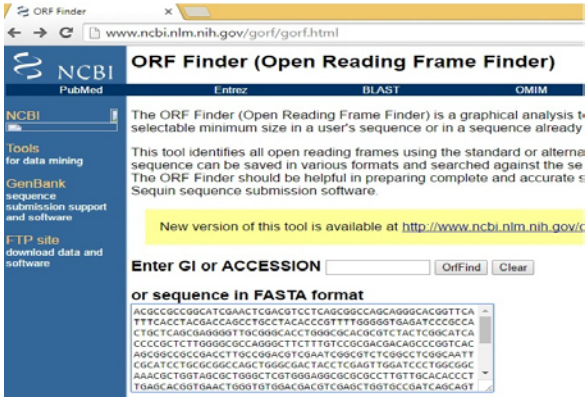

(A)

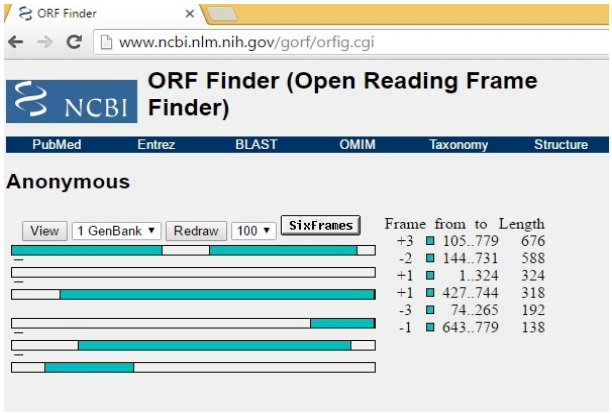

(B)

Figure 1. Translation of *dszB* gene (A) Nucleotide sequence of *dszB* gene of *Streptomyces* sp. VUR PPR 101 in FASTA format submitted to NCBI Open Reading Frame (ORF) finder; (B) Six reading frames generated in NCBI-ORF

The 259 amino acid sequence of the obtained DszB protein was:
AAGIELDVLSGQQGTVHFTYDQPAYTRFGGEIPPLLS EGLRAPGRTRLLGITPLLGRQGFFVRDDSPVTAAAD LAGRRIGVSASAIRILRGQLGDYLELDPWRQTLVAL GSWEARALLHTLEHGELGVDDVELVPISSPGVDVPA EQLEESATVKGADLFPDVARGQAAVLASGDVDALY SWLPWAGELQATGARPVVDLGLDERNAYASVWTV SSGLVRQRPGLVQRLVDAAVDAGLWARDHSDAVT SLHAANLGVST.

3.2. Sequence Alignment and Homology Modeling of DszB Protein

In SWISS MODEL WORKSPACE automated mode, fifty templates of query sequence (DszB protein sequence) were generated. The template, 2de2.1.A (Figure 2 C) demonstrated highest sequence identity to query sequence (Figure 2 A) and was used to develop the model of DszB protein (Figure 2 B). Tahri *et al*. (2015) also modeled the Thaumetopoein protein using SWISS MODEL WORKSPACE.

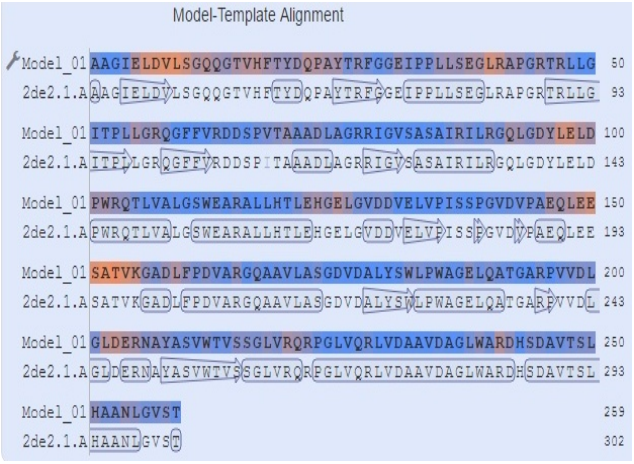

(A)

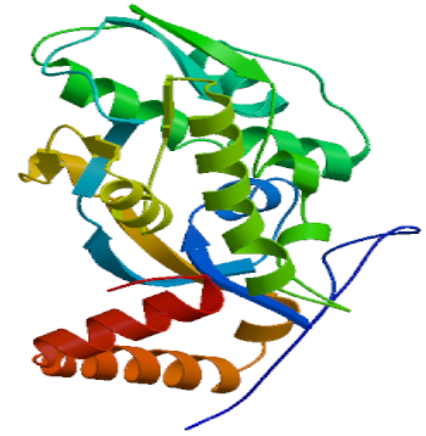

(B)

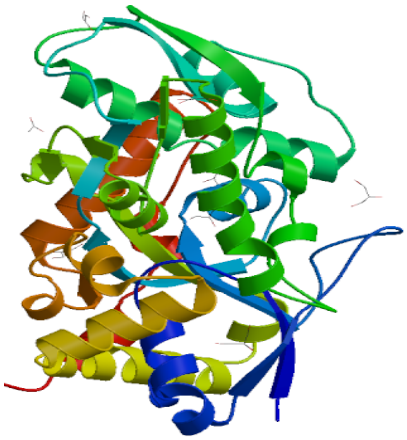

(C)

Figure 2. Homology modeling of DszB protein in SWISS MODEL WORKSPACE automated mode (A) Sequence alignment of DszB protein of *Streptomyces* sp. VUR PPR 101 with template, 2de2.1.A (B) Modeled structure of DszB of *Streptomyces* sp. VUR PPR 101; (C) Structure of template, 2de2.1.A.

3.3. Model Validation of DszB by Rampage

Table 2 depicts the Ramachandran plot values of modeled DszB protein and its template 2de2.1.A. In the Ramachandran plot generated for DszB protein of *Streptomyces* sp. VUR PPR 101, 94.9% residues were found in favoured, 4.7% residues in allowed, and 0.4% in outlier regions (Figure 3A). The Ramachandran plot of template 2de2.1.A showed 97.7% residues in favored, 2.0% residues in allowed, and 0.3% in outlier regions (Figure 3 B). The data of Ramachandran plot clearly indicate the reliability of the DszB protein model. Similarly, Bilal *et al.* (2009) validated the P2RY5 wild and mutant gene proteins by Rampage.

Table 2. Ramachandran plot values showing number of residues in favoured, allowed and outlier regions through RAMPAGE evaluation server

Structure	Number of residues in favoured region (%)	Number of residues in allowed region (%)	Number of residues in outlier region (%)
Modeled DszB	94.9%	4.7%	0.4%
Template (2de2.1.A)	97.7%	2.0%	0.3%

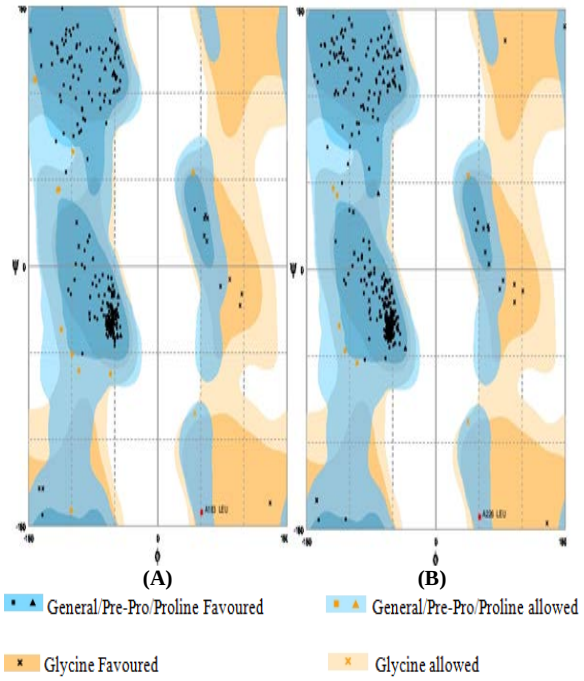

Figure 3. Validation of DszB protein model:(A) Ramachandran Plot of DszB protein of *Streptomyces* sp. VUR PPR 101; (B) Ramachandran Plot of template 2de2.1.A

3.4. Model Validation of DszB of Streptomyces sp. VUR PPR 101 in SPDBV

After superimposing main-chain atoms of modeled DszB protein on template, 2de2.1.A (Figure 4) in Swiss PDB Viewer (SPDBV), the Root-Mean-Square-Deviation (RMSD) was determined at 0.07 A^{o} which indicates close homology and ensures reliability of the model. Devi (2015) also superimposed Thyroid peroxidase (TPO) enzyme protein model on its template, 3BXI in SPDBV to validate the TPO model.

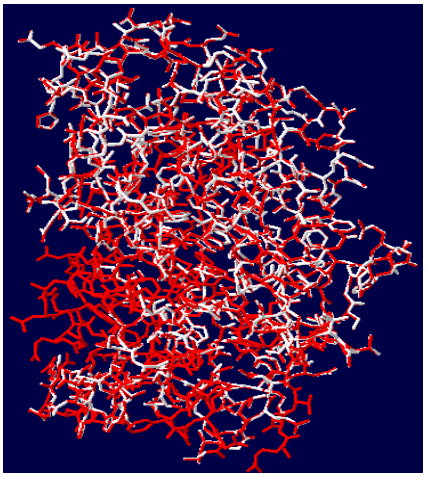

Figure 4. Superimposition of DszB protein of *Streptomyces* sp. VUR PPR 101 on template 2de2.1.A in Swiss PDB Viewer. Red color: Template, White color: DszB protein

3.5. Mutant Protein Construction

Mutant proteins, developed for DszB in DS, were Q65H with replacement of Glutamine by Histidine at 65 position (Figure 5A), Y63A with replacement of Tyrosine by Alanine at 63 position (Figure 5B), and Y63F in which Tyrosine was replaced with Phenylalanine at 63 position (Figure 5C). Ohshiro *et al.* (2007) in their *in vitro* experiment made replacements of same amino acids in same positions in DszB protein via site directed mutagenesis during their work on DszB protein of *Rhodococcus erythropolis* KA 2-5-1 to construct mutant DszB proteins to determine their catalytic efficiency over wild DszB protein and reported an increased catalytic activity in all the mutant proteins over wild DszB protein.

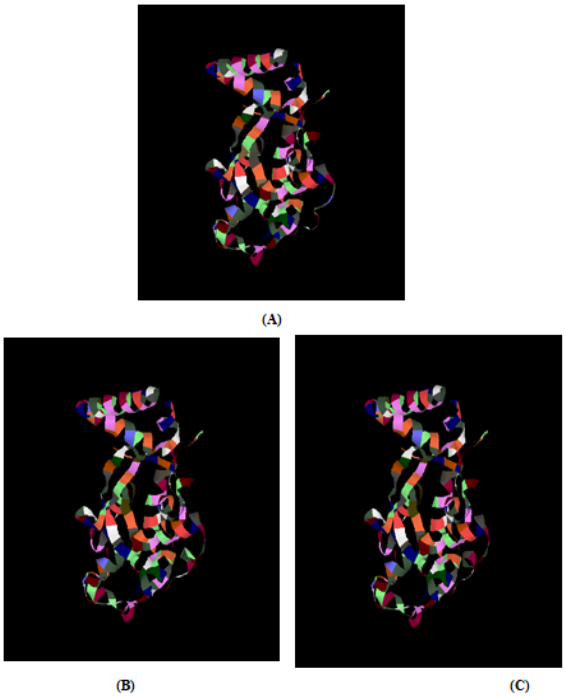

Figure 5. Structures of DszB mutant proteins of *Streptomyces* sp. VUR PPR 101. (A) Q65H mutant (B) Y63A mutant (C) Y63F mutant

3.6. Docking Studies

Molecular docking studies of wild type and mutant DszB proteins were performed with HPBS (mol format) in DS v2.1 using the Libdock algorithm. Binding modes of HPBS in the active sites of modeled wild type and mutant proteins were identified by this algorithm. Libdock makes use of protein site features, known as hotspots, which are of two types: polar and non-polar. The ligand (substrate) poses were fixed into the polar and non-polar receptor interaction sites (Kalani *et al.*, 2013; Alam and Khan, 2014). High Libdock scores were used to measure the ligand (substrate)-binding energies of top ranked conformations. In addition, other input factors, like Van der waal's forces and electrostatic interactions, were also considered for evaluating the docking efficacy of HPBS with modeled wild type and mutant DszB mutant proteins. Docking of HPBS into the active sites of the wild type and mutant models of DszB resulted in the generation of 10 conformations, however, only top ranked docked complex scores were considered for measuring binding affinity analysis (Table 3). Ligand (substrate) – receptor interaction plots for docked complexes were created in DS to determine the organization of key intermolecular interactions that aid in binding of HPBS to receptor sites of wild and mutant DszB proteins. The interaction of HPBS with wild DszB is depicted in Figure (6). The interaction of HPBS with mutant DszB proteins is shown in Figures 7A to 7C.

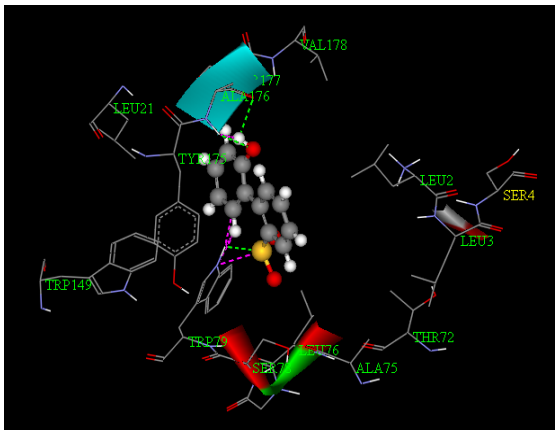

Figure 6. Interaction of HPBS at the active site of wild DszB protein of *Streptomyces* sp. VUR PPR 101

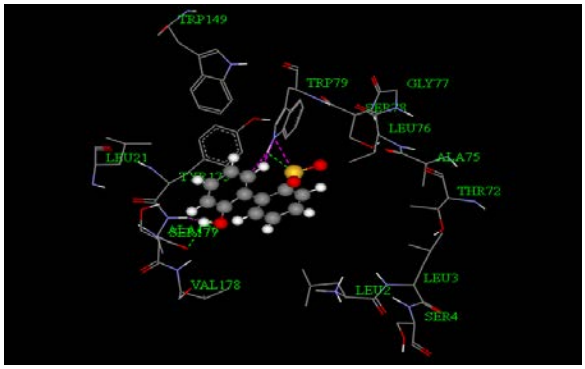

(A)

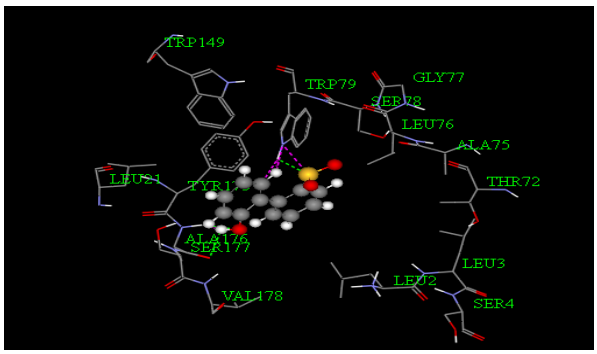

(B)

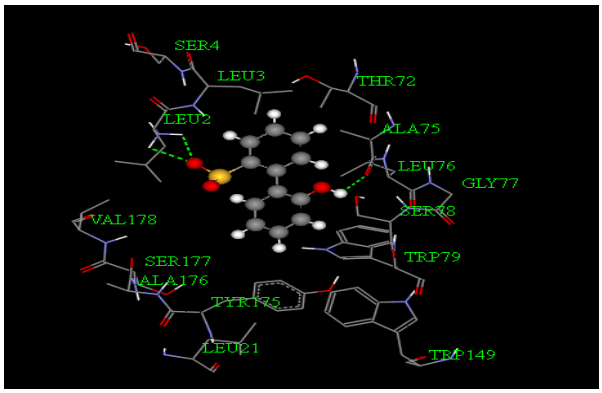

(C)

Figure 7. Interaction of HPBS at the active site of mutant DszB proteins. (A) Q65H mutant (B) Y63F mutant (C) Y63A mutant

Table 3. Docking studies between HPBS and DszB wild and mutant proteins of *Streptomyces* sp. VUR PPR 101

Enzyme protein And substrate	Libdock score (Binding energy)	Electrostatic Energy	Vanderwaal Energy	Number of Hydrogen bonds	Interacting aminoacids	Interacting atoms
Wild DszB + HPBS	60.757	10.832	5.115	3	Trp79 Ala176 Leu21 Tyr175 Val178 Trp149 Ser78 Leu2 Leu3 Ser4	A:TRP79:HE1 - Hydroxyphenylbenzosulfinate:S13 A:ALA176:HN - Hydroxyphenylbenzosulfinate:O16 Hydroxyphenylbenzosulfinate:H25 - A:ALA176:O Hydroxyphenylbenzosulfinate:C10 - A:TRP79:HE1 Hydroxyphenylbenzosulfinate:S13 - A:TRP79:NE1 Hydroxyphenylbenzosulfinate:H25 - A:ALA176:HN
Q65H mutant + HPBS	59.185	10.832	5.115	3	Trp79 Ala176 Leu21 Tyr175 Val178 Trp149 Ser78 Leu2 Leu3 Ser4	A:TRP79:HE1 - Hydroxyphenylbenzosulfinate:S13 A:ALA176:HN - Hydroxyphenylbenzosulfinate:O16 Hydroxyphenylbenzosulfinate:H25 - A:ALA176:O A:ALA176:HN - Hydroxyphenylbenzosulfinate:H25 A:TRP79:NE1 - Hydroxyphenylbenzosulfinate:S13
Y63F mutant + HPBS	56.605	10.832	5.115	3	Trp79 Ala176 Leu21 Tyr175 Val178 Trp149 Ser78 Leu2 Leu3 Ser4	A:TRP79:HE1 - Hydroxyphenylbenzosulfinate:S13 A:ALA176:HN - Hydroxyphenylbenzosulfinate:O16 Hydroxyphenylbenzosulfinate:H25 - A:ALA176:O A:ALA176:HN - Hydroxyphenylbenzosulfinate:H25 Hydroxyphenylbenzosulfinate:S13 - A:TRP79:NE1
Y63A mutant+ HPBS	61.497	10.832	5.115	3	Trp79 Ala176 Leu21 Tyr175 Val178 Trp149 Ser78 Leu2 Leu3 Ser4	A:LEU2:HT1 - Hydroxyphenylbenzosulfinate:O15 A:LEU2:HT2 - Hydroxyphenylbenzosulfinate:O15 Hydroxyphenylbenzosulfinate:H25 - A:ALA176:O A:TRP79:HE1 - Hydroxyphenylbenzosulfinate:S13 Hydroxyphenylbenzosulfinate:H19 - A:ALA176:HB2 Hydroxyphenylbenzosulfinate:H23 - A:SER78:HB1

HPBS: hydroxyphenyl benzene sulfinate

3.7. Interaction between DszB (Wild Type Protein) and Hydroxyphenyl Benzene Sulfinate (HPBS)

HPBS interacted with receptor site of wild type DszB (Figure 6) involving three hydrogen bonds. The binding energy (Libdock score) calculated during interaction between HPBS and receptor was 60.757 K.cal/mol. The amino acids interacting with HPBS in the active site were Trp79, Ala176, Leu21, Tyr175, Val178, Trp149, Ser78, Leu2, Leu3 and Ser4. The atoms of Trp79 (A:TRP79 : HE1 - Hydroxyphenylbenzosulfinate : S13), Ala176 (A : ALA176:HN – Hydroxyphenylbenzosulfinate : O16 ; Hydroxyphenylbenzosulfinate : H25 – A : ALA176 : O), Trp79 (Hydroxyphenyl benzosulfinate : C10-A : TRP79 : HE1 ; Hydroxyphenyl benzosulfinate : S13 - A : TRP79 : NE1) and Ala176 (Hydroxy biphenyl benzosulfinate : H25-A:ALA176:HN) were involved in bond formation. The remaining amino acids were involved in non-bonding interactions (Table 3).

3.8. Interaction between DszB Mutant Protein Q65H and HPBS

Three hydrogen bonds were observed between receptor site of mutant protein Q65H and HPBS, with a binding energy of 59.185 K.cal/mol (Figure 7A). The amino acids interacting with HPBS were Trp79, Ala176, Leu21, Tyr175, Val178, Trp149, Ser78, Leu2, Leu3 and Ser4. The atoms of Trp79 (A: TRP78: HE1 –

Hydroxyphenyl benzosulfinate: S13), Ala176 (A : ALA176 : HN – Hydroxyphenyl benzosulfinate : O16), and Trp79 (Hydroxyphenyl benzosulfinate : C10 – A : TRP79 : HE1) were involved in bond formation. The remaining amino acids exhibited non-bonding interactions (Table 3).

3.9. Interaction between DszB Mutant Protein Y63F and HPBS

Three hydrogen bonds were observed during the interaction between HPBS and DszB mutant Y63F (Figure 7B) with a calculated binding energy of 56.605 K.cal/mol. The amino acids interacting with HPBS were Trp79, Ala176, Leu21, Tyr175, Val178, Trp149, Ser78, Leu2, Leu3, and Ser4. The atoms of Trp79 (A : TRP78 : HE1 – Hydroxyphenyl benzosulfinate : S13), Ala176 (A : ALA176 : HN – Hydroxyphenyl benzosulfinate : O16; Hydroxyphenyl benzosulfonate : H25 – A : ALA176 : O; A : ALA176 : HN – Hydroxyphenyl benzosulfinate : H25), and Trp79 (Hydroxyphenyl benzosulfinate : S13 – A:TRP79 : NE1) were involved in bond formation. The remaining amino acids disclosed non-bonding interactions (Table 3).

3.10. Interaction between DszB Mutant Protein Y63A and HPBS

Three hydrogen bonds were formed during the interaction between HPBS and receptor site of mutant DszB Y63A (Figure 7C). The binding energy calculated during the interaction between receptor site and HPBS was 61.497 K.cal/mol. The amino acids interacting with HPBS were Trp79, Ala176, Leu21, Tyr175, Val178, Trp149, Ser78, Leu2, Leu3 and Ser4. The atoms Leu2 (A:LEU2:HT1-Hydroxyphenyl benzosulfonate:O15), Ala176 (Hydroxyphenyl benzosulfinate: H25-A:ALA176:O), Trp79 (A:TRP78:HE1 – Hydroxyphenyl benzosulfinate : S13), Ala176 (Hydroxybiphenyl benzosulfonate:H19-A:ALA176:HB2), and Ser78 (Hydroxybiphenyl benzosulfinate:H23 – A: SER78:HB1) were involved in bond formation. The remaining amino acids showed non-bonding interactions (Table 3).

Libdock score (binding energy) generated during the formation of docking complex was used to measure the affinity and binding strength between the substrate and protein. All docked poses of the complexes were ranked on the basis of Libdock Score (Zhou *et al.*, 2016). Libdock score is a measure of strength of binding affinity between ligand substrate and receptor protein (Rani *et al.*, 2014). That means the enzymatic protein that has maximum binding affinity towards HPBS exhibits highest Libdock score indicating highest activity (Chen *et al.*, 2015; Guo *et al.*, 2015). Highest Libdock score was observed for the docked complex which formed between Y63A mutant protein and HPBS, when compared to wild type DszB and other mutant DszB proteins docked complexes. The order of Libdock scores for the docked complexes was mutant Y63A > wild type DszB > mutant Q65H > mutant Y63F. Binding energy is the basic factor that influences the proximity, alignment effects, etc., during the enzyme-substrate interaction, which affects the catalytic activity of the enzyme (Dmitri *et al.*, 2015). Henceforth, docking studies reveal that mutant Y63A DszB protein of *Streptomyces* sp. VUR PPR 101 has increased affinity towards HPBS, therefore possessing higher DBT desulfurization activity.

4. Conclusion

DszB enzyme protein of *Streptomyces* sp. VUR PPR 101 was modeled in SWISS MODEL WORKSPACE and validated by Rampage and in SPDBV. Three mutant DszB proteins were constructed by replacing single amino acid residue at selected sites. The wild type and mutant DszB enzyme proteins were docked against the substrate HPBS. Highest Lipdock score (binding energy) was found during the interaction between Y63A mutant DszB protein and HPBS. Thus, Y63A mutant DszB protein may exhibit higher catalytic activity when compared to wild and other mutant DszB proteins. Based on the *in silico* and docking studies results of present study, similar mutations at the identified sites of *dszB* gene can be carried out using *in vivo* conditions through site-directed mutations which may pave the way for developing improved strain of *Streptomyces* sp. VUR PPR 101 with a modified *dszB* gene, that exhibit enhanced biodesulfurization activity. Such improved strains could gain ecological and commercial importance in Biodesulfurization of fuels.

References

Abdel-Hamid MK and Adam McCluskey A. 2014. In Silico docking, molecular dynamics and binding energy insights into bolinaquinone-clathrin terminal domain binding site. *Molecules*, **19**: 6609-6622.

Abo-State MA, EI-Gendy NS, AEI-Tentamy S, Mahdy HM and Nassar HN. 2014. Modification of basal salts medium for enhancing dibenzothiophene biodesulfurization by *Brevibacillus invocatus* C19 and *Rhodococcus erythropolis* IGTS8. *World Appl Sci J.*, **30 (2)**: 133-140.

Alam S and Khan F. 2014. QSAR and docking studies on xanthone derivatives for anticancer activity targeting DNA topoisomerase IIα. *Drug Design, Development and Therapy*, **8**: 183-195.

Archana CM, Harini K, Jerlin SJ and Geetha N. 2014. An In Silico Docking study of *Chromolaena odorata* derived compounds against antimalarial activity. *Inter J Pharmaceut Sci Business Manag.*, **2(9):** 42-58.

Badenhorst CJ. 2007. Occupational health and safety risks associated with sulfur dioxide. *J Southern Afr Inst Mining and Metallurgy*, **17**: 299-303.

Bai Q, Shao Y, Pan D, Zhang Y, Liu H and Yao X. 2014. Search for β2 adrenergic receptor ligands by virtual screening via grid computing and investigation of binding modes by docking and molecular dynamics simulations. *PLOS ONE*, **9(9)**: 1-10.

Bilal S, Iqbal H, Anjum F and Mir A. 2009. Prediction of 3D structure of P2RY5 gene and its mutants via comparative homology modeling. *J Computational Biol Bioinformatics Res.*, **1(1)**: 11-16.

Bordoli L, Kiefer F, Arnold K, Benkert P, Battey J and Schwede T. 2008. Protein structure homology modeling using SWISS-MODEL workspace. *Nature Protocols*, **4**: 1-13.

Calzada J, Zamarro MT, Alcon A, Santos VE and Diaz E. 2009. Analysis of dibenzothiophene desulfurizatin in a recombinant *Pseudomonas putida* strain. *Appl Environ Microbiol.*, **75 (3)**: 875-877.

Campos-Martin JM, Capel-Sanchez MC, Perez-Presas P and Fierro JLG. 2010. Oxidative processes of desulfurization of liquid fuels. *J Chem Technol Biotechnol.*, **85 (7)**: 879-890.

Chen J, Luo XJ, Chen Q, Pan J, Zhou J and Xu JH. 2015. Marked enhancement of *Acinetobacter* sp. organophosphorus hydrolase activity by a single residue substitution Ile211Ala. *Bioresources and Bioprocessing*, **2(39):** 1-8.

de Maglhaes CS, Barbosa HJC and Dardenne LE. 2004. A genetic algarithm for the ligand-protein docking problem. *Genetics and Mol Biol.*, **27(4)**: 605-610.

Devi D. 2015. In Silico studies on the disruption of the pituitarfy-thyroid axis by the dithiocarbamate fungicide mancozeb. *World J Pharmaceut Res.*, **4(3)**: 1569-1578.

Dmitri LMC, Rachelle JDA, Maynar OG, Lemuel AV and Junie BB. 2015. Piggyback drug development: (Molecular docking of Entacapone analogues as direct *M. tuberculosis* InhA inhibitors). *J Chem Pharmaceut Res.*, **7(5)**: 636-642.

Duarte GF, Rosado AS, Seldin L, de Araujo W and Elsa JDV. 2001. Analysis of Bacterial Community Structure in Sulfurous-Oil Containing Soils and Detection of Species Carrying Dibenzothiophen Desulfurization (dsz) Genes. *Appl Environ Microbiol.*, **67(3)**: 1052-1062.

Folsom BR, Schieche DR, Digrazia PM, Werner J and Palmer S. 1999. Microbial desulfurization of alkylated dibenzothiophenes from a hydrodesulfurized middle distillate by *Rhodcoccus erythropolis* 1-19. *Appl Environ Microbiol.*, **65(11)**: 4967-4972.

Guo S, Xu J, Pavlidis IV, Lan D, Bornscheuer UT, Liu J and Wang Y. 2015. Structure of product-bound SMG1 lipase: active site gating implications. *FEBS J.*, **282:** 4538-4547.

Hung CL and Lin CY. 2013. Open reading frame phylogenetic analysis on the cloud. *Inter J Genomics*, Article ID **614923**: 1-9.

Jin H, Zhou Z, Wang D, Guan S and Han W. 2015. Molecular dynamics simulations of acylpeptide hydrolase bound to chlopyrifosmethyl oxon and dichlorvos. *Inter J Mol Sci.*, **16**: 6217-6234.

Kalani K, Agarwal J, Alam S, Khan F, Pal A and Srivastava SK. 2013. In Silico and *in vivo* Anti-Malarial studies of 18 beta glycyrrhetinic acid from *Glycyrrhiza glabra. PLOS ONE*, **8(9)**: 1-11.

Mehta P. 2010. Science behind Acid Rain: Analysis of Its Impacts and Advantages on Life and Heritage Structures. *South Asian J Tourism and Heritage*, **3(2)**: 123-132.

Naika HR, Krishna V, Lingaraju K, Chandramohan V, Dammalli M, Navya PN and Suresh D. 2015. Molecular docking and dynamic studies of bioactive compounds from *Naravelia zeylanica*(L.) DC against glycogen synthase kinase 3β protein. *J Taibah University for Sci.*, **9**: 41-49.

Nousheen L, Akkiraju PC and Enaganti S. 2014. Molecular docking mutational studies on human surfactant protein-D. *World J Pharmaceut Res.*, **3(7)**: 1140-1148.

Ohshiro T, Ohkita R, Takikawa T, Manabe M, Lee WC, Tanokura M and Izumi Y. 2007. Improvement of 2-Hydroxybipheny-2-sulfinate desulfinase, an enzyme involved in the dibenzothiophene desulfurization pathway, by site-directed mutagenesis. *Biosci, Biotechnol, Biochem.*, **71(11)**: 2815-2821.

Park J, Rosania GR, Kerby KA, Nguyen M, Lyu N and Saitou K. 2009. Automated extraction of chemical structure information from digital raster images. *Chem Central J.*, **3(4)**: 1-16.

Prokop M, Dambosky J and Koca J. 2000. TRITON: in Silico construction of protein mutants and prediction of their activities. *Bioinformatics*, **16(9)**: 845-846.

Raghunathan G, Soundrarajan N, Sokalingam S, Yun H and Lee SG. 2012. Deletional protein engineering based on stable fold. *PLOS ONE*, **7(12)**: 1-14.

Rall DP. 1974. Review of health effects of sulfur oxides. *Environ Health Perspectives*, **8**: 97-121.

Rani N, Vijayakumar S, Palanisamy L, Velan T and Arunachalam A. 2014. Quercetin 3-O-rutinoside mediated inhibition of PBP2a: computational and experimental evidence of anti-MRSA activity. *Mol Biosyst.*, **10**: 3229-3237.

Read RJ, Adams PD, Arendall III WB, Brunger AT, Emsley P, Joosten RP, Kleywegt GJ, Krissinel EB, Lu tteke T, Otwinowski Z and Perrakis A. 2011. A New generation of crystallographic validation tools for the protein data bank. *Structure*, **19**: 1395-1412.

Rhee SK, Chang JH, Chang YK and Chang HN. 1998. Desulfurization of dibenzothiophene and diesel oils by a newly isolated *Gordona* strain, CYKS1. *Appl Environ Microbiol.*, **64(6)**: 2327-2331.

Savarino A. 2007. In Silico docking of HIV-1 integrase inhibitors reveals a novel drug type acting on an enzyme/DNA reaction intermediate. *Retrovirology*, **4(21)**: 1-15.

Shanthipriya S and Victor A. 2013. Active site prediction and targeting bipolar disorder through molecular docking techniques on protein kinase 3-β protein. *Inter J Sci Res.*, **2(6)**: 33-35.

Shavandi M, Sadeqhizadeh M, Khajeh K, Mohebali G and Zormorodipour A. 2010. Genomic structure and promoter analysis of the dsz operon for dibenzothiophene biodesulfurization from *Gordonia alkanivorans* RIPI90A. *Appl Microbiol Biotechnol.*, **87(4)**: 1455-1466.

Tahri D, Seba M and Benarous K. 2015. Structure homology modeling of thaumetopoein, an urticating protein from *Thaumetopoea pityocampa*, using SWISS-MODEL workspace. *Chem Informatics*, **1(2:13)**: 1-7.

Varshney CK, Garg JK, Lauenroth WK and Heitschmidt RK. 1979. Plant responses to sulfur dioxide pollution. *C R C Critical Reviews in Environ Cont.*, **9(1)**: 27-49.

Wondyfraw M. 2014. Mechanisms of effects of acid rain on environment. *J Earth Sci Climatic Change*, **5(6)**: 1-3.

Zhou X, Yu S, Su J and Sun L. 2016. Computational study on new natural compound inhibtors of pyruvate dehydrogenase kinases. *Inter J Mol Sci.*, **17(3)**: 1-13.

JJBS

Volume 10, Number 4,December 2017
ISSN 1995-6673
Pages 317 - 322

Jordan Journal of Biological Sciences

Bio-Insecticidal Potency of Five Plant Extracts against Cowpea Weevil, *Callosobruchus maculatus* (F.), on Stored Cowpea, *Vigna unguiculata* (L)

Ito E. Edwin[1,*] and Ighere E Jacob[2]

[1]*Department of Animal and Environmental Biology, Delta State University,* [1]*Tropical Disease Research Unit Delta State University, P.M.B 1 Abraka;* [1,2] *School of Applied Science and Technology, Department of Science Laboratory Technology, Delta State Polytechnic, Otefe-Oghara, Nigeria*

Received: March 15, 2017; Revised: August 3, 2017; Accepted: August 10, 2017

Abstract

It is estimated that the global post-harvest grain losses caused by insect damage and other bio-agents ranged between 10 to 40%. Small-scale farmers may lose up to 80% of their stock due to insect pest infestation after several months of storage. Control measures are necessary; they are proactive, cost effective and safe. The present study was conducted to evaluate the insecticidal effect of ethanol extracts from five locally available aromatic plants, namely *Allium sativum* L. (Garlic), *Cordia millenii* Baker (Manjack), *Monodora myristica* (Gaertn.) (Nutmeg), *Xylopia aethiopica* (Dunal) (Negropepper) and *Zingiber officinale* Roscoe (Ginger) against *Callosobruchus maculatus* (Cowpea weevil) infesting cowpea seeds (*Vigna unguiculata* L.). Bioassay was done by a direct contact application of the extracts using three concentrations (50, 75 and 100mg/ml) of each extract in 10g of previously disinfested cowpea seeds containing 10 adults of *C. maculatus* of 1-2 days old. The results revealed that all the plant species had lethal effects against the insect as compared with the untreated check. Considering the LC_{50} of the extracts 96 hours post-treatment as a main index *C. millenii* appeared superior (LC_{50} = 36.3mg), followed by *Z. officinale* (LC_{50} = 37.5mg), *X. aethiopica* (LC_{50} = 43.8mg), *M. myristica* (LC_{50} = 47.5mg) and *A. sativum* (LC_{50} = 55.0mg). All the tested plant species exhibited a toxic action against the cowpea weevils. These results have implications for cost effectiveness and safety that even the local farmers can use to protect stored cowpea seeds against the weevil.

Key words: Bio-insecticide, Cowpea weevil, Potency, Plant extract,Stored cowpea

1. Introduction

Cereals and grain legumes are the most commonly stored durable food commodities in the tropics (Odeyemi and Daramola, 2000). Cowpea grain (*Vigna unguiculata* L.) is a pulse crop produced and consumed largely by subsistence farmers in the semi-arid and sub-humid regions of Africa (DeBoer, 2003). It is an important cash and food crop for many poor farmers and also noted for its high nutritional value. It forms a major part of the diets of the people in West and East Africa, Latin America and the Carribean basin (DeBoer, 2003). It is a source of dietary protein in some parts of the world especially where there is a low availability and consumption of animal protein (Ofuya, 1991).

Insect pests are a major constraint on crop production, especially in developing countries. The cowpea weevil, *Callosobruchus maculatus*, F., (Coleoptera: Bruchidae) is a serious pest of stored grains in sub-sahara Africa (Al-Moajel and Al-Fuhaid, 2003). Postharvest losses of cowpea 3-4 months in storage caused by *C. maculatus* infestation have been reported as high as 50% in Northern Nigeria (Caswell, 1981) and 60% in Northern Ghana (Tanzubil, 1991). The loss of cowpea is a serious problem in Africa where as much as 20-50% of the grain is damaged by *C. maculatus* (FAO, 1985). The damage of this magnitude is incredibly high and demonstrates the destructive nature of the pest which can threaten food security at both household and national levels. This is a major agricultural problem for farmers in developing countries.

Weevil infestation causes weight loss, quality deterioration resulting in overall unacceptability in markets and impaired germinability of grains (Keita *et al.*, 2001). Infested grains are rendered unfit for consumption and sale. Consequently, farmers are compelled to sell their products early after harvest when prices are still low partly because of anticipated losses of the grain in storage.

Over the years, the destructive activities and menace of storage pests have been effectively suppressed with synthetic organochlorine and organophosphate compounds like carbon disulphide, phosphine, malathion, carbaryl, pirimiphos methyl and permethrin (Adedire *et al.*, 2011). The application of these chemicals as pest control agents is, however, fraught with problems, such as high persistence of the compounds, resurgence and genetic resistance of pests, negative effects on non -target

* Corresponding author. e-mail: ito.eddie@yahoo.com.

organisms, poor knowledge of application, direct toxicity to the users, non-availability of the chemicals and increasing costs of application (Berger, 1994; Sharma *et al*., 2006).

These deficiencies of synthetic insecticides have caused a shift of opinion away from their usage towards plants products in the control of pests with varying levels of effectiveness. The use of plants to protect agricultural products against insect pests is an age-long practice in many parts of the world (Dales, 1996). Botanicals are non-persistent and are known to have broad spectrum insecticidal properties. Plants with insecticidal properties offer a cheaper sustainable fumigation and thermal distribution methods. Besides, they are ecologically safer to non-target species (Ito and Ighere, 2017; Ellis and Baxandele, 1997), easily available and can be produced within farmer's vicinity, thereby providing a more sustainable approach to pest control (Berger, 1994). These qualities make plants ideal candidates for incorporation into an integrated pest management strategy.

It is common practice in traditional African communities to use locally available plants for medicinal purposes and in agriculture (Obeng-Ofori *et al*., 2006). Natural plants products possess insecticidal properties against a wide range of insect pests. For instance cowpea seeds treated with cashew nut liquid (Echendu, 1991), fruit powder from *Piper guineense* (Ivbijaro and Agbaje, 1986), certain spices (Igbai and Poswal, 1995), essential oil from sandbox (*Hura crepitans* L.) (Ajayi and Adedire, 2003) and leaves of Eucalyptus (Berger, 1994) were better protected than untreated seeds. Therefore, more investigations are necessary to explore the natural protectants available within the locality for a more sustainable approach in controlling storage pests.

The present study was undertaken to (1) evaluate the toxicity of five aromatic plant species against the cowpea weevil, *C. maculatus*, on stored cowpea, (2) ascertain whether the plants extracts could be used as protectants of cowpea against *C. maculatus*, (3) identify effective botanicals available within the farmers environment that can be recommended as alternative low cost technique for minimizing postharvest losses of cowpea from cowpea weevils, and (4) increase the data bank of natural products used in the control of stored insect pests.

2. Materials and Methods

2.1. Plants Materials and Extracts Preparation

Five plant species (bulb of garlic - *Allium sativum*; seeds of manjack - *Cordia millenii*; seeds of Africa nutmeg – *Monodora myristica*; fruit of negro pepper –*Xylopia aethiopica* and rhizome of ginger - *Zingiber officinale* identified by botanical taxonomist were selected for this insecticidal study. All the plants materials were obtained locally from markets in Abraka, Delta State, Nigeria. The materials were cut into pieces including the Africa nutmeg seeds which were hulled before slicing. The materials were sun-dried for seven days (Sowunmi, 1983) and later dried to constant weight in an oven maintained at 60^{o}C for three hours. After drying, each plant material was milled using an electric blender (Model BLG-400) and the powder sieved repeatedly through a 1 mm^2 perforation mesh to obtain the finest powder which was kept separately in a glass container with screw cap and stored at room temperature prior to use.

2.2. Extract Preparation

Fifty gram (50 g) powder of each plant species was soaked in 1000 ml ethanol solvent and macerated for 72 h with regular shaking and stirring with glass rod thrice daily. The mixture of solvent and powder was filtered through cheesecloth and Whatman No. 1 filter paper. The filtrate was extracted using Soxhlet apparatus for 5-6 h and concentrated under pressure to dryness in a rotary evaporator at 25-30^{0}C. The weights of the extracts were determined. *A. sativum* yielded 12.5 g, *C. millenii* 20.5 g, *M. myristica* 10.6 g, *X. aethiopica* 14.6 g and *Z. officinale* 15.8 g. The extracts were stored in a refrigerator maintained at 5-10 ^{0}C until ready for use. A technique described by (Ogunsina *et al*., 2011) was used to determine the percentage extract yield of each plant species. This involved dividing the extract mass obtained by sample mass used multiplied by 100. From each stock extract 1.5 g (=1500 mg) was weighed and dissolved in 30 ml ethanol solvent to give 50.0 mg/mL concentration. Two thousand two-hundred and fifty milligrams (2250 mg = 2.25 g) were dissolved in 30 ml ethanol to produce 75.0 mg/mL concentration. Similarly, three thousand milligrans (3000 mg = 3.0 g) were dissolved in 30 ml solvent to yield 100.0 mg/mL concentration. The extract concentrations (50.0, 75.0 and 100.0 mg/mL) of each plant species were used for the study.

2.3. Insect Culture

The insect pest used in this study was cowpea weevil, *C. maculatus* (F) (Coleoptera: Bruchidae). The weevils were reared on cowpea seeds (*V. unguiculata*) (L.) Walp in the laboratory to adapt them to the laboratory conditions using the method described by Sowunmi (1983). Cowpea seeds already infested with *C. maculatus* were collected locally in Abraka, Delta State, from traders of the food commodity. The adult weevils were isolated from the infested seeds. The cowpea seeds used as substrate to culture the weevils were thoroughly cleaned and exposed in an oven to ensure the absence of insects, mites and disease-causing microorganisms. Batches of one thousand (1000) treated seeds were placed in five different plastic containers previously washed, sterilized and dried. One hundred (100) weevils isolated from the infested cowpea seeds were introduced into each plastic container and covered with polythene net fastened tightly with rubber band. The cowpea seed-weevil mixtures were kept in the laboratory for 4 days to allow mating and oviposition to occur after which the parent weevils were removed. The rearing was given sufficient time (25-30 days) until new adult insects emerged. The first filial generations (F_1) adult weevils used for the experiment were 1-2 days old after emergence.

2.4. Toxicity Bioassay of Extracts

The plant extracts were assayed for insecticidal potency using the method described by Dharmasena *et al*. (2001). Cowpea seeds previously disinfested were divided into three lots of 10g each and replicated thrice. Each set of seeds was placed in a test tube (14.7x 2.4 cm) and treated with the plant extracts of different concentrations (50.0,

75.0 and 100.0 mg/mL). The tubes were manually rocked for two minutes to ensure that the seeds were coated with the extracts after which they were removed from the tubes and placed on filter papers for 24 h to allow the solvent to evaporate. Then each lot of seeds was placed in separate fresh test tubes and ten (10) adult weevils were introduced into the tubes and closed with plastic stoppers bearing gauze windows for ventilation. A control experiment, also replicated thrice, was constituted with identical amount of cowpea seeds and number of weevils but without the plant extracts. Mortality count of the insect pest was taken every 24 h for the exposure period of 96 h. The insect which did not respond when touched with a brush were considered killed and removed.

2.5. Statistical Analysis

Mortality data recorded every 24 h for 96 h exposure period were corrected for natural mortality of the insect pests in the control treatment using the formula proposed by Abbott (1925). The data were subjected to Analysis of Variance (ANOVA) and where significant differences existed treatment means were compared at 0.05 significant level using the New Duncan's Multiple Range Test (DMRT) (Zar, 1984). LC_{50} for each plant species at 96 h observation period was computed using regression analysis model (Finney, 1971).

3. Results

3.1. Mortality of C. maculatus

The result indicated that *C. millenii* gave the highest extract yield of 41.0%, followed by *Z. officinale* (31.6%), *X. aethiopica* (29.2%), and *A. sativum* (25.0%). The least extract yield of 21.2% was obtained from *M. myristica*. Table 1 shows the data of percentage mortality of the cowpea weevil, *C. maculatus*, observed on different days of treatment with ethanol plants extracts over 96 h.

Each value is a mean of triplicate data ± Standard Error with 10 weevils per replicate. Percentage values are in parenthesis. Column means followed by the same superscript letter are not significantly different ($p<0.05$) from each other using new Duncan Multiple range Test (DMRT).

Table 1. Cumulative mortality effect of five ethanol plant extracts on adult *C. maculatus*

Plant extract	Conc. (mg/ml)	Mean (%) mortality ± S.E at 24 to 96h Post-treatment*				
		24 h	48 h	72 h	96 h	Mean/24 h
A. sativum	50.0	2.33 ± 0.88	3.66 ± 0.33	4.66 ± 0.67	4.66 ± 0.67	3.83 ± 0.55
		(23.3)^{a}	(36.6)^{a}	(46.6) ^{a}	(46.6)^{a}	(38.3)^{a}
	75.0	2.66 ± 0.33	3.66 ± 0.33	5.0 ± 0.0	5.66 ± 1.20	4.25 ± 0.67
		(26.6) ^{a}	(36.6) ^{a}	(50.0)^{b}	(56.6)^{b}	(42.5)^{b}
	100.0	3.03 ± 0.06	4.33 ± 0.33	5.66 ± 1.20	6.66 ± 1.20	4.92 ± 0.79
		(30.3)^{b}	(43.3)^{b}	(56.6)^{c}	(66.6)^{c}	(49.2)^{c}
C. millenii	50.0	3.0 ± 1.0	4.83 ± 0.60	5.66 ± 1.20	6.36 ± 0.86	4.96 ± 0.58
		(30.0) ^{a}	(48.3)^{a}	(56.6)^{a}	(63.6)^{a}	(49.6)^{a}
	75.0	3.66 ± 0.33	4.99 ± 0.01	5.66 ± 1.20	6.66 ± 0.67	5.24 ± 0.63
		(36.6)^{a}	(49.9)^{a}	(56.6 ^{a}	(66.6)^{a}	(52.4)^{b}
	100.0	4.66 ± 0.67	6.33 ± 0.33	6.66 ± 0.67	8.36 ± 0.36	6.5 ± 0.76
		(46.6)^{c}	(63.3)^{b}	(66.6)^{b}	(83.6)^{b}	(65.0)^{c}
M. myristica	50.0	1.33 ± 0.33	2.66 ± 0.88	4.03 ± 0.57	5.33 ± 1.33	3.41 ± 0.86
		(13.3)^{a}	(26.6)^{a}	(40.3)^{a}	(53.3)^{a}	(34.1)^{a}
	75.0	2.33 ± 0.33	3.36 ± 0.32	4.36 ± 1.86	5.66 ± 1.20	3.93 ± 0.71
		(23.3)^{b}	(33.6)^{b}	(43.6)^{a}	(56.6)^{a}	(39.3)^{b}
	100.0	2.66 ± 0.33	4.03 ± 0.57	4.66 ± 0.67	5.66 ± 1.20	4.25 ± 0.67
		(26.6)^{b}	(40.3)^{c}	(46.6)^{b}	(56.6)^{a}	(42.5)^{c}
X. aethiopica	50.0	2.33 ± 0.88	4.66 ± 0.67	5.33 ± 1.33	6.36 ±0.86	4.67 ± 0.85
		(23.3)^{a}	(46.6)^{a}	(53.3)^{a}	(63.6)^{a}	(46.7)^{a}
	75.0	3.33 ± 0.67	5.33 ± 1.33	6.0 ± 1.53	7.33 ± 1.45	5.50 ± 0.83
		(33.3)^{b}	(53.3)^{b}	(60.0)^{b}	(73.3)^{b}	(55.0)^{b}
	100.0	3.33 ± 0.67	5.83 ± 1.15	6.33 ± 0.33	7.33 ± 1.45	5.71 ± 0.85
		(33.3)^{b}	(58.3)^{c}	(63.3)^{b}	(73.3)^{b}	(57.1)^{b}
Z. officinale	50.0	2.33 ± 0.88	3.33 ± 0.67	4.66 ± 0.67	5.66 ± 1.20	4.0 ± 0.73
		(23.3)^{a}	(33.3)^{a}	(46.6)^{a}	(56.6)^{a}	(40.0)^{a}
	75.0	3.13 ± 1.15	4.96 ± 0.58	5.33 ± 1.33	5.66 ± 1.20	4.77 ± 0.57
		(31.3)^{b}	(49.6)^{b}	(53.3)^{b}	(56.6)^{a}	(47.7)^{b}
	100.0	3.33 ± 0.67	5.86 ± 0.94	6.33 ± 0.33	7.66 ± 1.33	6.0 ± 1.53
		(33.3)^{b}	(58.6)^{c}	(63.3)^{c}	(76.6)^{b}	(60.0)^{c}

The insecticidal efficacies of the plant species on the adult *C. maculatus* over 96 h are presented in Figure 1.

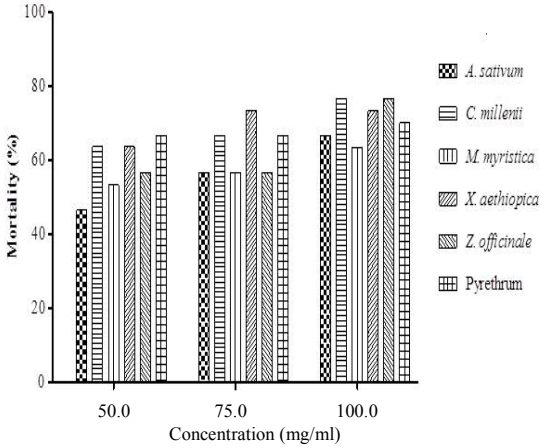

Figure 1. Cumulative mean mortality of *C. maculatus* exposed to various concentrations of plant extracts over 96 hours

The result showed that *C. millenii* and *X. aethiopica* extracts were most effective at 50 mg/mL concentration against the pest with respective mortality value of 63.3% at 96 h post-treatment. *Z. officinale* and *M. myristica* gave 56.6 and 53.3% mortality, respectively. The least percentage mortality of 46.6% over the 96 h exposure period was recorded in *A. sativum* extract. The highest mortality of 73.3% was observed in 75.0 mg/mL of *X. aethiopica* ethanol extract in 96 h exposure, followed by *C. millenii* (66.6%), while 56.6, 56.6 and 56.6% pest kill was exhibited by *A. sativum*, *M. myristica* and *Z. officinale* extracts, respectively, over 96 h. The extract of *C. millenii* at 100 mg/mL concentration gave the highest mortality of 83.6% compared to *Z. officinale* that caused 76.6% mortality of the pest after 96 h treatment. This was followed by *X. aethiopica* (73.3%), *A. sativum* (66.6%) and *M. myristica* (56.3%).

The overall mean percentage mortality data at all concentrations indicated that *C. millenii* extract gave better control of the cowpea weevil than the other extracts. The daily mean mortality of the pest at 100 mg/mL of *C. millenii* was 65.0%, followed by *Z. officinale* (60.0%), *X. aethiopica* (57.1%) and *A. sativum* (49.2%). *M. myristica* extract gave the least mortality of 42.5%. However, all the five treatment proved significantly better than the untreated check. Considering the mean daily percentage mortality of *C. maculatus* as main index the insecticidal efficacy of the five plants species is indicated as follows: *C. millenii* > *Z. officinale* > *X. aethiopica* > *A. sativum* > *M. myristica* (Table 2).

The efficacy and economic value of the five tested plants species are corroborated by the percentage yield of the extract (Table 1). The higher the yield the more efficacious was the plant extract.

Probit analysis of extract concentrations lethal to 50% (LC_{50}) of the adult cowpea weevil over 96h exposure is presented in Table 2.

Table 2. LC_{50} (mg/mL) of extracts on adult *C. maculatus*

Plants extract	LC_{50} at different time intervals			
	24h	48h	72	96h
A. sativum	-	-	75.0	55.0
C. millenii	-	75.0	42.5	36.3
M. myristica	-	-	-	47.5
X. aethiopica	-	50.0	46.3	43.8
Z. officinale	-	77.5	62.5	37.5

LC_{50} analysis of the extracts considered in 96 h post-treatment indicated that *C. millenii* was the most effective control agent of the target pest (LC_{50} = 36.3 mg/mL) followed by *Z. officinale, X. aethiopica, M. myristica* and *A. sativum* with respective LC_{50} of 37.5, 43.8, 47.5 and 55.0 mg/mL. The result revealed that the length of exposure time was a determining factor of the LC_{50}. The longer the period of treatment, the less was the LC_{50} of the extracts.

4. Discussion

The solubility of active ingredients in plants varies during extraction as observed in the extract mass and percentage yield of the tested plant species. Differences in toxicity may be related to the proportion of the active chemicals in the extracts due to differential solubility in the ethanol solvent. This probably was the reason for the high mortality of *C. maculatus* in *C. millenii* (manjack), *Z. officinale* (ginger) and *X. aethiopica* (negropepper) extract at all concentrations used since they gave higher percentage yield arising from their solubility.

The current study revealed that all the tested plants extracts were toxic and could be used as protectant against *C. maculatus*. However, the high toxicity of *C. millenii* (LC_{50} = 36.3mg/mL) was close to *Z. officinale* (LC_{50} = 37.5 mg/mL) against the target pest showed that it would be economical to carryout mass production of these plant species for use as protectant of grains since they were able to achieve 50% *C. maculatus* mortality with the least extract concentration within 96h exposure.

The results of this study are in conformity to some degree with the report of some workers, like Opareke and Dike (2005), Adedire *et al*. (2011), Mukanga *et al*. (2010), Ileke and Oni (2011), who observed that certain botanicals are effectively toxic against storage insect pests including *C. maculatus*. The resultant mortality rates of *C. maculatus* in this investigation could be attributed to the toxic effects of the chemicals in the tested plant species. Although all the plants showed promise as insecticides their toxicity against *C. maculatus* varied probably because of the different phytochemical contents.

C. millenii exhibited the strongest insecticidal effect due to oleanoic and triterpene derivatives (Chen *et al*., 1983), betulic and terpenoid quinones (Moir and Thomsom, 1973) as the main constituents. The high toxicity of *C. millenii* could be attributed to the terpenoids, which act as insecticides, repellants and antifeedants against insects (Detheir *et al*., 1996). According to Grøntved and Pittler (2000) *Z. officinale* has alpha-zingiberine as the major phytochemical which is believed to be toxic. The toxicity of ginger in the present study is somewhat corroborated by the report of Bandara *et al*.

(2006) that the ginger species, *Z. purpureum*, was ovicidal against *C. maculatus*. Ginger has been reported toxic to storage insect pests (Igbai and Poswal, 1995; Owolabi *et al*., 2009). Ginger has become a promising future alternative to expensive and toxic therapeutic agent because of the chemopreventive potentials of zingiberine (Duke and Ayensu, 1985). The principal chemicals in *X. aethiopica* are mono- and sesquiterpene hydrocarbons (Karioti *et al*., 2004) which may have caused the pest mortality. Terpenoids are the main chemical components in *A. sativum* (garlic) (Duke and Ayensu, 1985). Terpenoids act as fumigant causing insect death owing to anorexia arising from drastic reduction in insect respiratory activities as reported by Don-Pedro (1996e). Allitin, another chemical in garlic, inhibits cholinesterase activity in insects (David and Ananthakrishna, 2004). Garlic toxicity may have been caused by one or a combination of these chemicals. The mortality of *C. maculatus* by garlic and ginger in this study agrees with earlier reports that plants in the genera *Allium* and *Zingiber* to which garlic and ginger belong are insecticidal against various insect pests (Owusu *et al*., 2008). African nutmeg (*M. myristica*) has myristicine (Dales, 1996), p-cymene, alpha-phellandrene and other terpene hydrocarbons (Owolabi *et al*., 2009) as chemical constituents. Nutmeg toxicity may be due to the terpenes and their derivatives which are known to influence insect respiratory metabolism by disturbing mono-oxygenase enzymes activity (Bernard *et al*., 1989) and affect nervous system by inhibiting acetylcholinesterase enzyme activity (Keane and Ryan, 1999). Terpene 1,8-cineole is toxic against rice weevil (Byung-Ho *et al*., 2001) and cowpea weevil (Aggrawal *et al*., 2001). These chemicals in nutmeg notwithstanding the reportedly low toxicity of the extract may be as a result of low solubility of the active ingredients in the ethanol solvent.

5. Conclusion

All the tested plant species exhibited toxic action against the cowpea weevils. Therefore, they could be used by local farmers to protect cowpea seeds in storage against the weevil based on the available data. It is recommended that similar investigation on different parts of the tested plants species be carried out to further assess their efficacy against the weevil and other storage pests. Besides, the use of other extraction solvents for the tested plants is recommended in order to evaluate further their insecticidal potency. It is, therefore, expedient to control pest populations to low or zero levels in storage since higher bruchid populations result to higher level of stored grain damage.

Acknowledgment

The authors would like to thank Delta State University particularly Department of Animal and Environmental Biology/Tropical Disease Research Unit for providing facilities and enabling environments for this research.

References

Abbott WS. 1925. A method for computing the effectiveness of an insecticide. *J Econ. Entomol.,* **18**: 265-267.

Adedire CO. 2003. Use of nutmeg *Myristica fragans* (Houtt.) powder and oil for the control of cowpea storage bruchid, *Callosobruchus maculatus* (Fabricius). *J Plt Dis Prot.,* **109(2):** 193–199.

Adedire CO, Obembe OO, Akinkurolele RO, and Oduleye O. 2011. Response of *Callosobruchus maculatus* (Coleoptera: Chysomelidae: Bruchidae) to extracts of cashew kernels. *J Plt Dis Prot.,* **118(2):** 75-79.

Aggrawal KK, Tripathi KA, Prajapati V and Sushil K. 2001. Toxicity of 1,8-cineole towards three species of stored product coleopterans. *Insect Sci Appl.,* **21**: 155-160.

Ajayi OE and Adedire CO. 2003. Insecticidal activity of an under-utilized tropical plant; *Hura crepitans* (L.) seed oil on cowpea beetle, *Callosobruchus maculatus* (F) (Coleoptera: Bruchidae). *Nig J Entomol.,* **20**:74-81.

Al-Moajel NH and Al-Fuhaid WL. 2003. Efficacy and persistence of certain plant powders against Khapra beetle, *Trogoderma granarium*. (Everts), Fayoum. *J Agric Res Dev.,* **17**: 107-114.

Bandara P, Nimal KA, Kumar V, Ramesh C, Saxena RC and Puthenveetil K. 2006. Bruchid (Coleoptera: Bruchidae) Ovicidal Phenylbutanoid from *Zingiber purpureum. J Econ Entomol.,* **98*(4):*** 1163-1169.

Berger A. 1994. Using natural pesticides: current and future perspectives. A report for the plant protection improvement in Botswana, Zambia and Tanzania. http://www>blakherbals.com/ using_natural pesticides. Html: Downloaded 07/03/2005.

Bernard CB, Arnason JT, Philogene B, Lam J and Wadell T. 1989. Effect of lignans and other secondary metabolites of the Asteraceae on the mono-oxygenase activity of the European corn borer. *Phytochem.,* **25(5):** 1373-1377.

Byung-Ho L, Won-sik C, Sung-Eun L, and Byeoung-Soo P. 2001. Fumigant toxicity of essential oils and their constituent compounds towards rice weevil, *Sitophilus oryzae* (L). *J Crop Protect.,* **20**: 317-320.

Caswell GH, .1981. Damage to stored cowpea in the Northern part of Nigeria. *Samaru J Agric Res.,* **1**: 11-19.

Chen TK, Ales DC, Baenzinger NC and Wiemer DF. 1983. Anti-repellent triterpenes from *Cordia alliodora*. *J Org Chem.,* **48**: 3525-3531.

Dales MJ. 1996. A review of plant materials used for controlling insect pests of stored products. *NRI Bulletin 65 Chatman Natural Resources Institute, UK.*

David BV and Ananthakrishna TN. 2004. **General and Applied Entomology** 2nd Ed. Tata McGraw Hill education private limited, New Delhi, 1184 pp.

Deboer JL. 2003. Regional cowpea trade and marketing in West Africa. http;//www.isp.msu.edu/crsp/final report. D ownloaded 07/03/2005.

Dethier VG, Browne LB and Smith CN. 1996. The designation of chemicals in terms of the response they elicit from insects. *J Econ Entomol.,* **53(1):** 134-136.

Dharmasena CMD, Blaney WM and Simmonds SMJ. 2001. Effects of storage on the efficacy of powdered leaves of *Annona squamosa* for the control of *Callosobruchus maculatus* on cowpea (*Vigna unguiculata*). *Phytoparasitica,* **29(3):** 31-35.

Don-Pedro KN. 1996. Fumigant toxicity of citrus peels oils against adult and immature stages of storage insect pests. *Pesticide Sci.,* **47**: 213-223.

Duke JA and Ayensu ES. 1985. Medicinal Plants of China, Reference Publ., Inc. http://www.pakos.org/pjbot/PDFs/40% 284% 29/PJB40%284%291793.pdf, Downloaded 27/02/ 2010.

Echendu TNC. 1991. Ginger, cashew and neem as surface protectants of cowpeas against infestation and damage by *Callosobruchus maculatus* (F). *Trop Sci.,* **31**: 201-211.

Ellis MD and Baxendale FP. 1997. Toxicity of seven monoterpenoids to tracheal mites (*Acarina Tersonemidae*) and their honey bee (Hymenoptera Apidae) host when applied as fumigants, *J Econ Entomol.,* **90(5)**: 1087-1091.

Finney DJ. 1971. **Probit Analysis**. Cambridge University Press; 333pp.

FAO. 1985. Handling and storage of food grains. Food and agricultural organisation of United Nations, Rome. http://www>blakherbals.com/using_naturalpesticides. Downloaded 07/03/2005.

Grøntved A and Pittler MH 2000. Ginger root against sea sickness. A controlled trial on the open sea. *Brit J Anaesthesia,* **84 (3):** 367–71.

Igbai J and Poswal MAT. 1995. Evaluation of certain spices for the control of *Callosobruchus maculatus* (Fabricius) (Coleoptera:Bruchidae) in cowpea seeds. *Afr Entomol.,* **3***: 87-89.*

Ileke KD and Oni MO. 2011. Toxicity of some plant powders to maize weevil, *Sitophilus zeamais* (Motschulsky) (Coleoptera: Curculionidae) on stored wheat grains (*Triticum aestivum*). *Afr J Agric Res.,* **6(13):** 3043-3048.

Ito EE and Ighere EJ. 2017. **Basic Entomology and Pest Control**, 1st Edition. University Printing Press, Abraka, Delta State, Nigeria, 361pp.

Ivbijaro ME and Agbaje M. 1986. Insecticidal activities of *Piper guineense* Schum and Thonn and *Capsicum* species on the cowpea bruchid, *Callosobruchus maculatus. Insects Sci Appl.,* **7(4):** 521-524.

Karioti A, Hadjipavlou-Latina D, Mensah MLK, Fleischer TC and Skaltsa H. 2004. Composition and antioxidant activity of the essential oils of *X. aethiopica* (Dun) A. Rich (Annonaceae) leaves, stem bark and fresh and dried fruits, growing in Ghana. *J Agric Food Chem.,* **52**: 8094-8098.

Keane S, and Ryan MF. 1999. Purification, characterization, and inhibition by monoterpenes of acetylcholinesterase from the wax moth, *Galleria mellonella* (L.). *Insect Biochem Mol Biol.,* **29**:1097–1104.

Keita SM, Vincent C, Schmit JP, Arnason JT and Bélanger A. 2001. Efficacy of essential oil of *Ocimum basilicum* L. and *O. gratissimum* L. applied as an insecticidal fumigant and powder to control *Callosobruchus maculatus* (Fab.) (Coleoptera: Bruchidae). *J Stored Prod Res.,* **37***:* 339-349.

Moir M and Thomson RH. 1973. Naturally occurring quinones part XXII. Terpenoid quinones in *Cordia millenii* species. *J Chem Soc Perkin,* **1**: 1352-1357.

Mukanga M, Deedat Y, and Mwangala FS. 2010. Toxic effects of five plant extracts against the larger grain borer, *Prostephanus truncatus*. *Afr J Agric Res.,* **5(24):** 3369-3378.

Obeng-Ofori D, Jembere B, Hassanali A, and Reichmuth CH. 2000. Effectiveness of plant oils and essential oil of *Ocimum* plant species for protection of stored grains against damage by stored product beetles. Proceedings of the 7th International Working Conference on Stored-product Protection. Beijing – China, 799-808.

Odeyemi OO, and Daramola AM. 2000. Storage Practices in the Tropics, volume 1: **Food Storage and Pest Problems**, 1st edition MI. Nigeria: Dave Collins Publications. 253pp.

Ofuya TI. 1991. Observations on insect infestation and damage in cowpea (*Vigna unguiculata*) intercropped with tomato (*Lycopsicon esculentus*) in a rainforest area of Nigeria. *Exper Agric.,* **27**: 407 – 412.

Ogunsina OO, Oladimeji MO and Olajide L. 2011. Insecticidal action of hexane extracts of three plants against bean weevil, *Callosobruchus maculatus* (F.) and Maize weevil *Sitophilus oryzae* (Motsch). *J Ecol Nat Environ.,* **3(1):** 23-38.

Oparaeke A.M and Dike M.C. 2005. *Monodora myristica* (Gaertn), (Myristicaceae) and *Allium cepa* (Lilliaceae) as protectants against stored cowpea seed Bruchid *(Callosobruchus maculatus)* infestation. *Nig J Entomol.,* **22**: 84-92.

Owolabi MS, Oladimeji MO, Lajide L, Singh G, Marimuthu P and Isidorov V. 2009. Bioactivity of Three Plant Derived Essential Oils Agianst Maize Weevils *Sitophilus zeamais* (Motschulsky) and cowpea weevils *Callosobruchus maculatus* (Fabricius). *EJEAF Chem.,* **8(9):** 828-835.

Owusu EO, Akutse KS and Afreh-Nuamah K. 2008. Effect of some traditional plant components for the control of termites, *Macrotermes spp*. (Isoptera: Termitidae) *Afr J Sci Technol (AJST) Sci Eng Ser.,* **9(2):**82 – 89.

Sharma A, Kaushal P, Sharma R, and Kumar R. 2006. Bioefficacy of some plant product against diamondblack moth, *Plutella xylostella* (L.) (Lepidoptera: Yponomeutidae). *J. Entomol Res Soc.,* **30:** 213-217.

Sowunmi EO. 1983. Effect of storage length and insecticidal treatment on cowpea (*Vignaunguiculata).Trop Legume Bull.,* **27**: 21-27.

Tanzubil PB. 1991. Control of some insect pests of cowpea, *Vigna unguiculata* (L.) Walp with neem, *Azadirachta indica* A. Juss in northern Ghana. *Trop Pest Mgt.,* **37**: 216 – 217.

Zar JH. 1984. **Biostatistical Analysis**, 2nd ed. Prentice-Hill Intl. Englewood Cliffs, N.J.

JJBS

Volume 10, Number 4,December 2017
ISSN 1995-6673
Pages 323 - 327

Jordan Journal of Biological Sciences

Phytochemical Screening and Radical Scavenging Activity of Whole Seed of Durum Wheat (*Triticum durum* Desf.) and Barley (*Hordeum vulgare* L.) Varieties

Sofia Hamli[*1], Kenza Kadi[1], Dalila Addad[1] and Hamenna Bouzerzour[2]

[1] *Department of Agronomy, Faculty of Life and Natural Sciences, Abbas Laghrour Khenchela University, 40000;*

[2]*Valorization of Biological Natural Resources Laboratory, Faculty of Life and Natural Sciences, Setif-1 University, 19000, Algeria.*

Received: June 23, 2017; Revised: August 29, 2017; Accepted: September 4, 2017

Abstract

Three durum wheat (*Triticum turgidum* L. var. *durum*) cultivars, namely Bousselam, Vitron, and Gaviota *durum*, and one barley genotype (*Hordum vulgare* L.), Fouara, grown under semi-arid conditions were compared for their total phenolic and flavonoids content and antioxidant activities. Antioxidant activity was tested using DPPH radical scavenging assay method. The phytochemical screening revealed the presence of tannins, flavonoids, coumarins, saponins and phenolic compounds in each variety seeds. The results of the present study indicate significant differences among the evaluated varieties in terms of total phenolic and flavonoid contents and for radical scavenging capacity. Among the tested varieties Gaviota durum showed high total phenolic (95.32± 0.27 µg /mg) and flavonoid content (78.80 ± 0.27 µg/mg) and an intermediate radical scavenging capacity. While barley variety Fouara expressed high radical scavenging capacity (54.8% ±0.34) and intermediate total phenol and flavonoids contents. The tested durum wheat and barley varieties possessed varying but meaningful antioxidant activities which were not significantly correlated to their phenol and flavonoid contents. It is necessary to ensure that increased bioactive components in grains are combined with good agronomic performance, high grain yield and high quality for processing. The results of the present study should have significant implications for plant breeders as well as for grain and food processors.

Keywords: Wheat, Antioxidant, Barley, Flavonoids, Total phenolic content, DPPH.

1. Introduction

Cereals are an important component of the human diet, and are used in the production of many food products, providing energy based on t heir high protein and carbohydrate contents (Sarwar *et al*., 2013). They are also characterized by a high amount of insoluble and soluble bioactive components like fibers, vitamins, minerals, unsaturated fatty acids, tocopherols, lignans, flavonoids and phenolic acids (Okarter *et al.*, 2010). When facing oxidative conditions, caused by stresses such as heat, drought, UV radiation, chemicals or pathogens attacks, plants produce secondary metabolites as a self-protection mechanism to intercept oxidative reactions generating free radicals and converting them into harmless molecules (Manach *et al.*, 2004). In fact, reactive oxygen species and free radicals are constantly formed in the organism body by normal metabolic actions. Their effects are opposed by a balanced system of antioxidants and enzymes defenses. Unbalance between these two systems causes oxidative stress, which can lead to cell injury and death (Romano *et al.*, 2010).

Since synthetic antioxidants are suspected of being carcinogenic (Ratnam *et al*., 2006), much attention has been given to naturally occurring antioxidants, which are able to inhibit oxidative chain reactions within tissues (Nsimba *et al.*, 2008). According to Perez-Jimenez *et al*. (2008), increased intake of antioxidants rich food is associated with a lower risk of cardiovascular and cancer diseases. Naczk and Shahidi (2006) mentioned that phenolic compounds are employed in the treatment of cardiovascular diseases. Consumption of cereals containing high levels of antioxidants, mostly coming from phenols, has been recommended (Ward *et al*., 2008).

Anson *et al*. (2008) mentioned that the major components with antioxidant activity in wheat belong to the group of phenolic acids, which are mostly found in the bran, suggesting the use of wheat grain as whole instead of refined. Traditionally, wheat grain is milling to obtain the refined white flour by removing the bran. According to Dvorakova *et al*. (2010), barley is an excellent source of phenolic acids, flavonoids, tannins, proanthocyanidins and

* Corresponding author. e-mail: sofiahamli@yahoo.fr .

amino phenolic compounds. Adom *et al*. (2005) reported that antioxidant content depends on the cereal species, varieties, environmental conditions and treatment type.

The aim of the present study was to compare phenolic and flavonoid contents and their antioxidant activity in the seeds of three durum wheat (*Triticum turgidum* L. var. *durum*.) and one barley (*Hordeum vulgare* L.) varieties produced under semi-arid conditions.

2. Materials and Methods

2.1. Plant Materials

Three durum wheat (*Triticum turgidum* L. var. *durum*) cultuvars, namely Bousselam, Vitron, and Gaviota *durum*, and one barley variety (*Hordum vulgare* L.), Fouara, were used as plant material. Seeds were generously provided by Ain Babouche Cereals and Food Legumes Cooperative (Oum El Bouaghi, Algeria). These varieties were authenticated based on seed increase certificates delivered in June 2016, by the National Center of Seed Control and Certification, Khroub laboratory, Algeria (CNCC, Khroub, Algeria). Pedigree and cross origin of the durum wheat varieties were reported by Hamli *et al*. (2015**)** and the one of barley variety was reported by Bensemane *et al*., (2011). Seeds of the four varieties were cleaned and milled to a fine powder with cyclotec sample mill to pass through a 0.5 mm sieve.

2.2. Extracts Preparation

Extraction of the ground material was conducted according to Sultana *et al.* (2008) with some modifications. 10 grams of milled wheat and barley seed samples were extracted for 24 h w ith 100 m l of 70% aqueous methanol (v/v) at ambient temperature, in amber flasks in a shaking water bath. The supernatant was transferred to volumetric flask and the pellet was re-extracted for 24 h with another 100 mL of 70% aqueous methanol. Supernatants from both extractions were combined and the residues were separated by filtering through Whatman filter paper (No. 1, Whatman International Ltd., Kent, England). Methanol was evaporated using a rotary evaporator (HAHNVAPOR) under reduced pressure and mild temperature (<40°C).The combined crude extracts were weighed, and then kept in the dark until used for of various antioxidant bioassays and for determination of total phenolic, flavonoid content, and DPPH radical scavenging activity.

2.3. Qualitative Screening

2.3.1. Alkaloids and Flavonoids Screening

The presence of alkaloids was tested using Mayer reagent and according to the procedure described in the literature (Edeoga, 2005). Briefly, a 5 mL sample of the crude plant extract was added to a mixture of mercuric chloride and potassium iodide. The appearance of a white pale precipitate indicated the presence of alkaloids.

The presence of flavonoids was tested using the methods described by Edeoga (2005). Few drops of aluminium chloride solution (1 % $AlCl_3$ v/wt) were added to 5 mL of crude extract. The appearance of a yellow color indicated a positive result.

2.3.2. Tannins and Saponins Screening

The presence of tannins was tested by adding few drops of dilute iron chloride ($FeCl_3$, 2 %) to 5 m L of crude extract. According to Karumi *et al.* (2004), formation a dark blue colored precipitate indicated the presence of tannins. The presence of saponins was tested according to the procedure described by Karumi *et al.* (2004). Briefly, a mixture containing 5 ml of the crude extract in 10 ml distilled water was shaken vigorously for 2 m inutes. The formation of forth indicated the presence of saponins.

2.3.3. Coumarins Screening

The presence of coumarins is based on the Keller-Kiliani reaction **(**Edeoga, 2005). 1 ml of crude extract was dissolved in 5 m l of acetic acid containing one drop of ($FeCl_3$) solution and 5 mL of sulfuric acid were added to the mixture. The presence of coumarins is indicated by the formation of two phases, one red-brown colored suggesting the presence of acetic acid and the other blue-green colored, suggesting the presence of sulfuric acid (Edeoga, 2005).

2.4. Quantitative Analyses

2.4.1. Total Phenolic Content

The Total Phenolic Content (TPC) in the methanolic crude extract was determined using the Folin-Ciocalteu's reagent according to the method described by Singleton *et al.* (1999). The extract (0.2 mL) diluted ten times was left; react with 1 ml of the reagent of Folin-Ciocalteu, and then the mixture was neutralized with 0.8 ml of 20% sodium carbonate (w/v) solution. The mixture was then incubated at ambient temperature for 30 m in after which, the absorbance was measured at 760 nm using a helios spectrophotometer (thermo spectronic). A standard curve was prepared using gallic acid standard solutions of known concentrations, yielding a calibration curve having the following form: Y=0.0127X-0.0106 with a coefficient of determination $R^2 = 0.9988$, where Y= absorbance, and X= GAE concentration in µg/ml. The results are expressed as µg of gallic acid equivalent per mg of crude extract sample (µg GAE/mg sample). For each sample, three replicate assays were performed.

2.4.2. Total Flavonoid Content

Flavonoid contents of wheat and barley seed crude extract were assayed using the aluminum chloride colorimetric method described by Ordonez *el al.* (2006). Crude extract (0.5 mL) was mixed with 0.5 mL of 2 % methanolic solution of aluminum chloride (v $AlCl_3$/v Methanol). After incubation at room temperature for 10 min, the absorbance of the reaction mixture was measured at 420 nm with a helios spectrophotometer (thermo spectronic). The total flavonoid content was determined using a standard curve obtained from various concentrations of quercetin and expressed as µg of Quercetin Acid Equivalent (QAE) per mg of dry matter (µg QAE/mg). Calibration curve had the following form: Y=0.0334X-0.1031 with a coefficient of determination $R^2 = 0.9382$, where Y= absorbance, and X= quercetin concentration µg/mL.

2.4.3. Total Tanins Content

Total tanins content in extracts is carried out according to the method of Heimler *et al.* (2006). For 50 µL of the crude extracts we add 500 µL of vanillin (4% in methanol) and 1.5 mL of concentrated HCl. The mixture is incubated during 20 min and the absorbance was measured at 500 nm with a helios spectrophotometer (thermo spectronic). The total tanins content was determined using a standard curve obtained from various concentrations of catechine and expressed as µg of Catechine Acid Equivalent (CAE) per mg of dry matter (µg CAE/mg). Calibration curve had the following form: Y=0.133X-0.018 with a coefficient of determination $R^2 = 0.966$, where Y= absorbance, and X= catechine concentration in µg/ml.

2.4.4. Antioxidant Activity

The antioxidant capacity of the crude seed wheat and barley extracts was measured using the 2,2-diphenyl-1-picrylhydrazyl (DPPH) according to the method described by Huang *et al.* (2005). Samples of 0.2 mL of crude extracts were mixed with 1.8 mL of DPPH solution (0.04 g DPPH in 100 mL methanol) and incubated for 30 min at room temperature. Decline in absorbance of the reaction mixture at the end of the incubation period was measured using a helios spectrophotometer (thermo spectronic) at 517 nm. Free radicals scavenging capacity was calculated according to the following equation:

$$\mathbf{DPPH*scavenging}(\%) = \frac{\mathbf{absorbance_{control}} - \mathbf{Absorbance_{sample}}}{\mathbf{Absorbance_{control}}}\mathbf{x}100$$

2.5. Statistical Analyses

Data were subjected to an analysis of variance of randomized design with a single factor and three replications. Student-Newman-Keulstest was carried out to assess significant differences between treatment means, using SAS version 9.1.3., (2011). Spearman rang correlation coefficients (rs) were calculated to determine the relationships between measured variables at the 5% probability level of significance.

3. Results and Discussion

3.1. Qualitative Screening

Qualitative screening was performed in order to check for the presence/absence of secondary metabolites. The screening revealed the presence of tannins, flavonoids, coumarins saponins and phenolic compounds in each variety seeds .These results suggested that quantification of the targeted compounds could be carried out (Table 1).

Table1. Phytochemical screening of barley and wheat varieties

Parameters	Flavonoids	Tannins	Alkaloids	Coumarins	Phenols	Saponins
Wheat varieties	+	+	-	+	+	+
Barley	+	+	-	+	+	+

(+) = indicates presence of compounds, (-) = indicates absence of compounds

3.2. Quantitative Screening

3.2.1. Total Phenolic Content

Even though free polyphenols compounds are easily extracted using various solvents, such as methanol, ethanol, acetone, diethyl ether; studies of Ivanisova *et al.* (2014) indicated that antioxidants and polyphenols from cereals may be effectively extracted by methanol at laboratory temperature. Therefore, this solvent was used, in the present study, for the extraction and evaluation of antioxidants and polyphenols present in durum wheat and barley. Data analysis of variance indicated a s ignificant variety effect for total phenolic, flavonoid and the percentage of inhibition (I %) of crude extract of durum wheat and barley seeds and no significant variety effect for tannins contents (Table 2). Mean values of total phenolic content of crude extracts, ranged from 10.63± 0.35 µg /mg, measured in Bousselam variety to 95.32± 0.27 µg /mg, measured in Gaviota durum (Table 3).

Table2. Means squares of the analysis of variance of total phenolic, flavonoid and the percentage of inhibition (I %) of crude extract of durum wheat and barley seeds

Source	DF	Phenols	Flavonoids	Tannins	% I
Variety	3	4688.44**	3853.93**	6.23 **ns**	3045.97**
Error	8	0.07	0.09	0.05	2.77

****** = Significant variety effect at 1% probability. **ns** = no significant effect. I% = the percentage of inhibition= DPPH scavenging activity. DF: degrees of freedom

Table 3. Mean values of total phenolic, flavonoid and tannins contents of crude extracts of durum wheat and barley seeds

Varieties	Phenols (1)	Flavonoids (2)	Tanins	%I (3)
Gaviota durum	95.32^{a}±0.27	78.8^{a}±0.23	4.39^{a} ±0.16	38.17^{c}
Fouara	43.66^{b}±0.27	22.1^{b}±0.34	4.5^{a}± 0.27	54.80^{b}
Vitron	12.56^{c}±0.11	3.3^{c}±0.44	2.40^{b} ±0.23	0.18^{e}
Bousselam	10.63^{d}±0.35	2.7^{c}±0.06	1.62^{c} ±0.22	36.55^{d}
Ascorbic acid	-	-	-	88.00^{a}

(1) µg of gallic acid equivalent per mg of crude extract sample (µg GAE/mg sample). (2) µg of quercitin acid equivalent per mg of crude extract sample (µg EQ/mg sample). (3) µg of Catechin acid equivalent per mg of crude extract sample (µg EC/mg sample). Means followed by the same letter, within the same column, are not significantly different at 5% level according to the NK'S test. a,b,c and d: homogenized group. I% = the percentage of inhibition= DPPH radical scavenging activity.

Total phenolic content of Gaviota durum was 8.9 fold higher than the one of Bousselam, Vitron being more similar to Bousselam even though significantly different from it.

Fouara, barley variety presented an average value of 43.66 ± 0.27 µg /mg of total phenolic content. The current results are relatively lower than those reported by Amarowicz *et al.* (2002) (92.0 mg/g). Zeilinski and Hozlowoka (2000) as well as Liu and Yao (2007) noted that barley seeds expressed higher amount of phenolic content than common wheat. Comparatively, Abozed *et al.* (2014) reported lower values of total phenolic content

ranging from 3.88 to 4.66 µg /mg in the bran and from 1.78 to 2.57 µg /mg in whole grain of two common wheat varieties. Differences between and within species could originate from genetic factors, geographical and climatic factors, storage conditions and nature of solvent used for extraction.

Also note that despite these cultivars were obtained from the same region, it seems that they did not belong to the same collection period, thus in addition to the genetic factors, other factors including the collection period, drying method, storage conditions, extraction procedure and many other factors may affect the content of secondary metabolites.

3.2.2. Total Flavonoids Content

Mean values of flavonoids content of crude extracts, ranged from 2.70 ± 0.06 µg/mg, average value of Bousselam variety to 78.80 ± 0.27 µg/mg, measured in Gaviota durum (Table 3). Barley variety presented a mean value of 22.10 ± 0.34 µg/mg of flavonoids content. Gaviota durum presented high flavonoid content, 29.1 times fold higher than the flavonoid content of Bousselam, and 3.5 folds higher than barley variety Fouara. Bousselam and Vitron showed similar pattern of flavonoid content.

According to Satheeshkumar *et al.* (2011) flavonoids, based on their structure, are potential antioxidants, since they are able to scavenge, *in vivo* and *in vitro,* practically all known reactive oxygen species. Pinent *et al.* (2008) reported that flavonoids have positive effects on the regulation of glucose homeostasis and anti-inflammatory functions alleviating insulin-mediated chronic diseases, such as insulin resistance. Durum wheat variety Gaviota durum and barley variety Fouara could be recommended for the food industry as natural antioxidant ingredients because of their high level of flavonoid contents.

3.2.3. DPPH Radical Scavenging Activity

Roginsky and Lissi (2005) mentioned that DPPH radical test is based on the ability of this compound to react with hydrogen donor species, mainly polyphenols, and upon receiving proton from extract constituents, it loses its color, which changes from deep violet to yellow. As the concentration of phenolic compounds or degree of hydroxylation of the phenolic compounds increases, their DPPH scavenging activity increases too, correlating directly to the extent of Radical scavenging efficacy of the assessed plant material. Results of the present study show that the order of free radical scavenging activity of crude extracts from seeds of durum wheat and barley varieties was as follows: Fouara barley (54.8% ±0.34) > Gaviota durum wheat variety (38.0% ±0.28) > Bousselam variety (36.9% ±0.41) > Vitron seeds crude extract (0.18 % ± 0.10). Results are summarized in Table 3.

The results of the present study corroborate those of Abozed *et al.* (2014) who reported for two common wheat varieties strong DPPH free radical scavenging activities ranging from 28.07 to 36.82%, for bran samples. Amarowicz *et al.* (2002) reported that barley crude extract was found to afford the strongest free-radical scavenging activities at 43.6% efficacy, which was much stronger than those of the extracts prepared from rye, wheat and triticale caryopses. The results of correlation analyses between the total phenolic content, flavonoid and antiradical activity indicted that only TPC was positively and significantly correlated with flavonoid content (rs = 0.999, $P<0.000$), while these two parameters were not significantly correlated with % I (rs = 0.600, $P>0.050$). These results do not corroborate results reported by Siddhuraju and Becker (2003) who found a significant correlation and commented that antioxidant activity of phenolic compounds is mostly associated with their redox properties which allow them to act as anti-oxidative agents.

4. Conclusion

The results of the present study indicate significant differences among the evaluated varieties for total phenolic and flavonoid contents and for radical scavenging capacity. Among the tested varieties Gaviota durum showed high total phenolic and flavonoid content and an intermediate radical scavenging capacity. While barley variety Fouara expressed high radical scavenging capacity and intermediate total phenol and flavonoids contents. The tested durum wheat and barley varieties possessed varying but meaningful antioxidant activities which, however, were not significantly correlated their en phenol and flavonoids contents. Further studies are recommended to sample a l arger set of varieties, grain fractions and solvent types. The results suggested that selected durum and barley varieties may be considered as rich sources of natural antioxidants, which can ideally serve as basis for the development of functional foods designed to improve consumer's health. It is also necessary to ensure that increased bioactive components in grains are combined with good agronomic performance, high grain yield and high quality for processing. The results of the present study should have significant implications for plant breeders as well as for grain and food processors.

Acknowledgement

The authors are thankful to Mrs Bouakez Tahar for providing wheat grain samples by Ain Babouche Cereals and Food Legumes Cooperative (Oum El Bouaghi, Algeria).

References

Abozed SS , El-kalyoubi M, Abdelrashid A and Salama M.F. 2014. Total phenolic contents and antioxidant activities of various solvent extracts from whole wheat and bran. *Annals of Agric Sci.,* **59** (1): 63–67

Adom KK and Liu RH, 2005**.** Rapid peroxyl radical scavenging capacity (PSC) assay for assessing both hydrophilic and lipophilic antioxidants**.** *J. Agric. Food Chem* ,**53** :6572-6580.

Amarowicz R, Żegarska Z, Pegg R B, Karamać M and Kosińska A. 2007. Antioxidant and radical scavenging activities of a barley crude extract and its fraction. *Czech J. Food Sci*, **25**: 73–80.

Anson NM, Vanderberg R, Havenaar R, Bast A and Haenen M M. 2008.Ferulic acid from aleurone determines the antioxidant potency of wheat grain (*Triticum aestivum* L). *J Agric Food Chem*, **56**: 5589-5594.

Bensemane L, Bouzerzour H, Benmahammed A and Mimouni H. 2011. Assessment of the phenotypic variation within Two- and Six-rowed Barley (*Hordeum Vulgare* L.) breeding lines grown under semi-arid conditions. *Advances Environ Biol.,* **5**:1454-1460.

Dvorakova M, Dostalek P, Skulilova Z, Jurkova M, Kellner V and Guido L F. 2010.Barley and malt polyphenols and their antioxidant properties. *Kvasny Prum*, **56** : 160-163.

Edeoga HO, Okwu DE and Mbaebie BO.2005. Phytochemical constituents of some Nigerian medicinal plants. *Afr. J. Biotechnol.* **4 (7):** 685-688.

Hamli S, Labhilili, M, Kadi K, Kabthan A E H, Tagouti M, Kamar M, Kanzeri R, Alyadini M and Bouzerzour H. 2015.Heat shock effects on fluorescence, membrane stability, chlorophyll content and metabolites accumulation in durum wheat (*Triticum turgidum L. var. durum*) seedlings and relationships with stress tolerance indices. *Advances Environ Biol.,* **9**: 116-125.

Heimler D, Vignolini P, Giulia, Dini M, Francesco, Vincieri F and Rmani A.2006. Antiradical activity and polyphenol composition of local Brassicaceae edible varieties. *Food Chem.,* **99**:464-469

Huang D, Ou B and Prior RL. 2005. The chemistry behind antioxidant capacity assays. *J Agric Food Chem.*, **53**: 1841–1856.

Ivanisova E, Ondrejovic M, Chmelova D, Maliar T, Havrlentova M and Ruckschloss L.2014. Antioxidant activity and polyphenol content in milling fractions of purple wheat. *Cereal Res Commun.*, **42**:578-588.

Karumi Y, Onyeyili PA and Ogugbuaja VO. 2004.Identification of active principles of M. balsamina (Balsam Apple) leaf extract. *J .Med .Sci.*, **4(3):**179-182.

Liu Q and Yao H. 2007. Antioxidant activities of barley seeds extracts. *Food Chem.*, **102**: 732–737.

Manach C, Scalbert A, Morand C, Remesy C and Jimenez L. 2004. Polyphenols: food sources and bioavailability. *Am J Clin Nutr*., **79**: 727–747

Naczk M and Shahidi F. 2006.Phenolics in cereals, fruits and vegetables: occurrence, extraction and analysis. *J Pharm Biomed Analysis,* **41**: 1523-1542.

Nsimba RY, Kikuzaki H and Konishi Y. 2008. Antioxidant activity of various extracts and fractions of *Chenopodium quinoa* and *Amaranthus*spp. seeds. *Food Chem.,***106**: 760-766.

Okarter N, Liu CS, Sorrels ME and Liu RH. 2010. Phytochemical content and antioxidant activity of six diverse varieties of whole wheat. *Food Chem.*, ***119***, 249–257.

Ordoñez AAL, Gomez J D, Vattuone MA and Isla M I.2006. Antioxidant activities *Sechium dule* (Jacq.) Swart extracts*. Food Chem*., **97** : 452- 458.

Perez-Jimenez, J, Arranz S, Tabernero M, Duazrubio M E, Serrano J, Goni I and Saura-Calixto F. 2008.Updated methodology to determine antioxidant capacity in plant foods, oils and beverages: extraction, measurement and expression of results. *Food Res Intern.,* **41:** 274-285.

Pinent M, Castell, A, Baiges, I, Montagut G, Arola L and Ardevol A. 2008. Bioactivity of flavonoids on insulin-secreting cells. *Compr. Rev. Food Sci. F*, **7**:299-308.

Ratnam DV, Ankola DD, Bhardwaj V, Sahana DK and Kumar, RMNV. 2006. Role of antioxidants in prophylaxis and therapy: a pharmaceutical perspective. *J Contr Release*, **113**: 189–207.

Roginsky V and EA Lissi. 2005. Review of methods to determine chain breaking antioxidant activity in food. *Food Chem.*, **92**: 235-254.

Romano AD, Serviddio G, de Matthaeis A, Bellanti F and Vendemiale G. 2010. Oxidative stress and aging. *J Nephrol.,* **15:** S29-S36.

Sarwar MH, Sarwar MF, Sarwar MN and Moghal S.2013.The importance of cereals (Poaceae: Gramineae) nutrition in human health: A review. *J Cereals Oilseeds,* **4(3):**32-35.

Satheeshkumar D, Muthu KA and Manavalan R. 2011. *In vitro* free radical scavenging activity of various extracts of whole plant of Ionidium suffruticosum (Ging). *J. Pharm. Res.*, **4**:976–977.

Siddhuraju, P and Becker K. 2003. Antioxidant properties of various extracts of totalphenolic constituents from three different agroclimatic origins of drumstick tree (Moringaoleifera lam.) leaves. *J Agric Food Chem.,* **51**: 2144–55.

Singleton VL, Ortorfer R and Lamnela RM. 1999. Analyse of total phenols and other oxidation substrate and antioxydants by mean of Folin Ciocalteu reagent. *Academic press*, **5**:152-178

Sultana B, Anwar F, Rasi M and. Chatha SAS. 2008. Antioxidant potential of extracts from different agro wastes: Stabilization of corn oil. *Grasas Y Aceties,* **59:**205-217.

Ward JL, Poutanen K, Gebruers K, Piironen, V, Lampi AM, Nystrom L, Anderson, A A M, Aman P, Boros D, Rakszegie M, Bedo Z and Shewry PR, 2008. The health grain cereal diversity screen: Concept, results and prospects. *J Agric Food Chem.,* **56**: 9699–9709.

Zielinsky H and Kozlowska H.2000.Antioxidant activity and total phenolics in selected cereal grains and their different morphological fractions. *J Agric Food Chem., Davis*, **48**: 2008-2016,

Appendix A
Contents of Volume 10- 2017

Number 1

Original Articles

Number 2

Original Articles

Number 3

Original Articles

Short Communication

Number 4

Original Articles

Appendix B

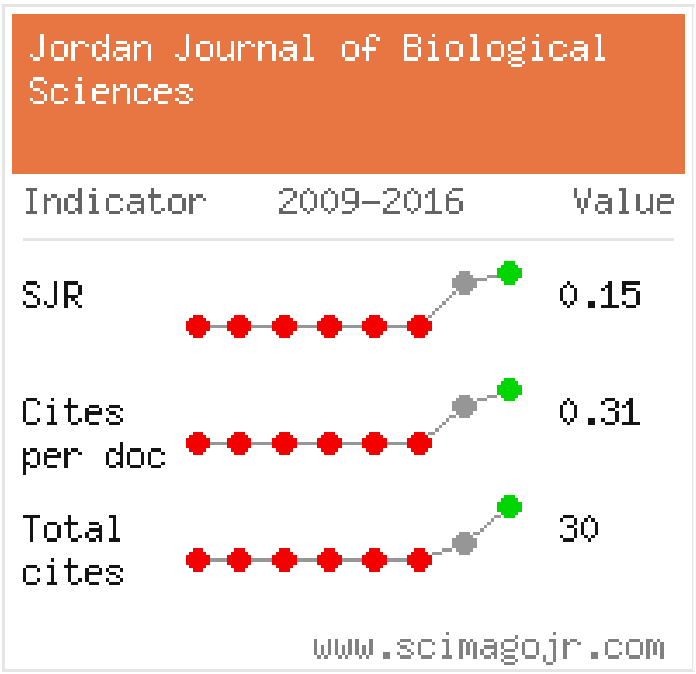

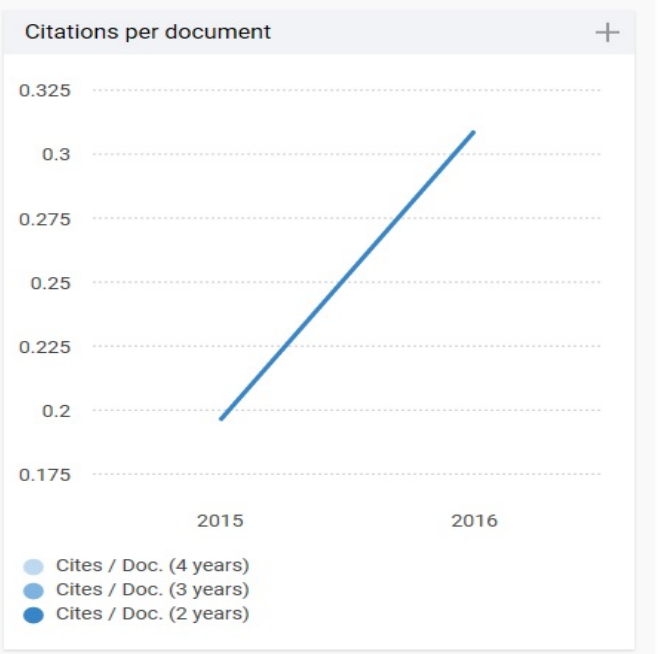

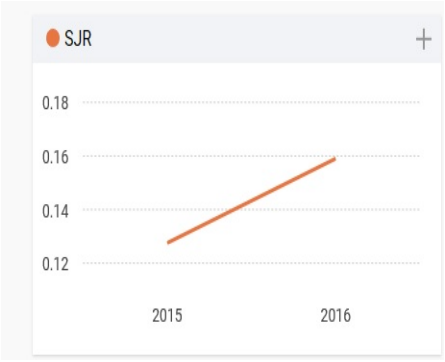

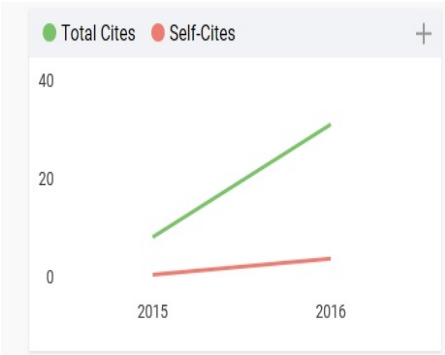

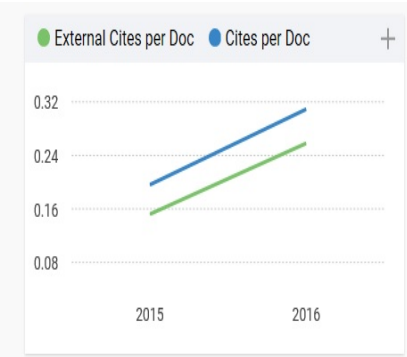

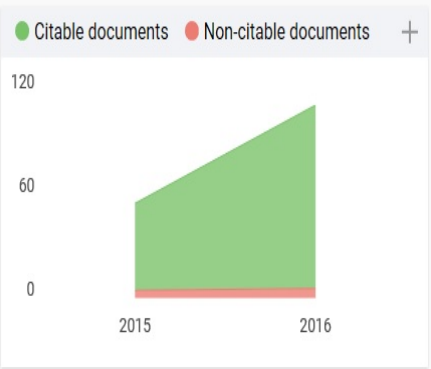

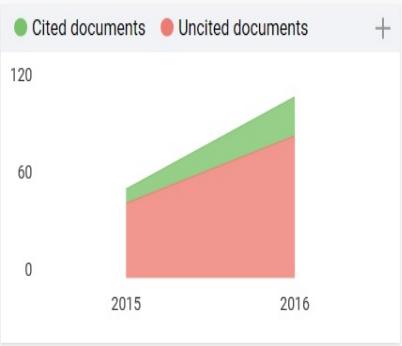

Title	Type	SJR	H index	Total Docs. (2016)	Total Docs. (3years)	Total Refs.	Total Cites (3years)	Citable Docs. (3years)	Cites / Doc. (2years)	Ref. / Doc.	
Jordan Journal of Biological Sciences	journal	0.146 Q4	3	30	102	974	30	97	0.31	32.47	

Subscription

Jordan Journal of
Biological Sciences

An International Peer – Reviewed Research Journal

Published by the deanship of Research & Graduate Studies, The Hashemite University, Zarqa, Jordan

Name: ..... الاسم:

Specialty: ..... التخصص:

Address: ..... العنوان:

P.O. Box: ..... صندوق البريد:

City &Postal Code:..... المدينة: الرمز البريدي:

Country: ..... الدولة:

Phone: ..... رقم الهاتف

Fax No.: ..... رقم الفاكس:

E-mail: ..... البريد الإلكتروني:

Method of payment: ..... طريقة الدفع:

Amount Enclosed: ..... المبلغ المرفق:

Signature: ..... التوقيع:

Cheques should be paid to Deanship of Research and Graduate Studies – The Hashemite University.

I would like to subscribe to the Journal

For

- ☐ One year
- ☐ Two years
- ☐ Three years

One Year Subscription Rates

	Inside Jordan	Outside Jordan
Individuals	JD10	$70
Students	JD5	$35
Institutions	JD 20	$90

Correspondence

Subscriptions and sales:

Prof. Ali Z. Elkarmi
The Hashemite University
P.O. Box 330127-Zarqa 13115 – Jordan
Telephone: 00 962 5 3903333 ext. 5157
Fax no. : 0096253903349
E. mail: jjbs@hu.edu.jo

المجلة الاردنية للعلوم الحياتية

مجلة علمية عالمية محكمة

المجلة الاردنية للعلوم الحياتية : مجلة علمية عالمية محكمة و مفهرسة و مصنفة، تصدر عن الجامعة الهاشمية و بدعم من صندوق البحث العلمي - وزارة التعليم العالي والبحث العلمي .

ترسل البحوث الى العنوان التالي :

رئيس تحرير المجلة الأردنية للعلوم الحياتية
الجامعة الهاشمية
الزرقاء ـ الأردن
هاتف : 0096253903333 فرعي 5157
Email: jjbs@hu.edu.jo, Website: www.jjbs.hu.edu.jo

المملكة الأردنية الهاشمية

المجلة الأردنية للعلوم الحياتية

مجلة علمية عالمية محكمة

تصدر بدعم من صندوق دعم البحث العلمي

http://jjbs.hu.edu.jo/

ISSN 1995-6673